studies in surface science and catalysis

124

EXPERIMENTS IN CATALYTIC
REACTION ENGINEERING

J.M. Berty

EXPERIMENTS IN CATALYTIC REACTION ENGINEERING

EXPERIMENTS IN CATALYTIC REACTION ENGINEERING

by

J.M. Berty
Berty Reaction Engineers, Ltd
Fogelsville, PA 18051-1501, U.S.A.

First edition 1999

Table of Contents

Preface

Many present day technologies were developed on an empirical basis, through much hard work and with remarkable success. However, all were achieved without benefit of a basic understanding of rate controlling processes, and the interaction of transport processes with chemical kinetics. These interactions are most important with fast reactions that are strongly exothermic or endothermic, exactly the ones preferred for industrial production. Therefore, many opportunities exist for improving present day production technologies through a better insight into the details of rate processes.

The influence of transport process in two–phase reaction systems depends on flow conditions, which change with the size of the equipment. This is the reason for the historic observation that performance changes as processes are scaled up and therefore scale–up should be done in several steps, each limited to a small increase in size. This is a slow and expensive method and still does not guarantee optimum design.

Effects of transport processes cannot be ignored in investigations aimed at more fundamental aspects of kinetics and catalysis. The interaction of chemical and physical processes was noticed a long time ago. M. V. Lomonosov mentioned in 1745:

> "I not only saw from other authors, but am convinced by my own art, that chemical experiments combined with physical, show peculiar effects."[1]

The need to design production units on a fundamental kinetic basis was recognized for a long time, yet the basic need to distinguish between rates influenced by transport and true chemical rates, was not fully comprehended and came only later.

---

[1] As quoted by Frank-Kamenetevskii (1961) in the preface to his book.

At the First European Symposium on Chemical Engineering, Amsterdam, (1957) the definition for Chemical Reaction Engineering was accepted as:

> "Chemical reaction engineering is part of chemical engineering in general. It aims at controlling the chemical conversion on a technical scale and will ultimately lead to appropriate and successful reactor design. An important part is played by various factors, such as flow phenomena, mass and heat transfer, and reaction kinetics. It will be clear that in the first place it is necessary to know these factors separately.
>
> Yet this knowledge in itself is insufficient. *The development of chemical conversion on a technical scale can only be understood from the relation and interaction between the above mentioned factors*".

Damköhler (1936) studied the above subjects with the help of dimensional analysis. He concluded from the differential equations, describing chemical reactions in a flow system, that four dimensionless numbers can be derived as criteria for similarity. These four and the Reynolds number are needed to characterize reacting flow systems. He realized that scale–up on this basis can only be achieved by giving up complete similarity. The recognition that these basic dimensionless numbers have general and wider applicability came only in the 1960s. The Damköhler numbers will be used for the basis of discussion of the subject presented here as follows:

$$Da_I = \frac{r\,l}{C\,u}, \quad Da_{II} = \frac{r\,l^2}{C\,D}, \quad Da_{III} = \frac{r(-\Delta H_r)l}{c_p \rho T u},$$

$$Da_{IV} = \frac{r(-\Delta H_r)l^2}{k_t T}, \quad Re = \frac{l\,u\,\rho}{\mu}.$$

In a later paper Damköhler (1937) also defined :

$$Da_V = Da_{IV}/Nu = \frac{r(-\Delta H_r)l}{hT}$$

This will be used here, too.

In the mid 1960s, computers became available and this made many calculations possible, including the simultaneous integration of several coupled differential equations. With this, the execution of many design

tasks—formerly very time consuming and approximate—became easy, fast and seemingly accurate. Publications proliferated, with computer solutions to many imagined and a few real problems. Only then was it realized that good kinetic results, free of transfer influences, were woefully lacking. This caused a general increase of interest in improving kinetic measurements.

In 1960 the author was charged with the review and improvement of the ethylene oxide technology of Union Carbide Corporation (UCC). A historic overview revealed some interesting facts. The basic French patent of Lefort (1931,1935) for ethylene oxide production was purchased by UCC in 1936. In 1937, a pilot–plant was operated and commercial production started in 1938. By 1960, UCC's production experience was several hundred reactor–years. This was expressed as the sum of the number of production reactors, each multiplied by the number of years it had been in operation. Research and development had continued since the purchase of the original patent and the total number of people involved in ethylene oxide related research at one time reached one hundred.

Development of the first recycle reactor was one of the consequences of a challenging situation. The ethylene oxide process had reached a high level of sophistication and excellent performance after 25 years of continuous R&D. To improve results achieved by so many excellent people over so many years was a formidable task.

In previous studies, the main tool for process improvement was the tubular reactor. This small version of an industrial reactor tube had to be operated at less severe conditions than the industrial–size reactor. Even then, isothermal conditions could never be achieved and kinetic interpretation was ambiguous. Obviously, better tools and techniques were needed for every part of the project. In particular, a better experimental reactor had to be developed that could produce more precise results at well defined conditions. By that time many home–built recycle reactors (RRs), spinning basket reactors and other laboratory continuous stirred tank reactors (CSTRs) were in use and the subject of publications. Most of these served the original author and his reaction well but few could generate the mass velocities used in actual production units.

Recycle reactors at that time were called "Backmix Reactors." They were correctly considered the worst choice for the production of a reactive intermediate, yet the best for kinetic studies. The aim of the kinetic study for ethylene oxidation was to maximize the quality of the information, leaving the optimization of production units for a later stage in engineering studies. The recycle reactors could provide the most precise results at well defined conditions even if at somewhat low selectivity to the desired product.

The RR developed by the author at UCC was the only one that had a high recycle rate with a reasonably known internal flow (Berty, 1969). This original reactor was named later after the author as the "Berty Reactor". Over five hundred of these have been in use around the world over the last 30 years. The use of Berty reactors for ethylene oxide process improvement alone has resulted in 300 million pounds per year increase in production, without addition of new facilities (Mason, 1966). Similar improvements are possible with many other catalytic processes. In recent years a new blower design, a labyrinth seal between the blower and catalyst basket, and a better drive resulted in an even better reactor that has the registered trade name of "ROTOBERTY®."

Many of the methods discussed in this book stem from the practical experience of the author, who worked for 20 years at Union Carbide Corporation. Other experience came from consulting work for over 30 companies, and from the laboratory of Berty Reaction Engineers, Ltd. The corresponding theoretical treatments were developed while teaching six professional short courses and lecturing at the State University of New York at Buffalo, NY, The University of Akron, at Akron, OH, and as a Senior Fulbright Scholar at the Technical University of Munich, Germany. The final assembly of the book was started when the author again taught a short course at the University of Veszprém in Hungary after a 36 year interruption.

The aim of the book is to give practical advice for those who want to generate kinetic results, valid for scale–up, and backed by sensible theory and understandable mathematical explanation.

Methanol synthesis will be used many times as an example to explain some concepts, largely because the stoichiometry of methanol synthesis is simple. The physical properties of all compounds are well known, details of many competing technologies have been published and methanol is an important industrial chemical. In addition to its relative simplicity, methanol synthesis offers an opportunity to show how to handle reversible reactions, the change in mole numbers, removal of reaction heat, and other engineering problems.

To facilitate the use of methanol synthesis in examples, the "UCKRON" and "VEKRON" test problems (Berty et al 1989, Árva and Szeifert 1989) will be applied. In the development of the test problem, methanol synthesis served as an example. The physical properties, thermodynamic conditions, technology and average rate of reaction were taken from the literature of methanol synthesis. For the kinetics, however, an artificial mechanism was created that had a known and rigorous mathematical solution. It was fundamentally important to create a fixed basis of comparison with various approximate mathematical models for kinetics. These were derived by simulated experiments from the test problems with added random error. See Appendix A and B, Berty et al, 1989.

The "UCKRON" AND "VEKRON" kinetics are not models for methanol synthesis. These test problems represent assumed four and six elementary step mechanisms, which are thermodynamically consistent and for which the rate expression could be expressed by rigorous analytical solution and without the assumption of rate limiting steps. The exact solution was more important for the test problems in engineering, than it was to match the presently preferred theory on mechanism.

Conclusions from the test problems are not limited by any means to methanol synthesis. These results have more general meaning. Other reactions also will be used to explain certain features of the subjects. Yet the programs for the test problem make it possible to simulate experiments on a computer. In turn, computer simulation of experiments by the reader makes the understanding of the experimental concepts in this book more profound and at the same time easier to grasp.

Literature

1. Árva, P. and F. Szeifert, **1989**, "Effect of Water–gas Reaction on Methanol Synthesis" *Chem. Eng. Comm.*, 76, pp 195–206.
2. Berty, J. M., J. O .Hambrick, T. R. Malone, and D. S. Ullock, **1969**, "Reactor for Vapor–Phase Catalytic Studies" Paper No. 42 E, presented at the Symposium on Advances of High Pressure Technology, Part II, 64th Nat. Meeting of AIChE, New Orleans, LA, March 16–20.
3. Berty, J. M., S. Lee, F. Szeifert, and J. B. Cropley, **1989**, "The 'UCKRON–I' Test Problem for Reaction Engineering Modeling" *Chem. Eng. Comm.*, 76, pp 9–34.
4. Damköhler, G. **1936**, "Einflüsse der Srömung, Diffusion und der Wärmeüberganges auf die Leistung von Reakcionsöfen" *Ztschr. Elektrochem*. Bd.42, Nr 12.
5. Damköhler, G. **1937**, "Einfluss von Diffusion, Strömung und Wärmetransport auf die Ausbeute bei chemisch–techniscen Reaktionen. Kap. II", 2. in A, Eucken und M. Jakob, editors, *Der Chemie–Ingenieur*. Band III.
6. Lefort, T. E., *Ethylene Oxide Production*, **1931**, Fr. Pat.729,952; 1935, U.S. Pat. 1,998,878.
7. Mason, Birny, **1966**, "Annual Report Almost Ready, Research Effort Highlighted," *The Hill-Topper*, a Union Carbide Publication, South Charleston, WV, March, page 1, No. 10.

Notations

Symbol	Definition	Units
A_i	chemical compound	mol
a	thermal diffusivity $= k_t / c\rho$	m^2/s
a_i	activity $= (f/f_o)$	–
C_i	concentration of species A_i	mol/m^3
c	specific heat of fluid	kJ / kg K
D_{AB}	diffusivity of A in B	m^2/s
d_P	particle diameter	m
d_t	tube diameter, inside	m
E	energy of activation	kJ/kmol
F	force = newton	$kg\ m/s^2$
F	total molar flow rate	mol / s
F_i	molar flow rate of A_i	mol / s
F'	volumetric flow rate	m^3/s
f	fugacity = pascal	Pa
G	mass velocity	$kg / m^2\ s$
g	acceleration of gravity = 9.81	m^2/s
ΔH	heat of reaction	kJ / mol
h_f	film coefficient for heat transfer	$W / m^2\ s$
K	equilibrium constant $= a_P{}^P/a_R{}^r$	–
k	reaction rate coefficient	1 / s
k_g	mass transfer coefficient	m / s
k_t	thermal conductivity	W / m K
k_m	momentum transfer coefficient	m / s
l	distance	m
M	molar density, 1/1000 MW	mol/kg
m	integral number	–
MW	molecular weight	kg / kmol
N	number of moles	mol
n	order of reaction	–
P	pressure	kPa
R	gas constant = 8.314	J/mol K
R_i	total rate of change of A_i	$mol / m^3\ s$
R_t	inside tube radius	m
r_i	rate of reaction i	$mol / m^3\ s$
q_{gen}	rate of heat generation	W/m^3
S	selectivity, fractional	–
S	surface	m^2
SS	steady state	–
T	temperature	K

Symbol	Definition	Units
t	clock time	s
u	linear velocity	m / s
U	overall heat transfer coefficient	$W / m^2 K$
U_0	time constant ratio	–
V	volume	m^3
W	weight of catalyst	kg
w	power = watts	W
x	mole fraction in liquid, on catalyst surface	–
X	conversion, fractional	–
y	mol fraction in gas	–
Y	Yield, fractional	–
Z	Efficiency, fractional	–

Greek Letters

α	stoichiometric coefficient	–
β	adiabatic temperature rise potential	–
γ	Arrhenius number = E / RT^2	–
δ	change in the sum of stoichiom. no.s	–
ε	void fraction in catalyst bed	–
η	kinematic viscosity	m^2 / s
η	catalytic effectiveness factor, fractional	–
θ	void fraction in catalyst pores	–
μ	dynamic viscosity	kg / m s
ρ	density	kg / m^3
τ	tortuosity factor	–
ϕ	Thiele modulus = $(d_p/3)(k/D)^{0.5}$	–
Θ	Weisz–Prater criterion = $\eta h \phi^2 = Da_{II}$	–

Superscripts

s   at standard temp and press. of 273.1 K and 101.3 kPa

Subscripts

b	bed	
f	fluid	–
i	reactions	–
j	compounds	
m	mass	–
o	feed conditions	–
p	particle	–
P	products	–
R	reactants	–
C	catalyst	
S	surface	–
s	solid	–
t	total	–

Dimensionless Numbers

'A'	momentum transfer / momentum cond., (analog to Sh and Nu numbers)	$= k_m \, l \, / \, \eta$
'B'	momentum production/momentum cond., (analog to St and f' / 2 numbers)	$= F / \rho \, \eta \, u \, l$
Bi	Biot (heat transfer/thermal cond. of solid)	$= Nu(k_t/k_{t,s})$
Bo	Bodenstein (Pe number for mass)	$= u \, l \, / \, D$
β	adiabatic temperature rise potential	$= C(-\Delta H)/\rho \, c \, T$
Ca	Carberry	$= r \, l \, / \, C \, k_m$
Da_I	Damköhler number – I	$= r \, l \, / \, C \, u$
Da_{II}	Damköhler number – II	$= r \, l^2 \, / \, C \, D$
Da_{III}	Damköhler number – III	$= r \, (-\Delta H) \, l/\rho \, c \, T \, u$
Da_{IV}	Damköhler number – IV	$= r \, (-\Delta H) \, l^2/ \, k_t$
Da_V	Damköhler number – V	$= r \, (-\Delta H) \, l \, / \, h \, T$
f / 2	Fanning friction factor	$= k_m/u$
'E'	momentum production/ conduction	$= F/\rho \, k_m \, u \, l^2$
Fr	Froud = 1/Fa = 1/Fanning	$= u^2/g \, l$
Ha	Hatta number	$= \sqrt{(kD)}/k_g$
j_D	Colburn factor for mass (Sh $Sc^{2/3}$)	$= (k_g \, l/ \, D)(\eta/D)^{0.66}$
j_H	Colburn factor for heat (St $Pr^{2/3}$)	$= (h \, /\rho \, c \, u)(\eta/a)^{0.66}$
Le	Lewis number	$= a \, / \, D$
Nu	Nusselt number	$= h \, l \, / \, k_t$
Pe	Peclet number	$= u \, l \, / \, a$
Pr	Prandtl number	$= \eta \, / \, a = c\mu/k_t$

Rc	Reynolds number	$= u\,l\,/\,\eta$
Sc	Schmidt number	$= \eta\,/\,D$
Sh	Sherwood number	$= k_g\,l\,/\,D$
St	Stanton number	$= h\,/\,\rho\,c\,u$
St′	Stanton number for mass	$= k_g\,/\,u$
We	Weber number	$= \rho\,u^2\,l^2\,/\,F$

A, **B**, **E** are unnamed numbers results of the systematization by László (1964).

The unnamed number **C** is now called the Carberry number, and **D** is identical with $\mathbf{Da_{IV}} = \mathbf{Da_V}$.

Introduction

Catalysis is a fascinating subject and many good books are available in the field. These books treat the subject all the way from the theoretical to the process chemistry end. In this book there is another goal and that is the engineering aspects of catalysis. In other words, this book aims to guide the reader through the path that leads from a catalytic discovery, or from a new and better laboratory result, to its industrial use. This activity is called "development" and when the interaction of chemical and transport rates are studied on a fundamental basis, it can also be thought of as "reaction engineering of catalytic processes."

The path that leads from a laboratory result to the large–scale production can also be called in a very general sense "scale–up." This definition sets the goal for scale–up but does not specify the method. In one sense, the word scale–up implies the method of an empirical and gradual increase of size to production level. The second definition of scale–up includes design, which means working from first principles toward a defined goal. In this case design means working from knowledge of intrinsic rates of chemical reactions and transport processes, toward the definition of a production reactor and its ancillary equipment.

The design approach is particularly feasible for those reactions in which chemical and pore diffusion rates are most important. For flow related phenomena semi–empirical, dimensionless correlations must be relied on. Therefore in this book scale–up will be used in the more general sense with the aim of using methods that are fundamentally based wherever feasible.

A few excellent books are also available on reaction engineering in the widest sense and from a fundamental point of view. These books treat the subject with mathematical rigor, yet are too inclusive to have any space left for details on experimental procedures. Here, the reader can find more insight and practical examples on the development and scale–up of

catalytic processes and on the experimental methods to collect results for this purpose. The book tries to give somewhat more than is usually present in a "How To" book, by giving reasons for the recommended actions. In other words, in addition to the "know how," the "know why" appears here, too.

Over fifty years of experience in this field taught the author that here, perhaps even more than in any other field, generalizations are dangerous. Yet there is no other choice, even at the risk of small mistakes or stretches of the imagination that go a little too far. This is the price of progress and the reader is encouraged to treat the conclusions critically, always asking the questions: "Can this be true?" "If it is true what are its consequences to my case?" and "How does this apply to my problem?" For the user's sake, an in–depth justification for rejecting any generalization is recommended. This way, as knowledge of the process increases, a review of the rejected generalization will be possible. An additional warning is also in order. Some of the fundamental differences among reaction chemistries may not be so critical or important when the reaction engineering aspects are considered. For example, in the petrochemical industry, the synthesis of methanol is more similar to that of ammonia than to that of ethanol from ethylene.

The reader will need some familiarity with the subject of catalysis and an elementary understanding of the reaction engineering subjects. These, in turn, require a conceptual grasp of calculus. To make good use of all this, a practical experience in computer programming is also required. The subjects, where practical, will be treated on an intuitive level. There is nothing wrong with intuition, only with the lack of it. To satisfy the purist, a rigorous mathematical presentation will be included mainly in the appendices, where it is justified for proof, and the reader will be able to skip most of these parts if so desired.

A few books useful to brushing up on the fundamentals are listed in the references. Some people naturally will have more in–depth knowledge of some aspects of the necessary subjects than others. In reality, few individuals will have the depth and breadth of knowledge necessary for success in developing catalytic processes. For a higher level of accomplishment, cooperation between chemists and engineers will be

needed. However, this will be fruitful only if both have enough knowledge of the partner's field to communicate intelligently and to appreciate the viewpoints and reasoning of the other.

Where useful, actual examples will be given and computer simulated experiments will be shown. In general, references to real life cases from the author's experience will be made available, when possible, to enlighten the subject.

In a more general sense, most of the concepts and techniques given in this book will be valid for homogeneous processes also, as long as there is a way to stop the reaction in the experimental studies suddenly by some means, e.g., by quenching or neutralizing. Some references will be given at the appropriate places in the book.

A surface scientist working on molecular scale of catalysis may become disappointed by seeing how little quantitative use can be made in reaction engineering of the newest and theoretically most interesting instrumental techniques. It may be of some solace to them that it is not their fault. The quantitative consequences of important insights will have to evolve from much closer cooperation between physicists, chemists and engineers. This will require people reasonably well informed in all three fields.

The successful accomplishment of a development project also requires cooperation between engineers and technicians in the development team and between engineers in R&D, design engineering and in management. All this will require some common background, clear reporting, and much patience.

In summary, the problem this book addresses is how to select a catalyst in laboratory experiments that will be the best for commercial processes and how to develop kinetic expressions both valid in production units and useful in maximizing profits in safe operations.

General References

1. Aris, R. **1969**, *Elementary Chemical Reactor Analysis*. Prentice–Hall, Englewood Cliffs, NJ.

2. Benson, S. W. **1960**, *The Foundations of Chemical Kinetics*. McGraw–Hill, New York, NY.

3. Boudart, M. **1968**, *Kinetics of Chemical Processes*, Prentice–Hall, Inc. Englewood Cliffs, NJ.

4. Brötz, W. **1965**, *Fundamentals of Chemical Reaction Engineering*. Addison–Wesley, Reading, MA

5. Butt, J. B. **1980**, *Reaction Kinetics and Reactor Design*. Prentice–Hall, Englewood Hills, NJ.

6. Carberry, J. J. **1976**, *Chemical and Catalytic Reaction Engineering*. McGraw–Hill, New York.

7. Delmon, B., Jacobs, P. A. and Poncelet, G. **1976**, *Preparation of Catalysts*. Elsevier Sci. Publ. Co., Amsterdam.

8. Gates, B. C., Katzer, J. R., and Schuit, G. C. A. **1979**, *Chemistry of Catalytic Processes*. McGraw–Hill, New York.

9. Fogler, H. S. **1998**, *Elements of Chemical Reaction Engineering* 2nd Edition, Prentice Hall, Inc., Englewood Cliffs, NJ

10. Froment, G. F. and Bischoff, K. B. **1979**, *Chemical Reactor Analysis and Design*. John Wiley & Sons, New York.

11. Gill, W.N., Garside, J. and Berty, J. M., Editors, **1989**, Special Issue on "Kinetic Model Development," *Chem. Eng, Comm*. 76.

12. Levenspiel, P. **1972**, *Chemical Reaction Engineering*. John Wiley & Sons, New York.

13. Petersen, E. E. **1965**, *Chemical Reaction Analysis*. Prentice–Hall, Inc., Englewood Cliffs, NJ..

14. Stiles, A. B. **1983**, *Catalyst Manufacture, Laboratory and Commercial Preparations*. Marcel Dekker, Inc., New York.

15. Thomas, C. L. **1970**, *Catalytic Processes and Proven Catalysts*. Academic Press, New York.

1. Effect of Scale on Performance

Developments in experimental and mathematical techniques in the 1970s have initiated an interest in the development of better laboratory reactors for catalytic studies. Besides the many publications on new reactors for general or special tasks, quite a few review articles have been published on the general subject of laboratory reactors for catalytic studies.

Most of the published reviews on reactors and on the testing of catalysts represent one special viewpoint because each author's own field of interest influenced the paper. Bennett et al (1972) reviewed gradientless reactors from the point of view of transient studies. Weekman (1974) evaluated various reactors for powdered catalysts used mostly in fluid bed processes as contrasted with particulate catalysts. Doraiswamy and Tajbl's (1974) review dealt primarily with fixed bed reactors. Difford and Spencer (1975) gave a brief review and recommendations on the use of different reactors for various purposes. Jankowski et al (1978) described the construction of various gradientless reactors. Cooke (1979) reviewed bench–scale reactors and tried to give a definition of the ideal reactor. Berty (1979) also reviewed the testing of commercial catalysts in recycle reactors. All these review papers will serve as general references for the indicated point of view, and where the following discussion cannot go into details the reader should consult these articles.

In reaction engineering, laboratory catalytic reactors are tools or instruments to study how catalysts behave in some desired reaction. Quantitatively, the investigator wants to know how much of the desired product can be made per unit weight of catalyst, how much raw material will be used, and what byproducts will be made. This is the basic information needed to estimate the costs and profitability of the process. The economic consequence of our estimates also forces us to clarify what the rate limiting steps are, and how much transfer processes influence the rates, i.e., everything that is needed for a secure scale–up. Making the

==desired product on a commercial scale, safely and economically, is the ultimate aim of catalytic reaction engineering.==

1.1 Scale–down to Laboratory Reactors

About sixty years ago, Damköhler (1936) investigated the possibility of a scale–up of laboratory reactors to production reactors on the basis of the theory of similarity. He concluded that, for tubular reactors that have temperature, concentration, and flow gradients, complete and simultaneous similarity is possible—of geometric, mechanical, thermal, and chemical properties—only if a single, well–defined reaction is occurring. This is valid for empty homogeneous reactors. For a packed bed catalytic reactor the similarity holds only for laminar flows. These cases are the least interesting industrial applications. Therefore, the dimensionless numbers derived by Damköhler were not initially appreciated. Later it was recognized that the Damköhler numbers represent fundamental dimensionless variables, with a wide range of applications. Smith (1968) considered the same scale–down problem as a part of an industrial research application.

In Figure 1.1.1 a,b an example is shown for scale–down to experimental conditions for the hydrogenation of crotonaldehyde to butanol:

$$CH_3CH=CHCHO + 2 H_2 \longrightarrow CH_3CH_2CH_2CH_2OH$$
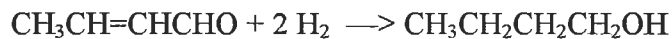
which, for conditions selected here, is practically irreversible (Berty 1983.)

Pressure (psig)	500	300
Temperature		
K	440	490
°C	167	217
°F	333	423
Density, ρ (kg/m^3) , where ρ_0=0.386	8.39	4.63
Superficial linear velocity (m/sec)	0.26	0.47
Mass velocity, G (kg/m^{2}sec)	2.18	2.18
Reynolds number, d_pG/μ	1150	932
GHSV (hr^{-1})	1876	1876

Figure 1.1.1a: Conditions that will be identical on all three scales at the two different P and T values.

Operating Conditions for the Recycle Reactor:

Flow cross–section for 2–inch basket $A=(2.54)^2(3.14)=20.27 cm^2$
$=2.03 \times 10^{-3} m^2$

Recycle flow	$F_0=GA/\rho_0=0.0115 \ m^3/sec=1457 \ SCFH$
Recycle ratio	$n=1457/1.83=800$
Rpm required	650 at 500 psig and 1150 at 300 psig
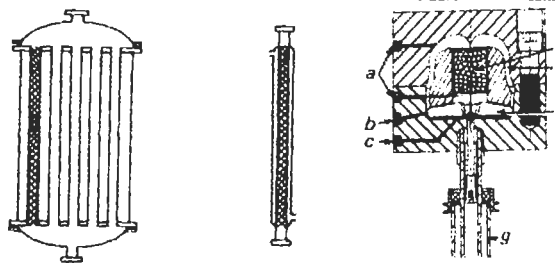
a–thermowell connection; b–inlet connection; c–outlet connection; d–catalyst basket; e–draft tube; f–impeller; g–magnedrive assembly

Scale–down ratio	1:1	1:4000	$1:1 \times 10^6$
Feed rate, aldehyde			
lb/yr	200×10^6	50×10^3	200
lb/hr *	33.3×10^3	8.33	33.3×10^{-3}
lb mol/hr	462	0.116	0.462×10^{-3}
lb mol, hydrogen**	4620	1.16	4.62×10^{-3}
Total Feed			
SCFH	1.82×10^6	455	1.82
g mol/hr	2.31×10^6	577	2.31
Tubes			
Number	4000	1	1
i.d. (inches)	1.12	1.12	2.0
Length (inches)	420	420	0.53
Length (feet)	35	35	0.044
Catalyst volume (ft³)	970	0.24	0.97×10^{-3}
Catalyst volume (m³)	27.5	6.9×10^{-3}	27.5×10^{-6}

The first data column at the top of Figure 1.1.1b represents a commercial reactor with a 1:1 scale–down ratio, and the conditions listed can be considered given. A laboratory reactor must be devised based on these conditions. The second data column represents a single tube identical to one of the 4000 tubes of the commercial reactor. This tube, if the heat transfer side is properly designed, can behave identically to an average tube in the large unit. But it is more of a pilot–plant reactor than a laboratory unit because of its size and feed requirements. It gives only overall performance results unless sample taps are built at equal distances and a thermowell with multiple sensors is built in. In this case, the single tube rapidly loses its close identity with the average tube and becomes complicated.

The third data column represents an internal recycle reactor where, using a 1 million scale–down factor, all the important flow, thermal, and chemical criteria can be maintained for the immediate surroundings of the catalyst From the operating conditions given in Figure 1.1.1a and the top of Figure 1.1.1b, holding the RPM constant and changing the fresh feed rate, various conversions can be achieved without changing the mass velocity.

The alternate possibility of building a laboratory tubular reactor that is shorter and smaller in diameter is also permissible, but only for slow and only mildly exothermic reactions where smaller catalyst particles also can be used. This would not give a scaleable result for the crotonaldehyde example at the high reaction and heat release rates, where flow and pore–diffusion influence can also be expected.

In the petrochemical industry close to 80% of reactions are oxidations and hydrogenations, and consequently very exothermic. In addition, profitability requires fast and selective reactions. Fortunately these can be studied nowadays in gradientless reactors. The slightly exothermic reactions and many endothermic processes of the petroleum industry still can use various tubular reactors, as will be shown later.

1.2 Performance of 12.0 & 1.2 Meter Long Methanol Reactors

Atwood et al, (1989) developed a reactor model that included axial and radial mass and heat dispersions to compare the performance of laboratory

and commercial tubular reactors. The UCKRON–I test problem was applied that uses the methanol synthesis as an example (Appendix A).

Both reactors used 38.1 mm Ø tubes. The commercial reactor was 12 m long while the length of the laboratory reactor was 1.2 m. Except for the 10:1 difference in the lengths, everything else was the same. Both reactors were simulated at 100 atm operation and at GHSV of 10,000 h-1. This means that residence times were identical, and linear gas velocities were 10 times less in the lab than at the production unit. Consequently the Re number, and all that is a function of it, were different. Heat transfer coefficients were 631 and 206 in watts/m^{2}K units for the large and small reactors.

Length, m	Coolant Temp, K	Gas Type	Inlet Velocity m/sec	Production rate, Kg/Hr
1.2	429	Real	0.0577	1288
1.2	429.5	Real	0.0577	1459
1.2	430	Real	0.0577	1811
1.2	434	Ideal	0.0577	1238
1.2	434.5	Ideal	0.0577	1380
1.2	435	Ideal	0.0577	1620
12	481.5	Real	0.577	44336
12	482	Real	0.577	51607
12	483	Real	0.577	110274
12	483	Ideal	0.577	34476
12	485.5	Ideal	0.577	53610
12	485.7	Ideal	0.577	60404

Inlet Pressure, 1012 kPa; Inlet Temperature, 473K; Inlet Composition, 0.772 Kg mol/cu m carbon monoxide, 1.801 Kg mol/cu m hydrogen.

Reproduced with permission from Atwood et al., Chem. Eng. Comm., 76, p. 137, © 1989 Gordon & Breach.

Figure 1.2.1: Methanol production rates.

The maximum attainable production was sought that did not cause thermal runaway. By gradually increasing the temperature of the water, boiling under pressure in the reactor jacket, the condition was found for the incipient onset of thermal instability. Runaway set in at 485.2 to 485.5 K for the 12 m reactor and at 435.0 to 435.5 K for the shorter, 1.2 m reactor. The smaller reactor reached its maximum operation limit at 50 K lower than the larger reactor. The large reactor produced 33 times more methanol, instead of the 10 times more expected from the sizes. This

included the heat generation rate also. The short tube is thus not a reliable basis for scale–up. Commercial reactors, designed on short tube results, can suffer economic, technical and human disasters.

Original calculations were made using ideal gas laws, and later ones with real gas laws. Only a few degrees of differences were observed between ideal and real gas cases and the difference between small and large reactors remained essentially the same. No significant radial concentration gradients were found in any cases investigated. See the table in Figure 1.2.1.

1.3   An Alternative Viewpoint For Scale–up

Figure 1.3.1 a: Scale–down of commercial catalytic converters.

Figure 1.3.1a, b illustrates an idea proposed by the author (Berty 1974): the basis for geometric similarity should be what the catalyst "sees" on the inside, instead of the gross features of a reactor that can be observed from the outside. Identity as well as similarity can be achieved on various scales if the investigator bases the criteria on the direct surroundings of the catalyst where flow, partial pressures, and temperature all are important.

Thermowell Connection

Thermowell Connection

Inlet Connection

Outlet Connection

Catalyst Basket

Draft Tube

Impeller

Magnedrive Assembly
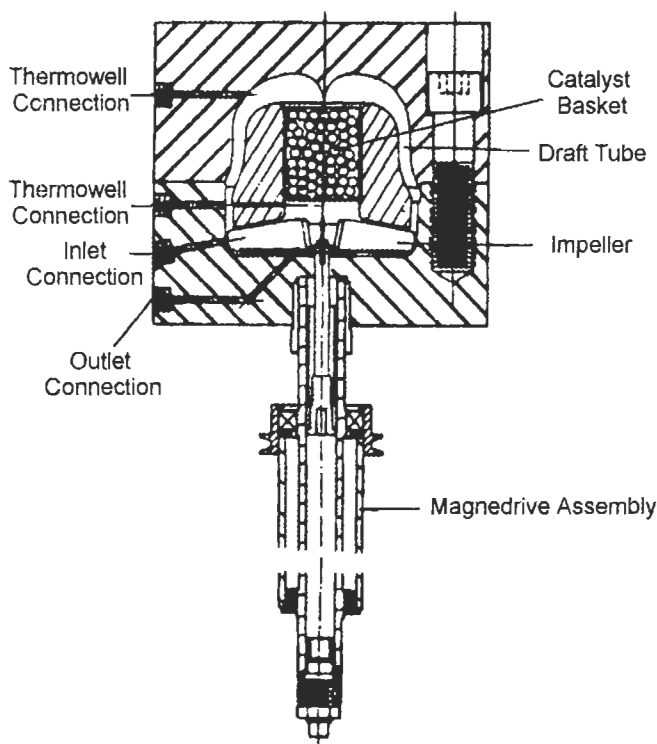
Reproduced from Chem. Eng. Progr. Vol. 70, No. 5, p. 79 with permission of the American Institute of Chemical Engineers, © 1974 AICHE. All rights reserved.

Figure 1.3.1 b: The first commercial design for a catalytic converter.

To achieve the goal set above, measurements for reaction rates must be made in a RR at the flow conditions, i.e., Reynolds number of the large unit and at several well–defined partial pressures and temperatures around the expected operation. Measurements at even higher flow rates than customary in a commercial reactor are also possible and should be made to check for flow effect. Each measurement is to be made at "point

conditions": one well–defined temperature and a set of partial pressures. The range of the measurements should include all conditions anticipated in a commercial reactor. The results must be summarized in kinetic equations or models. The integration of the kinetic equations with the proper boundary conditions pertaining to different reactors will give the best estimate for production performance. See Figure 1.3.1 b for the first commercial design.

The example in Figure 1.1.1 is really a scale–down and not a scale–up. Having some idea how these types of hydrogenations are executed on production scale, one can start by visualizing a production unit and estimate the approximate operating conditions from similar processes. In this case of crotonaldehyde hydrogenation to butyraldehyde, a 4000–tube reactor is assumed with other conditions given in the table. A single tube of this reactor can serve as a pilot–plant. The expensive pilot–plant studies must be cut to a minimum, mostly to those experiments that test the predictions of a kinetic model. For the development of the kinetic model, studies are planned in a recycle reactor that has only one millionth of the catalyst charge of the production unit. Although the scale–down ratio based on catalyst quantity is one–to–one million, in reality the conditions around the catalyst particles are the same, therefore, the test is made at one–to–one scale, i.e., without any scale change. The same conditions exist for flow, represented by identical particle diameters and Reynolds numbers, and at the same T, P, and concentrations and reaction rates.

The "Gradientless" recycle reactor still has a small gradient in the direction of the flow that can be calculated and is usually negligible. Tubular reactors have gradients both in radial and axial directions. The radial gradient is considered to be confined to the inside film in the tube in one–dimensional models. Thus, at any given tube length, the catalyst particles are assumed to work at the same average temperature. If the reaction has a large reaction enthalpy, two–dimensional models may also need to be investigated, taking into account the effect of radial gradient for temperature. Additional non–uniform performance among tubes, due to differences in packing densities of catalysts and consequent non–uniform flows per tube, can also be taken into account as Govil et al (1989) have shown. The most dangerous feature of scale–up—working at different Re

at various scales—is eliminated by this approach, even if some small differences to increased scale remain.

Commercial Reactor 6'9" Ø

Pilot-plant reactor 3" Ø

Basket Size for Recycle Reactor 2" Ø
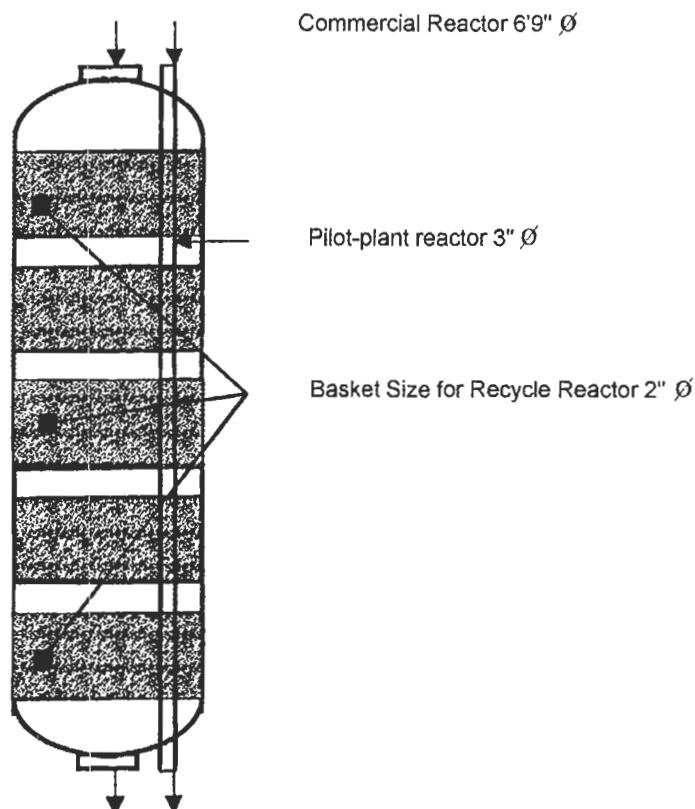
Both the pilot–plant and commercial reactors are the same length (60 feet), and all three use the same mass velocity and can be operated at various conditions.
Drawing by the author.

Figure 1.3.2: Five stage adiabatic reactor.

Figure 1.3.2 gives another perspective for scale–down to recycle reactor studies. In this actual case, after preliminary studies in a recycle reactor, a 5–stage adiabatic reactor was envisioned (Berty 1979.) Scaling down the proposed commercial reactor, a 3" diameter tube was designed with elaborate temperature compensation (heating and insulation) for pilot–plant studies (Berty 1968, 1969.) Small squares in the proposed reactor represent side views of cylindrical catalyst cutouts for the recycle reactor

study. Their location represents the range of the conditions that should be used in a statistically designed set of experiments for kinetic studies and not actual conditions at the particular location. This way, the same flow is again maintained on all three scales and the troublesome effect of changing flow conditions on scale–up can be eliminated. The proposed idea, for scale–up by scale–down from the view point of the catalyst, was proven to be effective in many industrial projects.

1.4 Flow and Pressure Drop in Catalyst Beds

Pressure drop in catalyst beds is governed by the same principles as in any flow system. Consequently, at very low flow, pressure drop is directly proportional to velocity, and at very high flow, to the square of velocity. These conditions correspond to the laminar and turbulent regimes of the flow.

In a packed bed, the transition from the laminar to the turbulent regime is much less pronounced than in empty tubes, and covers a wider range of flow. The cavities between particles form little mixing units that have several connections to adjacent cavities. Additional complications arise from the particle shape, from the surface smoothness, and from the particles' uniformity. These particle properties influence the packing density of beds. First, smooth particles usually pack more densely than those with rough surfaces. Second, pressure drop is higher on rough–surface particles than over smooth ones. Non–uniform particles pack to less void space than uniform ones. Finally, the ratio of the tube diameter to particle diameter also influences the bed density. Packing density at small ratios becomes a periodic function of the diameter ratios, further complicating the situation. For very exothermic reactions, ratios as small as 3 to 4 particle per tube diameter are used.

The void fraction, or porosity ε of the bed has the most significant influence on pressure drop. Charging catalyst to production reactors, especially to those with several thousand long and narrow tubes, is an art that requires special equipment and skills. In laboratory reactors, the problem is less pronounced but it is still easy to get 10–20 % deviations in pressure drop just by dumping and charging the same catalysts to the same tube again. Different generalized expressions to calculate pressure drop for catalyst–filled tubes can give up to 100 % different predictions. Error can

be lessened only if a calculation is made by a correlation that was developed on similar materials in the same size and flow range.

Energy needed for pumping can be a significant cost item for the inexpensive basic chemicals; therefore, pressure drop must be known more accurately than calculation methods can provide. The needed accuracy can be achieved only by measuring pressure drop versus flow for every new catalyst. This measurement can now be done much better and more easily than before. Even so, for a basic understanding of correlation between pressure drop and flow, some published work must be consulted. (See Figure 1.4.1 on the next page.)

Leva et al (1949) and Ergun (1952) developed similar useful equations. Later, these were refined and modified by Handley and Heggs (1968) and by MacDonald et al (1979). All these equations try to handle the transient regime between laminar and turbulent flow somewhat differently but are based on the same principles.

Leva's correlation (Leva 1949) is the easiest to use in manual calculation, especially when the particle diameter–based Reynolds number is high, i.e., above $Re_p \geq 1,000$. A changing exponent **n** in the Leva expression, shown below, accounts for the transient region as turbulence of flow increases. The dependence of **n** on Re_p was specified by Leva graphically (1949) as **n** growing with the Re_p between 1.0 and 2.0. The value reaches **n** = 1.95 at Re_p =1,000 thus approximating 2.0 closely.

$$\Delta h = \left[\frac{4f_m(1-\varepsilon)^{3-n}}{\Phi_s^{3-n}\varepsilon^3} \right]\left(\frac{1}{d_p} \right)\left(\frac{u^2}{2g} \right), \qquad n = f(Re_p), \qquad \Delta h = \frac{\Delta P}{\rho g}$$

This correlation was used earlier as can be seen in the 1974 paper because, at that time, interest was focused mostly on high flows with high Re_p.

The result of an actual pressure–drop versus flow measurement is shown in Figure 1.4.1. A separate flow tube was used and the measurement was made for the flow correlation of a catalyst to be charged to the older 5"–diameter reactor.

For the full range of flow, including the smaller flows and on smaller size catalysts, a more useful correlation for pressure drop is the Ergun

equation, as modified by MacDonald et al (110.) This is in rearranged and integrated form:

$$1.8 \frac{1-\varepsilon}{\varepsilon^3} \rho \left\{ \frac{L}{d_{eq}} \right\} \cdot u^2 \ + \ 180 \frac{(1-\varepsilon)^2}{\varepsilon^3} \frac{\mu}{d_{eq}} \left\{ \frac{L}{d_{eq}} \right\} \cdot u \ = \ \Delta P_{cat}$$

$$\text{or} \quad a \cdot u^2 \quad + \quad b \cdot u \quad = \quad \Delta P_{cat}$$
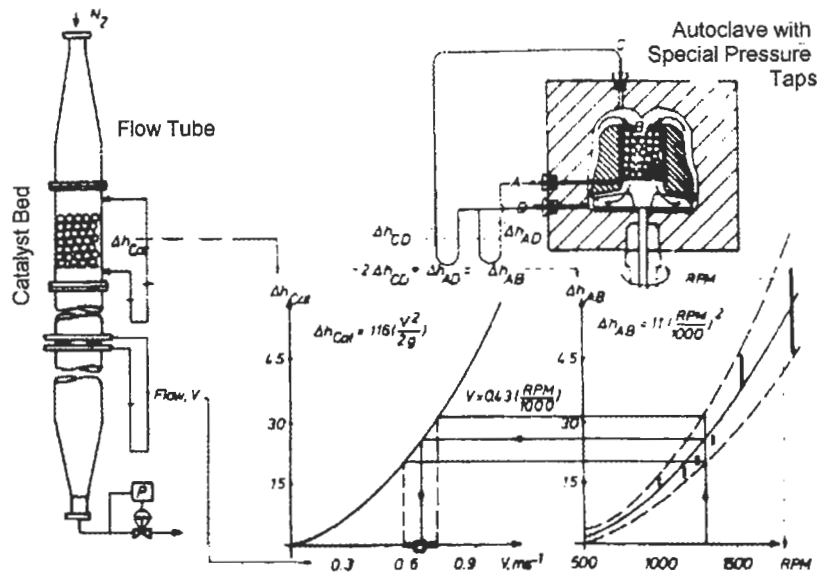
Figure 1.4.1: Pressure drop calibration and pump performance measurement.

The leading dimensionless coefficient of 1.8 pertains to smooth particles. For rough particles, 4.0 is recommended.

In the equation shown above, the first term—including ρ for density and the square of the linear velocity of u—is the inertial term that will dominate at high flows. The second term, including μ for viscosity and the linear velocity, is the viscous term that is important at low velocities or at high viscosities, such as in liquids. Both terms include an expression that depends on void fraction of the bed, and both change rapidly with small changes in ε. Both terms are linearly dependent on a dimensionless bed depth of L/d_p.

Flow distribution in a packed bed received attention after Schwartz and Smith (1953) published their paper on the subject. Their main conclusion was that the velocity profile for gases flowing through a packed bed is not flat, but has a maximum value approximately one pellet diameter from the pipe wall. This maximum velocity can be 100 % higher than the velocity at the center. To even out the velocity profile to less than 20 % deviation, more than 30 particles must fit across the pipe diameter.

In their experimental measurement Schwartz and Smith used circular–shape, hot–wire anemometers at several radii. These had to be placed somewhat above the top (discharge) end of the bed in up–flow operation, to dampen out large variations in velocity in the position of the anemometer. Right over a pellet the velocity was low and between the pellets it was high. These localized differences disappeared and a uniform velocity resulted somewhat above the bed.

Price (1968) made similar measurements, but placed a monolith right over the bed. This eliminated the radial components of the flow velocity after the fluid left the bed. Price also operated at an Re_p an order of magnitude higher than Schwartz and Smith and his conclusion was that the maximum is at a half–pellet diameter distance from the wall. Vortmeyer and Schuster (1983) investigated the problem by variational calculation and found a steep maximum near the wall inside the bed. This was considerably steeper than those measured experimentally above the bed.

All the above results are true and are caused by the increasing void fraction of the bed near the wall, as the previous authors recognized. Pressure drop is a very sensitive function of the void fraction. Because in a

tube the pressure drop across the tube must be uniform, the flow adjusts to the value that gives the corresponding pressure drop.

Several authors, quoting the correct conclusion of Schwartz and Smith, misinterpreted its significance by assuming that an even flow profile is desirable and that the maximum flow must be kept below a limit. This is not so. In industrial tubular reactors where the aspect ratio, (length over diameter) is several hundred, the radial–flow component is very large. In long tubes, this eliminates differences in gas concentration and temperature each length of every 1.5 times the tube diameter. The turbulent radial diffusivity reaches the permanent value in $Pe_r = 8 \sim 10$ above $Re_p > 200$. This means that the actual radial diffusivity is directly proportional to the axial velocity. At the opposite end of large–diameter industrial adiabatic beds, the cross–section for maximum flow is proportional to the perimeter times one particle diameter width, hence to the radius of the bed directly, while the total cross–section is proportional to the square of the radius. Thereby the contribution of the maximum flow to non–uniformity diminishes with increasing size. For laboratory reactors this effect must be checked.

1.5 Heat and Mass Transfer in Catalytic Beds

Flow in empty tubes has a relatively narrow band of velocities—or Reynolds numbers from 2000 to 10000—wherein the character changes from laminar to turbulent. In packed beds, even the laminar flow does not mean that motion is linear or parallel to the surface. Due to the many turns between particles, stable eddies develop and therefore the difference between laminar and turbulent flow is not as pronounced as in empty tubes.

At high velocities where turbulence dominates, the main body of flowing fluid is well mixed in the direction normal to the flow, minor differences in temperature and concentration can be neglected, and the film concept can be applied. This describes the flow as if all gradients for temperature and concentration are in a narrow film along the interface with the solid (Nernst 1904), and inside the film conduction and diffusion are the transfer mechanisms. This film concept greatly simplifies the engineering calculation of heat and mass transfer.

The basic correlation for packed tubes is derived from those of empty tubes by properly reinterpreting some critical variables. The most important change is in the characteristic distance that is changed from the tube diameter to the particle diameter. Other corrections are also used. The transfer correlations are based on dimensional analysis, expressed as either the Nusselt–type (1930) or the Colburn–type (1933) equations. For empty tubes at high Re numbers:

The Nusselt–type:

$$Nu = cRe^a Pr^b \quad \text{or} \quad \frac{h_f d_t}{\mu} = 0.023 \left(\frac{Gd_t}{\mu} \right)^{0.8} \left(\frac{c\mu}{k_f} \right)^{0.33}$$

The Colburn–type:

$$j_h = cRe^d \quad \text{where} \quad j_h \equiv StPr^{0.66} \quad \text{and}$$

$$\left(\frac{h_t}{\rho c u} \right) \left(\frac{c_p \mu}{k_f} \right)^{0.66} = 0.023 \left(\frac{Gd_t}{\mu} \right)^{-0.2}$$

For packed beds Gamson et al (1943) developed Colburn–type correlation for heat and mass from many experimental measurements for $Re_p > 350$ as:

$$j_h = 1.06 \, Re_p^{-0.41} \quad \text{and} \quad j_d = 0.99 \, Re_p^{-0.41}$$

$$\text{where} \quad Re_p \equiv \frac{Gd_p}{\mu} \quad \text{and} \quad Re_p \geq 350$$

Wilke and Hougen developed the same correlations for $Re_p < 350$ as:

$$j_h = 1.95 \, Re_p^{-.051} \quad \text{and} \quad j_d = 1.82 \, Re_p^{-.051}$$

$$\text{where} \quad Re_p \equiv \frac{Gd_p}{\mu} \quad \text{and} \quad Re_p \leq 350$$

From these unique functions of Re_p the numerical value of **j_h** and **j_d** can be calculated. From the definitions of the Colburn factors, the transfer coefficients **h_g** and **k_g** can be evaluated since all other variables are physical properties, independent of flow. For correctness, the physical properties

should be taken at film conditions, but as a first guess properties at bulk conditions will suffice.

$$j_h \equiv St Pr^{0.66}, \quad j_h = \left(\frac{h_t}{\sigma c u}\right)\left(\frac{c_p \mu}{k_f}\right)^{0.66}$$

$$h_t = j_h \, \sigma \, c \, u \left(\frac{c_p \mu}{k_f}\right)^{-0.66}$$

and in a similar way for the mass transfer coefficient:

$$j_d \equiv St' Sc^{0.66} \quad j_d = \left(\frac{k_g}{u}\right)\left(\frac{\mu}{\sigma D_i}\right)^{0.66} \quad k_g = j_d u \left(\frac{\mu}{\sigma D_i}\right)^{-0.66}$$

The Nusselt–type expression was used by Handley and Heggs (1968) to correlate heat transfer coefficients between particulate solids and fluid as:

$$Nu_p = \frac{0.255}{\varepsilon} Re_p^{0.66} \, Pr^{0.33} \quad \text{where} \quad Nu \equiv \frac{h_f d_p}{k_g}$$

$$\text{for} \quad Re_p > 100 \quad \text{and} \quad \frac{d_t}{d_p} > 8$$

These expressions are recommended for calculation of the transfer coefficients between the outside surface of the catalyst and the flowing fluid.

Yagi and Wakao (1959) used mass transfer measurement results to estimate the heat transfer coefficient at the tube wall. Material was coated on the inner surface of the packed tubes and the dissolution rate was measured.

Results were expressed as:

$$\overline{Nu}_f = 0.2 Pr^{1/3} Re_p^{0.8} \quad \text{at} \quad Re_p \, 40 - 2000 \quad \text{and}$$

$$\overline{Nu}_f = 0.6 Pr^{1/3} Re_p^{0.5} \quad \text{at} \quad Re_p \, 1 - 40$$

Kunii and Suzuki (1968) found in similar experiments:

$$Nu_f = CPr^{1/3}Re_p^{0.75} \quad \text{for} \quad Re_p \geq 100, \quad \text{where}$$

$$C = \frac{0.06}{e_w^2} \quad \text{and} \quad e_w \approx 0.5 \quad \text{hence} \quad C \cong 0.24$$

Dixon and Cresswell theoretically predicted (1979) in an elaborate work that:

$$Bi\left(\frac{d_p}{R}\right) = 3Re_p^{0.75}, \quad \text{where} \quad Bi = \frac{h_w R}{k_{r,ef}}$$

since $k_{r,eff}$ is difficult to estimate, a reasonable approximation for the above is:

$$h_w = \frac{c_p \mu}{3d_p} Re_p^{0.75}$$

Other correlations exist and each is good for the particular range where the experimental measurements were made. For searching out other more appropriate correlations, the reader is referred to the copious literature and to the major books on reaction engineering.

Examples for calculated heat transfer coefficients are shown in the table on Figure 1.5.1 The physical and other properties are used from the UCKRON-1 Example for methanol synthesis. These properties are:

$c_p = 2.93$ kJ/kg	$\mu = 1.6*10-5*$kg/m*s
$dp = 7.87$ mm (sphere)	$Pr = 0.7$
$dt = 38.1$ mm	$\varepsilon = 0.4$
$n = 3,000$ tubes	GHSV $= 10,000$/h
$L = 12$ m	$\rho o = 0.438*$kg/m^3 (70% H_2, 30% CO)

From these it follows that:

flow cross–section	$A = 3000*d_t^2*\pi/4$	$A = 3.42*$m^2
reactor volume	$V = A*L$	$V = 41.043*$m^3
feed flow	$F_o = V*$GHSV	$F_o = 4.104*10^5*$m^3/h
mass velocity	$G = F_o*\rho_o /A$	$G = 14.597*$kg/m^{2*}s
Reynolds No.	$Re_p = d_p*G/\mu$	$Re_p = 7.18*10^3$
therm. conductiv.	$k_t = \mu c/Pr$	$k_t = 6.7*10^{-5}*$kW/m*K

Gamson, Thodos and Hougen	$j_h=1.06*Re_p^{-0.41}$ $j_h=0.028$	$h_p =j_h*c_p*G*Pr^{-.066}$ $h_p = 1.51*kW/m^2*K$
Handley and Heggs	$Nu_p=0.648*Re_p^{0.66}*Pr^{0.33}$ $Nu_p = 198.8$	$h_p =Nu_p*k_t/d_p$ $h_p=1.69*kW/m^2*K$
Yagi and Wakao	$Nu_f=0.2*Re_p^{0.8}Pr^{0.33}$ $Nu_f = 216.2$	$h_w =Nu_f* k_t/d_p$ $h_w = 1.84*kW/m^2*K$
Kunii & Suzuki	$Nu_f=0.24*Re_p^{0.75}Pr^{0.33}$ $Nu_f = 166.4$	$h_w=Nu_f* k_t/d_p$ $h_fw = 1.42*kW/m^2*K$
Dixon & Cresswell	$h_w=c_p*m*Re_p^{0.75}/3*d_p$ 37 & 38 of the authors	$h_w = 1.55*kW/m^2*K$

Table compiled by the author.

Figure 1.5.1: Table of calculated heat transfer rates.

As can be seen in the table above, the upper two results for heat transfer coefficients h_p between particle and gas are about 10% apart. The lower three results for wall heat transfer coefficients, h_w in packed beds have a somewhat wider range among themselves. The two groups are not very different if errors internal to the groups are considered. Since the heat transfer area of the particles is many times larger than that at the wall, the critical temperature difference will be at the wall. The significance of this will be shown later in the discussion of thermal sensitivity and stability.

All correlations that are developed from measurements on non–reacting systems are valid for non–reacting systems, but not necessarily for systems where a chemical reaction is progressing. The behavior of a system comprising a catalyst–filled tube and air flowing through is not similar to the behavior of the same tube filled with the same catalyst and having the same air flow, if in the second case the air has some hydrocarbon in it that undergoes an oxidation reaction. Readers are referred to the book of Petersen (1965) for explanations.

It has been known for some time, although its significance is still not fully appreciated, that when exothermic reactions are progressing, the heat transfer can be several times higher than would be predicted from correlations from non–reacting systems. DeLancey and Kovenklioglu (1986) investigated this phenomenon numerically with the film theory on homogeneous reactions. They found that 100% enhancement of heat transfer is possible when reactions are present. In fixed bed reactors

several times higher transfer coefficients (than those calculated from the usual correlations) are mentioned by Petersen (1965), who gives some references.

In the case of exothermic reactions, underestimating the transfer coefficients makes the real gradients less than the estimated ones. As such, this makes our estimates conservative, in the sense that if a criterion calls gradients negligible then they surely are. The intent here is to do most of the kinetic study and catalyst testing at gradientless conditions and this book will make use of the Colburn–type correlations as developed by Hougen (1951) and his associates.

Reynolds (1839 & 1939) postulated first that a relationship exists between momentum and heat transfer. He did not deal with mass transfer. Bird et al (1960) set up criteria for a direct analogy between mass and heat transfer. Gupta and Thodos (1963) investigated this analogy for packed beds and concluded that the Colburn factor ratio of $j_h/j_d = 1.076$ is valid only for shallow beds. At deeper beds, j_d is significantly larger and that deviation increases as rates get higher. An exhaustive review was published by Gomezplata and Regan (1970). This review and the book of Bird et al (1960) serve as general references.

For conditions in industrial production reactors and in corresponding recycle reactors, the mass transfer coefficients of Gamson et al (1943) will be used. These are approximately correct and simple to use. There may be better correlations for specific cases and especially for larger molecules, where diffusivity is low and Schmidt number is high. In such cases literature referring to given conditions should be consulted.

In some special cases where very high mass velocities are used, for high transfer rates, the pressure gradient over the catalyst bed can reach or exceed 1.0 atm/m or 100 kP/m. In such cases a small flow can penetrate the catalyst particles. This is most likely with catalysts or carriers that have very large micropores: up to 0.1 mm. The flow can cut the concentration and temperature gradients way below the estimate based solely on diffusion. Although an insignificant fraction of the total flow moves through the catalyst particle, yet it is a very significant addition to the diffusional flux inside the catalyst.

1.6 Diffusion and Heat Conduction in Catalysts

The work of Thiele (1939) and Zeldovich (1939) called attention to the fact that reaction rates can be influenced by diffusion in the pores of particulate catalysts. For industrial, high–performance catalysts, where reaction rates are high, the pore diffusion limitation can reduce both productivity and selectivity. The latter problem emerges because 80% of the processes for the production of basic intermediates are oxidations and hydrogenations. In these processes the reactive intermediates are the valuable products, but because of their reactivity are subject to secondary degradations. In addition both oxidations and hydrogenation are exothermic processes and inside temperature gradients further complicate secondary processes inside the pores.

Many authors contributed to the field of diffusion and chemical reaction. Crank (1975) dealt with the mathematics of diffusion, as did Frank–Kamenetskii (1961), and Aris (1975). The book of Sherwood and Satterfield (1963) and later Satterfield (1970) discussed the theme in detail. Most of the published papers deal with a single reaction case, but this has limited practical significance. In the 1960s, when the subject was in vogue, hundreds of papers were presented on this subject. A fraction of the presented papers dealt with the selectivity problem as influenced by diffusion. This field was reviewed by Carberry (1976). Mears (1971) developed criteria for important practical cases. Most books on reaction engineering give a good summary of the literature and the important aspects of the interaction of diffusion and reaction.

Ordinary or molecular diffusion in the pores of a catalyst particle may become the rate–limiting step in fast liquid and gaseous reactions. At or below atmospheric pressure, if pore diameters are of the same magnitude as the molecular free path, then Knudsen diffusion may become limiting in gases. In this case, the collisions with the pore wall become more common than the intermolecular collisions. The configurational diffusion regime is reached as pore diameters approach the size of the molecules, much less than the size of the free path. Both Knudsen and configurational diffusion have significance in cracking reactions, mostly on zeolites. Testing for ordinary or molecular diffusion influence is the most important task.

The effectiveness of a porous catalyst η is defined as the actual diffusion–limited reaction rate divided by the reaction rate that could have been achieved if all the internal surface had been at bulk concentration conditions.

$$\eta \equiv r_d/r$$

For the effective diffusivity in pores, $D_e = (\theta/t)D$, the void fraction θ can be measured by a static method to be between 0.2 and 0.7 (Satterfield 1970). The tortuosity factor is more difficult to measure and its value is usually between 3 and 8. Although a preliminary estimate for pore diffusion limitations is always worthwhile, the final check must be made experimentally. Major results of the mathematical treatment involved in pore diffusion limitations with reaction is briefly reviewed next.

For the simplest one–dimensional or flat–plate geometry, a simple statement of the material balance for diffusion and catalytic reactions in the pore at steady–state can be made: that which diffuses in and does not come out has been converted. The depth of the pore for a flat plate is the half width L, for long, cylindrical pellets is $L = d_p/2$ and for spherical particles $L = d_p/3$. The varying coordinate along the pore length is x: $0 < x < L$.

$$D_e \frac{d^2 C_x}{dx^2} = r_d$$

or rearranged for first order reaction:

$$\frac{d^2 C_x}{dx^2} - \frac{k}{D_e} C_x = 0$$

This has the boundary conditions of $C_x = C$ at the surface, and $dC_x/dx = 0$ at the end of the pore. The well–known solution is:

$$C_x = M_1 e^{\frac{x}{L}\phi} + M_2 e^{-\frac{x}{L}\phi}$$

where:

$$\phi = L\sqrt{\frac{k}{D_e}}$$

is the Thiele modulus.

From these equations, the fraction of the bulk concentration inside the pores as a function of the pore depth x can be calculated to be:

$$\frac{C_x}{C} = \frac{\cosh(1-x/L)\phi}{\cosh\phi}$$

This, by evaluation of the average rate in the pores, gives the average concentration inside the pores as a fraction in the bulk at the outside of a particle:

$$\frac{\overline{C}_x}{C} = \frac{\tanh\phi}{\phi} \quad \text{and} \quad \text{when} \quad \phi\to\infty \quad \lim\frac{\tanh\phi}{\phi} = \frac{1}{\phi}$$

The limit is well approached when $\phi = 3$, due to the very steep nature of the hyperbolic tangent.

The diffusion limited rate is: $r_d = \eta\, k_o\, e^{-E/RT}\, C^n$

For first order reactions (n = 1) the rate is directly proportional to the concentration, therefore:

$$\frac{\overline{C}_x}{C} = \frac{r_d}{r} = \eta = \frac{\tanh\phi}{\phi} \quad \text{and when} \quad \phi\to\infty \quad \eta = \frac{1}{\phi}$$

and therefore at large values of ϕ, 3 and above:

$$r_d = (1/\phi)\, k_o\, e^{-E/RT}\, C^n$$

and finally:

$$r_d = \frac{1}{L}\, D_e^{0.5}\, k_o^{0.5}\, e^{-E/2RT}\, C^{\frac{n+1}{2}}$$

This latter equation offers opportunities for experimental tests.

Treatment of thermal conductivity inside the catalyst can be done similarly to that for pore diffusion. The major difference is that while diffusion can occur in the pore volume only, heat can be conducted in both the fluid and solid phases. For strongly exothermic reactions and catalysts with poor heat conductivity, the internal overheating of the catalyst is a possibility. This can result in an effectiveness factor larger than unity.

Temperature increase inside the catalyst pellet can be ignored in many cases. For these cases the treatment seen before can be satisfactory. In

other cases, neglecting heat effects would cause serious errors. In such cases the mathematical treatment requires the simultaneous solution of the diffusion and heat conductivity equations for the catalyst pores.

The governing equations for the combined effect of concentration and temperature gradient are:

$$D_e \frac{d^2 C_x}{dx^2} = r_d(C_x, T_x)$$

$$k_t \frac{d^2 T_x}{dx^2} = (-\Delta H_r) r_d(C_x, T_x)$$

where k_t is the effective thermal conductivity of the particle. The order of magnitude of this is $k_t = 0.4$ watts/(m K).

Prater (1958) has shown that without solving the complete equation the temperature increase can be related to the concentration drop inside the particle as:

$$T_x - T = \frac{D_e(-\Delta H_r^\circ)}{k_t}(C - C_x)$$

maximum when $C_x = 0$. In relative terms to the outside temperature this becomes:

$$\frac{(\Delta T_x)_{max}}{T} = \frac{(-\Delta H_r) D_e C}{k_t T} = \beta_c$$

This result is intuitively correct, since it says that at adiabatic conditions the maximum "fuel" delivered to the inside gives the maximum heat to be removed by heat conduction, and this gives the maximum inside temperature. Yet this is valid only for static or equilibrium conditions.

Tinkler and Metzner (1961) executed a large number of computations for simultaneous equations by approximate and exact methods and presented their results on numerous graphs. One of those is shown in Figure 1.6.1. Please note that on this figure the parameter is $\varepsilon = \gamma \beta D_e / a_t$ in the notation of this book, and the abscissa $\propto$ is the Thiele modulus.
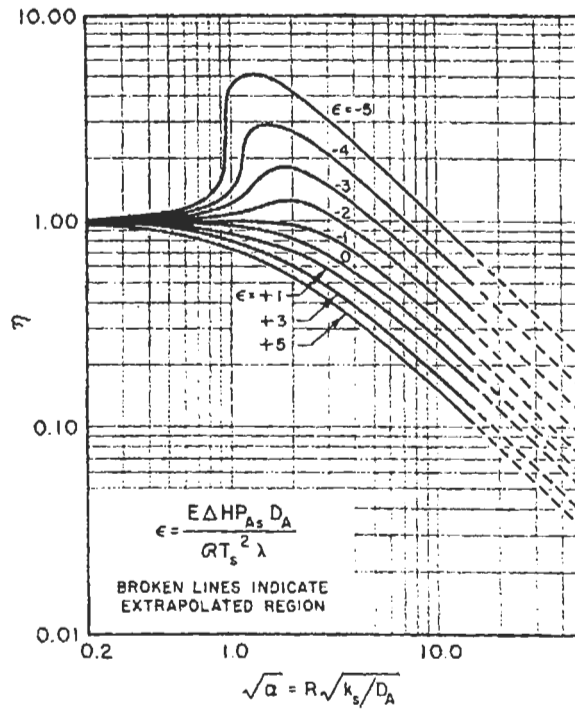
Reprinted with permission from Tinkler and Metzner in Ind. Eng. Chem., Vol. 53, No.8,
© 1961 American Chemical Society.

Figure 1.6.1: Comparison of asymptotic and exact solutions for a first order, non–isothermal reaction in a spherical catalyst pellet.

No industrially significant reaction has $\beta > 0.3$ (or with $\gamma \cong 20$, and D/a $\approx$ 1, $\delta > 5$) and only above this value are the interesting S–shaped curves possible. Of the three values of η, the effectiveness at one value of the Thiele modulus ϕ, the middle one is an artificial, non–existent solution. The two other values for η show the possibility of discontinuity inside the pellet. While this is possible, it is very unlikely to occur.

For additional details of the many possibilities, the reader should refer to the basic books on Reaction Engineering mentioned in the References.

2. Experimental Tools and Techniques

In classical examples of kinetics, such as the hydrolysis of cane sugar by acids in water solution, the reaction takes hours to approach completion. Therefore Whilhelmy (1850) could study it successfully one and a half centuries ago. Gone are those days. What is left to study now are the fast and strongly exothermic or endothermic reactions. These frequently require pressure equipment, some products are toxic, and some conditions are explosive, so the problems to be solved will be more difficult. All of them require better experimental equipment and techniques.

2.1 Batch Reactors

The well–known difficulty with batch reactors is the uncertainty of the initial reaction conditions. The problem is to bring together reactants, catalyst and operating conditions of temperature and pressure so that at zero time everything is as desired. The initial reaction rate is usually the fastest and most error–laden. To overcome this, the traditional method was to calculate the rate for decreasingly smaller conversions and extrapolate it back to zero conversion. The significance of estimating initial rate was that without any products present, rate could be expressed as the function of reactants and temperature only. This then simplified the mathematical analysis of the rate function.

Batch reaction still has some redeeming features, mostly for exploratory research using small amounts of material, so that tests are fast. With some care and skill, and for slow reactions, the kinetics can be followed by taking several samples in a few hours. The change in conversion with time can be observed by simple means like change in total pressure with gas reaction, or consumption or generation of gas volume to maintain constant pressure. It is no surprise that many ingenious ideas were developed to make batch reactors work. A simple batch reactor or "autoclave" is shown first and then an example will be shown: the falling basket reactor of Alcorn and Sullivan (1992) for liquid–gas reactions.
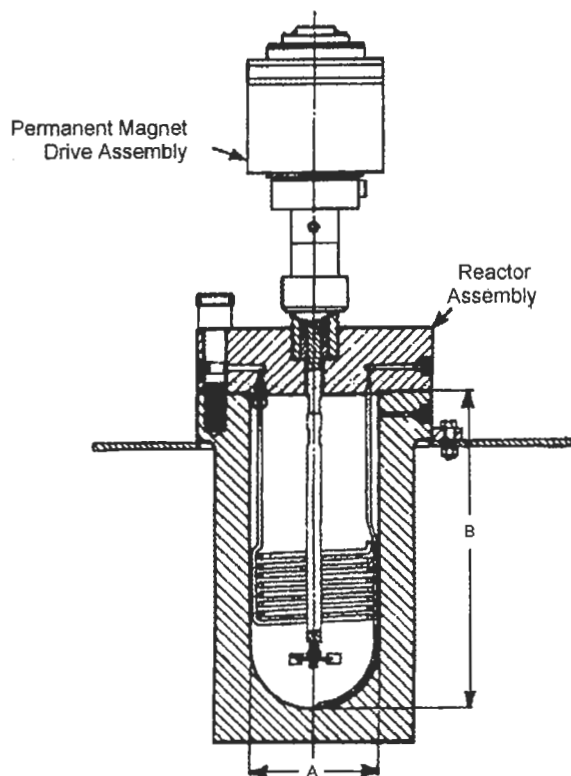
Reproduced courtesy of PPI.

Figure 2.1.1: A typical stirred autoclave reactor.

Stirred autoclave, the most common batch reactor

The most common heterogeneous catalytic reaction is hydrogenation. Most laboratory hydrogenations are done on liquid or solid substrates and usually in solution with a slurried catalyst. Therefore the most common batch reactor is a stirred vessel, usually a stirred autoclave (see Figure 2.1.1 for a typical example). In this system a gaseous compound, like hydrogen, must react at elevated pressure to accelerate the process.

The "Falling Basket" Reactor

Alcorn and Sullivan (1992) faced some specific and difficult problems in connection with coal slurry hydrogenation experiments. Solving these with the falling basket reactor, they also solved the general problem of batch reactors, that is, a good definition of initial conditions. The essence of their

falling basket reactor can be seen on Figure 2.1.2. Their cruciform basket holds the catalyst and is attached to the shaft of an ordinary, top–agitated autoclave. The shaft has a machined groove that keeps the catalyst basket above the liquid level during the initial heat–up and charging period while agitating the liquid. After the system has the solvent and the coal slurry charged and has reached the desired temperature and hydrogen pressure, agitation is stopped and momentarily reversed. This unlocks the basket and sends it down to the liquid phase; the reaction starts with minimal upset.
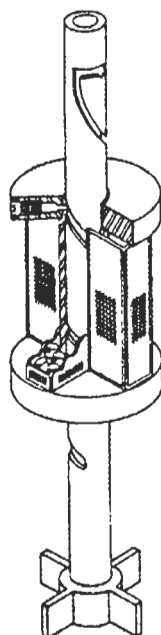
Reproduced from Alcorn and Sullivan 1992, courtesy of Englehard.

Figure 2.1.2: The "falling basket" reactor.

A temperature–time diagram is shown on Figure 2.1.3 on the next page.

2.2 Fixed–Bed Tubular Reactors

Tubular reactors have been the main tools to study continuous flow processes for vapor or gas–phase reactions. These are also used for reaction in two flowing phases over a solid catalyst. When the catalyst is in a fixed bed, the contact between the liquid on the outside surface of the particulate is uncertain. For slurry–type solid catalyst the residence time of the catalyst or the quantity in the reactor volume can be undefined.
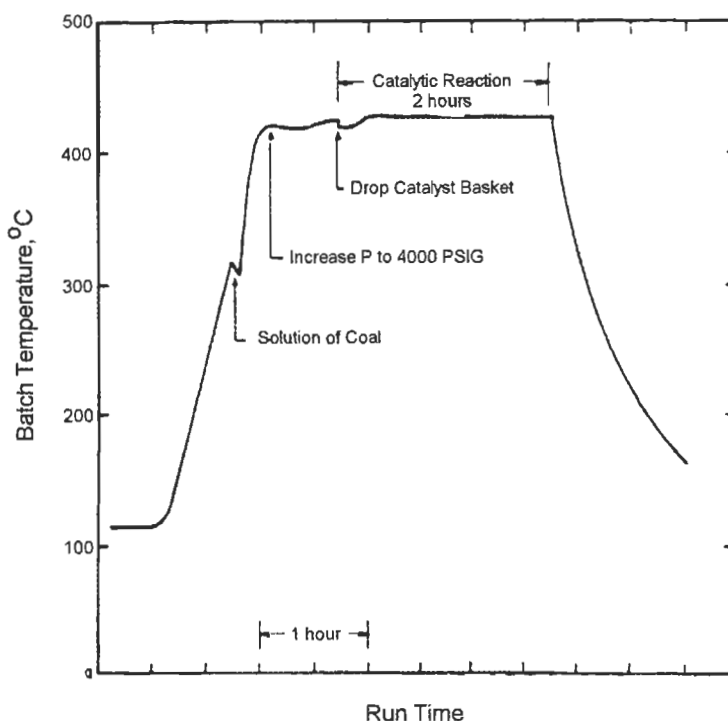
Reproduced from Alcorn & Sullivan 1982, courtesy of Englehard.

Figure 2.1.3: A temperature–time diagram.

Reactor for Microactivity Test

The microactivity test uses small quantities of catalyst, only 4 grams, and a feed of 1.33 g in 75 seconds, so it is a very fast test, but the test's empirical usefulness is strictly limited to one well–known technology, for an endothermic reaction and one very limited type of catalyst.

The ASTM testing procedure states:

"3.1. A sample of cracking catalyst in a fixed bed reactor is contacted with gas oil, an ASTM standard feed. Cracked liquid products are analyzed for unconverted material. Conversion is the difference between weight of feed and unconverted product. 3.2. The standardized conversion is obtained from the measured conversion and the correlation between ASTM reference catalysts and their measured conversions."

16 GA. 304 S.S. Tubing

Syringe Valve-to-Tube Fitting

Preheater

Catalyst

Discharge
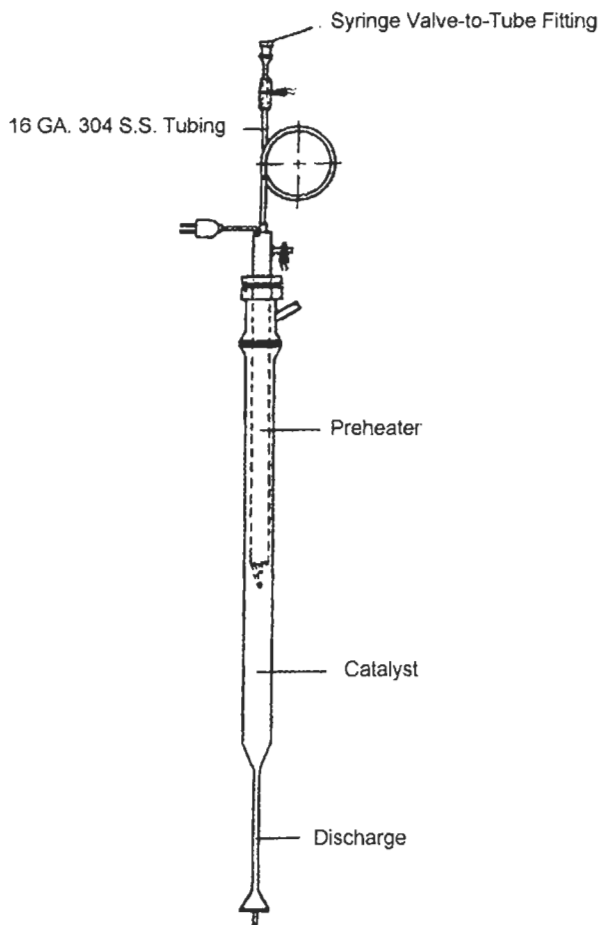
Figure 2.2.1: Reactor used for the microactivity test.

Figure 2.2.1 shows the simplified sketch of the reactor used for the microactivity test. As can be seen, a fluid–bed catalyst is tested in a fixed bed reactor in the laboratory to predict its performance in a commercial fluid bed reactor. This can be done only because enormous empirical experience exists that has accumulated throughout several decades in several hundreds of reactors both in production and in laboratories. The standard states:

"4.1. The microactivity test provides data to assess the relative performance of fluid cracking catalysts."

"4.1. The microactivity test provides data to assess the relative performance of fluid cracking catalysts."

Then the standard emphasizes that all operations such as catalyst pretreatment and analytical techniques must be done as standardized to obtain meaningful relative results.

Microreactors

The reactor built for this purpose is usually a 1/4–in. (~6 mm) tube that holds a few cubic centimeters of catalyst. A micro reactor is shown on Figure 2.2.2 that is typical in research work..
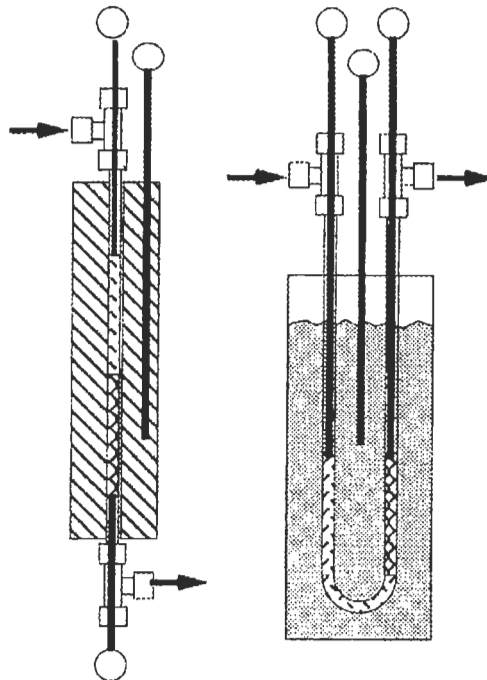
Drawing by the author.

Figure 2.2.2: A micro–reactor used in research work.

The tube is much longer than needed for the catalyst volume to provide a surface for preheating and to minimize temperature losses at the discharge end. The tube can be bent into a U shape and immersed in a fluidized sand bath, or it can be straight and placed inside a tubular furnace in a temperature–equalizing bronze block. Thermocouples are usually inserted

at the ends of the catalyst bed internally, since not much space is available. Outside wall temperature and bath temperature measurements are more commonly used, with the assumption that internal temperatures cannot be very different. This may be a good approximation for slow and not too hot reactions but certainly fails for very hot and fast processes. An exceptionally good reactor was proposed by Davis and Scott (1965). The single pellet string reactor has an I.D. of 1.1–1.4 times the pellet diameter and at high enough flow gives more reliable results than larger tubular reactors. This author used it for ^{14}C tracer studies, where feed was limited.

Good heat transfer on the outside of the reactor tube is essential but not sufficient because the heat transfer is limited at low flow rates at the inside film coefficient in the reacting stream. The same holds between catalyst particles and the streaming fluid, as in the case between the fluid and inside tube wall. This is why these reactors frequently exhibit ignition–extinction phenomena and non–reproducibility of results. Laboratory research workers untrained in the field of reactor thermal stability usually observe that the rate is not a continuous function of the temperature, as the Arrhenius relationship predicts, but that a definite minimum temperature is required to start the reaction. This is not a property of the reaction but a characteristic of the given system consisting of a reaction and a particular reactor.

Pulse Reactors

Tubular reactors can be made very small, connected directly to the feed line of gas chromatographs, and used as pulse reactors. Their usefulness is greatly reduced by transient operation, because the catalyst is never in a steady–state with regard to the flowing fluid components in an adsorption–desorption relationship. Results from pulse tests are very questionable, and the interpretation of these results is difficult. Generally their significance is limited to screening out completely inert or inactive catalysts from active ones, but no quantitative judgment of activity or selectivity can be rendered for commercial use. Some semiquantitative studies can be made in pulse reactors by repeated pulses for the measurement of adsorbed species and adsorbing poisons. The pulse reactor, because of its size and operation, is so far removed from industrial catalytic reactor operation that for practical purposes it is best to avoid its use. It fails so many of the

similarity criteria that it is not worth further elaboration. For an academic point of view, see Choudhary and Doraiswamy's (1971) review.

Various micro reactors serve a useful purpose in exploratory research. Even there, only totally negative results can be accepted, in which no significant reaction occurs at all. If a catalyst makes mostly or only undesirable byproducts, it still may be a good catalyst that cannot be controlled at very low flows and poor transfer conditions. In one case a catalyst that was supposed to oxidize propylene to acrolein in a 1"Ø and 10" long tubular reactor in an electric furnace was rejected as "hot spot type" because it did not produce acrolein at all. It made only a trace of acetic acid and mostly CO. This catalyst in a recycle reactor at high linear velocities gave 3–times more productivity and better selectivity than the previously selected "best" catalyst (Berty 1974.) This result was confirmed in a 30 foot pilot–plant tube—a single tube of the commercial reactor—and later in the production reactor itself. The lab selected the best catalyst for the lab, with its limited capabilities for heat transfer, and not for the commercial reactor where velocities, Re, and transfer conditions were an order of magnitude better.

Tube–in–Furnace Reactors

These were the main tools of catalytic studies in the 1950s. Hougen (1951) describes several successful models. Figure 2.2.3 shows a model, quoted by Hougen from Anderson and Rowe (1983). Most of these reactors have a 25–mm (1") reactor tube which holds 50–100 cm^3 of catalyst. Elaborate care is used in adding bronze block liners to reduce the longitudinal temperature gradient in the wall and by using multizone furnaces for the same reason. Because of their larger size as compared to the previously mentioned microreactors, the bronze liner and multizone heating do not help as much as for smaller microreactors.

Mass velocities are still much smaller than in production reactors, and Reynolds numbers based on particle diameter are frequently much less than 100. Consequently flow is not similar to that in commercial reactors, and heat and mass transfer are much poorer.

These reactors were, and unfortunately still are, used in a few laboratories for process studies on heterogeneous catalysis, frequently with the

disastrous results warned against by Carberry (1964.) The longer versions holding more (up to 500 cm^3) catalyst, especially in long and smaller–diameter tubes, have limited usefulness in the study of high–temperature endothermic reactions such as butane dehydrogenation. For exothermic reactions, very small diameter tubes with a single string of catalyst beads—sometimes even diluted with dummy carriers between every catalyst particle—make this reactor useful but not very advantageous.

Split-type Heating Element

4-5/8"

Bronze Block

Split-type Heating Element

Transite Flue Pipe, 10" I.D.

J.M. 450 Insulation, Packed Dry

Thermocouple

3'-3"
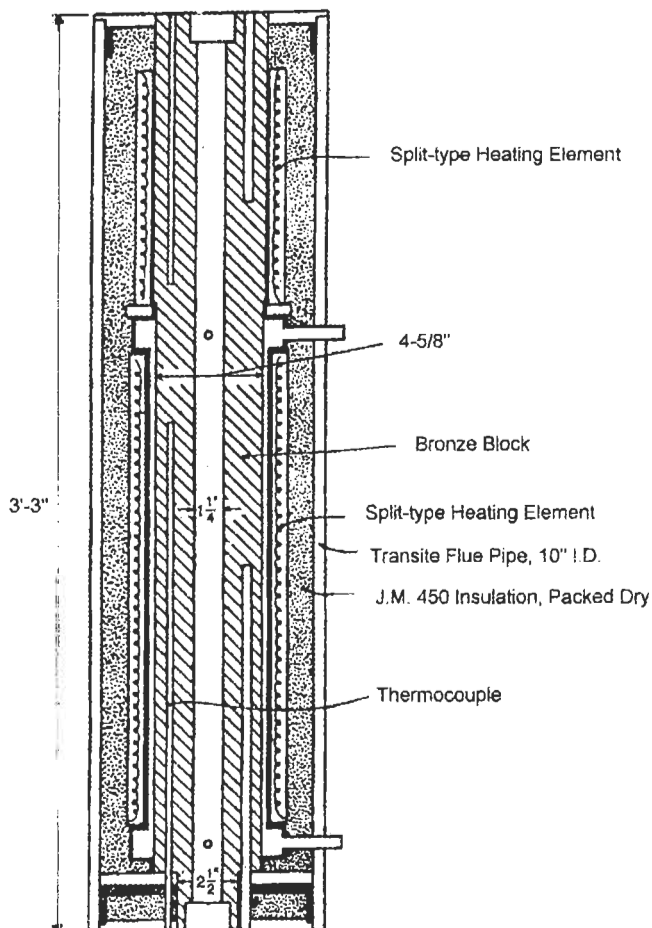
Reprinted with permission, © 1983 American Chemical Society.

Figure 2.2.3: The furnace from a tube–in–furnace reactor.

All the mentioned precautions do not make the operating mode of these tubular reactors close to that of large–scale reactors. The outside observer

may be mislead, because these reactors resemble, at least from the outside, commercial tubular reactors. Yet on the inside where the reaction occurs, conditions are far from that in commercial units.

Thermosiphon Reactors

Figure 2.2.4 (Berty 1983) shows a tubular reactor that has a thermosiphon temperature control system. The reaction is conducted in the vertical stainless steel tube that can have various diameters, 1/2 in. being the preferred size. If used for fixed bed catalytic studies, it can be charged with a single string of catalytic particles just a bit smaller than the tube, e.g., 5/16" particles in a 1/2"O.D. tube. With a smaller catalyst, a tube with an inside diameter of up to three to four particle diameters can be used. With such catalyst charges and a reasonably high Reynolds number—above 500, based on particle diameter—this reactor approximates fairly well the performance of an ideal isothermal plug–flow reactor for all but the most exothermic reactions.
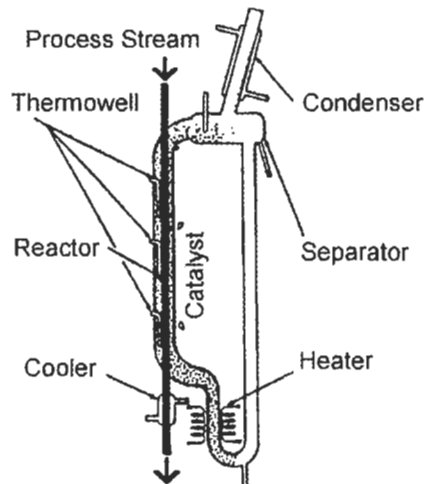
Reprinted with permission, Academic Press.

Figure 2.2.4: Thermosiphon jacketed reactor.

The temperature inside the tube is difficult to measure, and with a single string of catalyst one has to be satisfied with measuring it at the end of the bed. This can be accomplished by using a thermocouple inserted from the bottom. This thermocouple can also serve as the catalyst retainer, or bed

support. The temperature in the jacket can be kept constant by controlling the inert gas pressure at the reflux cooler's top. The downcomer line is filled with liquid, and the reactor jacket has vapor bubbles in the liquid and serves as a riser. The electric heater partially evaporates coolant in the boiler, and more is evaporated by absorbing the exothermic reaction heat in the jacket. The vapor–liquid mixture is lifted by the lower density, compared to the all liquid downcomer. This density difference creates circulation. Since the jacket side heat transfer is in the boiling mode, it is very high and the tube (reaction) side film coefficient is controlling.
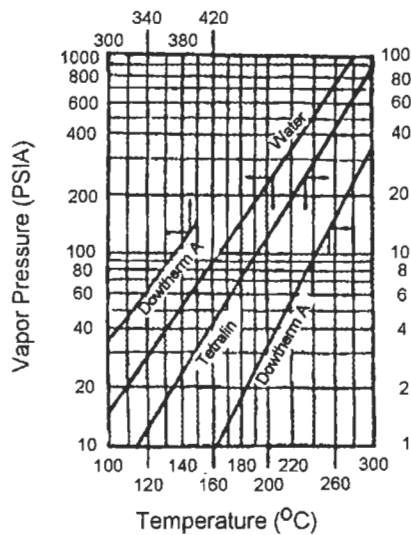
Reprinted with permission, Academic Press.

Figure 2.2.5: Vapor pressure–temperature relationship for coolants.

The thermosiphon circulation rate can be as high as 10 to 15 times the coolant evaporation rate. This, in turn, eliminates any significant temperature difference, and the jacket is maintained under isothermal conditions. In this case, the constant wall temperature assumption is satisfied. During starting of the thermosiphon, the bottom can be 20–30°C hotter, and the start of circulation can be established by observing that the difference between the top and bottom jacket temperature is diminishing. Figure 2.2.5 (Berty 1983) shows the vapor pressure–temperature relationship for three coolants: water, tetralin, and Dowtherm A.

The 1/2–in. O.D. reactor tube has the advantage of a relatively small wall thickness, even at higher pressures, hence permitting better heat transfer. The heating or cooling jacket can also be designed for high pressure. The 400–psig rating satisfies most needs, although higher jacket pressures can also be accommodated.

Interestingly, at high jacket pressures, a single Celsius temperature change can cause more than 1–psi pressure difference. Since pressure is relatively easy to control, excellent temperature control can be achieved in the jacket by maintaining constant pressure over the boiling liquid. Note that with water boiling in a 1000 psig jacket between 110 and 120°C, the pressure increases 18 psig, not quite 2 psi per °C. In the same jacket with water at 240–260°C the pressure increase is more than 200 psig or 10 psig per °C.

Liquid–Cooled Reactors

As the name implies, these reactors are mostly used for the study of exothermic reactions, although they can be applied to endothermic reactions, too. Figure 2.2.6 shows a liquid–jacketed tubular reactor (Berty 1989).
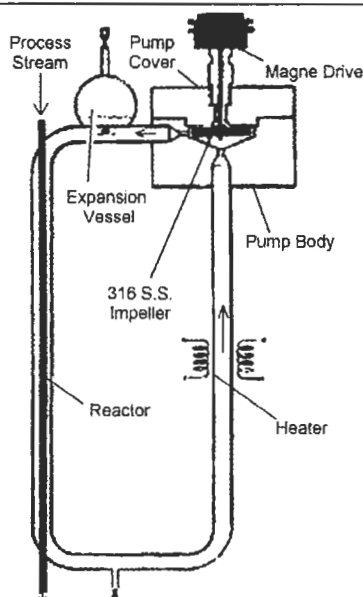
Reprinted with permission, Academic Press.

Figure 2.2.6: A liquid–jacketed tubular reactor.

In this arrangement, in contrast to the previous approach, the coolant is kept from evaporating by maintaining it under an inert gas pressure higher than its vapor pressure. A centrifugal pump is used to achieve high circulation rates. Besides the previously mentioned three coolants (water, tetralin, and Dowtherm A), other nonvolatile heat transfer oils as well as molten salts or molten metals can be used. These coolants are advantageous primarily at higher temperatures where, even if exothermic reactions are conducted in laboratory reactors, the heat losses are usually more than the reaction heat generated. A simple temperature controller, therefore, can be used to keep the electric heater adjusted by sensing with a thermocouple immersed in the return line. At a high recirculation rate of the liquid coolant, the constant wall temperature can again be approximated, but not as well as with boiling–type cooling.

On the other hand, this type of cooling permits the study of increasing or decreasing temperature profiles in the jacket and their influence on the inner temperature profile, reactor performance, and stability. For this type of study a reactor tube is needed that is large enough to accommodate an inner thermowell holding a multiple thermocouple assembly.

Recirculation of non–boiling liquids can be achieved by bubbling inert gas through the liquid in the reactor jacket. This is less practical for fluids with significant vapor pressure, because the jacket still must be under pressure, and a large condenser must be installed to condense the liquid from the vapor–saturated gas at the jacket temperature. It is more useful with molten metals and salts. For the design details of the reactor tube's inside, the same considerations apply as for a thermosiphon–controlled reactor.

Although fluidized sand or alumina can also be used in the jacket of these somewhat larger reactors, the size makes the jacket design a problem in itself, hence these reactors are seldom used. An advantage of the jacketed reactor is that several—usually four—parallel tubes can be placed in the same jacket. These must be operated at the same temperature, but otherwise all four tubes can have different conditions if needed. This type of arrangement saves time and space in long–lasting catalyst life studies. Jacketed tubular reactors come close, but still cannot reproduce industrial conditions as needed for reliable scale–up. Thermosiphon reactors can be used on all but the most exothermic and fast reactions.

Membrane Reactors

In these tubular reactors the reagents are separated by a membrane through which one of the reagents must diffuse. Another version is designed so that the product can diffuse through the membrane and thus avoid secondary degradation. Peña et al, (1998) show an example of ethylene epoxidation over a silver catalyst, where selectivity could be increased from 45% to the 50% level. This is an interesting case illustrating the concept, but of limited interest for an industry where selectivities in the laboratory are already at 76% in recycle reactors (Bhasin et al, 1980) and higher in production units.

2.3   Fluidized–Bed Reactors

As mentioned in Section 2.2 (Fixed–Bed Reactors) and in the Microactivity test example, even fluid–bed catalysts are tested in fixed–bed reactors when working on a small scale. The reason is that the experimental conditions in laboratory fluidized–bed reactors can not even approach that in production units. Even catalyst particle size must be much smaller to get proper fluidization. The reactors of ARCO (Wachtel, et al, 1972) and that of Kraemer and deLasa (1988) are such attempts.

The ARCO Reactor

Figure 2.3.1 (Wachtel, et al, 1972) shows the ARCO reactor that tried to simulate the real reaction conditions in a fluid cracking unit. This was a formal scale–down where many important similarities had to be sacrificed to get a workable unit. This unit was still too large for a laboratory study or test unit, but instead was pilot–plant equipment that could still give useful empirical results Since this serves a very large industry, it may pay off to try it, even if it costs a lot to operate.

The Fluidized Recycle Reactor of Kraemer and deLasa.

Figure 2.3.2 (Kraemer and deLasa 1988) shows this reactor. DeLasa suggested for "Riser Simulator" a Fluidized Recycle reactor that is essentially an upside down Berty reactor. Kraemer and DeLasa (1988) also described a method to simulate the riser of a fluid catalyst cracking unit in this reactor.
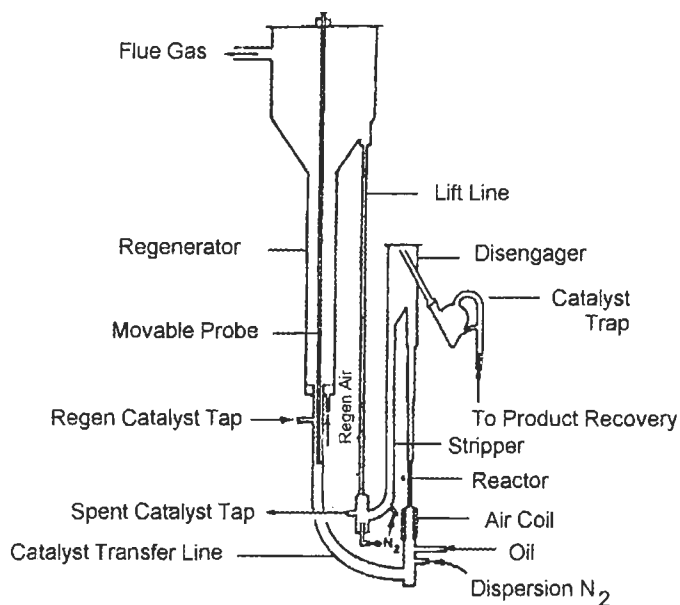
Figure 2.3.1: The ARCO reactor.
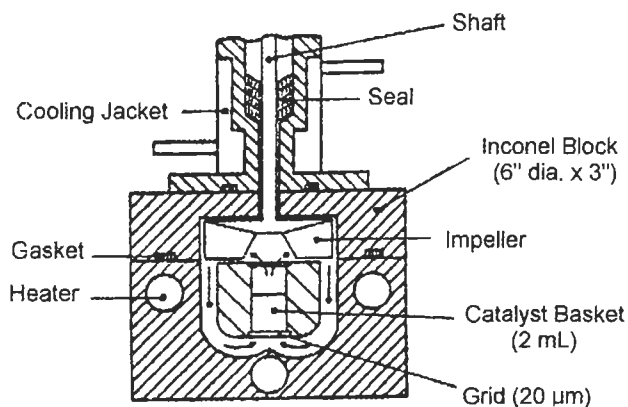
Figure 2.3.2: The fluidized recycle reactor of Kraemer and deLasa.

Actually, the very first homemade recycle reactors in 1965 at Union Carbide Corp. were of this type. In an ordinary one gallon top–agitated

autoclave, the shaft was cut short and an axial–centrifugal blower was installed at the top. An internal "draft tube" was installed in the center axially. In this central draft tube gas flowed upwards over the catalyst, which was charged and secured with a wire screen on the top. The screen on the top prevented the catalyst from fluidization and kept it in fixed bed condition. Gas returned downwards in the annular space between the draft tube and the reactor wall. Union Carbide donated such a reactor to Steven's Institute of Technology for the Department of Chemistry and Chemical Engineering. DeLancey and Kovenklioglu (1986) made their benzene hydrogenation experiments in fixed–bed operation in this top–agitated reactor. DeLasa (199X) recommended a new method of testing fluid–bed catalysts in this fluidized–bed reactor.

2.4 Gradientless Reactors

In gradientless reactors the catalytic rate is measured under highly, even if not completely uniform conditions of temperature and concentration. The reason is that, if achieved, the subsequent mathematical analysis and kinetic interpretation will be simpler to perform and the results can be used more reliably. The many ways of approximating gradientless operating conditions in laboratory reactors will be discussed next.

The Differential Reactor

In a differential reactor the concentration change, i.e., the conversion increase, is kept so low that the effect of the concentration and temperature changes can be neglected. On the other hand the concentration change must be quantitatively known because, multiplied by the flow rate and divided by the catalyst quantity, it measures the reaction rate as:

$$\Delta C / \Delta t = r_{av} = \frac{C_{in} - C}{V/F'}, \quad \lim_{(C.in - C) \to 0} r_{av} = r$$

This rate, measured the previous way, must be correlated with the temperature and concentration as in the following simple power law rate expression:

$$r = Ae^{-\frac{E}{R}\left(\frac{1}{T_2} - \frac{1}{T_1}\right)}[(C_{in} - C)/2]$$

There are two contradictory requirements here. The first is to keep the difference between Ci and C as small as possible so that it can be neglected. The second is to analyze these two only very slightly different concentrations with such precision that the difference will be significantly greater than the measurement error. This second need is for calculation of the rate of reaction, as shown in the first equation of this section.

This is an obviously difficult task, and it is rarely possible to satisfy both requirements reasonably and simultaneously. This difficulty is compounded by the need to use a preconverter to achieve the various conversion levels where the additional incremental increase in conversion can be measured. The alternative way to a preconverter is to feed the reactor various amounts of products in addition to the starting material. This does not ease the analysis difficulties.

In a differential reactor the product stream differs from the feed only very slightly, so the addition of products to the feed stream can be avoided if most of the product stream is recycled. The feed can be made up mostly from the recycle stream with just enough starting materials added to replace that which was converted in the reaction and blown off in the discharge stream. This is the basis of loop or recycle reactors, as will be explained later.

Continuous Stirred Tank Reactors

Jankowski et al (1978) discuss in detail the great variety of gradientless reactors proposed by several authors with a pictorial overview in their paper. All of these reactors can be placed in a few general categories: (1) moving catalyst basket reactors, (2) external recycle reactors, and (3) internal recycle reactors.

(1.) Reactors with a Moving Catalyst Basket

In moving catalyst basket reactors, the flow regime is ill–defined and the contact between catalyst and gas can be poor even if well–mixed conditions for the fluid phase are achieved. Perhaps the most successful representative of this category is the Carberry reactor (1964, 1966). Even in this model only a single layer of catalyst can be charged in the cruciform catalyst basket because the fluid flows in a radial direction outward and

does not penetrate much of the catalyst basket. This reactor is shown on Figure 2.4.1 (Berty 1983.)

(2.) External Recycle Reactors

Centrifugal blowers or turbines usually cannot generate enough pressure difference to overcome the added resistance of the recycle pipes. In addition, some components may condense out in the cooler, especially with high–boiling materials or at high pressures. These must be recycled by a liquid pump through an evaporator. This in turn makes them approach a steady–state slowly.
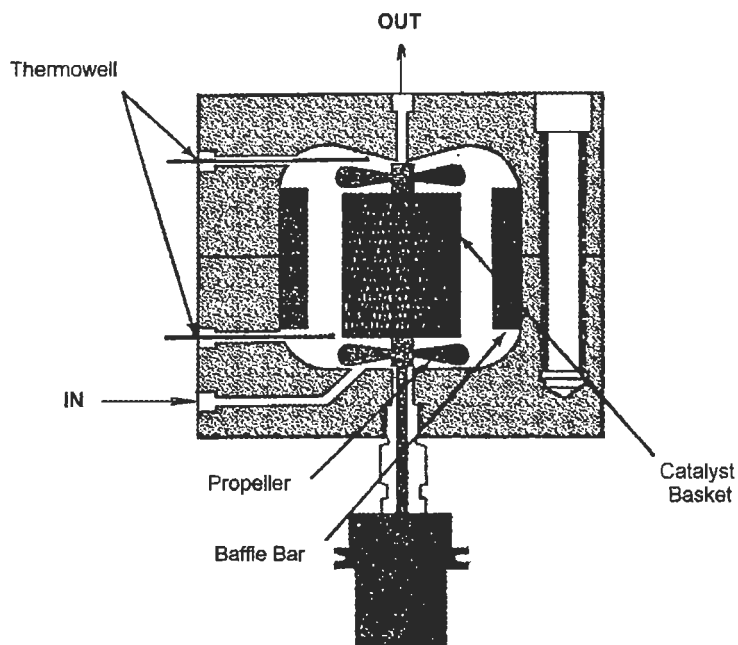
Reproduced courtesy of Autoclave Eng. Inc.

Figure 2.4.1: Carberry's spinning basket reactor.

The major difficulty with these reactors is in the outside recycle pump, especially at high temperatures. Reciprocating pumps require seal rings, and these cannot take the high temperature needed for most reactions. If the recycle gas is cooled down before entering the compressor, it must be reheated before it enters the reactor again. This makes them complicated in construction and excessive in cost.

In summary, external recycle reactors are expensive and their usefulness is limited. They can be practical for simple chemical systems where no condensation can occur and neither high pressure nor high temperature is needed. For example Carberry et al (1980) preferred an external recycle reactor over a spinning basket reactor for the study of CO oxidation in dry air at atmospheric pressure.

(3.) Internal Recycle Reactors

These are the most successful types of reactors presently available. The Internal reciprocating plunger types, for example, that of Nelles in Jankowski et al (1978), do not provide a steady uniform flow. Of those operating with rotating blowers or turbines, the best known are those of Garanin et al (1967), Brown and Bennett (1972), Livbjerg and Villadsen (1971). These and that of Römer and Luft (1974) are shown on Figures 2.4.2 a–d.
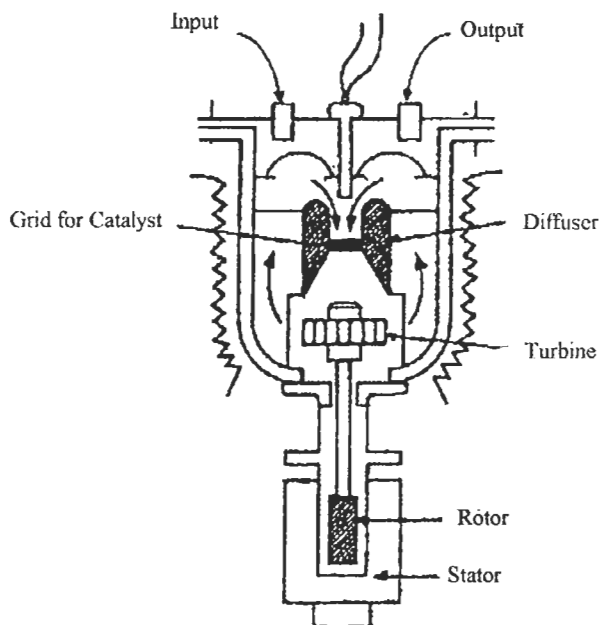
Reproduced courtesy of Plenum Publishing.

Figure 2.4.2 a: The Garanin reactor.
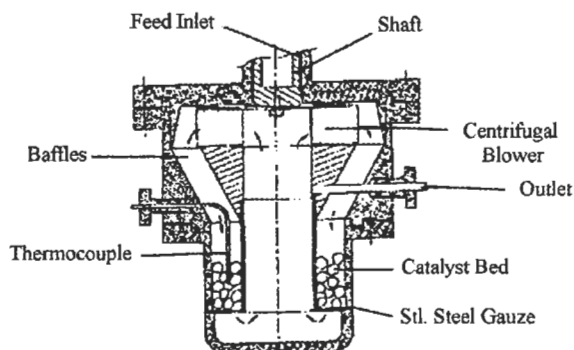
Reproduced with permission from Chem. Eng. Sci., 26, p. 1497, © 1971.

Figure 2.4.2 b: The Livbjerg–Villadsen reactor.
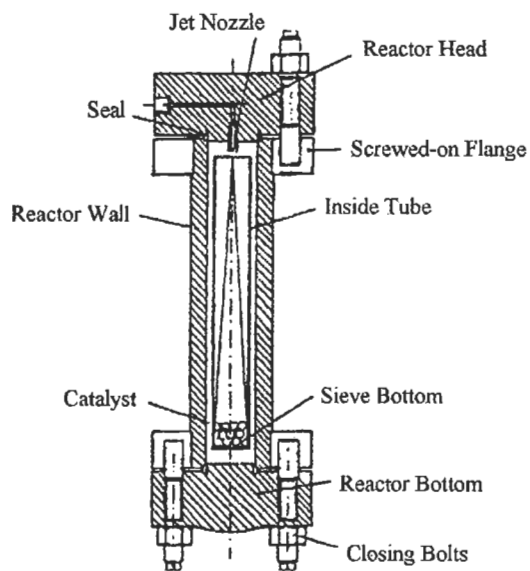
Reproduced with permission from Germ. Chem. Eng, Chem-Ing-Techn., 46, 15, © 1974.

Figure 2.4.2 c: The Römer–Luft reactor.
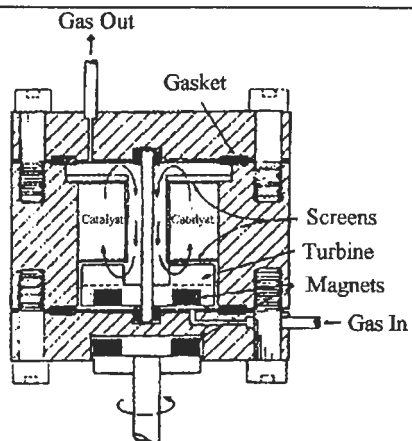
Reproduced with permission from Chem. Eng. Sci., 27, p. 2259, © 1972.

Figure 2.4.2 d: The Bennett reactor.
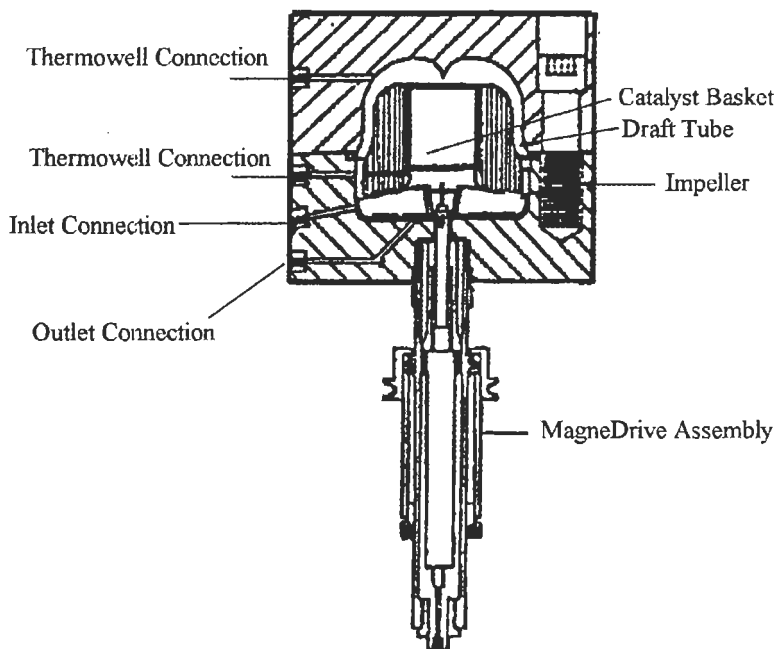
Reproduced with permission from Chem. Eng. Progr., 70, 5, p. 59, © 1974.

Figure 2.4.3 a: The 5–inch Berty reactor.
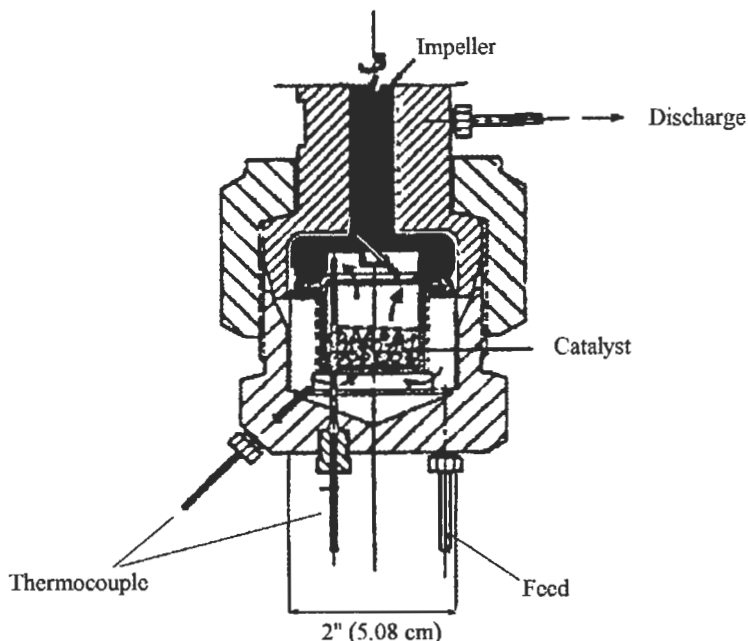
Figure 2.4.3 b: The 2–inch Berty reactor.

The older internal recycle reactors of Berty et al (1969), and Berty (1974) are shown on Figures 2.4.3 a, b. The reactor of Römer and Luft (1974) uses no mechanical moving parts. The recirculation is generated by the feed gas as it expands through a nozzle. A major disadvantage of using a jet is that feed rate and recirculation rate are not independent. Due to the low efficiency of jet pumps, recycle rates are quite low.

These reactors all work on very similar principles and will be discussed based on the example of the Berty[2] reactor, of which more than 500 are in operation around the world. The Berty reactor shown in Figure 2.4.3 a has much empty volume and is laborious to open and close. Another version of the Berty reactor (made by Basic Technology, Inc.) is shown in Figure 2.4.3 b. This 2–inch model was developed for quick exploratory studies on small samples of catalysts. The maximum catalyst sample volume is 15

---

[2] Carberry and Berty reactors were made by Autoclave Engineers, Inc., Erie, Pennsylvania.

mL, and the reactor has a single–thread–operated, quick opening closure. Smaller quantities of catalyst are easier to make in a research laboratory, and the smaller size also makes the use of expensive starting materials or labeled intermediates more efficient. This special model was developed at Design Technology, Inc., and is superceded now by the ROTOBERTY® model (Figure 2.4.4).
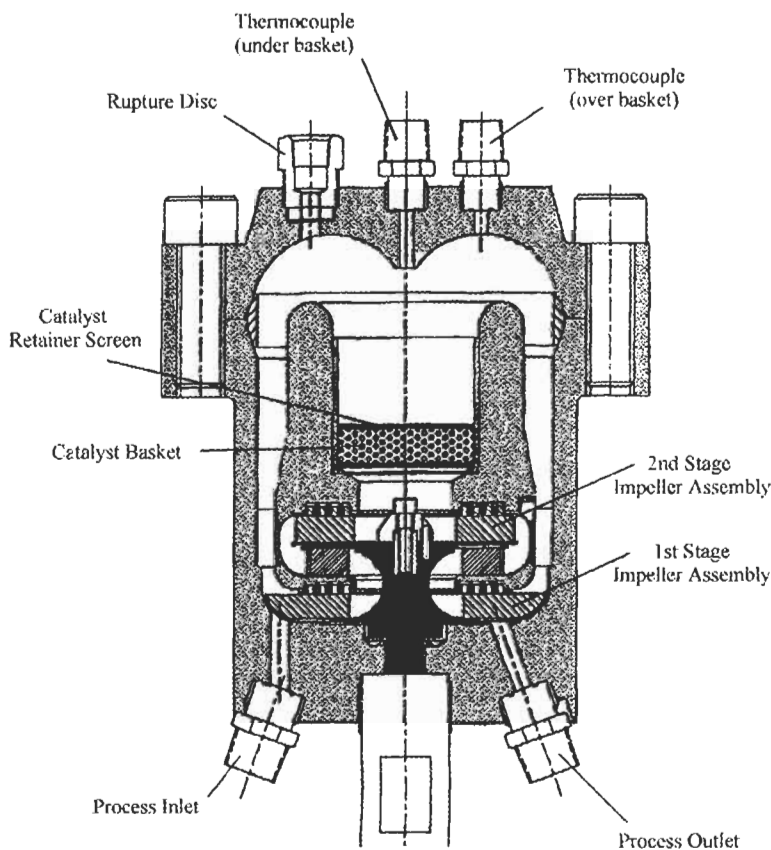
Reproduced courtesy of PPI.

Figure 2.4.4: The ROTOBERTY®.

The operational characteristics of the older Berty reactors are described in Berty (1974), and their use in catalyst testing in Berty (1979). Typical uses for ethylene oxide catalyst testing are described in Bhasin (1980). Internal recycle reactors are easy to run with minimum control or automation.

Complete automation with computer control and on–line data evaluation and reduction is also possible (Dean and Angelo 1971, Gregory and Young 1979, Larmon et al 1981.)

There are many catalytic reactors for various uses and the role of gradientless reactors for industrial use is expanding rapidly. Among these, internal recycle reactors are the most popular. These reactors can solve many problems, but not all. Tubular reactors will retain significance in testing the lifetime of slowly deactivating catalysts. Larger tubular reactors will be used in laboratory and in pilot–plant sizes to test predictions based on gradientless reactors.

3. The Recycle Reactor Concept

Various experimental methods to evaluate the kinetics of flow processes existed even in the last century. They developed gradually with the expansion of the petrochemical industry. In the 1940s, conversion versus residence time measurement in tubular reactors was the basic tool for rate evaluations. In the 1950s, differential reactor experiments became popular. Only in the 1960s did the use of Continuous–flow Stirred Tank Reactors (CSTRs) start to spread for kinetic studies. A large variety of CSTRs was used to study heterogeneous (contact) catalytic reactions. These included spinning basket CSTRs as well as many kinds of fixed bed reactors with external or internal recycle pumps (Jankowski 1978, Berty 1984.)

3.1 *Genealogy of Recycle Reactors*

The relationships among tubular, differential and recycle reactors are shown in Figure 3.1.1. On the left side, the "ideal, isothermal, tubular reactor" is illustrated with "m" segments of equal catalyst volume. After each segment, a sample can be taken out (not shown) for analysis to generate a curve of concentration vs. either tube length or catalyst volume. Differentiation of these curves would give the local rate of reaction at points where the concentrations are also known. Correlation of rates with the corresponding concentrations provides the rate functions. The process of differentiation increases the error of the original data. To avoid this, various curve–smoothing techniques were used. This is why statisticians prefer fitting different integrated rate equations to the original data and selecting the best fitting one.

The differential reactor is the second from the left. To the right, various ways are shown to prepare feed for the differential reactor. These feeding methods finally lead to the recycle reactor concept. A basic misunderstanding about the differential reactor is widespread. This is the belief that a differential reactor is a short reactor fed with various large quantities of feed to generate various small conversions. In reality, such a system is a short integral reactor used to extrapolate to initial rates. This method is similar to that used in batch reactor experiments to estimate

initial rates. The aim is to simplify the interpretation of kinetic laws by elimination of product influences. While this helps at the start, the effect of products eventually must be considered. Investigation of interaction effects of reactants with products at a later stage may make more experiments necessary or leave some effects unexplained.

Feeding of a differential reactor should always include some products, with the possible exception of the very first segment. Using a preconverter is one way of generating the necessary products for the feed. Mixing the products with the reactant in the feed is another method. Finally, consider that in a good, (short) differential reactor, the discharge is almost the same as the feed. Therefore, it is natural to use most of the discharge for the feed. Some venting is needed but only enough to discharge the products made in the last pass, made at the desired product concentration. The differences are made up with fresh feed. Thus the recycle concept is generated. This, with the advantage of replacing the inner balance with the more precise outer balance, then justifies the use of the recycle reactor as will be shown later.

In a recycle reactor, the representation of the performance of the X–th element of a tubular reactor is achieved only for the simplest case of A → B, a reaction where one reactant goes to one product. In cases of more product or more reactant (i.e., selectivity problems exist), feeding only the reactants results in a different composition in a recycle reactor than in the corresponding X–th element of a tubular reactor. This presents no major problem, because simulating the tubular reactor with a recycle reactor is not the goal. Rather, the goal is the study of kinetics, and the behavior of the catalyst, at wide ranges of concentration of all reactants and products. This can be made for several reactions at wide ranges of concentrations in recycle reactors.

Feeding a Differential Reactor

Integral Reactor   Differential Reactor   by A only, using a Preconverter   by Small Feed of A & Recycled Discharge

by Mixing Reactant & Product

$A=Ao$ $B=0$

1
2
3
⋮
x-1
x
⋮
m

$A=A(x-1)$
$B=Ao-A(x-1)$

$A=Ax$
$B=Ao-Ax$

1
2
3
⋮
x-1

$A=A(x-1)$, $B=Ao-A(x-1)$

$A=A(x-1)$
$B=Ao-A(x-1)$ $\Big\}=n+1$

$A=Ax$
$B=Ao-Ax$ $\Big\}=n+1$

$A=\dfrac{Ao-Ax}{n+1}$, $B=0$

$A=Ax/(n+1)$

$B=\dfrac{Ao-Ax}{n+1}$

n

as n $\longrightarrow$ ∞   limit of $[Ax-A(x-1)]/x=dA/dx$
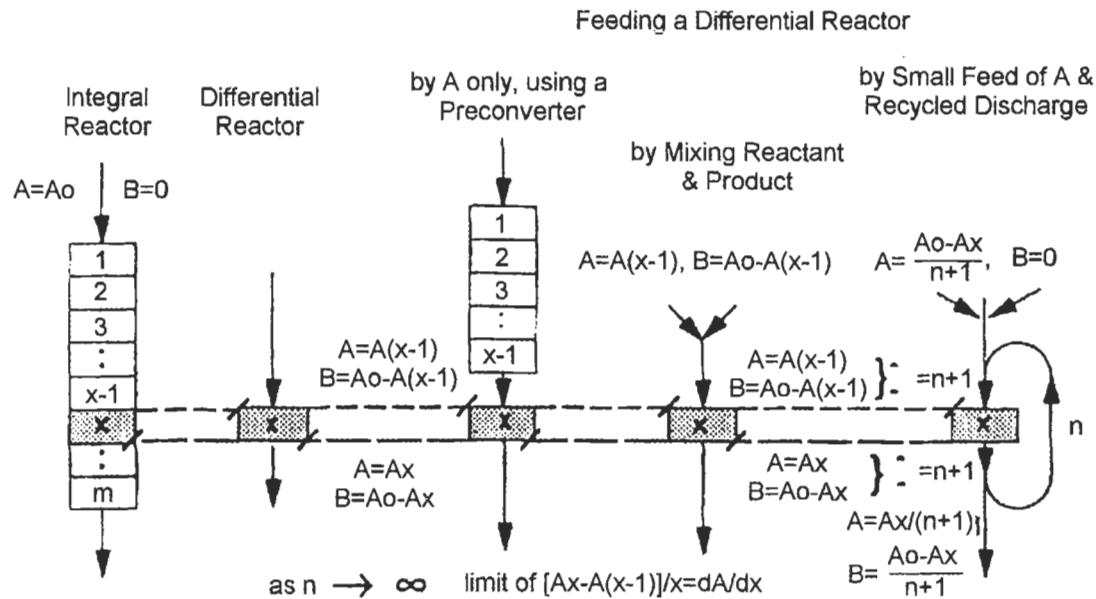
Drawing by the author.

Figure 3.1.1: Genealogy of recycle reactors; Reaction A→B, A and B in mol/sec.

Concentrations:

$$nF'C + F'C_0 = (n+1)F'C_1$$

$$C_1 = \frac{nC + C_0}{n+1}$$

Contact Times:

$$'t'_{perpass} = \frac{W}{(n+1)F'}$$

$$'t'_{overall} = (n+1)\frac{W}{(n+1)F'} = \frac{W}{F'}$$
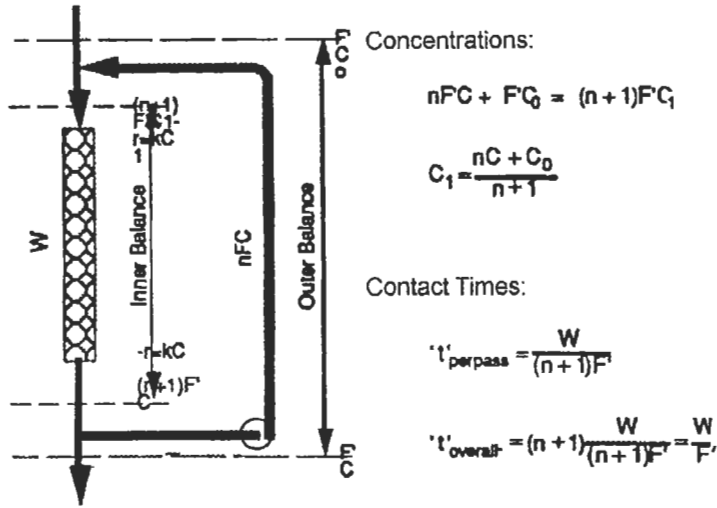
Integrating between the inner limits:

$$-(n+1)F'\frac{dC}{dW} = kC$$

$$-\int_{C_1}^{C}\frac{dC}{C} = \frac{k}{(n+1)F'}\int_0^W dW$$

$$-\ln\frac{C}{C_1} = \frac{kW}{(n+1)F'}$$

$$C = C_1 e^{\frac{-kW}{(n+1)F'}}$$

Adapted with permission from original in Catal. Rev.–Sci. Eng., 20, 1, pp. 75-95, © 1979 Marcel Dekker.

Figure 3.1.2: Tubular reactor with outside recycle.

Another view is given in Figure 3.1.2 (Berty 1979), to understand the inner workings of recycle reactors. Here the recycle reactor is represented as an ideal, isothermal, plug–flow, tubular reactor with external recycle. This view justifies the frequently used name "loop reactor." As is customary for the calculation of performance for tubular reactors, the rate equations are integrated from initial to final conditions within the inner balance limit. This calculation represents an implicit problem since the initial conditions depend on the result because of the recycle stream. Therefore, repeated trial and error calculations are needed for recycle

ratios in the finite range. For the extreme cases of very large, (approximating infinite) recycle ratio, the mathematical limits are shown on Figure 3.1.2 and Figure 3.1.3 (Berty 1979).

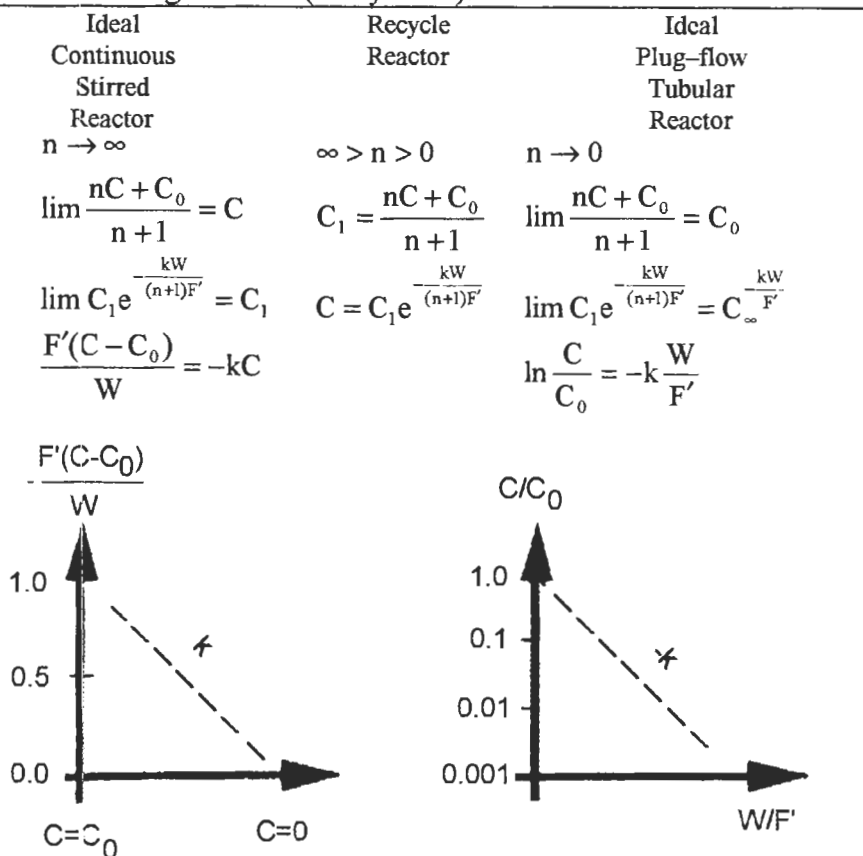| Ideal Continuous Stirred Reactor $n \to \infty$	Recycle Reactor $\infty > n > 0$	Ideal Plug–flow Tubular Reactor $n \to 0$
$\lim \dfrac{nC + C_0}{n+1} = C$	$C_1 = \dfrac{nC + C_0}{n+1}$	$\lim \dfrac{nC + C_0}{n+1} = C_0$
$\lim C_1 e^{-\frac{kW}{(n+1)F'}} = C_1$	$C = C_1 e^{-\frac{kW}{(n+1)F'}}$	$\lim C_1 e^{-\frac{kW}{(n+1)F'}} = C_\infty^{-\frac{kW}{F'}}$
$\dfrac{F'(C - C_0)}{W} = -kC$		$\ln \dfrac{C}{C_0} = -k \dfrac{W}{F'}$

Adapted with permission from original in Catal. Rev.–Sci. Eng., 20, 1, pp. 75-95, © 1979 Marcel Dekker.

Figure 3.1.3: Extreme conditions for recycle ratios.

As can be seen for infinite recycle ratio where $C = C_1$, all reactions will occur at a constant C. The resulting expression is simply the basic material balance statement for a CSTR, divided here by the catalyst quantity of W. On the other side, for no recycle at all, the integrated expression reverts to the usual and well known expression of tubular reactors. The two small graphs at the bottom show that the results should be illustrated for the CSTR case differently than for tubular reactor results. In CSTRs, rates are measured directly and this must be plotted against the driving force of

reactant concentration. For tubular reactors, the unconverted reactant fraction is plotted on a logarithmic scale versus residence time, as usual.

3.2 Overview of Laboratory Gradientless Reactors

Mixing of product and feed (backmixing) in laboratory continuous flow reactors can only be avoided at very high length–to–diameter (aspect) ratios. This was observed by Bodenstein and Wohlgast (1908). Besides noticing this, the authors also derived the mathematical expression for reaction rate for the case of complete mixing.
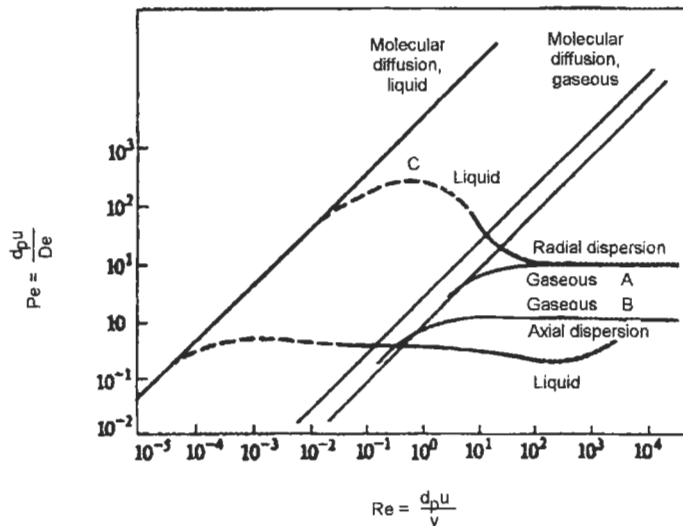
Reproduced with permission from Wilhelm, Pure Appl. Chem., 5, p. 403, © 1962.

Figure 3.2.1: Mixing in packed beds.

In tubes filled with particulate catalyst, it is somewhat easier to avoid mixing. Although every cavity between the particles corresponds to a mixing unit, the effect of these small mixers becomes inconsequential once the tube has a length of 100 to 150 particle diameters. In contrast, radial mixing in the small diameter tubes in cooled converters is very advantageous because it eliminates large radial gradients of concentration and temperature. Because avoiding mixing in catalyst–filled tubes is easier that in empty tubes, achieving complete mixing is more difficult with particulate catalyst present.

Figure 3.2.1 illustrates the mixing in packed beds (Wilhelm 1962). As Reynolds number approaches the industrial range Rep > 100, the Peclet numbers approach a constant value. This means that dispersion is influenced by turbulence and the effect of molecular diffusion is negligible.

Peclet number independent of Reynolds number also means that turbulent diffusion or dispersion is directly proportional to the fluid velocity. In general, reactors that are simple in construction, (tubular reactors and adiabatic reactors) approach their ideal condition much better in commercial size then on laboratory scale. On small scale and corresponding low flows, they are handicapped by significant temperature and concentration gradients that are not even well defined. In contrast, recycle reactors and CSTRs come much closer to their ideal state in laboratory sizes than in large equipment. The energy requirement for recycle reactors grows with the square of the volume. This limits increases in size or applicable recycle ratios.

Many ingenious devices were developed and used to achieve as complete mixing as possible. A good review was published by Jankowski (1978) on gradientless reactors and all laboratory reactors were reviewed by Berty (1983). In addition to differential reactors, various external and internal recycle reactor concepts are shown as well as reactors with fixed bed and axial flow through the beds. In all categories, where flow is generated by reciprocating piston action, the flow is periodic. This does not make the results useless, just very difficult to relate to the smooth, continuous flow conditions in industrial equipment. Where flow is generated by a centrifugal blower, the flow is continuous. Among these, the flow condition is only well defined where the flow is forced through an axial bed. The older model of the author is shown in Jankowski's figure also.

The jet pump is the simplest device to generate recycle flow. This was successfully applied by Römer and Luft (1978). The main disadvantage of the jet pump is that the control of the feed rate is interconnected with the recycle ratio. Therefore, jet pumps lack the great advantage of other recycle reactors, which is that mass velocity can be changed without changing space velocity and vice versa. Jet pumps are very inefficient in utilizing the energy of the jet stream; therefore, only shallow beds can be used and only low recycle ratios maintained. Jet pump driven recycle

reactors can be used for homogeneous reactions because energy is used only for mixing and no energy is dissipated as pressure drop over a catalyst bed. Jet pumps are also useful in production–size units for very fast homogeneous reactions (Johnson et al 1964).

Among the various rotating equipment used for CSTRs was Carberry's (1964) spinning basket reactor. This works well if the cruciform catalyst basket is charged with only one or two layers of catalyst. In particular, the gas penetrates the catalyst charged in the wings very poorly because the main direction of the flow is radially outward. The gas returns from the walls at the ends near the shaft in an axial direction. The wings are really vanes of a centrifugal blower and act as such. Baffles inside of the cylindrical body are helpful by causing turbulence. Yet, the actual contact of the catalyst by the fluid is uncertain and must be different between the leading face and the backside of the vanes. Neither of these are the same as contact among the catalyst particles in the interstitial spaces.

Positive displacement pumps were used by a few investigators. The main feature of reciprocating pumps is that they generate a high pressure difference. This is an advantage in overcoming a pressure drop even when used on a catalyst of fluidized bed size. The pulsating flow causes changing mass velocities and changing transfer coefficients periodically. Piston pumps inside the reactor must tolerate the pressure and temperature of the reaction. Of the two, the temperature is the most difficult problem. Piston pumps on the outside need better seals to provide even higher pressure increase, and must remain above the dew point for gases to avoid condensation. Teflon® and graphite seal rings are available for non–lubricated pumps but only for limited temperature and stroking speed ranges. If cooling, phase separation, heating and evaporation are needed, operation becomes complicated, difficult to control and expensive.

The most reliable recycle reactors are those with a centrifugal pump, a fixed bed of catalyst, and a well–defined and forced flow path through the catalyst bed. Some of those shown on the two bottom rows in Jankowski's papers are of this type. From these, large diameter and/or high speed blowers are needed to generate high pressure increase and only small gaps can be tolerated between catalyst basket and blower, to minimize internal back flow.

In the older model of the author (Berty 1974) the flow versus pressure drop over the catalyst charge was evaluated by outside, auxiliary equipment under conditions similar to those expected for the recycle reactor. The blower in the reactor was calibrated for differential pressure generated versus RPM. The two results together permitted a reasonable estimation of the inside flow during experiments. The main source of error was the measurement of the very low differential pressure that connected both results. In the newer model, flow is calibrated directly over the catalyst already charged to the reactor as a function of the RPM. This gives a very good basis for calculation of flow during experiments and for estimation of all transfer coefficients.

The spread of CSTR use for kinetic studies only started in the 1960s. References can be found even earlier than that of Bodenstein (1908) although most of these references discuss only the use for homogeneous kinetic studies. In view of this background, the story of the development at Union Carbide Corporation may be interesting.

The development of the recycle reactor was done at Union Carbide without publicity, but it was realized that people at other companies might face similar problems. Considering that these problems were being attacked by technical people of similar education and background, the odds were high that others would have the same idea. Therefore, Union Carbide management permitted the publication of the developments (Berty 1969). The corresponding lecture in the 1968 AIChE meeting did not create much enthusiasm and the publication was refused. It was deemed "not of general interest." Five years later, the very same editor was eager to publish a paper on the same subject after an invited lecture was presented at the AIChE Philadelphia meeting, because in–between, the general interest had developed. Due to other pressing problems, there was no time left for any updating, so the former paper, with minor additions, was submitted, accepted, and published. By the 1970s, recycle reactors became commonplace and their number and types proliferated.

3.3 The "ROTOBERTY"® Recycle Reactor

The original recycle reactor developed at Union Carbide Corporation in 1962 (Berty et al 1968) was modified or adapted by several people to different projects. Many recycle reactors were also designed by others for

similar purposes and some of these had little resemblance to the original concept. Yet the name "Berty Reactor" was still applied in general to many of these reactors. In order to clearly distinguish the latest reactor designed by the author, the ROTOBERTY trade name was registered. (Internal details are shown for the ROTOBERTY® in Figure 2.4.4.)

The ROTOBERTY® internal recycle laboratory reactor was designed to produce experimental results that can be used for developing reaction kinetics and to test catalysts. These results are valid at the conditions of large–scale plant operations. Since internal flow rates contacting the catalyst are known, heat and mass transfer rates can be calculated between the catalyst and the recycling fluid. With these known, their influence on catalyst performance can be evaluated in the experiments as well as in production units. Operating conditions, some construction features, and performance characteristics are given next.
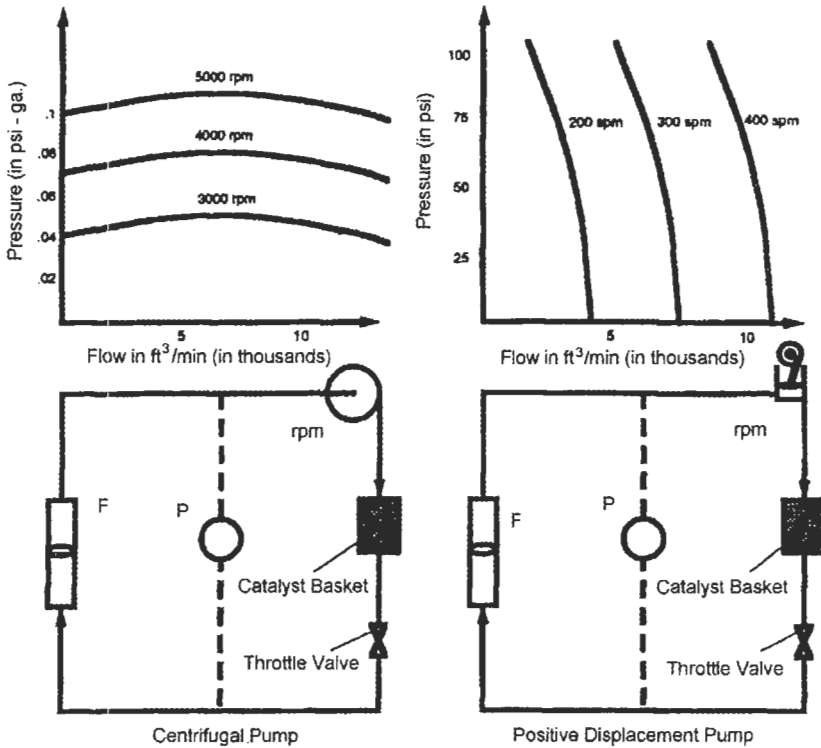
3.4 Pump Performance

Piston, or positive displacement pumps, are well known and much used. Centrifugal pumps are not as well understood. Consequently, piston pump performance is sometimes expected from centrifugal blowers. The main difference is that positive displacement or piston pumps generate flow, whereas centrifugal pumps produce pressure. With a piston pump, the pressure will increase to the level needed to maintain the flow set by the piston volume and stroking speed. In contrast, centrifugal pumps produce pressure; the flow will increase until the pressure drop, produced by the flow, matches the pressure produced by the pump.

The difference can be understood from the fact that the discharge flow from a centrifugal pump can be completely closed—that is, "dead headed"—and the machine will keep running, generating about the same pressure as with flow going through with the discharge valve open. Discharge valves of positive displacement pumps should not be closed while running. With a closed valve, the pump trying to deliver the same volume will generate a pressure high enough to open a pressure relief valve, or else the overload protector of the driving motor will cut off power.

Figure 3.4.1 illustrates the performance of the two different pumps. In the upper half of the Figure, conceptual pump–characteristic curves are given. These show the pressure produced versus the flow pumped at different RPM's. Performance can be generalized more easily if pressure is expressed in column–height of fluid pumped. In SI units, this is expressed in meters and can be converted to pressure in pascals by multiplying the head by density and acceleration of gravity:

$$\Delta p = \Delta h \, (\rho) \, g$$

Drawing by the author.

Figure 3.4.1: Piston and centrifugal pumps.

In the left upper corner of Figure 3.4.1, the centrifugal pump performance is shown. As can be seen, the head generated depends on RPM but is independent of the flow, within a 10 % error, up to a certain limit. The pressure starts to decline when that point is reached at which the flow is high enough that the pump itself limits the flow because of its cross–section.

With piston pumps, as shown on the right side of Figure 3.4.1, flow is independent of the pressure that must be overcome, again to a certain limit. This limit is reached when the unswept dead volume of the cylinder, the compressibility of the fluid, and some leaks become critical. The operation of both types of pumps is shown in two closed loop systems. With the centrifugal blower, as more and/or smaller–grain catalyst is charged or a valve is throttled, the flow will drop (indicated by a rotameter), yet pressure measured by the DP–cell remains constant. Doing the same with the positive displacement pump, the DP–cell will indicate a pressure increase while the flow will remain almost constant. An important consequence of this difference will be given after pressure drop in catalyst beds has been discussed in the next chapter. Other interesting results will be discussed in Chapter 7, Virtual and Real Difficulties with Measurements.
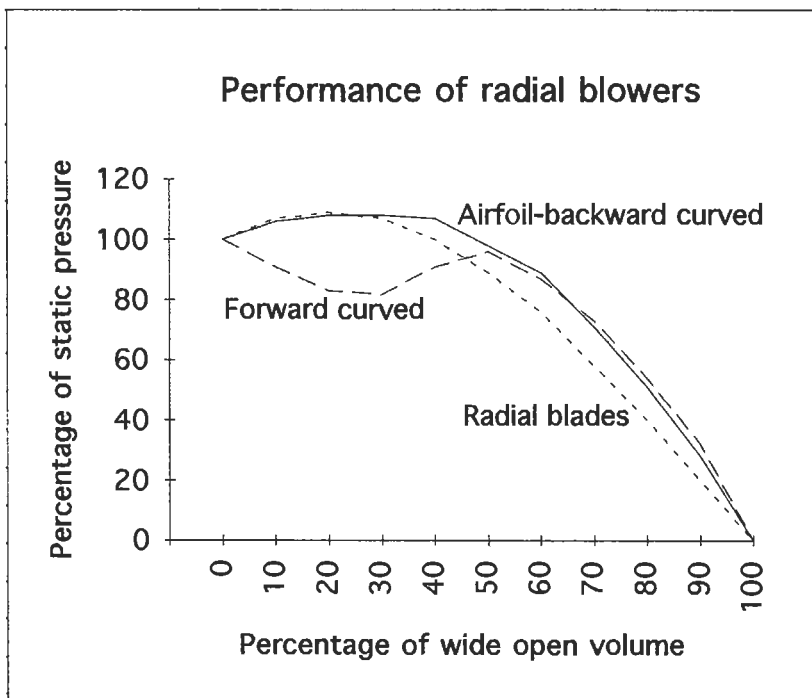
Graph by the author.

Figure 3.4.2: Performance of radial blowers.

Figure 3.4.2 gives a general view of centrifugal fans with different vane orientations. It should be noted that with the exception of the propeller–type fans, the other three radial blowers generate constant pressure within ±10% error limit in the flow range up to 50% of the highest flow. Recycle reactors should always be used within this range not because of efficiency concerns but because the simple and well–defined conditions in this range enable the calculation of flow conditions with good accuracy.

In Chapter 1, Figure 1.4.1 (Berty et al, 1969) shows the actual measurement results of the older 5" diameter recycle reactor performance, using two different types of equipment.

Two more consequences must be recognized about the very low pressure increases of 1 to 200 mm of water column made by the blowers. One is that those pressure surges, common in turbocompressors generating large pressure increases, are absent in these fans; therefore, these can be operated at low flows. The second is that, in calculation of energy consumption and dissipation, the expression for incompressible fluids can be used even for gases.

The following generalization is given by Perry for the performance of fans with a fluid of given density and an increasing RPM (see Figure 3.4.2).
   1)   Capacity varies directly as the speed ratio $F' \propto (RPM)$
   2)   Pressure varies as the square of the speed ratio $P \propto (RPM)^2$
   3)   Horsepower varies as the cube of the speed ratio $w \propto (RPM)^3$

Static head generated by a centrifugal blower depends on RPM alone for a given internal construction and a given set of dimensions. Pressure generated depends not only on RPM, but also on the density of the fluid. Flow depends on conditions outside the blower and so does the power needed. Therefore, blower performance should be characterized first by the head as a function of RPM; thereafter, studies can be extended to describe the flow.

Actual measurement results are shown in Figure 3.4.3 Here a ROTOBERTY® reactor was used with a two–stage blower pumping air at room conditions over three catalyst beds with 5, 10, and 15 cm^3 of catalyst volume. Pressure generated was measured by a water U–tube

manometer. The best fitting quadratic equation is also shown that has the form of:

$$\Delta p \text{ (mm of water)} = 1.18 \text{ (RPM/1000)}^2 = 1.18 \text{ (kRPM)}^2$$

where kRPM means the thousands of revolutions per minute. This can be converted to the "Head" expression by multiplying by the density ratio of water to air. The density of water is 1000 kg/m^3; the density of air is 1.29 kg/m^3. Their ratio is 775; therefore:

$$\Delta h \text{ (mm of fluid pumped)} = 912 \text{ (kRPM)}^2 \text{ or}$$

$$\Delta h \text{ (m of fluid pumped)} = 0.91 \text{ (kRPM)}^2$$
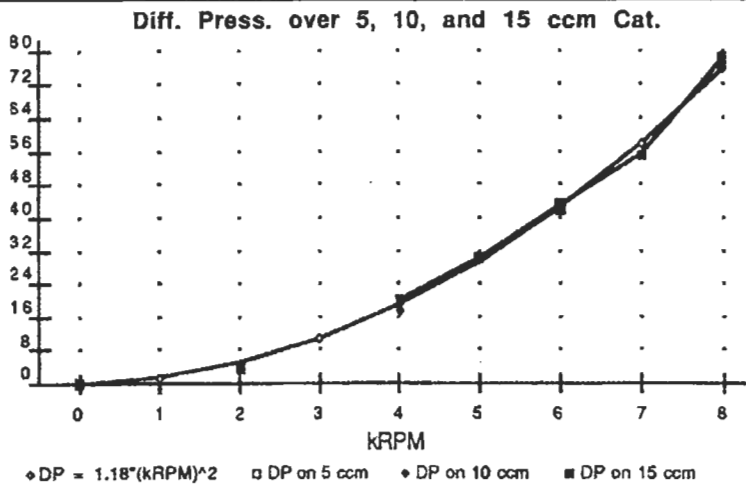
Graph by the author.

Figure 3.4.3: Graph of results; pressure generated vs. RPM.

Figure 3.4.3 shows that the measured results fit the quadratic equation well for pressure generated. It also shows that the pressure generated is independent of flow since three different quantities of catalyst were used. Since the pressure drop remained constant, then flow must have been different over the three quantities of catalysts. The flow adjusted itself to match the constant pressure generated by the blower.

The graph in figure 3.4.4 shows the pressure drop over 5.6 mm Ø glass balls. Generated pressure was not significantly different on these larger balls than it was over the 0.2 mm powder.

In the next chapter, flow over catalyst beds will be discussed and the relationship between blower performance and flow will be developed.
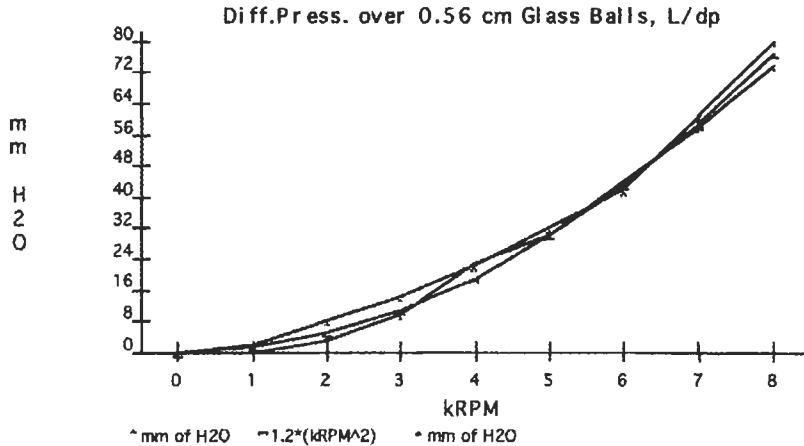
Graph by the author.

Figure 3.4.4: Pressure drop over 5.6 mm Ø glass balls.

## 3.5 Measurement of Flow in Recycle Reactors

A preliminary estimate is useful for the linear velocity to be used on the catalyst under study. The linear flow is known for an existing process. For a new process, it can be estimated from flow used in similar processes. An estimate can also be developed for the minimum flow to avoid gradients from calculations (to be presented in Appendix C.)

The measurement of the linear velocity as a function of shaft RPM can be done at room temperature and pressure in air. It is best to do this on the catalyst already charged for the test. Since **u** is proportional to the square of the head generated, the relationship will hold for any fluid at any MW, T, and P if the **u** is expressed at the operating conditions. The measurement can be done with the flow measuring attachment and flow meter as shown in Figure 3.5.1.

To measure the flow, do this:
1. Charge the catalyst and cover it with a screen on the top of the bed.
2. Start the blower and set it to 1 kRPM (=1000 RPM).

3. Place the measuring tube on the top of the basket holding with one
    hand. Be careful not to block the discharge flow at the open top of the
    reactor.
4. Turn the flow meter to the lower range and insert it in the side hole on
    the measuring tube to take readings. Move and turn the sensor slightly
    to be sure to get the highest reading. Record it.
5. Repeat everything at every thousand RPM, switching the instrument to
    the higher range when needed.
6. After the reading at the highest RPM, repeat the series once more.
7. Average the results and plot flow in m/s vs. kRPM.
8. Remember: diameters of the measuring tube and basket are different.
    Correct the linear velocity in the basket by reading the area differences.
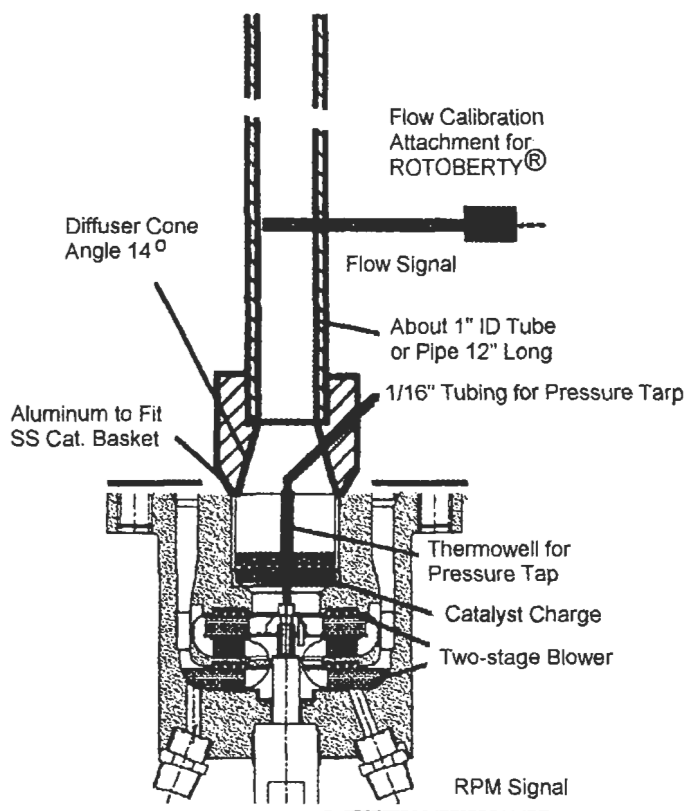

Drawing by the author.

Figure 3.5.1: Flow measuring attachment.

Some results of actual measurements are shown next on Figure 3.5.2 and Figure 3.5.3.

Explanation of Flow Calibration Results

The catalyst bed·that was charged to the reactor is now a restriction, calibrated for flow vs. pressure drop. The pressure drop equals the pressure generated by the blower, which in turn depends on the RPM. In essence, the differential pressure measurement was eliminated by calibrating the flow directly with RPM.
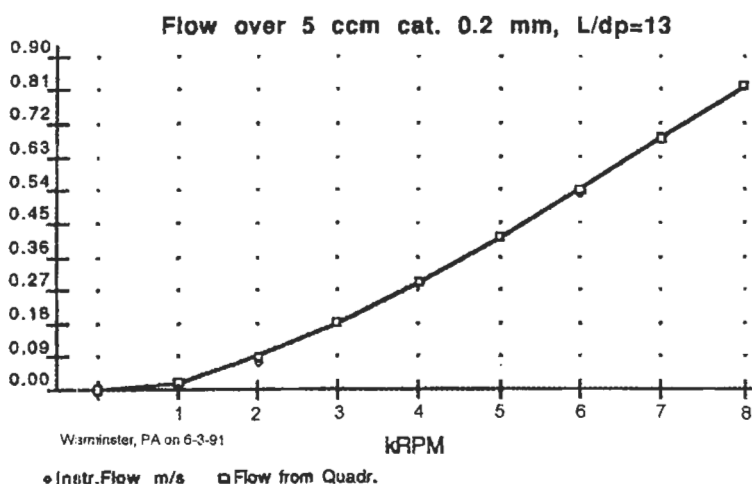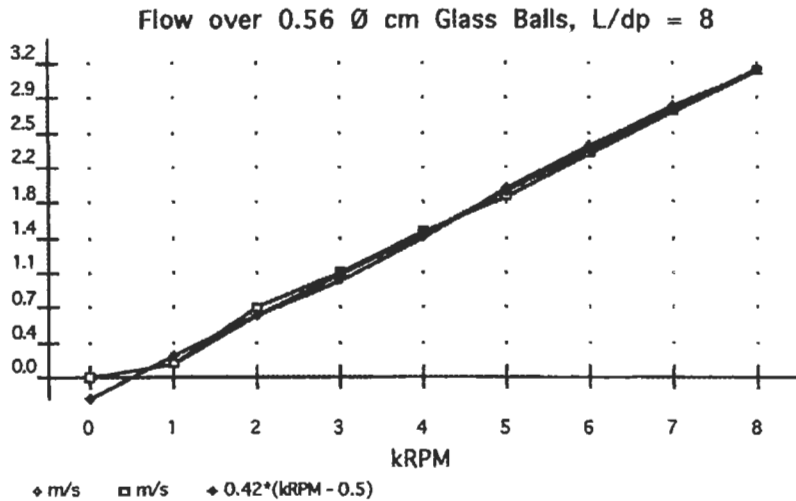

Graph by the author.

Figure 3.5.2: Graph of results (the Y–axis is m/sec.)

The flow that is shown in these figures is the instrument flow measured as m/s in the measuring tube. Multiplied with the flow cross–section of 5.59 cm², this gives the volumetric flow in the 2.67–cm diameter flow tube. Using a different catalyst basket or measuring tube will change this ratio. The volumetric flow is the same in the basket. Because the small basket has a 3.15 cm diameter and 7.79 cm² cross–section, the linear velocity will be 5.59/7.79 = 0.72 fraction of that in the tube.

The blower is calibrated at the factory for pressure generated vs. RPM. This can be checked with a U–tube or slanted tube for measuring the

differential pressure. The U–tube should be attached to the top of a 1/8" tube that was inserted through the catalyst basket before charging the catalyst, and penetrates the bottom screen. However, it will indicate pressure as mm of water column with questionable accuracy. Fortunately, this is not a problem because the blower generates the pressure, and the flow caused by this pressure can be measured directly. This made the measurement of the differential pressure unnecessary.

Graph by the author.

Figure 3.5.3: Graph of results (Y–axis is flow in m/sec.)

Figure 3.4.3 illustrated that the pressure drop is independent of the catalyst quantity charged at any one RPM. This must be so, as will appear later on the modified Ergun equation. Since RPM is constant, so is ΔP on the RHS of the equation. Therefore, on the LHS, if bed depth (L/dp) is increasing, **u** must drop to maintain equality. Results over 5, 10, and 15 cm^3 catalyst, and pumping air, all correlate well with the simple equation:

$$\Delta P = 1.18(kRPM)^2$$

expressed as mm of water. This, in meters of fluid pumped, is

$$\Delta P = 0.92(kRPM)^2$$

Figure 3.5.2 gives the instrument flow vs. kRPM on a very small catalyst particle, 0.2+ mm, which is close to the size used in fluidized beds. The

flow is therefore small but well above the terminal velocity in the fluid bed. The catalyst would be blown away in an up flow arrangement not restricted by screens. Here, it can be tested in fixed bed mode, where the velocity will be higher than the slip velocity is in a fluid bed. Therefore, heat and mass transfer between catalyst and gas will be even better than in a fluid bed. The flow correlates with the RPM as predicted by the Ergun equation. On higher flows, the line straightens out, indicating that now only the square of the velocity vs. the kRPM square term in the Ergun equation is significant.

Figure 3.5.3 shows the measured instrument flow vs. kRPM again on two repeated sets of measurements and one correlation. In Figure 3.5.2, the flow vs. kRPM over the small catalyst shows that the non–linear part of the correlation is important only at flows below 0.18–0.27 m/s. That flow range is on the curve of Figure 3.5.3 below 1 kRPM, which is not an important part in this latter case. Therefore, the very simple correlation of Instrument Flow = 0.59(kRPM–0.5) gives an excellent match above 1 kRPM.
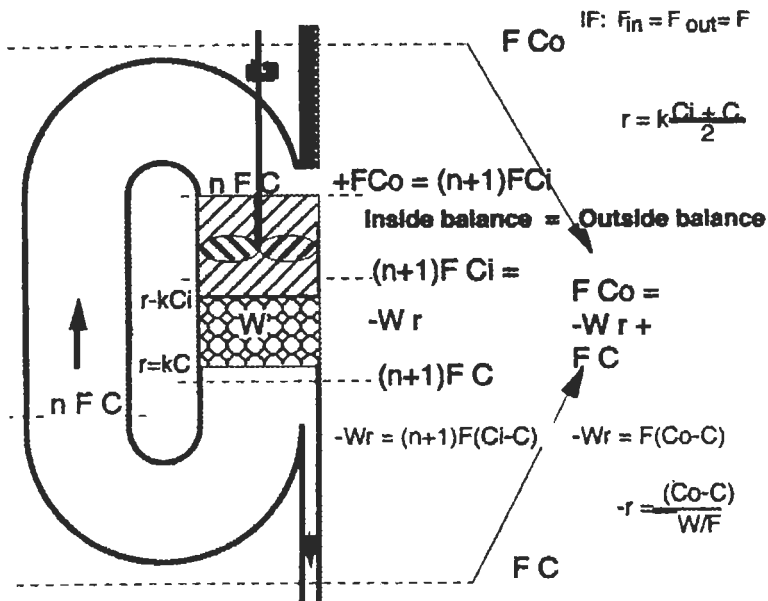
If similar measurements are made on the catalyst to be studied, then there is a good knowledge of the flow. Operating conditions should be calculated with the measured values and evaluated at the temperature and pressure of the experiment. If, in the calculated operating conditions, some important gradients are indicated, then a corrective action should be taken. These may include:
- increase RPM, increase P to maximum permitted by the process
- cut concentration, temperature, catalyst volume
- use larger particles.

If a catalyst is coking up or falling apart in a short time in the recycle reactor then flow will decrease and becomes unknown after a time. In this case is best to improve the life time or the mechanical properties of the catalyst before making tests in the recycle reactor.

3.6 Balance Calculations for Recycle Reactors

The general concept of balances, as explained in detail in Appendix 1, can be applied to a recycle reactor. Figure 3.6.1 shows the possibilities for balance calculations in a recycle reactor.

IF: $F_{in} = F_{out} = F$

F Co

$r = k\dfrac{Ci + C}{2}$

$n F C$ $+FCo = (n+1)FCi$

Inside balance ≈ **Outside balance**

$r-kCi$ $(n+1)F\,Ci =$ $F\,Co =$

$-W\,r$ $-W\,r\,+$

$r=kC$ $(n+1)F\,C$ $F\,C$

$n F C$

$-Wr = (n+1)F(Ci-C)$ $-Wr = F(Co-C)$

$-r = \dfrac{(Co-C)}{W/F}$

F C

Adapted with permission from original in Catal. Rev.–Sci. Eng., 20, 1, pp. 75-95,
©1979 Marcel Dekker.

Figure 3.6.1: Material balance of a recycle reactor.

Figure 3.6.1 (Berty 1979) is a Sankey (1898) diagram, used in power engineering, where the bandwidth is proportional (here qualitatively only) to the flowing masses. This illustrates the calculation results for a rather extreme case of an NO_x reduction problem. The case is extreme because the catalyst particle has a $d_p=0.2mm$, i.e., 200 microns. Flow resistance is very high, therefore an L=1 mm deep bend is used only. Per pass concentration drop is still high, $C_i-C=1.2ppm$, or $Da_I=0.11$. This was tolerated in this case, since it is between 11.2 and 10.00 ppm concentration, and nothing better could have been achieved.

In Figure 3.6.1 the inner balance accounts for differences between just before and just after the catalyst bed. In essence this is a balance for a differential reactor and written for a reactant:

$$(n + 1)\, F' \,(C - C_i) = -W\, r$$

The inner balance accounts for the chemical changes over the W kg catalyst by expressing the difference between the large flow times the small concentration change from in to out over the catalyst bed.

The outer balance gives the overall change between the outside boundaries of the RR system. The chemical change that occurred over the W kg catalyst is now expressed as the difference between the small flow times the large concentration change between in and out of the RR system.

If chemical reactions occur only over the catalyst and none on the walls or in the homogeneous fluid stream in the recycle loop, then conservation laws require that the two balances should be equal.

$$(n + 1) \, F'(C - Ci) \ = \ -W \, r \ = \ F' \, (C - Co)$$

$$r \ = \ (n + 1)(F'/W)(C - Ci) \ = \ (F'/W)(C - C_o)$$

3.7 Calculation of Gradients

Simple criteria are used for insight in transport limitation at catalytic processes. These are based on the Damköhler numbers and criteria presently in use. The basic approach is that the Damköhler numbers, which can be calculated from system properties, are connected to the driving forces. The explanations are made for the simplest cases and for one significant limiting step at a time. These can be extended and combined to more complicated conditions. The emphasis is here to get a clear understanding of the basic meaning of limiting conditions. While concern is expressed for gradients, the quantitative significance of transport processes can be gauged more easily from the magnitude of the driving forces. These will also be given.

For the following calculations it is assumed that experiments are conducted in a good recycle reactor that is close to truly gradientless. Conceptually the same type of experiment could be conducted in a differential reactor but measurement errors make this practically impossible (see later discussion.) The close to gradientless conditions is a reasonable assumption in a good recycle reactor, yet it would be helpful to know just how close the conditions come to the ideal.

Steady–state operation is considered. In this case to satisfy conservation laws it will be assumed that the stream of a component that crosses a boundary inward, and does not come out, has been converted by chemical reaction.

All criteria proposed here are constructed such that if absolutely no gradient of a particular type exists, then the value of the corresponding criterion is zero. For fast catalytic processes this is not reasonable to expect and therefore a value judgment must be made for how much deviation from zero can be ignored. For the dimensionless expressions the Damköhler numbers are used as these are applied to each particular condition. The approach is that the Damköhler numbers can be calculated from known system values, which are related to the unknown driving forces for the transport processes.

Gradients in the direction of the flow.

In a recycle reactor (RR), the conservation statement is that everything produced per pass must be removed, and everything consumed per pass must be supplied by the recycle flow. (See Figure 1.6.1.) The measured rate is "r", whatever causes it to be the given value. Here C is the concentration of the reactant and thus, the stoichiometric coefficient $\alpha=-1$.

The concentration gradient in the direction of the flow is calculated as:
From the inside material balance with $\alpha=-1$, $nF(C-C_i)=-V_r r$ and using

$$\frac{V_r/A}{nF/A} = \frac{L}{u}$$

the concentration difference is:

$$C_i - C = \frac{rL}{u} = Da_I C$$

which, divided by C, gives the ratio:

$$\frac{C_i - C}{C} = \frac{rL}{Cu} \equiv Da_I$$

and the longitudinal gradient is:

$$\frac{C_i - C}{L} = \frac{Da_I C}{L}$$

which can also be expressed as:

$$\frac{C_i - C}{L} = \frac{r}{u}$$

For high rates, high linear velocity is needed to minimize gradients.

The temperature gradient in the direction of flow can be measured directly with Pt–resistance thermometers, but it is difficult and expensive. When this is small, it is better to calculate from the material balance and thermochemical properties.

The inner heat balance is:

$$nF\rho c(T - T_i) = V_r(-\Delta H_r)r$$

where $(-\Delta H_r)r$ is the heat generation rate and the temperature change in direction of the flow is:

$$T - T_i = \frac{V_r(-\Delta H_r)r}{nF\rho c}$$

using :

$$\frac{V_r/A}{nF/A} = \frac{L}{u}$$

then:

$$T - T_i = \frac{rL}{u} \cdot \frac{(-\Delta H_r)}{\rho c_p} = Da_{III}T$$

and dividing this by T:

$$\frac{T - T_i}{T} = Da_I\beta = Da_{III}$$

the gradient can be expressed as:

$$\frac{T - T_i}{L} = \frac{r}{u}\frac{\beta}{C}T$$

The value of the difference $T-T_i$ is more useful than the gradient.

Gradients normal to the flow

For these cases, the conservation statement is made around the outside of the catalyst. In steady–state, everything that is consumed or produced inside the catalyst must go through the outside boundary layer of the fluid surrounding the catalyst. In case of serious selectivity problems with a desired and reactive intermediate, the criterion should be calculated for that component.

The concentration gradient normal to the outside of the catalyst particle. The rate is expressed on catalyst–filled reactor volume, with ε void fraction; for this smaller volume the rate must be higher to keep $V_r r = V_c r_c$. This is calculated from the continuity requirement that was mentioned above:

Reaction rate equals the mass transfer rate:

$$k_g S(C - C_s) = V_r r$$

The concentration difference is:

$$C - C_s = \frac{r\left(V_r \big/ S \right)}{k_g}$$

for spheres $V_c/S = d_p/6$, and $V_r/S = d_p/6(1-e)$, using this and dividing by C gives the Carberry number:

$$\frac{C - C_s}{C} = \frac{r d_p}{6(1 - \varepsilon) C k_g} \equiv Ca$$

the concentration difference is then:

$$C - C_s = Ca * C$$

the average concentration gradient is:

$$\frac{C - Cs}{\delta} = \frac{r d_p}{\delta k_g 6(1 - \varepsilon)}$$

To estimate the average gradient, the concentration difference should be divided by the unknown boundary layer depth δ. While this is unknown, the Carberry number (Ca) gives a direct estimate of what concentration fraction drives the transfer rate. The concentration difference tells the concentration at which the reaction is really running.

Temperature gradient normal to flow. In exothermic reactions, the heat generation rate is $q=(-\Delta H_r)r$. This must be removed to maintain steady–state. For endothermic reactions this much heat must be added. Here the equations deal with exothermic reactions as examples. A criterion can be derived for the temperature difference needed for heat transfer from the catalyst particles to the reacting, flowing fluid. For this, inside heat balance can be measured (Berty 1974) directly, with Pt resistance thermometers. Since this is expensive and complicated, here again the heat generation rate is calculated from the rate of reaction that is derived from the outside material balance, and multiplied by the heat of reaction.

Heat generation rate equals the heat transfer rate:

$$hS(T_c - T) = V_r(-\Delta H_r)r$$

the temperature difference is:

$$T_c - T = \frac{(-\Delta H_r)r(V_r/S)}{h}$$

this divided by the temperature:

$$\frac{T_c - T}{T} = \frac{(-\Delta H_r)r(V_r/S)}{hT} \equiv Da_V$$

using again $V_r/S = d_p/6(1-\varepsilon)$

$$\frac{(-\Delta H_r)rd_p}{6(1-\varepsilon)hT} = Da_V$$

the temperature difference at the catalyst surface and in the boundary layer is:

$$T_c - T = Da_V T$$

and from the outside materials balance:

$$T_C - T = \frac{(-\Delta H_r)rd_p}{6(1-e)}$$

the temperature gradient is:

$$\frac{T_c - T}{\delta} = \frac{(-\Delta H_r)(F/V_r)(C_o - C)d_p}{\delta 6h(1-e)}$$

the film thickness is missing for the gradient estimation, but the temperature difference gives an estimate of the temperature the catalyst is

really working at, and how much ΔT is needed for transfer of the generated heat.

Gradients inside the catalyst particle

For these gradients, continuity requires that everything that reacted inside, had to diffuse through the outside layer of the catalyst.

Concentration gradient inside the catalyst particle. The continuity statement, at the catalyst surface, is similar to Fick's first law for diffusion. The reaction rate is equal to the diffusion rate at the outside layer of the catalyst

$$-SD_e\frac{dC}{dx}\bigg|_{x=\sigma} = V_r r$$

using $(V_r/S)=d_p/6(1-e)$

$$\frac{dC}{dx}\bigg|_{x=\sigma} = \frac{rd_p}{D_e 6(1-\varepsilon)}$$

is the concentration gradient, the driving force for diffusion.

This divided by $C/(d_p/2)$ gives

$$Da_{II} \equiv -\frac{\dfrac{dC}{dx}\bigg|_{x=\sigma}}{C/(d_p/2)} = \frac{rd_p^2}{CD_e 12(1-\varepsilon)}$$

but here, since the measured rate is used that includes the effectiveness factor, it is the Weisz–Prater number (1954) and this gives a relative measure for the driving force for diffusion.

This expressed with the measured rate becomes:

$$Da_{II} = \Phi$$

The r is the "observable rate" calculated from the outside balance. Therefore everything in Da_{II} is measurable but the D_e. If no reliable value exists for this, then from the relationship

$$D_e = (\theta/\tau)D_A \cong 0.1 D_A$$

D_A can serve as an initial guess.

Temperature gradient in the catalyst particle. Continuity in the outermost layer of the catalyst requires that all the heat generated inside has to cross this layer. The continuity statement in the outermost layer is now similar to Fourier's law for thermal conduction.

The heat generation rate in a pellet must equal the thermal flux in the outermost layer of the pellet:

$$-Sk_t \frac{dT}{dx}\bigg|_{x=\sigma} = V_r(-\Delta H_r)r$$

using again $(V_r/S)=d_p/6(1-e)$

$$-\frac{dT}{dx}\bigg|_{x=\sigma} = \frac{(-\Delta H_r)rd_p}{k_t 6(1-\varepsilon)}$$

is the temperature gradient, the driving force for thermal conduction.

This divided by $T/(d_p/2)$ gives Da_{III}

$$\frac{-\dfrac{dT}{dx}\bigg|_{x=\sigma}}{T/(d_p/2)} = \frac{(-\Delta H_r)rd_p^2}{k_t T12(1-\varepsilon)}$$

Here k_t is the thermal conductivity of the system, consisting of the porous solid and the reacting fluid inside the pores. This is the most uncertain value, while everything else is measurable. Two things must be remembered. First, data on thermal conductivity of catalysts are approximate. The solid fraction of the catalyst $(1-\theta)$ always reduces the possibility for diffusion, while the solid can contribute to the thermal conductivity. Second, the outside temperature difference normal to the surface or Da_{IV}, will become too high, much before the inside gradient can cause a problem. See Hutching and Carberry (19), Carberry (20).

Suggested critical values
The exact numerical values of the criteria proposed here have no major significance because the interest is usually in knowing which extreme is close. The desire is mostly to be as close to zero as possible to avoid falsification of chemical rates by transport resistances. In spite of this, some numerical values are proposed in the final table to give some orientation about the magnitudes. These estimates are based on the

experience that it is difficult to measure reaction rates with less than 10% error for fast and exothermic processes. With exceptional care the error can be reduced to 5%. Therefore, errors of this magnitude should not make the results hopeless.

In the direction of the flow:

$$Da_I \quad = \quad \frac{r\,L}{C\,u} \quad = \quad \frac{C_i - C}{C} \quad \leq \quad 0.05$$

$$Da_{III} \quad = \quad \frac{r\,L}{C\,u} \cdot \frac{(-\Delta H_r)C}{\rho\,c_p\,T} \quad = \quad \frac{T - T_i}{T} \quad \leq \quad 0.002$$

Normal to the flow:

$$C_a \quad = \quad \frac{r\,dp}{6\,(1-\varepsilon)\,C\,k_g} \quad = \quad \frac{C - C_s}{C} \quad \leq \quad 0.05$$

$$Da_{IV} \quad = \quad \frac{(-\Delta H_r)\,r\,l}{6\,(1-\varepsilon)\,h\,T} \quad = \quad \frac{T_s - T}{T} \quad \leq \quad 0.002$$

Inside the pellet:

$$\Phi, Da_{II} \quad = \quad \frac{r\,dp^2}{12\,(1-\varepsilon)\,C\,D_e} \quad = \quad \frac{dC/dl}{C/l} \quad \leq \quad 0.05$$

$$Da_{IV} \quad = \quad \frac{(-\Delta H_r)\,r\,dp^2}{12\,(1-\varepsilon)\,k_t\,T} \quad = \quad \frac{dT/dl}{T/l} \quad \leq \quad 0.002$$

4. Experimental Systems and Methods

Any method and system that would be suitable for all possible reactions would be too complicated, difficult to operate, and expensive. Evaluating material balances and kinetic results from a complicated system would be laborious and even questionable in quality. Therefore in the following pages the simple conceptual system will be shown first and the method to operate it will be given. This will be enough to explain the concepts and the reasoning behind it. Then a few systems will be discussed, those that were built to study specific processes. These will include simple systems and more complete units built for on–line computer evaluation and unattended operation. Illustrating a few specific cases should give a good start to build your unit to satisfy the needs of you process studies. Even a well–conceived experimental system needs later modification after some knowledge is gained. This results from the very nature of experimentation, in which one deals with subjects that are not well known.

4.1 Conceptual Flowsheet

An elementary explanation is given below for one of the cherished examples of Chemical Engineering: the first order, monomolecular, irreversible reaction without change in mol numbers:

$$A \rightarrow B, \text{ where the rate is expressed as } r = kf(C)_A,$$
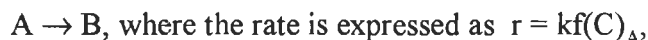
$$\text{and}$$

$$r \equiv - dC_A/d(V/F') = dC_B/d(V/F')^3$$

The material balance for steady–state operation of a perfectly mixed reactor is:

$$F'(C_{Ao} - C_A) = VkC_A$$

Showing this all together on a conceptual flow sheet gives Figure 4.1.1.

To calculate the rate, the values of F', C_{Ao}, and C_A must be measured, since $r = F'(C_{AO} - C_A)/V$. The measurement of all three variables involves

---

[3] For a detailed discussion of rate and its definitions, see Appendix II.

errors. Especially, when conversion is low and the concentration difference $(C_{Ao} - C_A)$ is small, errors can be high. In this simple case the $F'C_B$ should be measured, which has much less error. Assume here that reaction volume V can be measured without significant error.

$$F'C_{Ao} \qquad -VkC_A \ = \qquad F'C_A$$
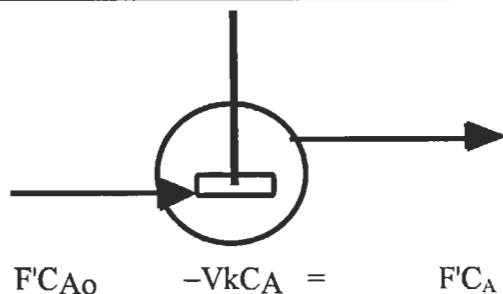
Drawing by the author.

Figure 4.1.1: Conceptual flowsheet.

Now retain this favorite reaction but abandon all assumptions. If one even assumes the solid catalyzed dimerisation reaction of:

$$2A \rightarrow B$$

and suspects that:

$$r = kC_A^n$$

then things get more complicated. The situation appears on Figure 4.1.2:

$$F'_oC_{Ao} \ - VkC_A \ = \ F'C_A , \ \text{in mol/s}$$
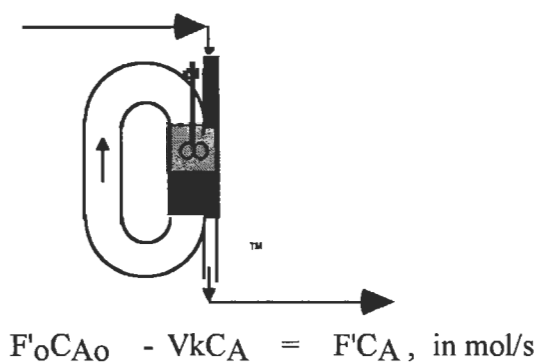
Drawing by the author.

Figure 4.1.2: Dimerization reaction

While everything said before still stands, a few more changes must be considered. According to the chemical reaction shown above, for every

mole of B formed two moles of A disappear, therefore the total volume changes, too. Measuring F' and C_B at the discharge is still the best method, unless F' is difficult to measure for some reason, such as the risk of condensation.

4.2 Test for the Recycle Reactor

Flowsheet for the experimental unit

The following flowsheet represents the simplest connections combined with good, inexpensive manual regulation required to execute valid experiments. This is the recommended minimum starting installation that can be expanded and made more sophisticated as need and budgets permit. The other extreme, a fully computer controlled and evaluated system that can be run without personnel will be shown later. The concepts, mentioned in Chapter 3, are applied here for the practical execution of experiments in recycle reactors.

For a first test of the reactor and all associated service installations it is recommended that experiments for methanol synthesis should be carried out even if this reaction is not especially interesting for the first real project. The reason for this recommendation is that detailed experimental results were published on methanol synthesis (Berty et al, 1982) made on a readily available catalyst. This gives a good basis of comparison for testing a new system. Other reactions that have been studied in detail and for which the performance of a catalyst is well known can also be used for test reactions.

Necessary Supplies

The catalyst should be the copper–based United Catalyst T–2370 in 3/16", reduced and stabilized, in extrudate form. Initially, 26.5 g of this should be charged to the catalyst basket. This catalyst is not for methanol synthesis but for the low temperature shift reaction of converting CO to CO_2 with steam. At the given conditions it will make methanol at commercial production rates. Somewhat smaller quantity of catalyst can also be used with proportionally cut feed rates to save feed gas.

The feed gas should be mixed to the desired composition of 70% H_2, 15% CO, 10% CO_2, and 5 % CH_4 as given in Table 2, of the cited paper. Later,

if the interest remains in studying methanol synthesis in more detail, consider building a feed system.

The flowsheet for the recommended test system appears on the next page in Figure 4.2.1. Parts mentioned in the bill of materials below the flowsheet are examples for successful models. Other good parts can also be used.

Description of the experimental unit

The synthesis gas cylinder should be installed with an instrument–quality forward pressure regulator, since this will control the experimental pressure of the whole unit. The nitrogen cylinder can have an ordinary regulator, because it is used only for flushing the unit.

The feed line runs through a surge check valve (also called a flow limiting valve) to the reactor. This is a safety device that stops flow completely if flow exceeds a certain high value. Excess flow can be caused by failure of a fitting or by breakage in any instrument that would cause sudden release of a large quantity of gas. Flooding of the experimental unit with combustible gas can be dangerous and the surge check valve protects against this event. Another protection against ignition of combustible gas is the pressure switch; in case of a sudden drop in operating pressure to below a given limit, it shuts off electric power for the heater and the motor. Once the surge check valve is closed, and the cause for the action is identified and corrected, it can be opened. For this the bypass valve is needed to equalize the pressure around the surge check valve.

The nitrogen line pressure is set to a level much less than the experimental pressure. With the nitrogen cylinder open, a check valve prevents the feed gas from getting into the nitrogen cylinder. When the surge check valve cuts off the synthesis gas feed, the unit becomes depressurized. Then pressure drops below the nitrogen pressure level, nitrogen flow will start and flush out the system.

The reactor should be connected to a power source for heating and running the motor. Wall thermocouples should give a signal to a temperature controller. Inside thermocouples should be read and the set point changed on the wall temperature controller to get the desired result

inside. The wall and inside temperatures can be a few degrees different and a better control action can be achieved from the wall temperature even if the internal temperature is important. A cascade scheme can also be applied, where the inside gas temperature can change the set point on the wall temperature controller. See Silva (1987).
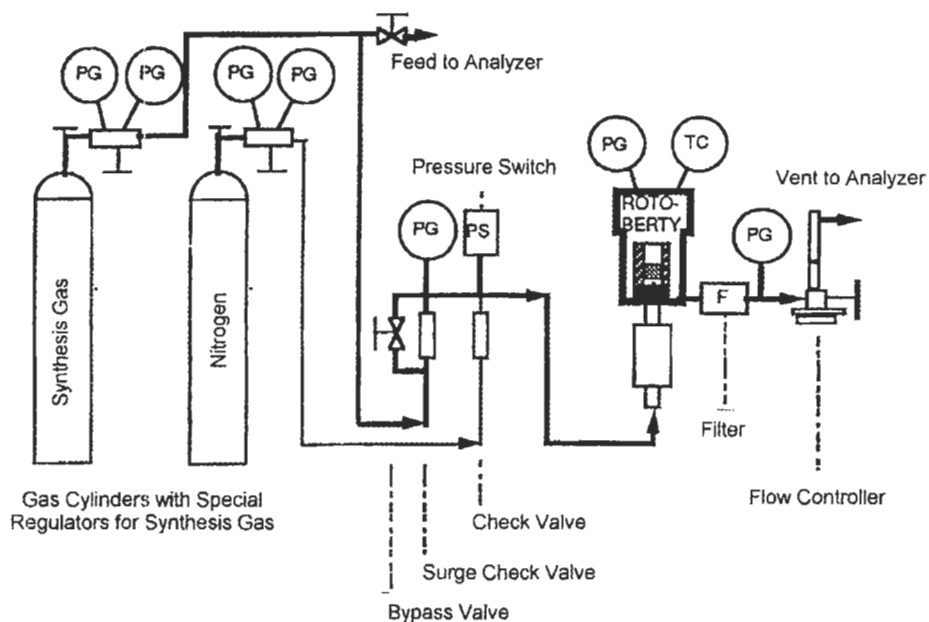
Bill of Materials (Fittings for ¼" Swagelock connections are not listed.)		
Item	**Manufacturer**	**Model**
Recycle Reactor	PPI	ROTOBERTY®
Bypass Valve	NUPRO	SS–B–4JN
Surge Check Valve	PPI	¼" tubing size
Check Valve	NUPRO	SS–4C–VI
Pressure Switch	SOR, Inc.	OMNI*
Filter	NUPRO	S–4TF–40
Integral Flow Controller	BROOKS	8805D**

*Max. pressure 1800 psig
**Max. pressure 1000 psig limiting the total system.
Drawing and table by the author.

Figure 4.2.1: Installation for methanol synthesis experiments.

After the reactor, a filter protects the flow controller from any catalyst dust. Caution must be applied because, if significant catalyst dust collects, results can be ruined even if the filter is at a lower temperature than the reactor. The flow controller also indicates the volumetric flow of the experiment. To operate properly, the flow controller needs a minimum 5 psig pressure at the gauge before the controller. This is important at low pressure experiments.

At high pressure experiments the reactor should be installed in a pressure cell. All check valves before it, and the filter with the flow controller after it, can be kept in the vented operating room. As a minimum, the bypass valve and the flow controller must be accessible to the operator. This can be done by extended valve stems that reach through the protecting wall. Both the operating room and the pressure cell should be well ventilated and equipped by CO alarm instruments.

Planning the experiments

The experimental unit, shown on the previous page, is the simplest assembly that can be used for high–pressure kinetic studies and catalyst testing. The experimental method is measurement of the rate of reaction in a CSTR (Continuous Stirred Tank Reactor) by a steady–state method.

It is assumed that the experiments will be conducted at 70 atm (7.1kPa) pressure or lower. Here the pressure rating of the flow controller limits the maximum pressure for the entire unit. The ROTOBERTY® is rated for higher pressure, and upgrading the rest to higher pressure can be done when needed.

The synthesis gas comes premixed for the desired composition in a high pressure cylinder, e.g., DOT3AA6000 that has 1.5 ft^3 = 42 liter volume. If this cylinder is charged to 380 atm and used down to 80 atm it holds as useful volume (380 - 80)*42 = 12,600 normal liter of synthesis gas. This is 562 g–mol.

The catalyst is a commercial low–temperature Cu–based shift catalyst that makes methanol at high pressure. Of this, V = 20 cm^3, equal W = 26.5 g is charged in form of 3/16"(4.76 mm) regular cylinders.

If using GHSV = 10,000 h^{-1}, the feed is, F = V*GHSV = 20*(10^4) cm^3 or 200 liters/h. Therefore, the 12.600 normal liters in the cylinder will be enough for 60 hours of operation. During these 60 hours, effects of temperature and conversion (by changing space velocity) can be studied at the one, given gas composition in the cylinder.

Internal recycle flow rate created by the blower was 620 times larger than the make–up feed rate in an actual experiment. At this recycle flow, a particulate based Re_p = 3050 was achieved. The corresponding transfer coefficients were very high and gradients were negligible.

More details of operation in an actual study can be seen in: Berty et al, (1982). In this work, a condenser and a liquid–gas separator were used in the product line before the pressure let–down. Keeping the products all in the vapor phase was difficult. Other improvements later included a continuous, four–component, feedgas make–up system with a compressor.

Experimental operation of the unit

1. After catalyst charging and the flow vs. RPM measurement is done, the reactor should be closed and flushed out with nitrogen while the impeller runs, until O_2 drops below a few tenths of a percent. Then a static pressure and leak test should be made by turning off the forward pressure controller and the flow controller. If an observable drop of pressure occurs within 15 minutes, all joints and connections should be checked for leaks and fixed before progressing any further.

2. With all leaks stopped, and the reactor under test pressure with nitrogen, set the nitrogen pressure regulator to the lowest pressure on the controller, but above 0.3 atmosphere or 5 psig. Now open the flow controller and set the N_2 flow to 66 mL/s, equivalent to 10.5 mols/hr rate, to start the flow. Also start heating the unit.

3. Open the feed gas cylinder and regulate it to the proper pressure, 52.0 atm, (5.27 MPa, or 764 psig) for this recommended test experiment. The flow will start and the feed gas will gradually replace the nitrogen in the unit. While the unit is heating and the nitrogen is being replaced, the analysis of the feed can start. After the experimental temperature is reached and becomes stable, the analysis of the discharge gas can start

too. Analyze the discharge repeatedly until it does not seem to change anymore. After this the measurement period can start.

4. For the experiment proper, take samples from the feed and discharge alternately and repeatedly. If no change is observed, then the system has reached a steady–state (SS). Take a few more pairs of samples, (called cycles), analyze them and calculate rates for methanol and water production as well as material balances. Averaging a few of the samples and calculating standard deviation for concentration and rates will give some insight how steady the operation is. Another method would be the calculation of a student's t–test comparing the averages of a first few results with a few following results. This could distinguish between random changes and drifting results (Box et al, 1978).

5. After enough results are collected from steady–state measurements, the experiment can be terminated or conditions switched to the next experiment. If the unit is to be shut down, turn off the heating and leave the impeller running. Turn off the feed gas cylinder and after the pressure drops below the level of the nitrogen cylinder, nitrogen flow will start flushing out the system. After combustible gases are below 1 % total by analysis, turn off the nitrogen.

To open the reactor for inspecting or changing the catalyst, extreme caution must be used. A used catalyst is completely reduced and has some methanol and other combustibles adsorbed on the surface. The used catalyst can heat up when exposed to air and even ignite. A catalyst overheated this way is not useful for further studies and a burned–down laboratory is not useful at all.

The proper method to remove the catalyst involves stabilization. The method for this is usually recommended by the catalyst manufacturer. With the reactor still closed, cold and flushed with nitrogen, admit nitrogen with less than 1 % oxygen in it, while the impeller is running. This oxidizes the organics and the metallic surface of the catalyst under well–controlled conditions after which the catalyst can be exposed to air without danger of overheating.

All equipment should be used according to manufacturer's specifications and in compliance with all applicable regulations.

Please notice that in a well–ventilated laboratory and a pressure cell, these experiments can be executed safely. In seven years of graduate research activity at the Chemical Engineering Department of the University of Akron, only one catalyst ignition and one real CO alarm occurred. Several false CO alarms were sounded until someone noticed that they always happened about 2:30 PM. As it turned out, one maintenance employee parked his old car right in front of the air intake to the lab ventilation. He warmed up his car for a while before he started to go home after his shift, and the motor exhaust gas set off the false alarms.

4.3 An Experimental Unit for Reacting Liquid and Gaseous Feeds in the Vapor Phase, or in a Two–Phase System

Only parts needed above but for the vapor–phase reactor are listed here.
Most of the description for the installation for methanol synthesis experiments (Figure 4.2.1) holds for this installation, too. In the mentioned unit, product was blown down while still hot, thus keeping all product in a single vapor phase. This simplifies material balance calculations. When avoiding condensation is difficult, cooling and separation becomes necessary. This method was used in the cited AIChEJ publication.

When liquid content of the feed is high, a condenser and a separator are needed. The liquid–to–gas ratio can be as high, so that even at reaction temperatures a liquid phase is present. The reactor still performs as a CSTR, however the response time for changes will be much longer than for vapor phase alone. Much lower RPM will be needed for liquid–phase studies (or liquid and gas phase experiments) since the density of the pumped fluid is an order–of–magnitude greater than for vapor phase alone. In this case a foamy mixture or a liquid saturated with gas is recirculated.

The illustrated unit can be used to study vapor–phase reforming of kerosene fractions to high octane gasoline, or hydrogenation of benzene, neat or in gasoline mixtures to cyclohexane and methylcyclopentane. In liquid phase experiments hydrotreating of distillate fractions can be studied. The so–called "Solvent Methanol Process" was studied in the liquid phase, where the liquid feed was a solvent only, a white oil fraction,

while methanol was made of the CO, CO$_2$ and H$_2$ content of the feed gas. (Krishnan, et al, 1991.)
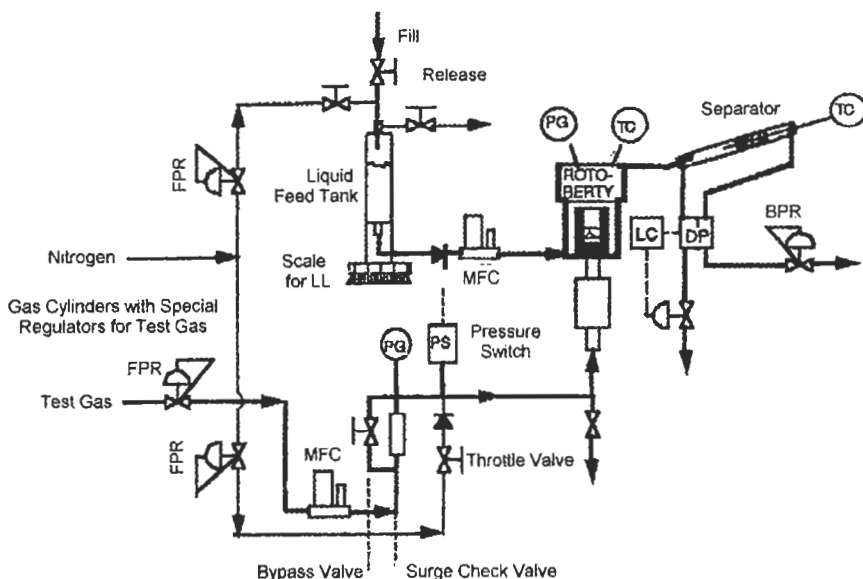
Item	Model	Manufacturer
Liquid feed tank	4HDM300 (300 ccm)	HOKE Inc.
Liquid mass flow controller	LCA–42–2–C–1	Porter Instr.
Separator	Made of Swagelok fittings	Swagelok Inc.
Differential pressure cell	P305D	Valedyne Corp.
Level control valve	same as flow meter	Porter Instr.
Electronic scale	Brainweigh B3000D	OHAUS Scale

Figure 4.3.1: Experimental unit for reacting in the vapor phase, or a two–phase system, and the major parts required.

At the time of the solvent methanol experiments a metering pump was used. In some experiments the pulsating action of the pump can be disturbing, so a high–pressure syringe–type pump can be used. Since mass flow controllers are available now, the combination of a gas–pressurized feed tank on an electronic scale for liquid level indication and a mass flow controller seems to be a good choice. Both the feed tank and separator can be heated or cooled. In the case of the solvent methanol experiments,

electrical heating tapes allowed the separator to be kept at the same temperature as the reactor. This way during the kinetic study, vapor–liquid equilibrium measurements were also accomplished.

The Valedyne Differential pressure cell is a miniature aerospace product. Its membrane can be damaged easily by accidental overloading, yet it is easy to exchange. DP cells used in the process industry are not suited for experiments in grams/ hour flows. These are large, usually larger than the reactor, so these would introduce large hold–up volumes and delay times. Because of the very small flows, these can be fed through the DP cell. This practice is, of course, not recommended in plant operations.

The Back Pressure Regulator (BPR) shown at the end can be a gas dome–loaded Grove Inc. regulator or a spring–loaded Tescom model. The same holds for the forward pressure regulators. Instead of regulators, controllers can be used too, especially since small electronic control valves are now available.

The bill of materials under the picture includes only the important parts that are needed in addition to those already listed on the vapor phase methanol flow sheet in Figure 4.2.1

Operating with a liquid phase present in the recycle reactor requires special care at start–up and shut–down. It is good to avoid letting liquid in the shaft cavity, because it may damage bearings and makes cleaning out after the run difficult. Therefore, always start up the empty reactor with a N_2 flow and blower running at 1000 RPM. Then start the liquid flow and the synthesis gas flow. The discharge gas flow will start slowly and it will take several hours to reach a steady–state.

After a run is finished and the reactor will be shut down, first terminate the liquid feed and the heating of the reactor. After the reactor cools down, which can be accelerated by blowing compressed air through the cooling coils embedded in the bronze heating mantle, depressurize by changing the BPR to lower and lower settings. At low enough pressure the N_2 flow will start and the syngas can be shut down Drain the liquid from the reactor by a valve at the bottom (not shown). During this time a gas flow through the shaft should be maintained and the impeller should be running.

When no more liquid drains from the reactor and the system is depressurized, open the top of the reactor, while the shaft is still running and the N_2 is still flowing. This condition will be a surrogate way of stabilizing the catalyst if no 1% O_2 containing N_2 has been installed for this purpose; no such feed is shown on Figure 4.3.1. After some time, for example 30 minutes, if no heating of the catalyst occurs, N_2 flow can be turned off. Now check the drain valve at the bottom of the shaft drain off any liquid that has entered the shaft cavity. The catalyst can be removed and the open reactor covered with a plastic sheet to protect the sealing faces from dust.

No safety devices are shown on the flowsheet and installation of those is the responsibility of the operator of the unit.

4.4   Installation for Ethylene Oxidation Experiments

The unit shown on the next page in figure 4.4.1 is a somewhat simplified version of a tested, actual unit. The six gaseous feed components enter through check valves at a pressure regulated to about 4 atm higher pressure then experimental pressure, e.g., 22 atm. Six mass flow controllers set the flows and all but the nitrogen lines are secured with power to open solenoid valves (SV).

In case of high temperature, pressure, oxygen concentration, or at low RPM or power failure, all solenoids close and the system is purged with nitrogen. When the SV for the O_2 line is open, it lets the oxygen flow through, and when it closes the O_2 feed line, it also opens the third branch in–between, while a check valve closes the feed manifold. This is for safety, to prevent any mixing between O_2 and any other gases that may leak through this valve. Ethane is added to control the dechlorination of the catalyst. Methane, which is inert in this system, is the carrier gas for ethyl chloride and is saturated at ice–water temperature. From the known vapor pressure of ethylchoride, the total pressure of the saturator and the flow rate of the ethylchloride saturated methane the concentration of ethylchloride in the feed can be calculated (Berty et al, 1989).

The total feed flow is set for a higher level than it is needed for the experiment. The excess feed is released by a back pressure regulator (BPR at the bottom of the picture), e.g., at 21 atm and is led to the analyzer. The

total feed is controlled by a seventh mass flow controller. Conceptually, the total feed FC could be exchanged with the BPR after the reactor, but the gas has to be hot upon release to prevent condensation, and FCs are not available for high temperatures. However BPRs can take somewhat higher temperatures than FCs. The best method to measure the volumetric flow would be at the discharge (as explained in figure 4.1.2) and that can be done using more complicated and much more expensive controllers.
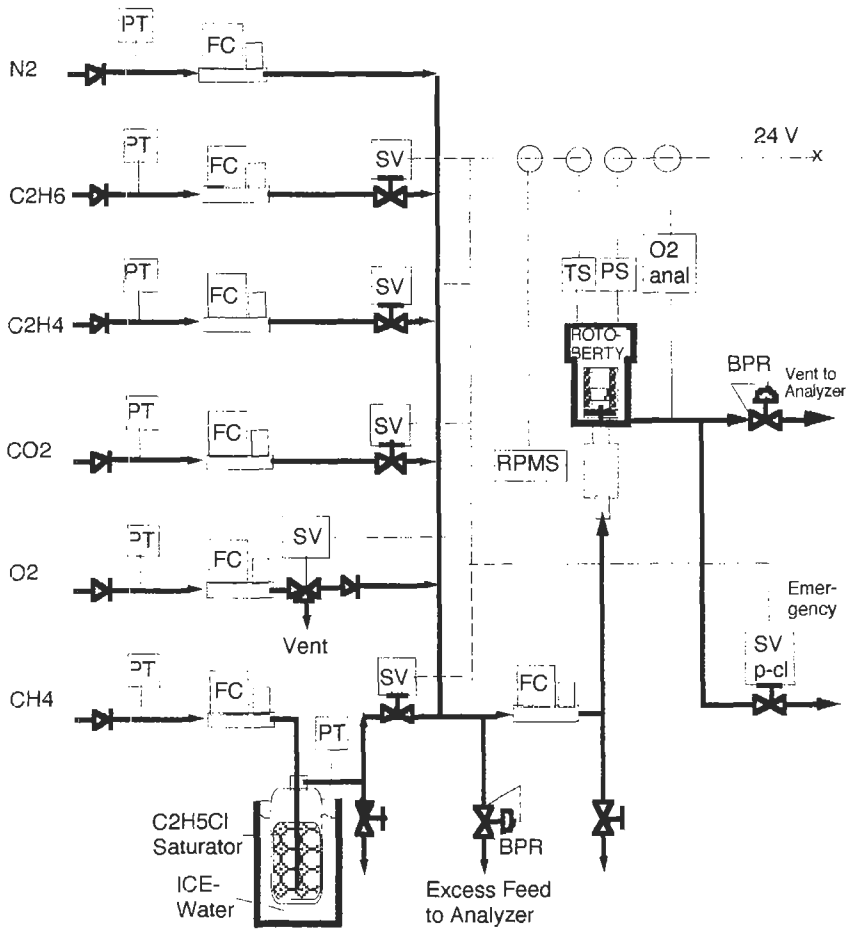
Drawing by the author.

Figure 4.4.1: Installation for ethylene oxide units

In actual experiments (Berty et al, 1989) the method recommended by Bhasin, et al, (1980) was used, and the following conditions applied:

- $V = 80$ cm^3, $W = 68$ g of catalyst was charged.
- The total feed was $F = 10.63$ normal liter/ min. corresponding to about GHSV = 8000 h^{-1}.
- The feed had 8 mol % C_2H_4 and 6 % O_2, and 7.5 PPM inhibitor.
- Ethylene oxide product concentration was about 1.5 %.
- Operating pressure was 17.8 atm and median temperature was 260°C.

Other details can be found on page 99 and in Chapter 9. Many other safety actions are needed, for which the operator of the unit must take responsibility.

4.5 A semi–batch method for gas–solid reactions.

The destruction and removal of trichloroethylene (TCE) by reaction with OXITOX®, (sodium carbonate activated by Mg and Mn oxides and carbonates), proceeds through the following stoichiometric reaction:

$$2\,C_2HCl_3 + 3\,O_2 + 3\,Na_2CO_{3(s)} \xleftarrow{\text{Mn, Mg}} 6\,NaCl_{(s)} + 7\,CO_2 + H_2O$$
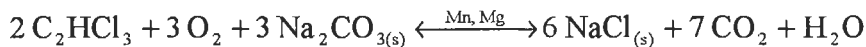
For example in paint shops, TCE evaporates and causes air pollution. The contaminated air has 250 ppm TCE in it and this can be fed to a moving bed reactor at 300°C that is charged with OXITOX (Chován et al, 1997) The kinetics must be studied experimentally. The experimental setup is shown in Figure 4.5.1 and the following description explains the recommended procedure. In the experimental unit shown, the feed is contained under pressure in a gas cylinder. Two percent of the feed is saturated by TCE and diluted with the rest of the feed. The rate is calculated as:

$$F(250-500) = -Vr$$

where **V** is fixed, **r** is changed by temperature, **F** is the response variable, and the quantity (250-500) is fixed as (ppm out - ppm in).

A forward pressure regulator (FPR) reduces the pressure and keeps the reactor at 7.5 psig. Reactor pressure is Indicated and recorded by (PIR) and temperature by (TIR). Discharge flow from the reactor is measured by a flow transmitter (FT) and after correction for temperature and pressure the Flow is Recorded on (FR).

The experimental setup uses the ROTOBERTY® internal recycle reactor. The catalyst basket of this is charged with W = 35.5 g or V = 44.3 cm^3 of OXITOX that contains 0.25 mol, i.e., 26.5 g of sodium carbonate.

First it is important to study how the gradual conversion of soda will influence the rate of reaction. Initially, keep all other conditions constant that can influence the rate: oxygen and water concentration, and the mole fraction of TCE in the reactor. This last is the same as the TCE in the discharge flow from the reactor.

Overall reaction: $2C_2HCl_3 + 3O_2 + 3Na_2CO_3 \rightarrow 6NaCl + H_2O + 7CO_2$
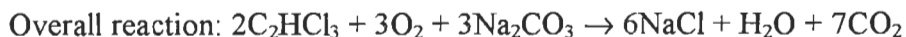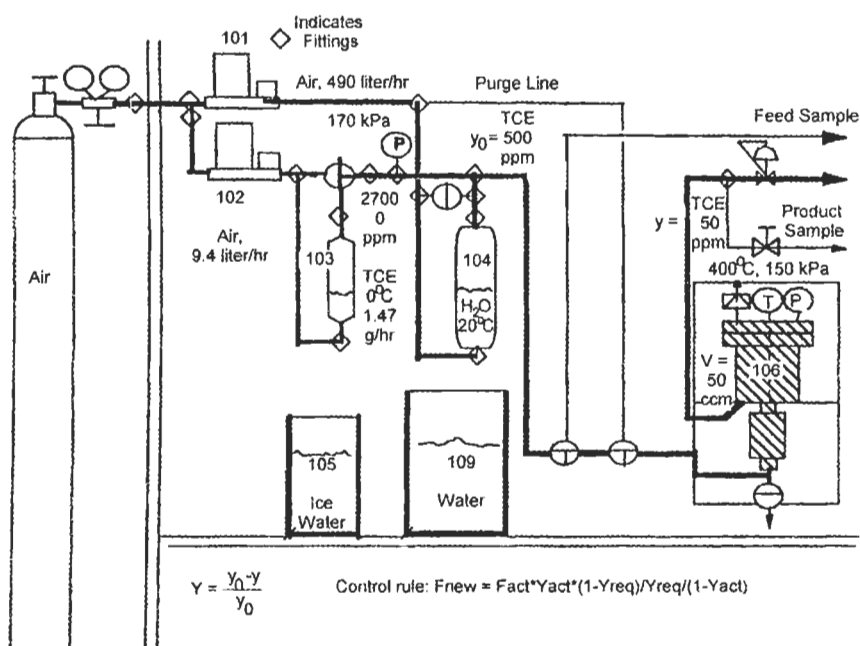
Drawing by the author.

Figure 4.5.1: Exper. setup for kinetics studies; material flows during experiment in installation for Veszprém Oxitox studies, 10–5–95.

After the flow measurement, sample the discharge stream to a continuous Flame Ionization Detector (FID) that works as an Analyzer Indicator Transmitter (AIT). The Flow Controller (FC) reads the TCE concentration signal and adjusts the flow to keep the TCE at the set level of, say, 250 ppm.

The material balance of the working unit can be formulated as follows: moles per hour of TCE (out - in) = (3/2) moles per hour soda converted.

$$- (y_0 - y)dN/dt = (3/2) N_S d(X)/dt \quad \text{in (mol of TCE)/h units}$$

where $dN/dt = F$ is the changing flow, N gives the total gaseous moles, and y and y_0 are discharge and feed mol fractions of TCE. N_S gives the initial moles of soda charged to the catalyst basket and X is the fractional conversion of the soda. Dividing both sides by the constant OXITOX volume results in the rate of reaction. The 3/2 comes from the stoichiometric coefficients in the chemical equation. Although it is not possible to measure the conversion of the solids directly and continuously, the changing flow can be measured and recorded and the TCE mol fraction difference kept constant by the FID analyzer and flow control. This is equivalent to 3/2 mol of the converted soda.

A numerical value is obtainable by integrating the trend curve for the flow received from the Flow Recorder (FR), from the start of the reaction to a time selected. Doing this from zero to each of 20 equally spaced times gives the conversion of the solid soda. Correlating the rates with the calculated X's, a mathematical model for the dependence of rate on X can be developed.

Therefore at constant temperature of 300°C and 7.5 psig of pressure, the system uses air that has 500 PPM TCE in it. Complete oxidation of 500 PPM TCE would consume only 750 PPM of oxygen as can be seen from the stoichiometric reaction. This is not a significant change from the oxygen content of air.

The experiment should be conducted at constant TCE concentration of 250 PPM. For this purpose, discharge enough flow from the reactor to maintain the concentration of TCE in the discharge flow at 250 PPM level. The forward pressure regulator keeps the reaction pressure constant. The difference between 500 and 250 PPM multiplied with the molar flow rate gives the moles per hour converted that may change continuously as the soda is consumed.

The above example was made simple to clarify the concept. Other arrangements may be more practical and some of these will be shown later.
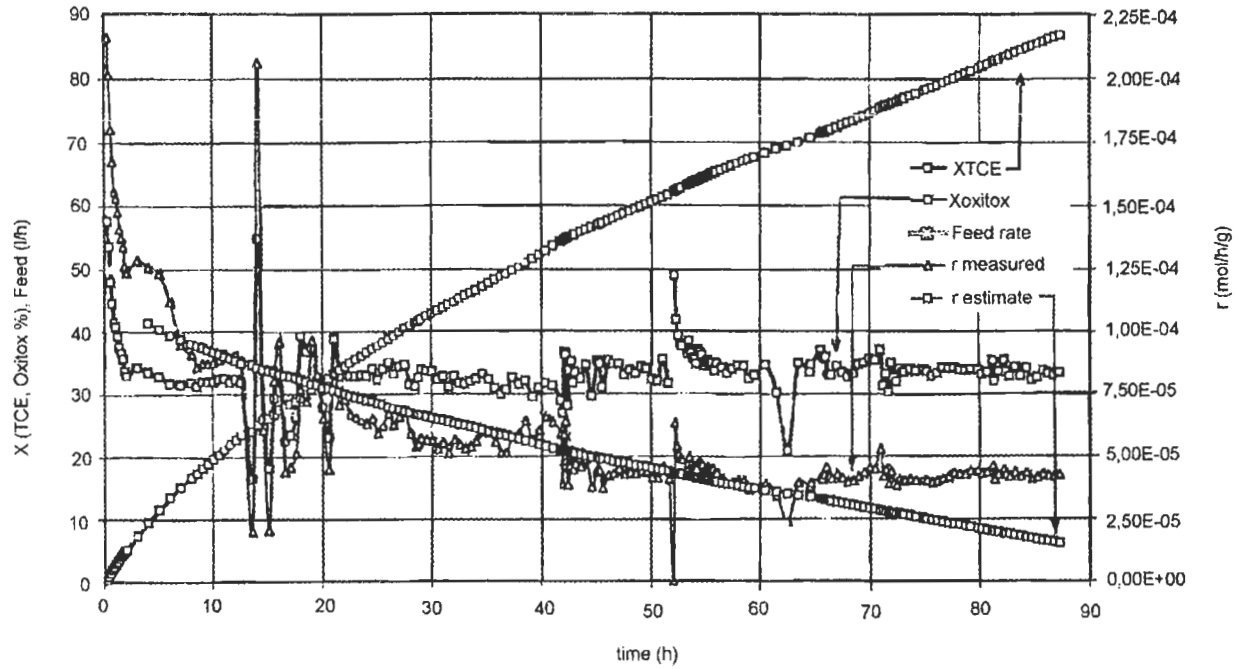
Adapted from Chován et al, 1997.

Figure 4.5.2: Conversion of solid phase in 90 hours.

4.6 The Batch Method of Silva

Silva (1971) used the Berty reactor to execute exploratory measurements on vapor–phase hydrogenation of organic substrates that had little vapor pressure at room temperature. The substrate was measured by weight in a small ceramic boat and put on the catalyst screen beside a few particles of catalyst, also measured by weight. Then the stirring started, and the autoclave was heated to the reaction temperature. Finally the desired hydrogen pressure was applied suddenly and the reaction started.

After hydrogen consumption slowed down, as judged from drop of total pressure, samples were taken for GC analysis for determination of total conversion. This is a reasonable method for preliminary evaluation of activity and selectivity of a catalyst. The method has an advantage: due to the high internal recycle flow, the outside transport limitation and catalyst overheating were avoided. This preempted the possibility of disqualifying a catalyst that was too active and could have "hotspotted" in a small tubular reactor, and given thereby very poor selectivities. Disqualifying the best catalyst, by testing in a short tube, was observed by the author (Berty, 1974).

5. Executing the Experiments

In a study of heterogeneous catalysis many different goals can emerge. Most of these can be grouped into a few categories:

- Quality control for an existing installation where a proven quality must be maintained within given tolerance limits; see section 5.1.
- An improved catalyst for an existing process, where variations in experimental condition are possible only in a limited range; see section 5.2.
- Testing catalyst for a new process; see section 5.3.

If a catalyst is tested for commercial use, it is also important to know under production conditions how much rates are influenced by various transfer processes. Recycle reactors can execute all these tests and give information on transfer influences. In advanced research projects it is enough to know the transfer interaction during the study so that physical processes are not misinterpreted as chemical phenomena.

5.1 Routine tests for Quality Control
The Ethylene Oxide Example
In well–established processes, like ethylene oxidation to ethylene oxide, quality control tests for a routinely manufactured catalyst can be very simple if the test is developed on the basis of detailed kinetic studies and modeling of the performance in a commercial reactor. Tests must answer questions that influence the economics of the commercial process. The three most important questions are:
- What is the product concentration?
- What is the production rate?
- What is the selectivity?

Product concentration influences the separation cost and the cost of recycling unconverted reactants. Production rate has a strong effect on investment cost for the full synthesis loop. Selectivity sets the raw material

costs and also the cost of disposal of unwanted byproducts. These questions are interrelated; therefore some standardization and simplifications are needed. For quality control tests of catalysts, a practical simplification is to require that a standard product concentration should be reached at a standard set of conditions (except temperature, which is the response variable). The desired product concentration should be less in a recycle reactor than in production units since in a CSTR everything is produced in the presence of everything. This kind of test was suggested by Bhasin et al (1980) for ethylene oxide catalysts.

In ethylene oxidation over a silver catalyst three overall reactions occur:

$$C_2H_4 + 0.5\ O_2 \Rightarrow C_2H_4O \qquad \Delta H_{r1} = -117\ \text{kJ/mol}$$

$$C_2H_4 + 3.0\ O_2 \Rightarrow 2\ CO_2 + 2\ H_2O \qquad \Delta H_{r2} = -1334\ \text{kJ/mol}$$

$$C_2H_4O + 2.5\ O_2 \Rightarrow 2\ CO_2 + 2\ H_2O \qquad \Delta H_{r3} = -1217\ \text{kJ/mol}$$

Considering the above three reactions, only two are independent stoichiometrically, but the third has limited significance according to studies with ^{14}C tagged ethylene oxide. Therefore, viewing the first and second will give a satisfactory picture of catalyst performance. For 75% selectivity, 3 out of 4 ethylene molecules react by the first reaction and the last by the second or third reaction. This results in a significant rate of heat production; a good recycle reactor is required to keep the reaction isothermal during studies.

The standard conditions used by Bhasin (1980) and by Nielsen and La Rochelle (1976) are shown in the table on Figure 5.1.1.

The test recommended by Bhasin et al (1980) is a search for the temperature where ethylene oxide concentration in the discharge reaches 1.5 vol.% in Recycle Reactor (RR) at fixed feed rate and feed concentration. Starting at low temperature, this search is a series of small increases in temperature and short relaxation time until the system reaches a steady–state, and when the results are stabilized the rates are measured.

Test Conditions	UCC (Bhasin, et al 1980)		Shell in lab*	Shell	
Reactor	5" Berty		microtube	5" Berty	
Pressure, psig	275		200	200	
Temp (ref), °C	260		260	260	
RPM	2000			3000	
Composition	feed	reactor		feed	reactor
ethylene, mol%	8.0	6.7	30.0	30.0	28.2
ethane, mol%	0.5	0.5		0.5	0.5
oxygen, mol%	6.0	4.5	8.0	8.0	5.8
CO_2, mol%	6.5	7.2			1.0
EO, mol%		1.0			1.5
water, mol%		0.7			1.0
nitrogen, mol%	79.0	79.4	62.0	61.5	62.0
EDC inhibitor, ppm	7.5	7.5	5-8	10.0	10.0
Physical properties					
c_p, kJ/kg	1.19		1.46	1.46	
MW, av. Kg/kmol	29.31		28.34	28.34	
ρ, kg/m^3, T_r, P_r	13.25		9.16	9.16	
μ, kg/(m–s)	22×10^{-6}		22×10^{-6}	22×10^{-6}	
Catalyst charge					
vol, cm^3	80.0[c]		2.57[b]	40.0[c]	
wt, g	68.0[a]		3.5[c]	34.0[a]	
shape	rings		crushed	rings	
size, cm	.79x.79		0.03	.79x.79	
6 vol/surface, cm	0.696		0.03(?)	0.696	
void vol fraction	0.484		0.43	0.484	
flow x sect, cm^2	15.56		0.508	15.56	
bed depth, 1/dp	6.5		423.3	3.25	
Flow conditions					
GHSV, h^{-1}	7,975		3,300	6,555	
makeup feed, cm^3/min, STP	10,632		2,200	4,370	
superfic. lin vel, u, cm/s,$T_r P_r$	82.59		1.58	116.8	
recycle ratio	74.16		none	185.0	
mass flow, m, kg/s	0.017			0.017	
mass vel, kg/(m^2-s)	11.10		0.145	11.04	
Reynolds no. (p)	3410		2.0	3390	
Schmidt no.	0.857			1.219	
Prandtl no.	0.606			0.713	
mass transfer coeff, m/s	0.039			0.044	
heat transfer coeff, W/(m^2–s)	768.0			857.0	
[C_2H_4O] inc. between top and bottom of bed, mol%	0.014			0.008	
concn diff between catalyst surface and gas, %	0.012			0.018	
per pass adiabatic temp rise in the catalyst bed, K	3.105			1.550	
temp diff between catalyst surface and gas, K	1.585			1.760	

*Nielsen and La Rochelle, 1976; [a]estimated; [b]calculated; [c]given

Reprinted with permission from Berty, © 1989 American Chemical Society.

Figure 5.1.1: Test Conditions.

Time, h	EO, mol%	CO₂, mol%	eff	temp, °C	EO rate[a]	CO₂ rate[a]	Heat generation		
							kJ/h	W	kW/m³
1.67	0.858	0.440	0.796	252.2	0.1004	0.0514	46.06	12.79	319.84
2.37	1.023	0.567	0.783	260.8	0.1197	0.0663	58.24	16.18	404.47
3.05	1.057	0.600	0.779	262.8	0.1237	0.0702	61.26	17.02	425.43
3.70	1.104	0.637	0.776	264.4	0.1292	0.0746	64.84	18.01	450.28
4.37	1.207	0.721	0.770	267.4	0.1412	0.0844	72.78	20.22	505.43
5.78	1.269	0.758	0.770	268.0	0.1485	0.0887	76.52	21.26	531.39
6.45	1.284	0.767	0.770	268.2	0.1502	0.0897	77.42	21.51	537.67
7.15	1.318	0.792	0.769	268.9	0.1542	0.0926	79.82	22.17	554.32
7.95	1.364	0.833	0.766	270.1	0.1596	0.0975	83.69	23.25	581.20
8.58	1.389	0.853	0.765	270.4	0.1625	0.0998	85.60	23.78	594.42
9.27	1.416	0.870	0.765	271.0	0.1657	0.1018	87.26	24.24	605.97
9.92	1.448	0.900	0.763	271.7	0.1694	0.1052	90.01	25.00	625.04
[b]10.57	1.480	0.925	0.762	272.3	0.1731	0.1082	92.39	25.66	641.61
[b]11.90	1.482	0.921	0.763	272.2	0.1734	0.1077	92.12	25.59	639.72
[b]13.08	1.508	0.942	0.762	272.6	0.1764	0.1102	94.14	26.15	653.75
[b]13.72	1.500	0.932	0.763	272.7	0.1755	0.1090	93.24	25.90	647.49
24.62	1.720	1.153	0.749	276.8	0.2012	0.1349	113.49	31.52	788.12
25.40	1.745	1.170	0.749	276.6	0.2041	0.1368	115.14	31.98	799.57
26.20	1.730	1.159	0.749	276.3	0.2024	0.1356	114.15	31.71	792.70
26.92	1.664	1.086	0.754	274.9	0.1947	0.1270	107.49	29.86	746.49
27.47	1.656	1.081	0.754	274.9	0.1937	0.1264	106.98	29.72	742.90
28.53	1.639	1.064	0.755	274.3	0.1917	0.1244	105.43	29.29	732.16
29.57	1.587	1.019	0.757	273.2	0.1857	0.1192	101.22	28.12	702.91
30.08	1.572	0.987	0.761	272.7	0.1839	0.1155	98.56	27.38	684.44
30.63	1.603	1.012	0.760	273.4	0.1875	0.1184	100.93	28.04	700.94
31.18	1.565	0.983	0.761	272.5	0.1831	0.1150	98.12	27.26	681.39
[b]31.72	1.532	0.952	0.763	272.0	0.1792	0.1113	95.23	26.45	661.30
[b]32.48	1.514	0.946	0.762	271.7	0.1771	0.1106	94.51	26.25	656.35

[a]mol/h; [b]catalyst performance evaluation conducted with these points, [c]Same conditions as in the third column of Figure 5.1.1. Feed=4510cm³/min at STP; ΔH_{r1}=-117kJ/mol; ΔH_{r2}=-1334kJ/mol; cat vol=40cm³. Means: eff=0.7625; temp °C=272.25. STD: eff=0.0005; temp °C=0.37

Reprinted with permission from Berty, © 1989 American Chemical Society

Figure 5.1.2: Test results.[c]

Tests according to Bhasin's recommended experiments were executed at the laboratory of Berty Reaction Engineers, Ltd. on a test unit built for an export order. (The test unit was shown in Figure 4.4.1.) Results of this study were reported by Berty et al, (1989) and are reproduced here in the table on Figure 5.1.2.

As can be seen on Figure 5.1.2, at slightly above 272°C, the ethylene oxide concentration reached the goal of 1.5 vol.%. These results are marked [b]. At 272.35 ± 0.37°C efficiency reached 76.25 ± 0.05 % at the desired product concentration of 1.497 ± 0.014 vol.%.

As in most systematically done and well–controlled experimental series, results can be reevaluated later on for additional purposes. In this set, the heat generation rates were evaluated with the help of the heats of reaction, at every temperature used. These in turn formed the basis for evaluation of temperature runaway conditions, as will be shown in Chapter 9.

The pollution control example.

Control of pollutants by oxidation is another exothermic process in which high conversion is the most important performance criterion. Interest in efficiency is limited to minimize byproduct formation; the byproducts can be more damaging and more refractory than the original pollutants were. Commercially, most adiabatic reactors used for pollution control are of the least expensive construction.

Complete or very high conversion requires the study of catalyst at very low concentrations. At such conditions, close to equilibrium (Boudart 1968), all reactions behave according to first order kinetics. Study at very low concentrations is also helped by the very small heat generation, so these studies can be executed in small tubular reactors, placed in simple muffle furnaces. Such studies were made by Kline et al (1996) at Lafayette College and were evaluated by Berty (1997).

Evaluation of catalyst for oxidation of pollutants usually involves an "Ignition Curve" determination. This is a slightly overused expression, because only heat generation is evaluated, not heat removal. For a true ignition curve representation, heat removal evaluation would also be required.
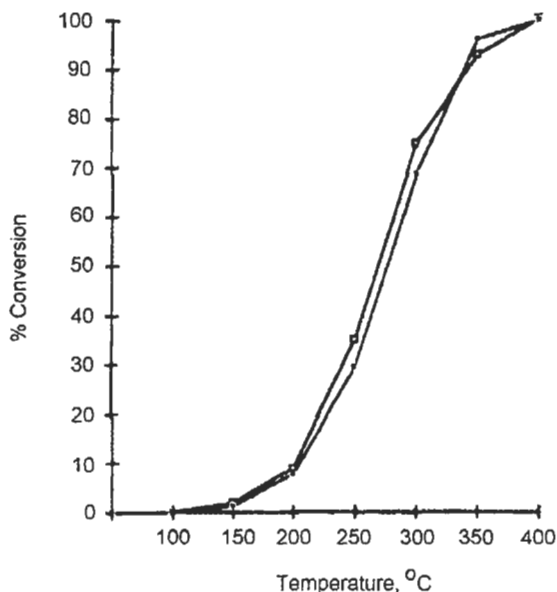
Figure 5.1.3: Graph for the Ignition Curve measurement.

From the heat generation alone the maximum tolerable temperature difference between catalyst and gas can be evaluated, as will be shown in a later chapter. This is never done in pollution control catalyst testing. Due to the simple conditions at very low concentration, the "Ignition Curve" can be evaluated for first order kinetics.

In a small integral reactor at each step of the stepwise increasing temperature, one point on a conversion versus temperature curve is received. These are all at the same feed rate and feed composition, constant pressure, and each is at a different but practically constant temperature along the tube length within every step. Since the reactor is small the attainment of steady–state can be achieved in a short time. The steadiness of conditions can be asserted by a few repeated analyses.

The kinetic equation is, for very low concentration of pollutants:

$$-\frac{dC}{dt} = kC \qquad -kt = \int_{C}^{C_o} \frac{dC}{C} \qquad -kt = \ln\frac{C}{C_o} \qquad e^{-kt} = \frac{C}{C_o}$$

$$X = \frac{C_o - C}{C_o} \qquad 1 - X = \frac{C}{C_o}$$

$$\frac{dX}{dt} = k(1-X) \qquad kt = \int_{1}^{1-X} \frac{dX}{1-X} \qquad -kt = \ln(1-X) \qquad e^{-kt} = 1 - X$$

These equations hold if an "Ignition Curve" test consists of measuring conversion (X) as the unique function of temperature (T). This is done by a series of short, steady–state experiments at various temperature levels. Since this is done in a tubular, isothermal reactor at very low concentration of pollutant, the first order kinetic applies. In this case, results should be listed as pairs of corresponding X and T values. (The first order approximation was not needed in the previous ethylene oxide example, because reaction rates were measured directly as the total function of temperature, whereas all other concentrations changed with the temperature.) The example is from Appendix A, in Berty (1997). In the "Ignition Curve" measurement a graph is made to plot the temperature needed for the conversion achieved.

Here, since the measurements were done in an integral reactor, calculation must start with the Conversion vs. Temperature function. For an example see Appendix G. Calculation of kinetic constants starts with listed conversion values as vX and corresponding temperatures as vT in array forms. The Vectorize operator of Mathcad 6® tells the program to use the operators and functions with their scalar meanings, element by element. This way, operations that are usually illegal with vectors can be executed and a new vector formed. The v in these expressions indicates a vector.

Then vkt is calculated from the vX values as (-ln(1-vX)). The independent function Temperature vx is expressed as 1000*K/vT for the Arrhenius function. Finally the independent variable vy is calculated as ln(vkt). Next a linear regression is executed and results are presented as y_i plotted against $x_{i..}$ The results of regression are printed next. The slope and intercept values are given as a, and b. The multiple correlation coefficient is given as c.

In the results it can be seen that c = -0.996, that 99.6% of the variance in the data is accounted for by the Arrhenius temperature function. The Energy of Activation = 60,250 J/mol or 14,400 kcal/mol is a little less than published, for diffusion in the solid phase. This was expected in the second reaction, the regeneration of the catalyst in a solid–solid system. Some diffusional limitation by the reacting gas was observed in the pores of the catalyst and this could lower the expected value even more.

5.2   *Improved Catalyst for an Existing Process*

Finding a better commercial catalyst for an existing production unit requires a wide search, keeping in mind the operation limitations of the commercial unit. Similar catalysts made by different manufacturers (supported nickel, for example) may vary in trace chemical composition, surface area, pore structure, and so on. While the overall chemistry of the process may not change much, the basic rate limiting process can be different, and alter the kinetics and the response of the catalyst to operating conditions.

Commercial units always have built–in limitations due to their design. These are not limited to maximum temperature and pressure ratings but also to flow rate, heat exchange capacity, raw material availability and storage capacities. Therefore, the search for a better catalyst should be limited to the unit's range of operability.

Preliminary tests can use the existing quality control method (discussed in Chapter 5.1) for orientation but only very inactive catalysts should be rejected on the basis of older norms. For new catalysts that at first glance seem little better than current ones, an optimization should be performed. Catalysts should be compared at optimum performance within the constrained domain.

Before an optimization is started, it is usually practical to find out what kind of limiting process affects the new catalyst. This can be done by studying the effect of temperature, inert gas pressure and a variable that is critical for profit making, usually conversion with a given feed or product concentration.
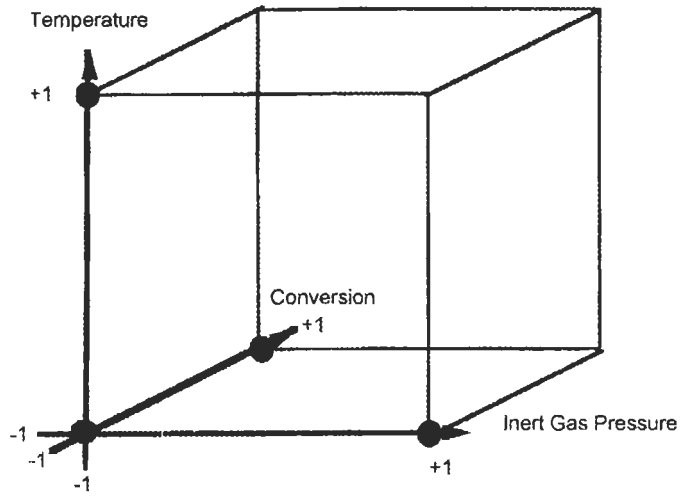
Drawing by the author.

Figure 5.2.1: One variable at a time.
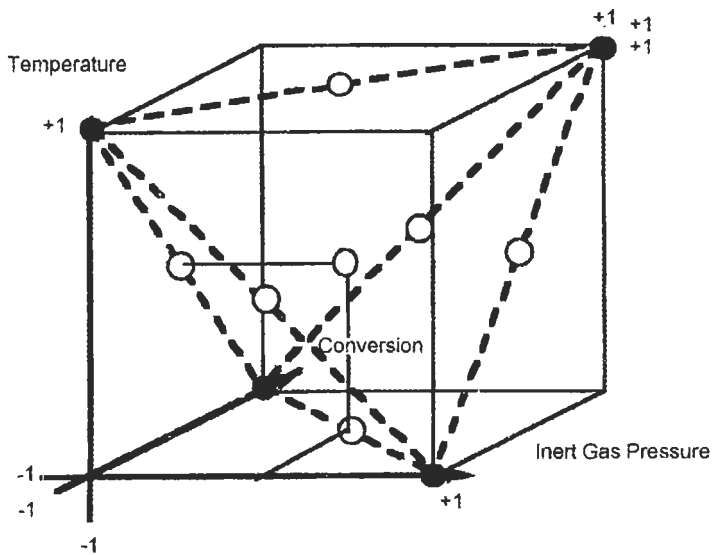
Drawing by the author.

Figure 5.2.2: Statistical design of experiments.

The study of three variables can be done by the older method of making a single change at each experiment. This is shown on Figure 5.2.1. In addition to this method, on Figure 5.2.2 a very simple example shows how this can be done by statistical design of a set of experiments. The difference is in economy of experimentation. While in the older way two experimental results can be used to evaluate the effect of a single variable, in this oversimplified example for statistical design, all experiments are used in evaluating all the variables.

Figure 5.2.1 illustrates the traditional method of changing one variable at a time. In this method the experimenter selects an anchor point, usually close to present operating conditions. After executing the anchor point experiment, the inert gas pressure alone is changed to a higher level. In the next experiment inert gas is changed back to the base case (illustrated here as -1,-1,-1, indexed point.), where it remains as temperature alone is increased. Finally, both pressure and temperature are held at base level and the conversion is changed to its higher level for the final experiment. In evaluating each of the effects, only two results can be used.
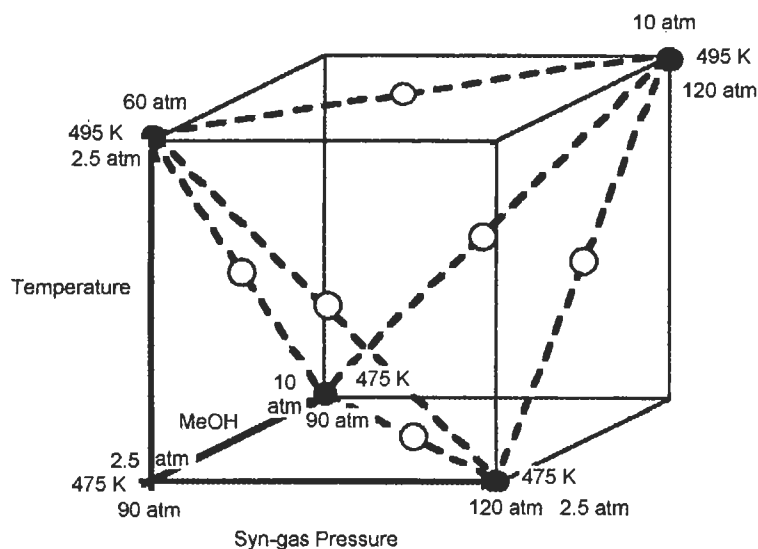
Drawing by the author.

Figure 5.2.3: Reaction conditions.

Figure 5.2.3 shows a very simple, even simplistic, example for the statistical design of experiments. This experimental plan is the simplest 2

level, 3 variable design. Here $2^3 = 8$ experiments are needed for a full replica. The full set of all the experiments needed is listed below. To simplify, temperature is coded as **T**, inert gas pressure as **Pi** and conversion as **X**. The levels of variables are simplified to + and - , since there are only two.

Experimental plan for full replica

No.	P_i	T	X
1	+	+	+
2	+	+	-
3	+	-	+
4	+	-	-
5	-	+	+
6	-	+	-
7	-	-	+
8	-	-	-
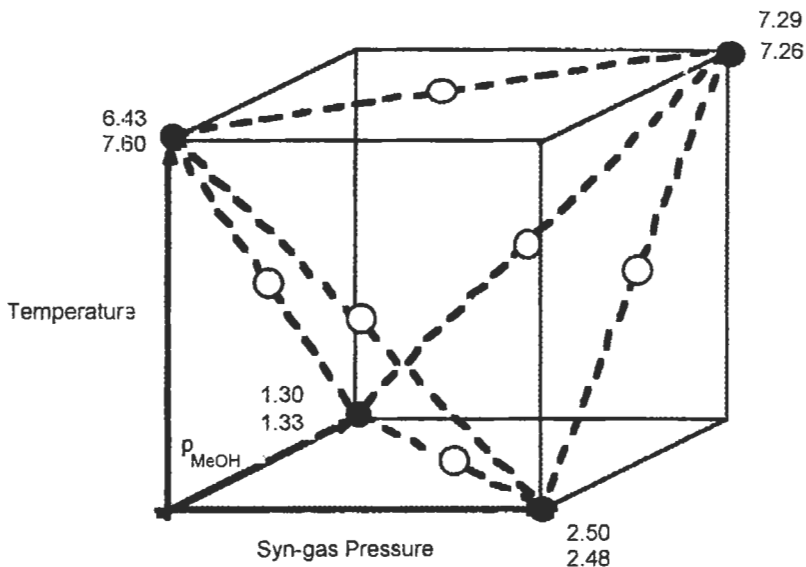
Drawing by the author.

Figure 5.2.4: Measured reaction rates, mol/m^3.s.

In such small designs it is advisable to carry out all 8 experiments, adding perhaps as the 9th experiment an additional center point condition. This

would be coded as 000 in the middle of the cube. For comparison with the traditional plan, only four experiments will be considered here. This is called the half replica. The points considered are marked by solid black dots and connected by dotted lines for easier visualization in space.

The statistical design has the advantage of using all 4 experimental results for evaluating the effect of each of the 3 variables. The illustrated half replica consists of experiments 1, 4, 6 and 7. Refer to Figure 5.2.3. On any plane of the cube, two experimental conditions are shown and it is customary to write the numerical results there. On the planes, one variable for both experiments is at one level and the other two are on opposite levels. Therefore, the two results can be averaged and assigned to the center of the plane, since the two variables that are on opposite levels are canceling themselves out. This can be done for all 6 planes and effects can be evaluated from opposing pairs of averages. Therefore, it is a much better use of the four experimental results. More information on statistical design and evaluation of experiments is available in the literature on the subject. A good compilation of several years of actual experience is summarized in Box et al, (1978).

Inert gas pressure, temperature, and conversion were selected as these are the critical variables that disclose the nature of the basic rate controlling process. The effect of temperature gives an estimate for the energy of activation. For a catalytic process, this is expected to be about 90 to 100 kJ/mol or 20–25 kcal/mol. It is higher for higher temperature processes, so a better estimate is that of the Arrhenius number, $\gamma = E/RT$ which is about 20. If it is more, a homogeneous reaction can interfere. If it is significantly less, pore diffusion can interact.

Inert gas pressure does not have any effect on the surface catalysis controlling the rate. If diffusion is slowing down the rate, high inert gas pressure will cut the diffusion coefficient and the rate will be less than at low Pi. If both this and a low energy of activation is are observed, a diffusional effect is very likely.

The effect of conversion is mostly an economic indicator. Additionally, a strong slowdown can indicate a reversible reaction. If this possibility is excluded by thermodynamic estimates, a strong inhibition of the rate is

indicated by some product. If selectivity drops with increased conversion a consecutive reaction may also be in progress. The above observations will give a direction and estimate on what way, and how much can be gained from the new catalyst.

5.3 Range Finding Experiments.

The UCKRON test problem was introduced in the Preface on page viii and mentioned a few more times since. The Appendix contains a FORTRAN listing and a EXCEL program to calculate and use UCKRON for studies.

The UCKRON test problem will be used here to simulate experiments in a Continuous Stirred Tank Reactor (CSTR). For this preliminary study, fix the feed composition to a mol ratio of 2 mol of H_2 to 1 mol of CO with no methanol in the feed. This is $2/3 = 66.7$ vol. % H2 and $1/3 = 33.3$ vol. % CO. Select for the tetrahedral experimental design the three axis as temperature, partial pressure of H_2/CO 2:1 mixture, and partial pressure of methanol, all in the exit (as well as in the reactor) with the above specified feed. The experimental design for the four experimental conditions and values for the independent variables shown on the left side of Figure 5.3.1. The numbers in parentheses refer to the full replica presented previously. All four experiments were run twice. That is, the four exact rates were calculated from the "true" kinetics and each of these were adjusted with two different random errors to get the eight "experimental" results.

Experiment number	Pressure of C/H atm	Temp. T, K	MeOH M, atm/atm	Rate truc exact	Rate ± 5% crror	Rate ± 5% crror
1 (1)	120	495	10	**7.14**	**6.78**	**7.37**
2 (5)	90	495	2.5	**7.77**	**7.53**	**7.52**
3 (7)	90	475	10	**1.28**	**1.29**	**1.31**
4. (4).	120	475	2.5	**2.58**	**2.54**	**2.53**

Table compiled by the author.

Figure 5.3.1: Experimental design for four experimental conditions.

In the above table the dependent variables are in bold face. H + C are not separated as variables, but these must be inserted in the program as H and C separately. Rates are calculated for the simulated experiments by the explicit rate form, as is detailed on the Excel Table in the Appendix D (pages 1–4.) The four results, exactly as "true" rates are given and listed

twice more with 10 % standard error added . The errors were calculated by using a random number generator.
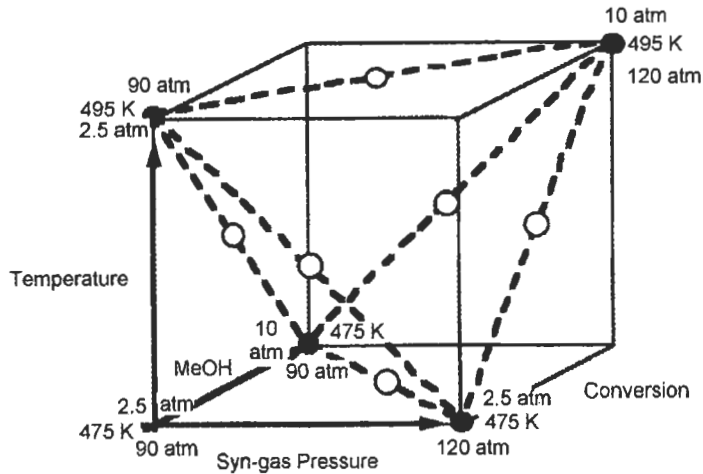
Drawing by the author.

Figure 5.3.2: Reaction conditions.
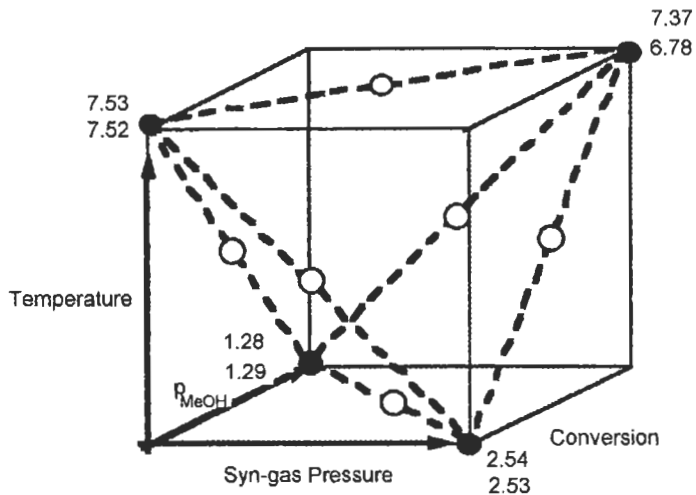
Drawing by the author.

Figure 5.3.3: Measured reaction rates, mol/m^3.s.

On the upper Figure 5.3.2 the tetrahedron indicates the values of the independent variables. On the lower picture Figure 5.3.3 the results of the

experiments are given at the corners of the tetrahedron. From the experimental result shown in the picture with the tetrahedron, the following results can be calculated.

$$Rate = k*exp(-E/2303*R)(1000/T)(C^m)(M^n),$$

where E, m, and n are the unknown coefficients.

$$log\ rate = log(k) -(E/2303*R)(1000/T) + m*log(C) + n*log(M)$$

Averaging the results on the upper plane results in:

at 495 K, 1000/T = 2.020   log(7.145) = 0.854

Now averaging the results on the bottom plane gives:

at 475 K, 1000/T = 2.105   log(1.902) = 0.283

In Figure 5.3.2, between the upper and lower planes, only the temperatures differ. All other reaction conditions average out. This can also be observed on Table 5.3.1 by inspecting the columns for C and M. Therefore, the difference in rates can be considered as caused by temperature alone.

Log rate(495) = log(k) - (E/2303*R)*(2.020) + m*log(C) + n*log(M)
-[log rate(475) = log(k) - (E/2303*R)*(2.105) + m*log(C) + n*log(M)]
----
log rate(495) - log rate(475) = (E/2303*R)(2.105-2.020)

The difference between the log rates at the two temperatures gives the last equation. From this the Energy of Activation is calculated as:

$$E = 2303*1.98*\frac{0.854-0.283}{2.105-2.020} = 30,740$$

Multiple regression analysis can be executed by various programs. The one shown in the Appendix is from Mathcad 6 Plus, the "regress" method. Taking the log of the rates first and averaging later gives somewhat different result.

In summary, the Energy of Activation calculated from repeated experiments with 5% random error is:

By manual averaging the arithmetic rates: 30,740 cal/mol
By multiple regression: 30,031 cal/mol
By manual averaging the log of rates: 32,190 cal/mol

The manual evaluation and the multiple regression results are in good agreement. The result from the log rates is still very close The evaluation by multiple regression is shown in Appendix E. The reader is encouraged to do the manual evaluation of effects of C and M (m and n exponents) and compare those with the multiple regression results.

5.4   *The Ethane Story*

An appreciation of statistical results can be gained from a study conducted to support the first application of computer control for an ethylene oxide production unit at Union Carbide Corporation in 1958. For the above purpose, twenty years of production experience with many units was correlated by excellent statisticians who had no regard for kinetics or chemistry. In spite of this, they did excellent, although entirely empirical work. One statement they made was: "…[ethane has a significant effect on ethylene oxide production.]" This was rejected by most technical people because it did not appear to make any sense; ethane did not react, did not chemisorb, and went through the reactor unchanged.

Much later (Marcinkowsky and Berty 1973) it was proven that ethane did indeed have an effect. In the study of the inhibitor action of chlorinated hydrocarbons it was discovered that these compounds chlorinate the silver catalyst and ethane removes the chlorine from the catalyst by forming ethyl chloride. Since the inhibitor was in the 10 ppm range and similar quantities were used from the ethane present in about one volume percent, the small difference could not be calculated from material balance. The effect of ethane was only noticed as significant by the statistics, which justifies the statement made by Aris (1966) that, "The need for sophistications should not be rejected unsophisticatedly."

6. Kinetic Measurements

Chemical kinetics is a part of chemistry that studies the change in time of the composition of a reacting system. The specific rate of reaction (see Appendix H for details) is expressed as:

$$r = C_o \frac{dX}{dt}$$

where X is the mole fraction of the initial reactant chemically converted.

Knowledge of the rate is important to design chemical reactors for industrial production. It is also important for optimizing the production and to define the safety limits of operation. As was mentioned in the introduction, various transfer processes can influence chemical rates. The recognition of such interference is of primary importance during any study of kinetics, especially in those studies that will serve as the basis of design for production reactors.

The many methods used in kinetic studies can be classified in two major approaches. The classical study is based on clarification of the reaction mechanism and derivation of the kinetics from the mechanism. This method, if successful, can supply valuable information, by connecting experimental results to basic information about fundamental steps. During the study of reaction mechanisms many considerations are involved. The first of these is thermodynamics, not only for overall reactions, but also on so–called "elementary" steps.

In looking for the mechanism, many intermediates are assumed. Some of these are stable molecules in pure form but very active in reacting systems. Other intermediates are in very low concentration and can be identified only by special analytical methods, like mass spectrometry (the atomic species of hydrogen and halogens, for example). These are at times referred to as active centers. Others are in transition states that the reacting chemicals form with atoms or radicals; these rarely can be isolated. In heterogeneous catalytic reaction, the absorbed reactant can

form a transition state complex with a surface atom and another reactant, and these are hard to identify.

It is difficult to give definite instruction in reality for kinetic studies. Although in general all studies have common features, each one is somewhat different, so once a general idea is formed how to do it, go ahead and start. The first study will teach what should have been done. This learning period may repeat itself a few times. Scientific publications usually report the last and finally successful set of experiments and do not list the many less successful tries.

6.1 Recent History of Kinetic Studies.

In today's competitive climate, investigators cannot spend much time on the clarification of the kinetics for a new process. At Union Carbide Corporation in the 1970s the study to replace the old and not very efficient butyraldehyde hydrogenation was done in three months. In another three months a kinetic model was developed and simultaneously tested in an existing single tube in a pilot–plant (Cropley et al,1984). Seldom is a completely new process studied for which no similar example exists in the industry.

Preliminary kinetics usually can be developed in a short time, good enough to explain the major effects of the process. Then as the process produces and the competition begins catching up, further refinements of kinetics and the catalyst will protect the company's position. Again at Union Carbide (based on anecdotal records), the high pressure polyethylene manufacturing started during World War II. From the results of a few experiments in a 10 cm^3 shaking autoclave, a continuous production unit was built. The tube of the reactor was made from gun barrels.

The first reactor plugged up irreversibly in the first minutes of operation. A second reactor was made and production started. The polyethylene was dark and stinking but the Navy needed the material. As the war ended, the product was improved; when competition started, quality accelerated significantly. Fourteen year after production started, the first pilot–plant was built, since the continuous process was difficult to study in small scale. A few more years later, three polyethylene pilot–plants were running day

and night to support the production. Not everything goes logically or "by the books."

Humans can not know the ultimate and detailed true reaction mechanism of any reaction, or the kinetics that can be derived from it.. Bodenstein (1906) studied the mechanism of the $H_2 + Br_2 = 2$ HBr reaction and after several decades of work and dozens of publications wrote the final paper on the subject. Within a few years one of his students published a correction to Bodenstein's explanations.

The present author was worried about the lack of knowledge concerning the quality of the kinetic models used in the industry. A model is by definition a small, scaled–down imitation of the real thing. (Men should remember this when their mothers–in–law call them model husbands.) In the industry all we require from a kinetic model is that it describe the chemical rate adequately by using traditional mathematical forms (Arrhenius law, power law expressions and combinations of these) within the limits of its applications. Neither should it rudely violate the known laws of science.

No industrial process enjoys a knowledge of mechanism and kinetics so complete that models can be compared to it. Aris (1975) and Cropley (1978) simulated experimental results using a rate model. From the data a new model was derived and compared with the original.

Therefore the author decided to create an artificial "true" mechanism, derive the kinetics from the mechanism without any simplification, and solve the resulting set of equations rigorously. This then can be used to generate artificial experimental results, which in turn can be evaluated for kinetic model building. Models, built from the artificial experiments, can then be compared with the prediction from the rigorous mathematical solution of the kinetics from the "true" mechanism.

Methanol synthesis served as the model for the "true" mechanism. Stoichiometry, thermodynamics, physical properties, and industrial production rates were all taken from the methanol literature. Only the reaction mechanism and the kinetics of methanol synthesis were discarded. For the mechanism a four step scheme was assumed and from this the

kinetics was derived. This can be seen on Figure 6.1.1. There, A is H_2, B is CO, and C is methanol. From the active centers, X_1 is the empty surface, X_2 is the chemisorbed hydrogen. X_3 is an intermediate, existing on the surface only and having the chemical composition of formaldehyde. Finally X_4 is the chemisorbed product, the methanol (Berty et al, 1989.)

Figure 6.1.1 represents a four step mechanism consisting of the following steps:

$$2(A + X_1 = X_2)$$

$$B + X_2 = X_3$$

$$X_3 + X_2 = X_4 + X_1$$

$$X_4 = C + X_1$$
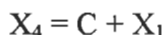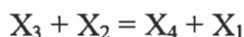
On Figure 6.1.1, the four consecutive reaction steps are indicated on a vertical scale with the forward reaction above the corresponding reverse reaction. The lengths of the horizontal lines give the value of the rate of reaction in mol/m^3*s on a logarithmic scale. In steady–state the net rates of all four steps must be equal. This is given on the left side with 4 mol/m^3*s rate difference, which is 11 mm long. The forward rate of the first step is 4.35 mol/m^3*s and the reverse of the first reaction is only 0.35 mol/m^3*s, a small fraction of the forward rate.

The second forward rate is five orders of magnitude larger. From such a large number the difference of four is well within the error limit and can be neglected. On a linear scale, compared to the 11 mm net rate this would be 31 m long. If the forward and reverse rates are large and about the same, it is possible to consider these two at quasi–equilibrium. Hence the first rate can be called the rate determining step and the second can be considered practically at equilibrium. The third step is only 8 meters long on a linear scale, but still can be considered to be at equilibrium. The fourth forward step is only twice as large as the first one. This cannot be neglected, and in this reaction system there are two slow steps. In deriving the rigorous solution for UCKRON, no assumption of equilibrium or limiting step was made.
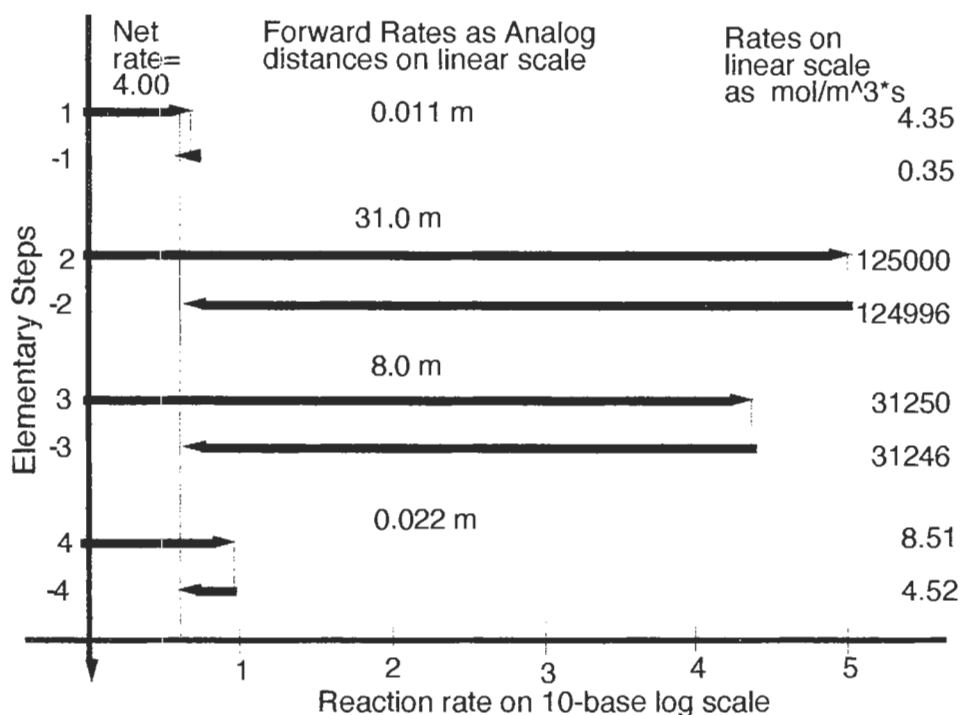
Drawing by the author.

Figure 6.1.1: Four consecutive reaction steps.

If a sequence of reaction steps consists only of irreversible steps, then all forward rates must be equal. When this occurs, the intermediates or active centers' concentrations will adjust themselves to achieve this. The reaction that consumes the active center or intermediate of the highest concentration is the rate limiting step. Even in this case all rates must be equal. One should be cautious when speaking about the slowest rate; perhaps the smallest rate constant would be somewhat better.

In the case of parallel reactions, the fastest reaction will set or control the overall change. In all rate determining cases, the relative speed of the reactions will change with the temperature. This is caused by different energies of activation among the steps in the sequence. This is just one more reason for limiting rate predictions from measurements within the studied domain: to avoid extrapolation.

Heterogeneous catalytic studies should also be concerned with the significance of adsorption and desorption rates and equilibria of the reactants, intermediates and products. Yang and Hougen (1950) tabulated the expressions for surface catalyzed reactions controlled by various steps.

The rate expression consisted of three groups:

$$\text{rate} = \frac{(\text{kinetic factor})(\text{driving } -\text{force group})}{(\text{adsorption group})}$$

Expressions for the three groups and exponents were tabulated separately.

These expressions give valuable direction, but using them should not be done mechanically. Always test the consequence of the implied assumptions. Ask the question: if this is true, what follows from it? For example, if the adsorption of A is controlling, then the effect of the other reactant B should be zero or even negative.

The rigorous solution in algebraic form is in Appendix A, then in FORTRAN IV executable form in Appendix B. The executable form gives the rate of reaction in mol/m^3s at the temperature T in, and partial pressures of H, C, and M (for H_2, CO, and MeOH) in atmospheres are supplied. The program allows experimentation, but instead of putting the catalyst in the reactor, put a the disk containing the UCKRON[4] program in the computer. The program on the disk will give the rate of reaction of methanol synthesis at the specified values of T, H, C, and M in a CSTR. Therefore this is the composition of the discharge as it is from CSTRs. For example, at T = 485 K, and H = 70 atm, C = 25 atm. M = 5 atm, the program calculates the rate to be 4.00 mol/m^3s.

The University of Veszprém in Hungary extended UCKRON with the water–gas shift reaction. This modification, which has six steps in its mechanism, is called the VEKRON test problem. (Árva and Szeifert 1989).

Boudart (1956) and Weller (1956) discussed the applicability and need of Langmuir–Hinshelwood kinetics to describe the rate of industrially

---

[4] The name of the program for the mathematical exercise is UCKRON, since it was made in cooperation of Union Carbide Corporation and the University of AKRON (Berty 1989.)

important reactions. With the increasing knowledge and improved computational techniques some of the differences between the two viewpoints lost their significance. It is still interesting that the fundamental forms of kinetic equations fit very well with industrial data, perhaps in a narrow range of conditions.

The systematic use of classical catalytic kinetics is always a useful approach in modeling (Boudart 1986). Even if these models do not reflect the true mechanism in the case of structure–sensitive catalysts, they are a formally correct representation of the observed facts. As Boudart sees it in the case of structure–insensitive reactions, it can also be the real thing.

The UCKRON test problem assumes the simplest uniform surface implicitly, because adsorbed hydrogen coverage is directly proportional to the partial pressure of gaseous hydrogen and adversely affected by the partial pressure of the final products. Such a simple mechanism still amounts to a complex and unaccustomed rate expression of the type solved by second order algebraic equations.

The best fit, as measured by statistics, was achieved by one participant in the International Workshop on Kinetic Model Development (1989), who completely ignored all kinetic formalities and fitted the data by a third order spline function. While the data fit well, his model didn't predict temperature runaway at all. Many other formal models made qualitatively correct runaway predictions, some even very close when compared to the simulation using the "true" kinetics.

If the UCKRON expression is simplified to the form recommended for reactions controlled by adsorption of reactant, and if the original "true" coefficients are used, it results in about a 40% error. If the coefficients are selected by a least squares approach the approximation improves significantly, and the numerical values lose their theoretical significance. In conclusion, formalities of classical kinetics are useful to retain the basic character of kinetics, but the best fitting coefficients have no theoretical significance.

6.2 General rules

Boudart (1968) proposed five basic rules for rate functions of *single reactions*. These are of general validity and if an exception applies, it usually points to some interesting details. In heterogeneous catalysis at least one chemisorption step is always involved. Therefore "single" reactions are seldom seen, but frequently complications can be neglected, and a complex set of reaction steps treated as if it would be a simple one. This is valid for a narrow range of conditions, especially when one step is much slower than the rest. A good example is presented by Mears and Boudart (1966) where the logic and reasoning can be seen clearly.

The five rules of Boudart are the following:

I.   The rate **r** usually declines as conversion increases.

II.   The rate can be expressed for irreversible reactions as $r = kf(C_i)$, where **k** is independent of concentrations.

III.   The rate constant **k** is a function of the absolute temperature in the form that Arrhenius (1889) found:

$$r = k_0 exp(-E/RT)$$

IV.   The function of rate on concentrations $f(C_i)$ is usually independent of temperature and can be written as:

$$f(C_i) = \prod_i C_i^{n_i}$$

where the product $\prod$ is taken over all concentration of components on the system. The exponent n_i generally does not agree with the stoichiometric number α_I in the chemical equation when more than one step is involved. The agreement was suggested by Guldberg and Waage (1867) for the elementary equation participating in the equilibrium.

V.   For reversible reactions the net rate of reaction can be expressed as the difference between forward and reverse reactions:

$$r = \overrightarrow{r} - \overleftarrow{r}$$

When Rule II applies to the rate functions

$$\overrightarrow{r} = \overrightarrow{k} f(C_i) \quad \text{and} \quad \overleftarrow{r} = \overleftarrow{k} f(C_i) \quad \text{then}$$

the rate constants are related to the equilibrium constant of the reaction by means of the equation:

$$\frac{\overrightarrow{k}}{\overleftarrow{k}} = K^n$$

where n is the is the one over the stoichiometric number of the rate determining step. (See Boudart at loc.cit, page 87.)

For a sequence of reaction steps two more concepts will be used in kinetics, besides the previous rules for single reactions. One is the steady–state approximation and the second is the rate limiting step concept. These two are in strict sense incompatible, yet assumption of both causes little error. Both were explained on Figure 6.1.1; Boudart (1968) credits Kenzi Tamaru with the graphical representation of reaction sequences. Here this will be used quantitatively on a logarithmic scale.

6.3   *Kinetic Model for a new Process*

This task demands the most circumspect considerations, because only very general guidance can be given, and making mistakes and learning from them is the way to success. Once the desired chemistry of a new process is defined, and some knowledge is gained about the undesired side reactions, some catalyst types can be marked as potential candidates for testing. Some of the catalysts may be commercially produced for other reactions. In this case it is practical to check out some of them, before a major effort is started to modify an existing catalyst, or to make new ones.

Testing conditions are not as constrained as for catalysts in an existing production unit, but other conditions may set some limits, like explosive range, start of a homogeneous reaction, corrosion, polymerization, etc. Literature should be searched for this limitation, in addition to other information on the main reaction. Literature gives much more information if interest is not limited to the main reaction but is extended to analogous processes as well.

Screening of the catalysts can be done at conditions estimated for the new process. A minimum performance usually can be defined, for example, a minimum product concentration and a minimum selectivity at reasonable temperature and pressure. After setting the estimated conditions, except for the temperature, this variable should be gradually increased until some reaction is observable. Catalysts can be compared at fixed feed condition since not enough is known about the process. Fixed discharge may not be feasible at this time since discharge may differ widely from catalyst to catalyst.

Only catalysts that are completely inactive within reasonable condition should be rejected. Finding better conditions for a catalyst that shows some promise is best left for the catalyst manufacturer or the investigator. Those most familiar with process chemistry and recycle reactors will be best able to find the optimum condition for a promising catalyst.

An investigation of a limited domain can be done as before, with the main difference that ranges can be wider than for existing processes. Temperature is again the most important variable, and inert gas pressure can be replaced by total pressure. According to Hougen (1951) the effect of total pressure gives the most information on a new process. For the critical variable, initial economic evaluations will give advice, and product concentration will be usually the most important.

After the preliminary tests are made on a promising catalyst and some insight gained on the process, it is time to do a kinetic study and model development. The method of a kinetic study can be best explained on an actual industrial problem. Because more can be learned from a failure than from a success, the oxidation of propylene to acrolein is an instructive attempt at process development. (Besides, to get permission to publish a success is more difficult than to solve the problem itself.) Some details of the development work follow in narrative form to make the story short and to avoid embarrassing anyone.

Propylene oxidation to acrolein example
After several years and millions of dollars were spent to develop a homogenous gas–phase oxidation process to produce propylene oxide, the development was terminated. This was a reaction classified as a

"Degenerate Explosion"; it was a free radical autocatalytic process and control was difficult, but manageable. The main disadvantage was that it produced as much or more acrolein as propylene oxide. Because no market existed for acrolein at that time, the project was abandoned. Within two years, the acrylic market developed and a new project was initiated to make acrolein and acrylic acid by vapor–phase catalytic oxidation of propylene.

The project was justified by decades of experience of the company in commercial catalytic oxidation processes, and some preliminary results gained in laboratory tubular reactors. Due to the similarity to other oxidation technologies, it was decided to skip the pilot–plant step and design a production unit based on other experiences and laboratory studies in 1"Ø and 12" long tubular reactors. All the corresponding analogies were listed and none of the differences were recognized. Nobody studied the homogenous oxidation results, where important lessons were learned at considerable expense.

Skipping the pilot–plant saved 1 to 2 million dollars and made it possible for the company to enter the acrylic market a full year ahead of the competition. It was assumed that the savings would be enough to pay for any changes in the production unit that might be needed.

The development proceeded without the involvement of this author. When the construction of the commercial unit started he was invited to the first major project review, where he was obliged to express his opinion. This was that the acrolein process would not work as designed, and even if it could be modified somewhat to make it work, it would never be profitable due to the cost of the necessary changes. That opinion irritated the working group, who failed to heed the advice until reports of glowing hot discharge at the end of the short, one inch diameter tubular reactor surfaced. Alarmed, management decreed that the author must attend the technical meetings as an advisor, and that the working group had better listen to the advice.

By this time, the construction of the production unit was underway, and in a great hurry a pilot–plant was constructed, the size of a single tube of the 4000 tube commercial reactor. Interestingly, when the glowing discharge

occurred, a significant drop in oxygen concentration also occurred, but there was no loss of acrolein concentration. This demonstrated the autocatalytic nature of the homogeneous reaction. The ignition danger in the bottom head of the commercial reactor became substantial. A finned–tube heat exchanger was recommended for installation right at the discharge end of the tube containing shell of the commercial reactor and above the bottom dished head.

In the laboratory, a recycle rector was installed right after the tubular reactor. The tube was used as a preheater only, and a few experiments were made with the catalyst in the recycle reactor. This exploration of a limited domain already suggested that the operating pressure had to be cut by half to avoid ignition. This agreed with the experience in the homogeneous oxidation, where rates increased with the 3 to 4 order of pressure. During these studies a new lab was installed with two recycle reactors to study the kinetics. The lab was built for computer control and on–line evaluation of experiments with a direct coupled process gas chromatographs. A typical printout of the computer on–line calculation is shown on Figure 6.3.1. (Please notice that this was made in 1972 and the less than perfect look is due to the IBM typewriters since no small printers were available that time. It was felt that a poor quality copy of the archaic original is more valuable than a retyped version.)

On Figure 6.3.1 the first line tells the date and duration of the experiment. In the third line the number of cycles is five. This indicates that feed and product streams were analyzed five times before an evaluation was made. The concentrations, and all other numbers are the average of the five repeated analyses with the standard deviation given for each average value. The RATE as 1/M means for each component the reaction rate in lb–moles per 1000 lbs of catalyst.

Efficiency means component 1 made per component 3 converted, all in molar units. Data show that 89.7% of the converted propylene was accounted for by the formed acrolein. An additional 9.8% efficiency is indicated for acrylic acid. Efficiency to total useful product was 99.5% as long as ignition of homogeneous reaction could be avoided

CATALYTIC REACTION LABORATORY: INITIAL RUNS IN GAS AUTOCLAVES

```
FROM 205R  7-17 10   2346   7-17-72
SUMMARY LOG NO.   87
AUTOCLAVE 2          NO. OF CYCLES   5      VFA
                 ACR    AA    C3H6    02     CO     CO2    HAC    ACET   C3H8    N2      H2O

FEED PCT
        AVG     .000   .000   5.546  5.454  .011   .007   .000   .002   .004   70.448  14.861
        STD     .000   .000   .040   .041   .001   .000   .000   .003   .000    .368    .171
MOLES/HR        .000   .000   .960   .944   .001   .001   .000   .000   .000   12.192   2.572
PART.PR.        .00    .00    6.37   6.26   .01    .00    .00    .00    .00    80.89    17.06

VENT PCT
        AVG    1.167   .128   4.275  3.793  .078   .036   .025   .037   .004   70.820  16.105
        STD     .028   .002   .029   .029   .005   .006   .003   .003   .000    .561    .064
MOLES/HR        .201   .021   .736   .653   .013   .006   .004   .006   .000   12.191   2.772
PART.PR.       1.34    .15    4.91   4.35   .09    .04    .02    .04    .00    81.32    18.49

RATE 1/M
        AVG    3.255   .356  -3.630 -4.716  .186   .080   .071   .097  -.000    .000    3.255
        STD     .092   .006   .148   .169   .015   .019   .002   .013   .000    .000    .092

EFF) PCT       1/3     2/3
        AVG   89.718   9.329                TOTAL FEED ANALYSIS =   96.3 PCT
        STD    1.413    .500                TOTAL VENT ANALYSIS =   96.5 PCT

BAL PCT        C        H       O
        AVG  101.713 100.446  98.278
        STD     .576    .583    .530

TEMP   C  BED IN  BO OUT  WALL    VENT
        AVG 350.280 358.720 354.120 118.040
        STD     .177    .000    .306    .710

PRE PSIG  AUTO    VENT
        AVG 100.120  15.348
        STD     .322    .033

FLO SCFM  FEED    VENT
        AVG  62.128  61.800
        STD     .714    .326
```

Printout by the author.

Figure 6.3.1: Table showing computer on–line calculation.

This was a very clean and efficient process. The total feed or vent analysis was made of a constant volume injected in Vapor Fraction Analyzer (VFA) (a process gas chromatograph.) Balances were also reasonable and conditions of pressure and temperatures were stable. The large increase, more than 8.5°C between the in and out thermocouples, indicated that the recycle ratio was not high enough, at about 8 to 1. Normally this is not enough for a kinetic study, but for this emergency project it was judged to be adequate. (This was done more than 25 years ago and more than a decade after the same quality data at much higher recycle ratio were generated for the ethylene oxide project.)

To avoid ignition of homogeneous oxidation, a special insert was made to cut the free gaseous space in the recycle reactor to a minimum. Recycle flow had to be large, too, in order to keep the per–pass residence time in the empty vapor phase less than the induction period of the homogeneous rate. The catalytic reaction was very fast and the fresh or makeup feed was large. This cut the recycle ratio down although the mass velocity in the catalyst basket was high.

The kinetic study was made in two parts. First, a feed–forward design was executed based on variations in feed conditions. A larger study was made by feed–back design, where conditions were specified at the discharge of the reactor. Details of the two designs can be seen on the tables in Figures 6.3.2 and 6.3.3.

Figure 6.3.2 shows the feed–forward design, in which acrolein and water were included, since previous studies had indicated some inhibition of the catalytic rates by these two substances. Inert gas pressure was kept as a variable to check for pore diffusion limitations. Since no large diffusional limitation was shown, the inert gas pressure was dropped as an independent variable in the second study of feed–back design, and replaced by total pressure. For smaller diffusional effects later tests were recommended, due to the extreme urgency of this project.

The catalyst used for these studies was one that had been rejected by laboratory short tubular reactor experiments as a "hotspot–type" catalyst. This same type was recommended by another corporate lab with experience in catalyst formulations. The "hotspot–type" catalyst gave 3–

times larger productivity and better selectivity than the previously selected "best" catalyst judged by the short lab reactor. All that was needed was a reactor whose heat transfer ability did not limit the catalyst. The higher productivity was taken advantage of, by lowering the temperature to meet the expected lower production rate. This also helped to avoid ignition.

		C_3H_6	O_2	Acrolein	H_2O	N_2
Experiment	T	p_A°	p_m°	p_B°	p_E°	p_I°
1	+	+	+	+	+	+
2	+	+	-	+	-	-
3	+	-	+	-	+	-
4	+	-	-	-	-	+
5	-	+	+	-	-	+
6	-	+	-	-	+	-
7	-	-	+	+	-	-
8	-	-	-	+	+	+
C.P.	0	0	0	0	0	0
Variable	High Level (+)		Low Level (-)		Center Point (0)	
T °C	340		325		332	
*p_A° (C_3H_6)	0.54		0.23		0.39	
*p_m° (O_2)	0.54		0.23		0.39	
*p_B° (Acr.)	1.00		0.034		0.068	
*p_E° (water)	1.57		0.78		1.17	
*p_I° (N_2)	6.80		4.76		5.78	

*in atmospheres

Adapted with permission from original in Catal. Rev.–Sci. Eng., 20, 1, pp. 75-95, © 1979 Marcel Dekker.

Figure 6.3.2: Feed–forward design.

The feed–back design (Figure 6.3.3 on the next page) was a 2–level, 6–variables central composite plan that required 2^6 = 64 experiments for the full replica. A 1/4 replica consisting of 16 experiments was made with an additional centerpoint. This was repeated after every 3 to 4 experiments to check for the unchanged condition of the catalyst. The execution of the complete study required six weeks of around the clock work. In the next six weeks, mathematical analysis and model–building was done and some additional check experiments were made.

Several models were developed and the one shown on Figure 6.3.4 was found to be the simplest. This model accounted for most of the results, conformed with kinetic expressions, and was useful for design purposes.

The predictions checked in the pilot–plant reactor were reasonable. Later, when the production unit was improved and operators learned how to control the large–scale reactor, performance prediction was also very good. The highest recognition came from production personnel, who believed more in the model than in their instruments. When production performance did not agree with model predictions, they started to check their instruments, rather than questioning the model.

Experiment	P_A	P_M	P_E	P_B	T	P
16	-	-	-	-	-	-
2	+	-	-	-	-	+
3	-	+	-	-	+	-
13	+	+	-	-	+	+
12	-	-	+	-	+	-
6	+	-	+	-	+	-
7	-	+	+	-	-	-
9	+	+	+	-	-	-
1	-	-	-	+	+	+
15	+	-	-	+	+	-
14	-	+	-	+	-	+
4	+	+	-	+	-	-
5	-	-	+	+	-	+
11	+	-	+	+	-	+
10	-	+	+	+	+	+
8	+	+	+	+	+	+
C.P.	0	0	0	0	0	0
Variable	Low Level (-)		High Level (+)		Center Point (0)	
P_A (atm, C_3H_6)	0.23		0.54		0.39	
P_M (atm, O_2)	0.23		0.54		0.39	
P_E (atm, H_2O)	0.78		1.57		1.17	
P_B (atm, acr.)	0.034		0.095		0.105	
T°C	323		338		330	
P atm	6.46		9.18		7.82	

Adapted with permission from original in Catal. Rev.–Sci. Eng., 20, 1, pp. 75-95, © 1979 Marcel Dekker.

Figure 6.3.3: Feed–back design.

The startup of the production unit was exciting. The extended surface cooler on the discharge end was installed and about half of the design pressure was used to avoid ignition. In spite of this, on the first day an ignition was observed and emergency shut down was activated. Removing the bottom closure it became evident that the square form of the cooler

left many channels in the circular bottom for the discharge gas to bypass the cooler and to create a large whirlpool of gas under it. This served as a recycle reactor, advantageous for ignition. The free spaces were filled up with firebrick and gas was forced through the cooler.

$$r_B = a_B Exp(22.6 - 12.650\,T)\frac{p_A^{0.5}\,p_M^{0.5}}{1+3.2p_B} \cdot R_B^2 = 0.92$$

acrolein

$$r_C - a_C Exp(25.0 - 14.700T)\frac{p_B^{0.5}\,p_M^{0.5}}{1+3.2p_B} \cdot R_C^2 = 0.92$$

acrylic acid

$$r_D - a_D Exp(22.5 - 13.350T)\frac{p_B^{0.5}\,p_M}{1+3.2p_B} \cdot R_D^2 = 0.92$$

carbon dioxide

$$r_E - a_E Exp(28.1 - 16.600T)\frac{p_B^{0.5}\,p_M^{1.5}}{1+3.2p_B} \cdot R_E^2 = 0.82$$

carbon monoxide

$$r_F - a_F Exp(27.2 - 17.500T)\frac{p_A^{0.75}}{1+3.2p_B} \cdot R_F^2 = 0.90$$

acetaldehyde

$$\text{Where}: r[=]\frac{g.\,mole}{hr.\,kg.\,catalyst} \qquad p[=]atm.\,abs. \qquad T[=]^\circ K$$

The 'a's are dimensional constants, with a value of 1. R^2 is the multiple correlation coefficient, the fraction of total variance in the data accounted for by the model.
Adapted with permission from original in Catal. Rev.–Sci. Eng., 20, 1, pp. 75-95, © *1979 Marcel Dekker.*

Figure 6.3.4: Kinetic model for example.

On the second startup no ignition in the bottom occurred, but it was observed here also that a significant drop in oxygen concentration occurred between the reactor bottom and the heat exchanger, without loss of acrolein concentration. The homogeneous reaction also produced acrolein, just in much lower selectivity. Then, on the third day of

operation, a flame ignition occurred in the pipe connecting the reactor and the heat exchanger. Emergency shutdown did its duty again. The heat exchanger was sited on the opposite side of a road, apparently for aesthetic layout. The connecting pipe was 16 inches in diameter and 70 ft long. Replacing this by a 14 inch pipe increased linear velocity and cut residence time in the pipe just below the induction time for the homogeneous reaction. This avoided further ignition there.

After a few weeks of trouble–free, but low productivity operation it was decided to increase production by increasing temperature and pressure somewhat. The increase agreed with that predicted from the model. After a week another ignition occurred in the heat exchanger. This was also expected qualitatively for some time, but this ignition occurred in the cold, reheating side of the exchanger. The gas went through a scrubber in between, which should have removed the acrolein, but enough remained to start the ignition.

An investigation of the scrubber revealed that a large part was blocked by polymers, cutting much of its efficiency. A material balance also indicated that about half of the acrolein produced was missing, as determined by analysis of the discharge gas from the converter. This was more than needed to explain the ignition on the reheating side of the exchanger. Yet the question remained: where did the approximately 2 ton/hr of acrolein go?

Since the oxidation was done by air, significant blow–off stream vented to a very tall flare, where most of the acrolein survived the flame as it did in many previous ignitions and dispersed in the atmosphere. Acrolein is as toxic as hydrogen cyanide but few people are killed from it since traces of it are strong lacrimants and can be recognized much before it can reach toxic levels. By the way, at the production unit no smell of acrolein could ever be detected, due to the very good construction work. The unit could be operated but never economically; eventually it was scrapped and replaced by a purchased technology. The company permitted use of this example for educational purposes.

6.4 The Workshop Test Problem

Testing kinetic models against a "true" and detailed kinetic expression was the aim of the International Workshop on Kinetic Model Development at the Denver AIChE Meeting in August, 1983 and at the Chicago 1985 Symposium. The UCKRON test problem was described earlier and is presented in Appendix A and B. For more details see Berty et al, (1989.)

Using the UCKRON test problem the results of simulated experiments were calculated for four variables (T, and partial pressures of MeOH, H_2, and CO) at two levels for expressing the rate of methanol synthesis as:

$$r = f(T, p_{MeOH}, p_{H2}, p_{CO}) .$$

This resulted in a $2^4 = 16$ factorial experiments. To these were added 8 "outlayers" and 3 repeated centerpoint: altogether 27 experiments. The levels of variable are shown on the table in Figure 6.4.1.

Five percent random error was added to the error-free dataset to make the simulation more realistic. Data for kinetic analysis are presented in Table 6.4.3 (Berty 1989), and were given to the participants to develop a kinetic model for design purposes. For a more practical comparison, participants were asked to simulate the performance of a well defined shell and tube reactor of industrial size at well defined process conditions. Participants came from 8 countries and a total of 19 working groups. Some submitted more than one model. The explicit models are listed in loc.cit. and here only those results that can be graphically presented are given.

The main lessons learned from the workshop were (with some 5–year old afterthoughts added in parentheses):

- Solutions submitted by workshop participants exhibited more variation in reactor performance than had been expected.
- Much of the variation was caused by the difference in temperature profiles, which were in turn caused in large measure by differences between kinetic models.
- The variations were mainly due to operating conditions very close to the parametrically sensitive region, i.e., to the incipient temperature runaway. Small errors in the estimation of temperature effects caused runaways and, consequently, large differences.
- If results of runaway cases were disregarded and the one very low result with decimal point error neglected, the rest of the results were

between 22 and 44 metric tons/h around the "true" 35 tons/h value. Not outstanding, but it could be corrected in reality by small changes in operating temperature if the system was far from the temperature sensitive conditions. (The temperature where 35 ton/h production could be achieved should also have been required from participants.)

- The mathematical form of the models (and possibly the techniques used to develop them) appeared to be most important in the prediction of the temperature profile.
- The choice of integration technique or algorithm was unimportant as long as the grid size was fine enough to produce accurate results.
- The need for improving and testing temperature effects with exothermic, fast reactions was obvious.
- Mathematical models that ignored kinetic forms may fit the "experimental" results very well but fail to predict critical performance attributes. For example, neglecting the well known exponential form of the Arrhenius function made one, entirely mathematical, model fail in predicting the thermal runaway.
- Although "experimental" results could be fitted well with irreversible rate models, ignoring thermodynamic facts could be disastrous. Although reversibility moderated the maximum temperature at runaway, it was not the most important qualitative result. In fact, the one dimensional (directional, or irreversible, correctly) model was not realistic at these conditions. For the prediction of incipient runaway and the ΔT_{max} permissible before runaway, the reversibility was obviously important.
- This type of testing is worth continuing and should be extended to more complex cases.

Exp.No	Variable	Units	--	-	0	+	++
A.	T	K	470	475	485	495	500
B.	p_{MeOH}	kPa	172	253	507	1013	1520
C.	p_{CO}	kPa	1276	1530	2533	4052	4862
D.	p_{H2}	kPa	5369	5906	7091	8309	9330

Reproduced with permission from Chem. Eng. Comm, 76, pp. 9-33, © 1989 Gordon and Breach.

Figure 6.4.1: Levels of effect variables.

Expt.	Rate mol/m³/s	T Kelvin	Partial CH₃OH	Pressures, CO	kPa H₂
A	7.4224	495	1013	4052	8509
B	5.3572	495	1013	4052	5906
C	6.8278	495	1013	1530	8509
D	4.7978	495	1013	1530	5906
E	9.9904	495	253	4052	8509
F	7.6482	495	253	4052	5906
G	9.3842	495	253	1530	8509
H	7.0958	495	253	1530	5906
I	1.7270	475	1013	4052	8509
J	1.2412	475	1013	4052	5906
K	1.7236	475	1013	1530	8509
L	1.2212	475	1013	1530	5906
M	2.6778	475	253	4052	8509
N	2.0442	475	253	4052	5906
O	2.7114	475	253	1530	8509
P	2.0556	475	253	1530	5906
CP	4.000	485	507	2533	7091
AA	10.2162	500	507	2533	7091
BB	1.3516	470	507	2533	7091
CC	2.6006	485	1520	2533	7091
DD	4.9664	485	172	2533	7091
EE	3.9717	485	507	4862	7091
FF	3.7734	485	507	1276	7091
GG	4.9790	485	507	2533	9330
HH	3.1560	485	507	2533	5369

Reproduced with permission from Chem. Eng. Comm, 76, pp. 9-33, © 1989 Gordon and Breach.

Figure 6.4.2: Table of error–free kinetic data from CSTR simulation.

Expt.	Rate[a] mol/m³/s	Temp Kelvin	p_MeOH	p_CO	kPa H₂
A	6.753	495	1013	4052	8509
B	4.819	495	1013	4052	5906
C	6.270	495	1013	1530	8509
D	4.928	495	1013	1530	5906
E	10.115	495	253	4052	8509
F	7.585	495	253	4052	5906
G	9.393	495	253	1530	8509
H	7.124	495	253	1530	5906
I	1.768	475	1013	4052	8509
J	1.177	475	1013	4052	5906
K	1.621	475	1013	1530	8509
L	1.293	475	1013	1530	5906
M	2.827	475	253	4052	8509
N	2.125	475	253	4052	5906
O	2.883	475	253	1530	8509
P	2.035	475	253	1530	5906
CP1	4.030	485	507	2533	7091
CP2	3.925	485	507	2533	7091
CP3	3.938	485	507	2533	7091
AA	10.561	500	507	2533	7091
BB	1.396	470	507	2533	7091
CC	2.452	485	1520	2533	7091
DD	5.252	485	172	2533	7091
EE	3.731	485	507	4862	7091
FF	3.599	485	507	1276	7091
GG	5.085	485	507	2533	9330
HH	3.202	485	507	2533	5369

[a]Rates are moles methanol formed per cubic meter of catalyst packed reactor volume per second
Reproduced with permission from Chem. Eng. Comm, 76, pp. 9-33, © 1989 Gordon and Breach.

Figure 6.4.3: Data for kinetic analysis. Simulated CSTR results with random error added to UCKRON–I.
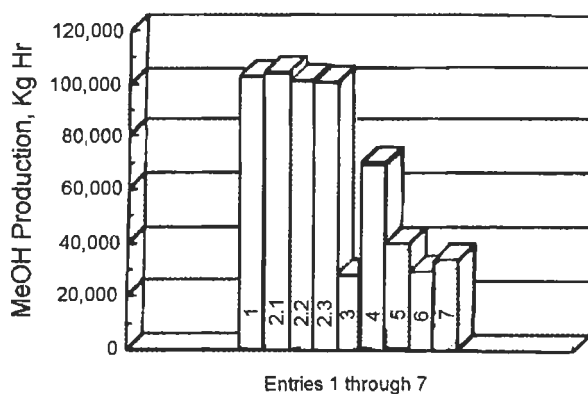
Entries 1 through 7

Figure 6.4.4: Distribution of performance, entries 1–7.
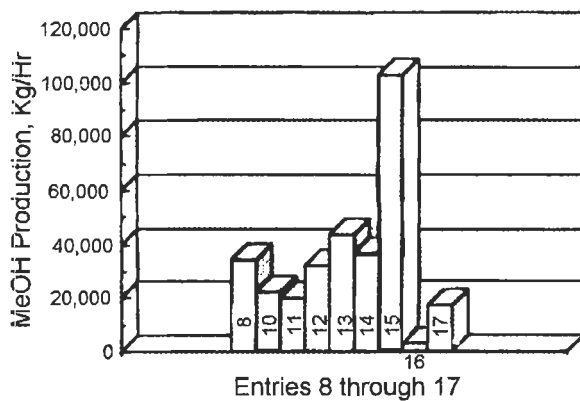
Entries 8 through 17

Figure 6.4.5: Distribution of performance, entries 8–17.
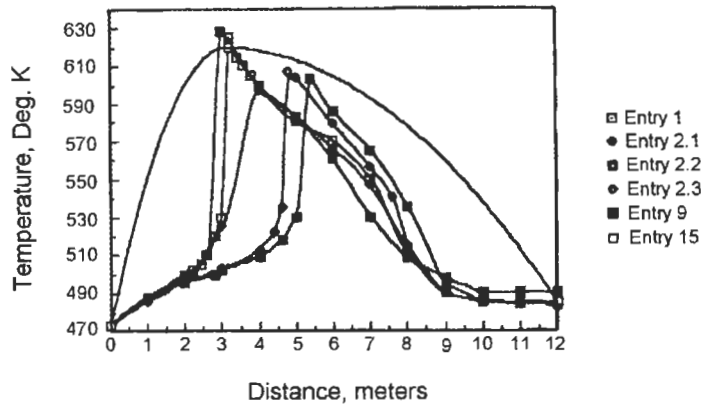
Figure 6.4.6: Models that showed runaway behavior.
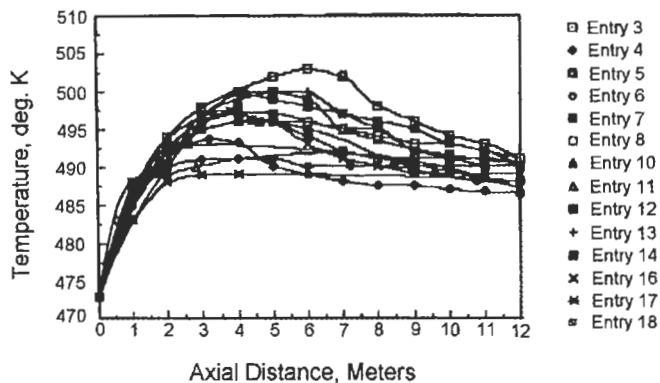
Figure 6.4.7: Models that showed controlled behavior.

Some additional observations from the result

In the original announcement of the workshop the participants were told that everything was to be taken from methanol synthesis except the kinetics. Some may have interpreted this to mean that the known thermodynamic equilibrium information of the methanol synthesis is not valid when taken together with the kinetics. This was not intended, but

many ignored the reversibility of the reaction with disastrous consequences as mentioned above.

Those entries that incorporated the reversibility of the reaction in the kinetics came closer to the "exact" performance. Submission 5, L. H. Hosten and J. J. Perou, assistants of professor G. F. Froment at Gent, Belgium used the table of Yang and Hougen to assemble the model. They used only one temperature dependent term, the energy of activation. The value for this in their correlation was E= 30,376 cal/mol from 27 experimental results. This almost matches the results derived in Chapter 6.3 from 8 experimental results at 4 conditions.

The results of P. Valko and J. Holderith, working with professor P. Benedek in Budapest, Hungary used the same basis, but incorporated 3 temperature terms. This gave the Energy of Activation of 15,561*1.98=30,811 This also matches the value obtained in the previous chapter. The temperature terms in the denominator have a small but significant effect. The model of professor Benedek's assistants was about the best–fitting and best–behaving of the proposed models. This is shown in the following equation:

$$r = \frac{1.16(10^{-3})e^{-15,561(1/485-1/T)}(p_H - p_M/((K/101.3^2)p_C p_H))}{1.0 + 1.35(10^{-3})e^{-3,049(1/485-1/T)}p_M + 5,67(10^{-5})e^{6.227/(1/485-1/T)}pH}$$

Students of professor R. G. Anthony at College Station, TX used a mechanism identical (by chance) to that in UCKRON for derivation of the kinetics. Yet they assumed a model in which the surface reaction controls, and had two temperature dependent terms in the denominator as 13,723 and 18,316 cal/mol. Multiplying both the numerator and the denominator with exp(-15,000) would come close to the E_a/R about 15,000 cal/mol, with a negative sign, and a denominator similar to that in the previously discussed models.

The model that best describes the mechanism is usually very complicated. For dynamic studies that require much more computation (and on a more limited domain) a simplified model may give enough information as long as the formalities of the Arrhenius expression and power law kinetics are incorporated. To study the dynamic behavior of the ethylene oxide reactor,

a simple Arrhenius function and a first order dependence on oxygen concentration was sufficient 25 years ago.

The fitting of these complicated rate expressions requires the use of non–linear least square techniques. Discussing this subject goes beyond the aim of this book. A good reference that helps the understanding of statistics and various mathematical techniques is Box et al, (1978). Here is a field where the skilled experimenter definitely should seek the cooperation of a statistician. The experimenter should also be prepared for some misgivings from statisticians, who do not consider a few expensive results to be amenable to statistical analysis, nor even fewer repetitions a reasonable basis upon which to estimate experimental errors. Unfortunately, both camps are correct; statisticians require more data, and experimenters have budget limitations. Many readers will recognize this scenario: to save money, management stopped a project after fifteen of a required sixteen experiments were completed. While preparations for a new project were underway, the last experiment was sneaked in and the project completed while the investigators were still asking permission to do so.

6.5 Formalized Methods

Some authors have not only given advice but have created methods to execute experiments to generate kinetic models. The "Heuristic Approach to Complex Kinetics" of Cropley (1978) which is well tested, is one that will be described next. Then, other recommendations will be discussed briefly.

Heuristic Approach to Complex Kinetics

Cropley made general recommendations to develop kinetic models for complicated rate expressions. His approach includes first formulating a hyperbolic non–linear model in dimensionless form by linear statistical methods. This way, essential terms are identified and others are rejected, to reduce the number of unknown parameters. Only toward the end when model is reduced to the essential parts is non–linear estimation of parameters involved. His ten steps are summarized below. Their basis is a set of rate data measured in a recycle reactor using a sixteen experiment fractional factorial experimental design at two levels in five variables, with additional three repeated centerpoints. To these are added two outlier

experiments for each variable. All together twenty nine experiments are recommended.

Rule 1: Develop an exponential or power–law model in dimensionless form. This later is achieved by dividing the partial pressures of each variable by their centerpoint value.

$$\ln(r) = f[\ln x_i, (\ln x_i)^2, (\ln x_i)(\ln x_j)]$$

where x_i is the temperature term.

The last term indicates interaction of temperature and partial pressure ($x_j = p_j/p_{j,cp}$)

$$r = k_o e^{\frac{-E}{R}\left(\frac{1}{T}-\frac{1}{T_{cp}}\right)} \prod j \left(\frac{p_j}{p_{j,cp}}\right)^m$$

temperature interactions are in some exponents.

Rule 2. Eliminate any variable that was not significant in the exponential model.

Rule 3. Eliminate temperature terms in the denominator. (Terms with negative exponents in the power law model are considered to belong to the denominator, in the hyperbolic model. *Author.*)

Rule 4. Develop (e.g., write) the hyperbolic equation in terms of the dimensionless variables. This breaks the interdependence of exponential and pre–exponential terms.

$$r = \frac{k_o e^{\frac{-E}{R}\left(\frac{1}{T}-\frac{1}{T}\right)} \prod j \left(\frac{p_j}{p_{j,cp}}\right)^{m_j}}{1+\sum Kj \left(\frac{p_j}{p_{j,cp}}\right)^{n_j}}$$

Rule 5. Arbitrarily assign exponents to terms in the denominator (as shown above, $n_J = 0.5, 1.0, 2.0$.)

Rule 6. Use for E the value obtained in the exponential model.

Rule 7.   Determine the pre–exponential term by setting all variables to center point value, where everything becomes one except the pre–exponential factor, because:

$$\bar{r}_{cp} = \frac{k_0}{1+\sum K_j} \qquad k_0 = \bar{r}_{cp}(1+\sum K_j)$$

Substituting the expression for k_0 in the equation above Rule 5, the expression is ready for non–linear estimation of the coefficients.

Rule 8.   Set the initial value of exponents in the numerator between 0 and 2. The K's should be between 0 and 5. This last range sets the K's to be significantly larger or smaller than 1.

Rule 9.   Estimate by non–linear methods the exponents and K's.

Rule 10.   Adjust exponents to their nearest sensible value and run the non–linear estimation once more to get the best value for E, and K's.

To test the model, first check against experimental values within the design. Second, check against rates not involved in the design. Third, predict rates and execute experiments to check the results.

As expected, a lot of work, estimation and guessing goes into model development. In this estimation the developer should rely on the help and advice of both a chemist knowledgeable about similar mechanisms, and a statistician versed in the appropriate mathematics.

Other approaches and recommendations

Timoshenko et al (1967) recommended running a set of experiments in a CSTR on feed composition (now called feed–forward study), and then statistically correlating the discharge concentrations and rates with feed conditions by second order polynomials. In the second stage, mathematical experiments are executed on the previous empirical correlation to find the form and constants for the rate expressions. An example is presented for the dehydrogenation of butane.

Foment and Mezaki (1969) present a sequential method of experiments aimed at optimum discrimination between rival models as proposed by Box and coworkers. Their example is for tubular reactor data and uses the integral type of kinetic analysis. An example is given for the isomerization of pentane. The concept can be used for CSTR results. An early mistake in the approximation can lead the sequence in the wrong direction, which can generate a large quantity of largely useless data. It was found that executing a limited experimental design at start gives protection against starting in the wrong direction.

Kelkar and McCarthy (1995) proposed another method to use the feed–forward experiments to develop a kinetic model in a CSTR. An initial experimental design is augmented in a stepwise manner with additional experiments until a satisfactory model is developed. For augmenting data, experiments are selected in a way to increase the determinant of the correlation matrix. The method is demonstrated on kinetic model development for the aldol condensation of acetone over a mixed oxide catalyst.

7. Virtual and Real Difficulties with Measurements

According to Murphy's Law, whatever can go wrong, will. To this Jean Cropley added that Murphy was an optimist. Many things can go wrong in a recycle reactor, too. One of these is running at a low recycle ratio. The old advice of James Carberry that a recycle ratio of 20 is about enough in most applications is just general advice. Calculating the gradients or driving forces as suggested in Chapter 3.7 will give a clear picture of what is needed in an application. If the recycle ratio is reasonably high, many other defects in the catalyst charge will be made insignificant, as some calculation examples will show.

A second source of difficulty is caused by the unavoidable empty space in recycle reactors. This limits their usefulness in some studies. Homogeneous reactions in the empty gas volume may interfere with heterogeneous catalytic measurements. Transient experiments could reveal much more information on various steps in the reaction mechanism but material in the empty space can obscure sharp changes.

7.1 Effect of Recycle Ratio

Pirjamali et al (1972) developed a correction procedure for interparticle gradients in recycle reactors. Their study involved recycle ratios n from 36 to 1000 (as defined in this book) that relates to their recycle ratio β

$$n = \beta/(1-\beta)$$

The most important conclusions of their work were that the inter–particle effects are reasonably small for the particular recycle reactor design, and that kinetic constants determined in the recycle reactor were trustworthy.

Schermuly and Luft (1978) reported that in their jet–pump type recycle reactor they could achieve up to $n = 25$ recycle ratios and that was enough to study the kinetics of methanol synthesis. The greatest advantage of their design was that it had no moving parts. This advantage was undercut, however, by the low recycle ratios. Any change in recycle ratio required a change to different sized nozzles.

Georgakopoulos and Broucek (1987) investigated the effect of recycle ratio on non–ideality, both mathematically and experimentally. They investigated two cases from which the bypass case "b" was completely uninteresting, because total bypass of the catalyst bed could be avoided by feeding the makeup directly to the location of highest sheerfield, at the tip of the impeller blade. For their case "a" they showed on their Fig. 3. that from a recycle ratio of about $10^{1.5} = 32$ there was no observable falsification effect. This matched well the conclusion of Pirjamali et al.

Cropley (1967) pointed out that if product concentration influences reaction rate, then feeding only reactants to a CSTR can lead to fallacious results. His argument stated that if no product was fed, the rate could be expressed as $r = C_P (F/V)$ and it followed that $C_P = r V/F$, where C_p is the concentration of the product. Substituting this expression in the place of C_P in the rate function and lifting r out of the right hand side, the resulting equation gave completely wrong results. Feeding product in a feed–forward design was necessary. If the design were made in terms of the discharge concentrations this problem would have been avoided, but to carry out experiments on these terms was difficult, (although not as bad as was anticipated.)

7.2 Catalyst Bed Non–Idealities

Shape of the catalyst bed

Frequently, experimenters who wanted to use just a little catalyst tried to narrow down the basket cross–section by making an insert (a bushing.) This is not the right choice, illustrated by the following calculation.

Select a volume $V = 19.64$ cm^3 of catalyst to be charged both in the regular basket (case A) and in a basket (case B) that is half of the diameter of A. In cases A and B the ΔP and RPM are kept the same. In Cases A and C the volumetric recycle flow remains the same. In row 1 and 2 on Figure 7.2.1, if the diameter drops to half, the height must increase four times (for constant catalyst volume.) In row 4, L/d_p increases four times as well. In row 5, for cases A vs B, if L/d_p increases four times, u^2 has to drop to one quarter, hence u will be one half to maintain constant ΔP. In row 6, for u in A and B and flow cross section 1/4, the volumetric flow will be 1/8 and the recycle ratio also 1/8. In row 7, or u four times larger,

ΔP will be sixteen times higher and for L/d_p of four times longer, the total ΔP will be $4*16 = 64$ times larger. For A and C, if the volumetric flow remains unchanged through a one–quarter flow cross–section, **u** increases four times, and $\mathbf{u}^2$ increases sixteen times. No small pump exists that can take the temperature and pressure of this system.
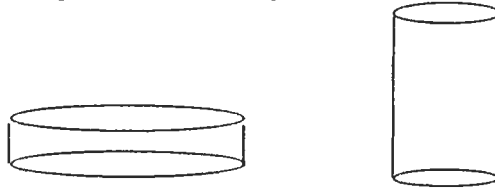
	Case A	Case B	Case C
1. Flow cross section cm^2	19.64	4.91	4.91
2. Bed height, cm	1.00	4.00	4.00
3. Catalyst particle $\varnothing$, cm	0.25	0.25	0.25
4. L/d_p	4	16	16
5. u, linear velocity m/s	1.4	0.7	5.6
6. n recycle ratio at const, ΔP of 2.4 cm of H$_2$O	300	37.5	
7. ΔP in cm H$_2$O at constant recycle ratio	2.4		153.6

Table compiled by the author.

Figure 7.2.1: Shape of the catalyst bed.

Effect of non–uniform flow in non–uniform beds

For the discussion of this problem the extreme case of a bed divided in two halves will be used, with a different size of catalyst in each half.

The catalyst volume is the same on both sides. It is assumed that no diffusional rate limitation exists even in the larger pellets. That is, the chemical reaction rate is controlling. Pressure drop must be the same for both sides, so the flow has to be less over the smaller pellets to maintain the $\Delta P \propto (L/d_P)(u^2/2g) = $ constant.
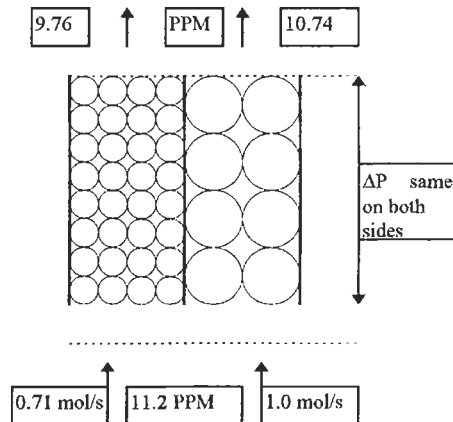
Figure 7.2.2: An idealized non–uniform bed. *Drawing by the author.*

For this to be constant, if L/d_P doubles then u^2 must become one half, or u to be $(1/2)^{0.5} = 0.71$ over the smaller pellets. Since the reaction rate is the same and the catalyst volumes are the same, the number of moles converted are the same. This constant number of moles will result in the 71% flow over the smaller pellets in $1/0.71 = 1.41$ times larger reactant decrease than over the larger pills. The flow volumes are relative, not absolute values.

If the recycle ratio is $n = 71.4$, the concentration gradient—or rather the difference along the length of the bed—is from 11.2 to 10.0 ppm If x part of this 1.2 ppm difference is more and y part is less, then:

$$V * r = nF * \Delta C$$

from the inside balance:

$$V * r = 1.71 * (11.2 - 10.0) = 2.052 \, mol/s$$

$$(V/2) * r = 0.71 * (11.2 - x) = 1.026 \, mol/s, \ x = 9.755 \, PPM$$

$$(V/2) * r = 1.00 * (11.2 - y) = 1.026 \, mol/s, \ y = 10.174 \, PPM$$

Uneven flow, caused by packing differences in the bed, creates differences in discharge concentration, but these will remain insignificant. This will be so if recycle flow is high and the gradient along the catalyst bed is small.

Channeling in shallow beds

Assume that a channel develops in a shallow bed (in fluidization this is called a rat hole) that lets about the same quantity flow through the channel unchanged as is flowing through the catalyst charge. In Figure 7.2.3, as assumed above, equal volumes flow through the channel and through the catalyst bed. This increases the discharge concentration from 6.189 vol % to 6.190 vol %.

Rate is calculated from the outside balance, therefore the concentration difference will not be the correct one, which is:

8.158 - 6.189 = 1.969, but the error laden 8.158 - 6.190 = 1.968

or: 100*(1.969 - 1.968)/1.969= 0.05 % error, which is negligible.

This example shows again that if the recycle ratio is high, errors do not cause much of a problem. In reality, it is not the recycle ratio, but rather the high recycle flow and the very small concentration change through the catalyst bed that helps to cut the significance of mistakes.

F = 2.37 cm3/s
Co = 182 mol/m3

CHANNEL

Ci = 138.119, mol/m3
or 6.191 vol %

Trough cat.   hole

C = 138.071, C = 138.119
     mol/m3   mol/m3
or   6.191   6.189
       vol %   vol %
on average:
     C = 138.095 mol/m3
or   6.190 vol %

C = 138.090 mol/m3
or   6.190 vol %

n =
911
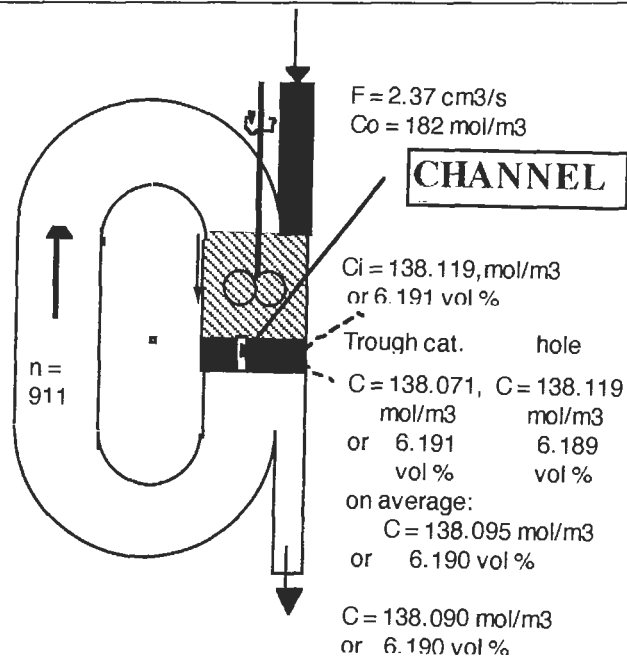
Drawing by the author.

Figure 7.2.3: Channeling in methanol synthesis.

Note that the above case is not the same as Case B of Georgakopoulos and Broucek (1987), for which the make–up feed bypasses the mixing zone and the catalyst bed. That crude mistake can be easily avoided. Instead of a channel, the higher flow can occur at the larger empty volume near the perimeter. This can cause a similar error as a channel can, which is a real error, as discussed Chapter 1.4, but which is negligible as long as the recycle flow is high and the concentration change per pass is low.

7.3 Influence of Empty Space

Homogeneous reactions

In tubular reactors, empty space at the discharge can have a significant effect if some of the products produce radicals. In such cases a free radical reaction may start in the product gas and falsify the measurement results. If this is small it may be hard to prove its presence. In recycle reactors the same problem may look different; the empty space can be an order of magnitude larger than the catalyst filled volume. At every recycle the reacting gas goes through both the catalyst charge and the empty space once.

Many chain reactions are of an autocatalytic nature. This means that a certain "induction" time is needed for the reaction to reach a certain speed. If this is longer than the residence time during one return pass, the homogeneous reaction may not have a chance to reach any speed and little or no harm will be done to the catalytic measurement. The catalyst itself may be generating radicals or just the opposite: it may terminate radicals. The construction material of the reactor may have a similar role. In oxidation of hydrocarbons the steel wall had a chain starting effect when oxygen concentration was high and a terminating effect when it was low.

The check for homogeneous reactions should be done by repeating some experiments with different quantities of catalyst charge. For example, make measurements over 20, 40 and 80 cm^3 of catalyst charges with proportionally increased makeup feed rates. Change the RPM to keep the recycle ratio constant (if possible) or the linear rate **u** constant. The measured catalytic rate should remain the same if nothing happens in the empty space.

If the rate changes, homogeneous gas reactions may be present. To test further, the empty space can be filled up with metal turnings of the construction material used for the reactor. The RPM should be increased to maintain constant linear velocity over the catalyst bed. If a free radical reaction is in progress it will show some change in the results. If it slows down, use it as is or insert special fins that increase surface, but do not create significant resistance to the flow. If additional construction material surface area accelerates the homogeneous rate, then the surface should be coated or treated. A thin gold coating has been used successfully.

The catalytic effect of the reactor wall may also cause problems. Especially when a stainless steel reactor gets overheated in a reducing atmosphere, the outside chromium oxide protective layer gets reduced and nickel can migrate to the surface. After a reactor reaches this state, previously high efficiency catalyst may never perform well again. Repair of the overheated surface may be possible, although extreme caution is required. Try a nitric acid/hydrofluoric acid wash—*very dangerous!*—followed by a water rinse, a sodium carbonate rinse, and a final water rinse. Then run the system empty for a day with air at 100 kPa pressure and a temperature of 450°C. Poisoning the catalytic activity of the walls of an empty reactor

with thiophen is also possible, but risky, because afterwards it is difficult to completely remove all the catalyst poisons.

New reactors should also be treated in air as mentioned above, before they are first used. After the treatment the light yellowish hue indicates the presence of the chromoxide layer on the surface.

7.4 Transient measurements

Transient response techniques supply far more information on any dynamic system than a steady–state test can. In multi–step processes where an overall change is accomplished through a series of elementary steps, the rate of all steps has to be equal to maintain a steady state. When a system in steady state is disturbed by a sudden change in one of its parameters or driving forces, then the different elementary steps will react to the disturbance at different speeds. During the upset, the elementary steps reveal their significance or the lack of it. With proper instrumentation, transient signals can be recorded and analyzed for their information content. The experimentally applied disturbing signals are the pulse (spike, or Dirac delta), the square pulse, frequency change of sinusoidal signals and square step up or down. The most appropriate one depends on the system to be tested, on the instrument that monitors the signal, and on the mathematical techniques available to analyze the resulting exit signal. The simplest and most frequently used is the step change technique.

Any variable or parameter that influences kinetics can be used if well–defined perturbation can be achieved. Temperature was the early favorite in kinetic studies, but in catalysis the heat capacity of the catalyst makes the response for temperature changes very sluggish. A sudden change in one or more of the product or reactant concentrations can be executed faster and usually gives a better response signal.

A good review of the transient response method in heterogeneous catalysis was published by Kobayashi and Kobayashi (1974). These authors credit Bennett (1967) for applying this previously microcatalytic research technique to recycle reactors and thereby, in view of this author, to engineering problems.

Empty volume of recycle reactors

Evaluations of the measurements are based on the transient material balance equation for CSTR:

$$F'(C - C_0) - Vr = -V\frac{dC}{dt}$$

For empty volume determination, when no reaction will proceed, the reaction rate term can be left out. The measurement will be done by running a CSTR with pure methane, and then switching over at zero time to methane with C_0 concentration of carbon monoxide containing methane at unchanged F' flow. The concentration of CO in the reactor and the discharge will grow gradually. It is assumed that neither methane nor carbon monoxide is reacting or adsorbing on the catalyst.

$$F'(C - C_0) = -V\frac{dC}{dt}$$

where at t=0, C=0 and at t=t_1, C=C_1. After rearrangement and integration the discharge concentration will be:

$$C_1 = C_0(1 - e^{-(F/V)t_1})$$

from this it follows that:

$$V = \frac{-F't_1}{\ln(C_0 - C_1)/C_0}$$

The small volumes of the feed line from the switching valve to the reactor and the discharge line to the analyzer can be corrected for, since they will have plug flow. This will only displace the zero time on the recorder and it can be easily corrected.

Multiples of Residence Time	Fraction of Inlet Concentration
1	0.632
2	0.865
3	0.950
4	0.982
5	0.993

Table compiled by the author.

Figure 7.4.1: Flushing of a perfectly stirred vessel.

It is worth noting on Figure 7.4.1 how much time it will take to purge a CSTR of existing compounds. For example if the previous composition

has to be dropped to 2% or less, then a feed equivalent to four residence times must be fed to the system.

Chemisorption measurement

The previous volume measurement was done by methane because this does not react and does not even adsorb on the catalyst. If it did, the additional adsorbed quantity would make the volume look larger. This is the basis for measurement of chemisorption. In this experiment pure methane flow is replaced (at t = 0) with methane that contains $C = C_0$ hydrogen. The hydrogen content of the reactor volume—and with it the discharge hydrogen concentration— increases over time. At time t = t_2 the hydrogen concentration is $C = C_2$. The calculation used before will apply here, but the total calculated volume now includes the chemisorbed quantity.

$$V = V_E + V_C \quad \text{and} \quad V_C\, C_2 = W\, C_M$$

where V_C is the additional "empty" volume with a gas composition of C_2 that must contain equal amounts of hydrogen chemisorbed on active sites with the concentration of C_M mol/kg–catalyst on W kg catalyst.

Remember, H_2 chemisorbs on the surface but it does not react with the inert methane. H_2 concentration is monitored and the pure CH_4 flow is not significantly different from the H_2 containing CH_4 flow; both are the same as in the previous volume test. In this, as well as in the previous experiment, it was important to purge the reactor with CO containing methane until all H_2 and O_2 were removed from the surface, and thereafter to purge long enough to remove all CO by purging with pure methane.

The plot of the following function is given in Appendix F.

$$C/C0 = 1 - \exp(\theta), \quad \theta = -F'/v*t$$

As can be seen on the figure in Appendix F, if the adsorbed "volume" is 25% more than the reactor volume, a good measurement is possible. At a dimensionless time of θ = 2.0, the discharge concentration is 10% lower when adsorption occurs. For a reactor volume of 1000 cm^3 the adsorbed volume is 250 cm^3, which is 250/22412 = 0.011 mol. This much has to be adsorbed on 80 cm^3 = 50 g of catalyst, and this is 0.011/0.05 = 0.22 mol/kg.

An important improvement would be the significant reduction of the empty volume in the recycle reactor. This calls for a special insert to block out most of the empty space without choking the flow. A practical solution of this type is on the drawing board.

The conclusion is that for chemisorption measurements in a CSTR, the matter in the empty space must be minimized, which calls for low (atmospheric) pressure, and low concentration of the chemical, in a low flow of carrier gas. Even at low pressure it will work only for very large surface area materials, like molecular sieves or active charcoals.

The most interesting of transient measurements would consist of tracing the chemisorbing component with an isotope, like in CO hydrogenation, using deuterium. Bennett (1967) suggested this by a step function type disturbance. The Happel method (1977) does not disturb the system's steady state. He only replaces the CO (the adsorbing species in his case of CO oxidation) at time zero by ^{13}CO and follows the changes with a mass spectrometer.

Measurements in tubular reactors

Tubular reactors have empty spaces only between the catalyst particles. This eliminates one big disadvantage of CSTRs. On the other hand, the mathematical description and analysis of the data become more complicated. For chemical reaction studies it is still useful to detect major changes or differences in reaction mechanism.

Ethylene adsorption on oxygenated silver was investigated using frontal chromatography by Marcinkowsky and Berty (1973). A 1/4 inch stainless steel tube was charged with 13 w% silver-containing catalyst and placed in a muffle furnace. Installation was similar to the U-shape tube in Figure 2.1.1. At that time the existence of two different forms of chemisorbed oxygen was generally accepted. That no ethylene adsorption occurs on oxygen free silver was known. Few if any papers were presented on the adsorption of oxidation products.

Before the start of the measurement the catalyst was kept in air at 285°C for 2 hours. Then it was purged with nitrogen and set to the experimental temperature. At time zero, nitrogen containing non-adsorbing methane

and adsorbing ethylene was switched on. At discharge, the gas was monitored by a hydrogen flame ionization detector. The output of the detector is shown on Figure 7.4.2.
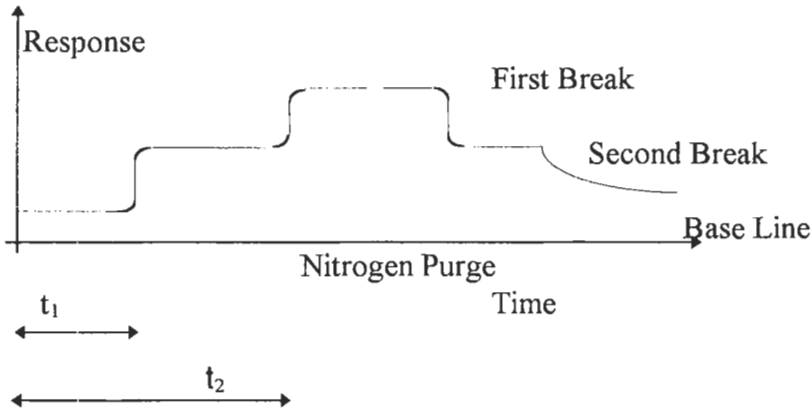
Figure 7.4.2: Ethylene chemisorption on silver.

The retention time of the non–adsorbing methane (t_1) is the measure of the column void volume or holdup. Ethylene is adsorbed by the catalyst, hence it does not reach the detector until the available surface is saturated, at which point ethylene breaks through and is detected by the sensor (t_2). The adsorbed volume of ethylene is given simply by:

$$V_E = F'(t_2 - t_1) \, y_E$$

where F' is in cm^3/s, t is in s, and y_E is mole fraction of Ethylene. Figure 7.4.3 gives the results of adsorption experiments.

Notice on this graph that the 25°C experiments were informative, and results were in the measurable range. At 135°C some intermediate, semi–quantitative results could be seen. At 285°C no detectable adsorption could be seen. Taking the high adsorption result at 25°C as 22.4 mL/kg, this converts to 0.001 mole/kg. Compare this with the 0.22 mole/kg needed for measurable result in the CSTR case in the previous section.

Ethylene oxide secondary oxidation with ^{14}C–tagged ethylene oxide, to clarify the source of CO_2, was done at Union Carbide but not published. This was about 10 years before the publication of Happel (1977). With very limited radioactive supply only a semi–quantitative result could be gained but it helped the kinetic modeling work. It became clear that most CO_2 comes from ethylene directly and only about 20% from the secondary oxidation of ethylene oxide.

Pore diffusion limitation was studied on a very porous catalyst at the operating conditions of a commercial reactor. The aim of the experiments was to measure the effective diffusivity in the porous catalyst and the mass transfer coefficient at operating conditions. Few experimental results were published before 1970, but some important mathematical analyses had already been presented. Publications of Clements and Schnelle (1963) and Turner (1967) gave some advice.

For this measurement a single tube (from a reactor containing several thousand) was installed in a large–scale lab, penetrating several floors. The tube was charged with the commercial catalyst and equipped with several sampling points on the side. The first was about 0.5 m from the bottom entrance and the last about the same distance before the exit at the top. This was done to avoid difficulties with the boundary value definitions of the bed. The samples were negligible in quantity compared to the nitrogen flow rate, and only the first and the last sample points were used. Analysis of the samples was done by continuously operated hydrogen flame detectors. The feed was nitrogen containing a few vol.% of added ethane.

A frequency response technique was tried first and some results were received. The useful frequency domain was less than one order of magnitude, while in electrical problems five orders of magnitude can be scanned. The single pulse technique was more revealing, but evaluation by moments had the usual accumulation of errors. Fourier transform of the pulse test results was the final method.

Results were surprising. By getting Def $> \theta * D^{E/N}$, i.e., the effective diffusivity of ethane in nitrogen was larger than predicted by the formula of:

$$\text{Def} > (\theta/\tau)D_{E/N}$$

which requires $\tau < 1$, and this could be explained by assuming that the laminar flow was passing through the catalyst, enhancing the diffusional molecular flux. The evaluation of the mass transfer coefficient was only partially successful. Experimental errors causing the joint confidence interval such that it obscured the result. Qualitatively it could be estimated that it was high enough so its effects could be ignored.

Transient Studies in an Adiabatic Packed–Bed Reactor was the title of a publication by Berty et al (1972). This was in connection with thermal runaway of reactors. The pertinent subject will be discussed in a following chapter in which the interest is focused on how to avoid the onset of a runaway. Here the object of the experiment was to see what happens after a runaway has started.

Although very few papers exist on experimental work in this area, many theoretical and computational studies were published. Generating data was a longer range objective of this experimental work, largely to check the usefulness of various models. The experimental reactor was an adiabatic unit chosen to generate results in one spatial dimension for easier mathematical analysis. The flowsheet for the experimental unit is given in Figure 7.4.3.
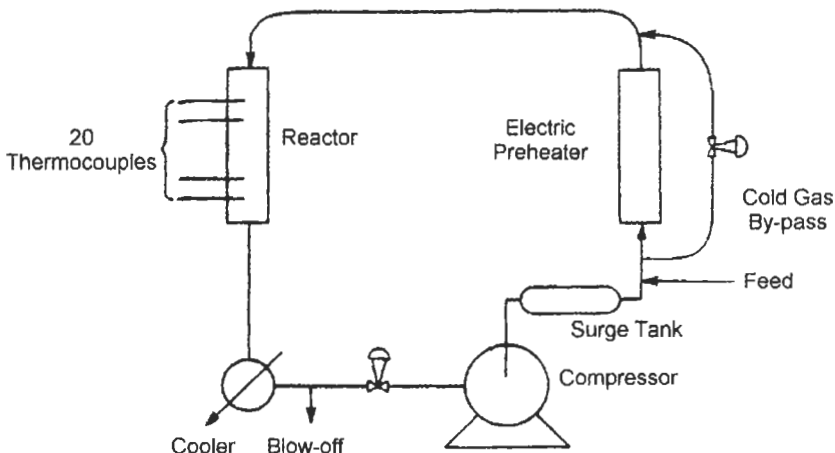
Reproduced from Proceedings of the Fifth European and Second Int. Symposium on Chemical Reaction Engineering, B, 8–27–38, © 1972 Elsevier.

Figure 7.4.3: Single–stage adiabatic reactor system.

The unit was built in a loop because the needed 85 standard m^3/hour gas exceeded the laboratory capabilities. In addition, by controlling the recycle loop–to–makeup ratio, various quantities of product could be fed for the experiments. The adiabatic reactor was a 1.8 m long, 7.5 cm diameter stainless steel pipe (3" sch. 40 pipe) with thermocouples at every 5 centimeter distance. After a SS was reached at the desired condition, the bypass valve around the preheater was suddenly closed, forcing all the gas through the preheater. This generated a step change increase in the feed temperature that started the runaway. The 20 thermocouples were displayed on an oscilloscope to see the transient changes. This was also recorded on a videotape to play back later for detailed observation.

Ethylene oxidation was studied on 8 mm diameter catalyst pellets. The adiabatic temperature rise was limited to 667 K by the oxygen concentration of the feed. With the inlet temperature at 521 K in SS and the feed at $p_{O2, o}$=1.238 atm, the discharge temperature was 559 K, and exit $P_{O@}$=1.187 atm. The observed temperature profiles are shown on Figure 7.4.4 at various time intervals. The 61 cm long section was filled with catalyst.
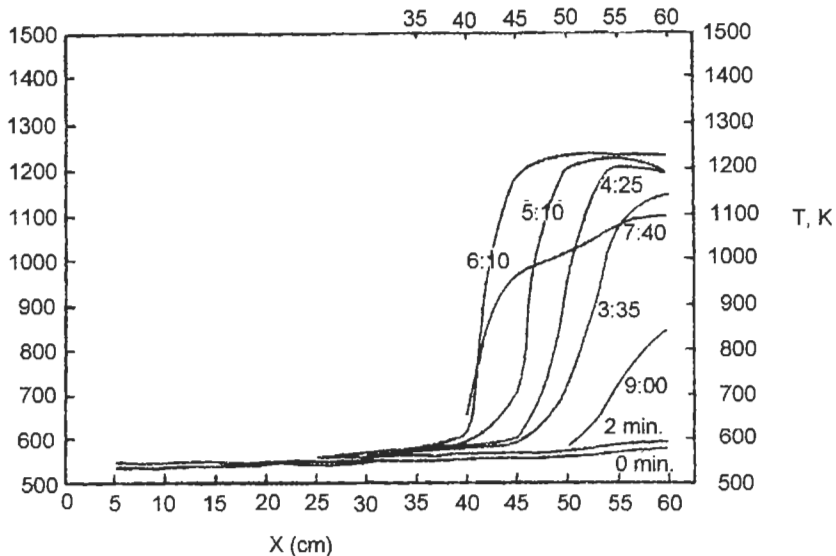
Figure 7.4.4: Observed temperature profiles.

After the 20K step increase in feed temperature, not much change could be observed for two minutes. Then the last thermocouple started to increase from 560 to 1200 K level, and the hot zone widened. The forward migration rate of the hot zone was about 5 cm/min. After about six minutes, the oxygen content of the cycle gas became very low and temperature slowly started to decline. With this the experiment terminated.

For simulation on the IBM 360/65 computer, the reaction was represented as first order to oxygen, the limiting reactant, and by the usual Arrhenius form dependency on temperature. Since the changes here were rapid, various transport processes had significant roles. The following set of differential equations was used to describe the transient system:

Concentration in fluid:

$$M(p_{j-1} - p_j) - (p_j - P_j) = a_1 \frac{dp_j}{d\theta}$$

Temperature of the fluid:

$$H(t_{j-1} - t_j) - (t_j - T_j) = a_2 \frac{dt_j}{d\theta}$$

Concentration in the particle:

$$(p_j - P_j) - k_j P_j = a_3 \frac{dP_j}{d\theta}$$

Temperature of the particle:

$$(t_j - T_j) + k_j \beta p_j + R(T_{j+1}^4 + T_{j-1}^4 - 2T_j^4) = a_4 \frac{dT_j}{d\theta}$$

The initial conditions, t_j, p_j, T_j, P_j, $j=1,2,3...N$, $\theta=0$, and boundary conditions $t_1(\theta)$, $p_1(\theta)$, at $\theta>0$ are specified.

The various equation coefficients are derived from physical properties:

$$a_1 = \frac{\varepsilon \rho_f}{k_g a_v \overline{PM}}, \text{minutes} \qquad a_2 = \frac{\varepsilon \rho_f c_f}{h_f a_v}, \text{minutes}$$

$$a_3 = \frac{d_p}{6} \frac{\theta \rho_{fs}}{k_g PM}, \text{minutes} \qquad a_4 = \frac{d_p}{6} \frac{\rho_s c_s}{h_f}, \text{minutes}$$

$$H = \frac{Gc_f}{h_f a_v} \frac{1}{l} = H_h \frac{1}{l} \qquad M = \frac{G}{Pk_g a_v \overline{M}} \frac{1}{l} = H_g \frac{1}{l}$$

H_h and H_g are the height of heat and mass transfer units, respectively, in multiples of the cell height, l. H and M are the same in dimensionless units.

$$k_j = \frac{d_p}{6} \frac{\rho_s S_g k_o'}{k_g} e^{-\frac{E}{RT_j}} = k_o e^{-\frac{E}{RT_j}}$$

$$R = \frac{\varepsilon' \phi}{2h_f} \sigma, \ K^{-3}, \ \beta = \frac{-k_g}{h_f} \Delta H_r$$

Here R=r is the parameter for radiative heat transfer in K^{-3} units.

β is a heat of reaction term, in K/atm units

t_j is the fluid temperature in the j–th axial position

ε' is the particle emissivity

l   is the cell dimension in m

θ is the clock time in minutes

The rest of the symbols are in the dimensions of the notation in this book, even if not in the same units.

Results of the simulation are given on Figure 7.4.5, with the important parameters specified. In the simulation $a_1=a_2=a_3=0$ was used since these were orders of magnitude smaller than a_4. More details are given in the original paper.

Conclusions were:
1. Simulation by the improved Euler method has shown that a significant radiative heat transfer must be present before reaction zone migration can be demonstrated.
2. An order of magnitude higher radiation parameter R was needed than reported in the literature to match the observed migration rate.
3. With the chosen coefficient the general character of the simulation agreed with the experimental data. For better agreement, a more detailed kinetic model would be needed.
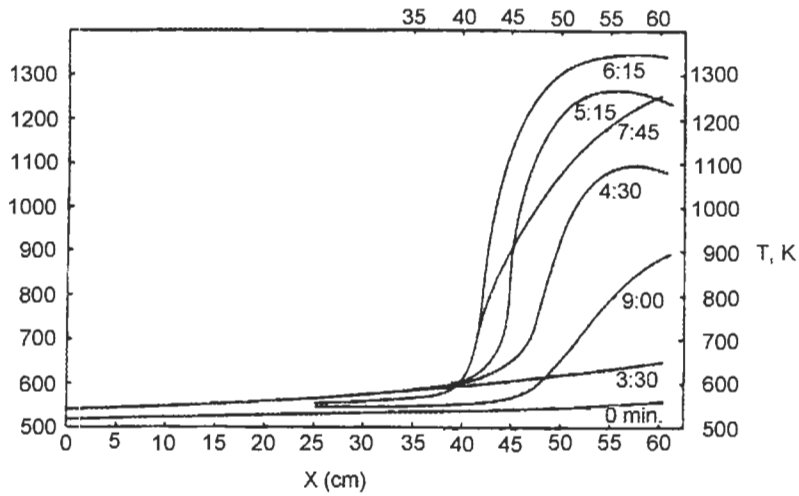
Simulation with $a_4=0.164$ min., $k=Exp(10.79-9040\ K/T)$, and $r=7.1 \times 10^{-11} K^{-3}$

Reproduced from Proceedings of the Fifth European and Second Int. Symposium on Chemical Reaction Engineering, B, 8-27-38, © 1972 Elsevier.

Figure 7.4.5: Simulation results.

8. Reactor Design

The basic problem of design was solved mathematically before any reliable kinetic model was available. As mentioned at start, the existence of solutions—that is, the integration method for reactor performance calculation—gave the first motivation to generate better experimental kinetic results and the models derived from them.

Commercial or production reactors for heterogeneous catalytic processes are versions of the so–called integral reactors, so the fundamental process of design is integration. In particular, the necessary catalyst–filled reactor volume must be calculated that will give a desired production rate. This then includes finding conditions to achieve the desired production, at a certain selectivity and minimal operating costs and investment, to maximize the return on investment.

The achievement of an economic optimum is limited by requirements of selectivity, energy efficiency, safety, and pollution control. The total design of production reactors therefore involves a few more tasks than the basic integration method.

In this chapter the interest will be limited to a few basic technical tasks; detailed economic considerations are outside the scope of this book. A brief story is included here as an important general lesson. In 1963, Union Carbide Corp. was building the first very large "world–scale" ethylene oxide plant. During that time, a statistically designed set of evaluations was executed, consisting of more than one hundred design calculations for the complete synthesis loop, to find the most economic operating conditions. When the results were inspected, the most economical condition was not at the maximum efficiency, as everyone had assumed. It took days to analyze and understand the unexpected result.

The surprise was finally clarified by remembering that this was an air operated plant built in a thermodynamic cycle, (the Brayton or gas turbine cycle) with a 18,000 HP air compressor. This generated 5 MW of salable

electric power from the reaction heat. The worth of total salable products, ethylene oxide and power peaked at less than the maximum efficiency of the system. For the maximum efficiency of ethylene oxide production, a lower temperature was required that in turn cut the thermal generating efficiency. An overall scheme of this technology is shown on Figure 8.0.1 (Berty 1983), where the ethylene oxide plant is only one block in the energy generating scheme.

$$10\ C_2H_4 + 5\ O_2 \longrightarrow 10\ C_2H_4O$$

$$3.3\ C_2H_4 + 10\ O_2 \longrightarrow 6.6\ CO_2 + 6.6\ H_2O$$
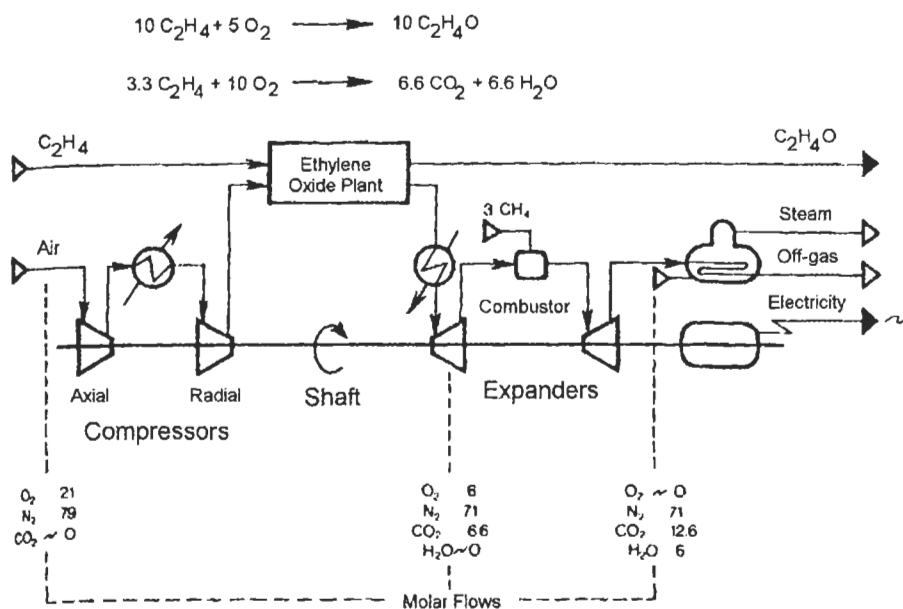
Reproduced with permission, © 1983 Academic Press.

Figure 8.0.1: Cogeneration of ethylene oxide and energy in a Brayton cycle.

In general, for basic petrochemicals that are not much more expensive than fuel (energy) itself, the energy recovery or use is important. Therefore, exothermic reactions should be executed at the highest temperature and endothermic reaction at the lowest, within the range that the reaction permits. In addition, reactors should not be optimized only for their own performance, but also for the optimum economy of the full synthesis loop or the full technology.

8.1 Integration Methods

In a catalytic reactor, concentrations and temperature change along the flow path of the reactants, and in some cases also normal to the flow. The sum of all these changes over the catalyst–filled volume in time will give the production of the reactor. There are several methods to account for all these changes, illustrated on Figure 8.1.1.
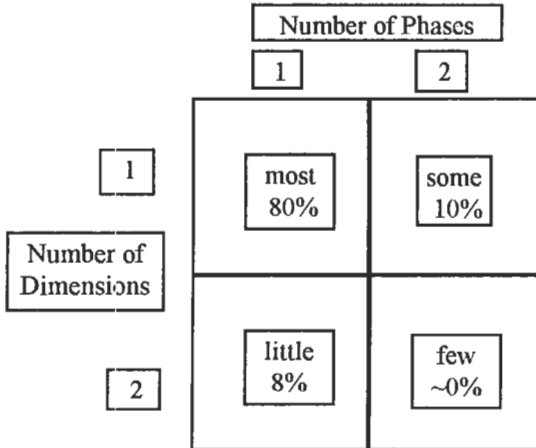
Drawing by the author.

Figure 8.1.1: Integration methods.

The one–dimensional, single–phase model is used mostly to design tubular reactors. These handle the heterogeneous reaction as a quasi–homogeneous process in the catalyst–filled volume. Plug–flow assumption is used and all the temperature gradients are considered to be in the film on the inside of the tube. At high enough flows and a large aperture ratio ($L/d_P > 150$) axial mixing can be ignored as negligible. Radial mixing at the small ratio of $d_T/d_P < 6$, and high $Re_P > 100$ can be considered complete, that is, no significant concentration gradient is in the radial direction and the plug–flow assumption applies. This model was used by most of the Workshop participants (Berty et al, 1989)

The two–phase model is used mostly to check very exothermic or endothermic reactions, to calculate the temperature difference between catalyst and gas at extreme conditions, or when accounting for changes in both phases is needed. This model was applied to the two–phase counter–

current operation of the OXITOX® reactor at steady–state for integrating the UCKRON test problem (Berty 1997.)

The two–dimensional model is also used for checking and for studies. Atwood et al (1989) used this to compare two methanol tubular reactors, one 1.2 m long and the other 12.0 meters long. Except for the difference in length, the two reactors were identical in all aspects, and ran at the same space velocity, that is, the shorter reactor operated at one tenth the linear velocity and Re_P, of the longer one. The two–dimensional two–phase model is seldom used and then only for simulation of transient operation. Usually one spatial dimension and time are the coordinates. It was used to simulate the consumption of the solid reactant soda during the startup of the OXITOX reactor (Berty 1997.) In the following, a few examples of integration methods will be given; a complete review of this field is left for others.

One dimensional, one–phase model

Here the integration method will be shown that was used for the workshop program (Berty et al, 1989) to integrate the UCKRON rate equations. Since this is about methanol synthesis the reaction is shown here with the stochiometric coefficients:

$$CO + H_2 = CH_3OH$$
$$-1 \quad\;\; -2 \quad\;\; +1$$
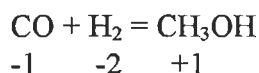
From the equation it is obvious that a large contraction of volume takes place. For every mole of methanol made, two mole volumes disappear. The volumetric flow and superficial linear velocity will change substantially, with some physical properties changing too. Only the mass velocity will remain constant, and the Reynolds number will change little with the changing viscosities. All this will influence pressure drop, and must be taken into account. The heat transfer coefficient will change very little and can be neglected. A diagram for model development appears in Figure 8.1.2.

The change of the molar flow of the components can be expressed as:

$$\frac{d(F'C_M)}{dx} = Vr,$$

$$\frac{d(F'C_{II})}{dx} = -2Vr,$$

$$\frac{d(F'C_C)}{dx} = -Vr$$

The fractional distance from the inlet is **x**, and **r** is the kinetic expression. In the quoted case, it was the UCKRON test problem that is detailed in the Appendices. The change in volumetric flow rate due to the reaction can be considered by the above equations as follows. Since:

$$C_{total} \equiv C_H + C_C + C_M = \frac{P}{RT}$$

$$\frac{dF'}{dx} = -\frac{2RT}{P}Vr$$

$$F'_0, \ C_{H,0}, \ C_{C,0}, \ C_{M,0},$$

$$\frac{d(F'C_M)}{dx} = Vr, \quad r = f(T, \Pi C_i)$$

$$\frac{dT}{dx} = \frac{(-\Delta H_r)}{\rho c F'}Vr - \frac{U}{\rho c}\frac{V}{F'}\frac{4}{d_t}(T - T_w)$$

$$\frac{dP}{dx} = \left(\frac{fL}{d_p}\right)\frac{16F'^2 \rho}{n_t d_t^4 \pi^2}\frac{1}{1000}$$
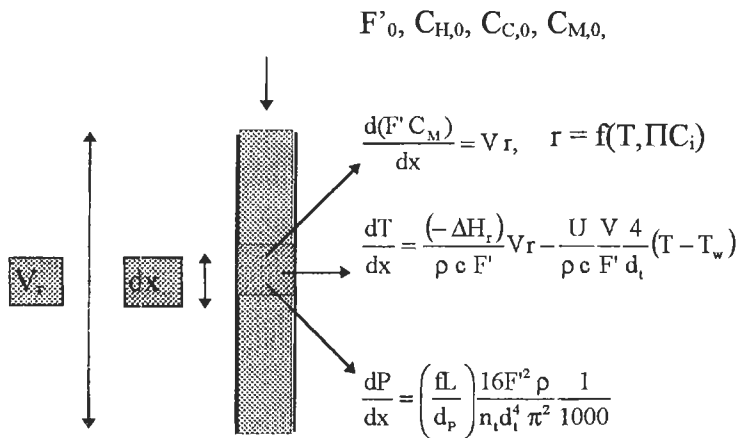
Drawing by the author.

Figure 8.1.2: Diagram for model development.

Pressure drop in the tube can be expressed with the use of the friction factor from the Ergun equation:

$$\frac{dP}{dx} = \left(\frac{fL}{d_P}\right)\frac{16F'^2}{n_t d_t^4}\frac{\rho}{\pi^2}\frac{1}{1000}$$

in kPa, where:

$$f = \frac{1-\varepsilon}{\varepsilon^3}\left(1.75 + 150\frac{1-\varepsilon}{Re_P}\right) \qquad Re_P = \frac{4F'\rho a}{d_P \pi \mu} \qquad \rho = \sum_i 1000 MW_i C_i$$

Temperature change along the tube is expressed as:

$$\frac{dT}{dx} = \frac{(-\Delta H_r)}{\rho\, c\, F'}Vr - \frac{U}{\rho\, c}\frac{V}{F'}\frac{4}{d_t}(T - T_w)$$

Initial conditions for the system of differential equations shown before are given by the values of state variables known at the inlet of the reactor:

$$F', C_i \,(i = CH_3OH, CO, \text{ and } H_2), T, \text{ and } P \text{ are given at } x = 0.$$

Some systems may show "stiff" properties, especially those for oxidations. Here the system of differential equations to be integrated are not "stiff". Even at calculated runaway temperature, ordinary integration methods can be used. The reason is that equilibrium seems to moderate the extent of the runaway temperature for the reversible reaction.

Shell–side temp., K	473.0	483.0	485.0	485.1	493.0	513.0
Max. tube–side temp, K	478.2	498.2	515.4	555.6	601.3	613.0
Location from inlet of max. temp, m	3.29	4.82	7.19	9.04	2.80	1.50
Outlet temp., K	477.0	490.8	491.72	492.05	497.56	522.22
Outlet [McOH], vol %	2.639	6.899	12.230	22.78	27.38	33.56
Fraction of equil.value	0.0013	0.0080	0.0178	0.0499	0.0942	0.4678
Production rate, kq/hr	14,697	35,546	57,624	91,760	103,739	117,741

Reproduced with permission, © 1989 Gordon and Breach.

Figure 8.1.3: Results of reactor simulation with "true" kinetics (with pressure drop).

To check the effect of integration, the following algorithms were tried: Euler, explicit Runge–Kutta, semi–implicit and implicit Runge–Kutta with stepwise adjustment. All gave essentially identical results. In most cases, equations do not get stiff before the onset of temperature runaway. Above that, results are not interesting since tubular reactors should not be

operated there. The location of the runaway limit is important only to know how to avoid it. Figure 8.1.3 (Berty et al 1989) and Figure 8.1.4 (Berty et al 1989) show the results. In this illustrations the workshop task is answered . This included the answer to the question of the production rate of a 4000 tube reactor (assumimg that all tubes perform the same) although the performance of a single tube was calculated and multiplied by 4000.
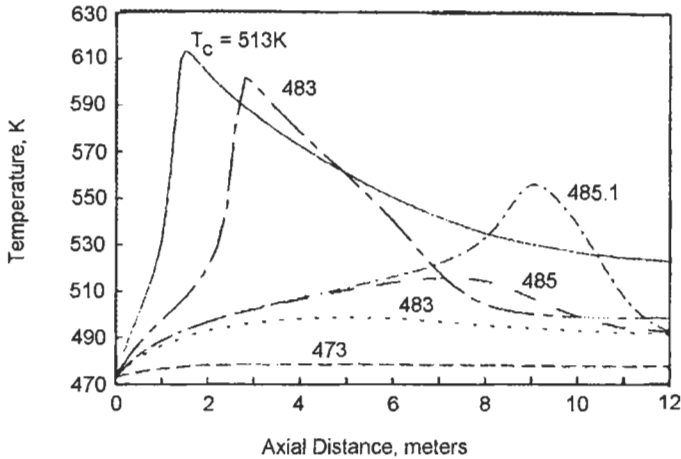
Reproduced with permission, © 1989 Gordon and Breach.

Figure 8.1.4: Simulated temperature profiles with "true" kinetics and coolant temperature as parameters.

Total # of Steps	500	1000	2000	5000
Max. tube–side temp, K	613.0	613.0	613.0	613.0
Location from inlet of max. temp., m	1.49	1.50	1.50	1.50
Outlet temp., K	522.2	522.2	522.2	522.2
Outlet [MeOH], vol %	33.587	33.572	33.562	33.546
Fraction of equil. value	0.4682	0.4680	0.4679	0.4677
Production rate, kg/hr	117,799	117,768	117.747	177.714

Reproduced with permission, © 1989 Gordon and Breach.

Figure 8.1.5: Effects of stepsize on integration results at 513 K.

Figure 8.1.5 (Berty et al 1989) shows the effect of step size on integration results at a 513 K shell temperature with boiling water. This is the

condition well beyond temperature runaway and hence in a sensitive region. Yet results show practically no difference using between 500 and 5000 steps.

The effect of integration method and stepsize must be checked for every application where temperature runaway is possible. Those will be mostly oxidations, but other reactions can be very exothermic, too. During the 1973/74 oil crisis, when synthetic "natural" gas projects were in vogue, one of the CO hydrogenation technologies was found to be very exothermic and prone to runaway also.

One dimensional, two–phase model

In the steady–state operation of the OXITOX reactor, pelletized solid of catalytically activated sodium carbonate slides down a "Silo" type reactor. Counter–current to the solid flow, the polluted air rises through the sliding bed of solids. At reaction temperature the following reaction occurs:

$$Mn/Mg$$
$$2\ C_2HCl_3 + 3\ O_2 + 3\ Na_2CO_3 \Rightarrow 6\ NaCl + H_2O + 7\ CO_2$$
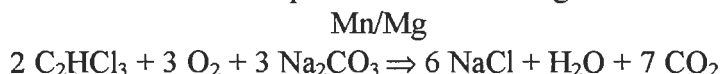
The trichloroethylene is oxidized, the gaseous products are removed by the flowing air, and the chlorine is captured by the solid soda and forms salt. The solid salt is removed by discharging the used OXITOX at the bottom of the reactor. This is a relatively slow reaction and the central interest is in removing the last traces of toxic chlorinated compounds (for which TCE is only a model compound), therefore a very simple model was used. Based on conservation principles, it was assumed that chloride removed from the gas phase ends up in the solid phase. This was proven in several material balance calculations. No HCl or other chlorinated compound was found in the gas phase. The consumption rate for TCE was expressed as:

$$\frac{F_y(-dy)}{\alpha_y dV_r} = kC_0 y \frac{6(1-\varepsilon)(1-X)^{2/3}}{d_p}$$

$$\frac{F_y(-dy)}{\alpha_y dV_r} = \frac{F_s dX}{\alpha_x dV_r} \quad \text{or} \quad K = \frac{\alpha_x F_y}{\alpha_y F_s} \text{and} dX = K(-dy)$$

F_y and F_S are molar flow rates of gas and solid, $\alpha_y = -2$, and $\alpha_X = -3$, are the stoichiometric numbers for TCE and soda. The rate is now a unique function of y for the moving bed reactor, and k is in m/s.

Taking the upward direction as positive, when both $F_y < 0$ and $F_S < 0$, represents a co–current downflow operation, if $F_S < 0$, but $F_y > 0$ means a counter–current operation. The rest of the equation defining the system can be seen in Berty (1997). Integration was done by the Romberg method as is used in Mathcad PLUS 6 (1996) software.

Two–dimensional, one–phase model.

This model was used by Atwood et al (1989) to compare the performance of 12 m and 1.2 m long tubular reactors using the UCKRON test problem. Although it was obvious that axial conduction of matter and heat can be expected in the short tube and not in the long tube, the second derivative conduction terms were included in the model so that no difference can be blamed on differences in the models. The continuity equations for the compounds was presented as:

$$\left(\frac{\partial^2 C_i}{\partial r^2} + \frac{1}{r}\frac{\partial C_i}{\partial r} \right) + \frac{Pe_r R_i^2}{Pe_z L^2}\frac{\partial^2 C_i}{\partial z^2} + \frac{R_i^2 Pe_r}{u_z d_p}\sum_j r_j \alpha_{i,j} = \frac{R_i^2 Pe_r}{L\, d_p u_z}\frac{\partial u_z C_i}{\partial z}$$

A diagram to explain the notation for the model is given in Figure 8.1.6.
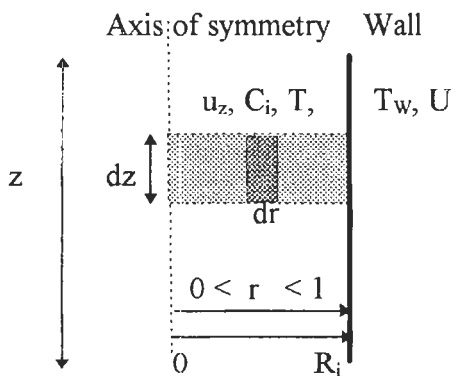
Drawing by the author.

Figure 8.1.6: Notation for the model.

Boundary conditions:

$$\frac{\partial C_i}{\partial r} = (0, z) = 0 \qquad C_i(r,0) = C_i^0$$

$$\frac{\partial C_i}{\partial r} = (1, z) = 0 \qquad \frac{\partial C_i}{\partial r}(r,1) = 0$$

The continuity equation for temperature is:

$$\left(\frac{\partial^2 T}{\partial r^2} + \frac{1}{r}\frac{\partial T}{\partial r}\right) + \frac{Pe_r}{Pe_z}\frac{R_i^2}{L^2}\frac{\partial^2 T}{\partial z^2} + \frac{R_i^2 Pe_r}{G_z d_p c}\sum_j r_i\left(-\Delta H_j\right) = \frac{R_i^2 Pe_r}{L d_p u_z}\frac{\partial u_z T}{\partial r}$$

and the boundary conditions are

$$\frac{\partial T}{\partial r}(0,z) = 0. \quad T(r,0) = T_0, \quad \frac{\partial T}{\partial r}(1,z) = -\frac{U d_p}{k_t}(T - T_r), \quad \frac{\partial T}{\partial z}(r,1) = 0$$

Axial pressure drop was calculated using the Ergun equation:

$$\frac{dP}{dz} = \left[150\left(\frac{1-\varepsilon}{d_p u_z / \eta}\right) + 1.75\right]\left[\left(\frac{1-\varepsilon}{\varepsilon^3}\right)\right]\left[\frac{\rho u^2}{d_p}\right]$$

The implicit Crank–Nicholson integration method was used to solve the equation. Radial temperature and concentrations were calculated using the Thomas algorithm (Lapidus 1962, Carnahan et al,1969). This program allowed the use of either ideal or non–ideal gas laws. For cases using real gas assumptions, heat capacity and heat of reactions were made temperature dependent.

Two–dimensional, two–phase model

In contrast with the previous sophisticated method, the example for this case is greatly simplified. The subject is the same oxidation of trichlorethylene (TCE) as a pollution control task. While the mentioned methanol synthesis is a highly exothermic process, the oxidation of 100 PPM of TCE hardly makes any heat. Therefore, the concentration change is followed in the reactor and any change in temperature is neglected (isothermal behavior is used). The aim of this work was to clarify the concentration changes during startup of the oxidizer. The two dimensions monitored here were bed length and time. Concentration or conversion both in the gas and solid phases have been calculated. The fraction of unconverted solid is shown on Figure 8.1.7 by volume and time. The equations to be integrated are:

$$\rho_s \frac{-\partial y}{\partial t} + \frac{F_y(-\partial y)}{\alpha_x \partial V_r} = k'(C_0 y)\rho_s (1-X)^{2/3}, \qquad dX = K(-dy)$$

The integration was executed similarly to the Grossman (1946) method of double stepwise integration on an Excel spreadsheet. For a preliminary estimate a rough grid was outlined. Column 1 to 100 represented time in hour units, while rows gave the reactor volume in 1 to 30 liters. Results of the integration can be seen on Figure 8.1.7 (Berty 1997). On this figure, the unconverted fraction of the solid soda is on the ordinate, reactor volume is on the abscissa, and time is the parameter. In general this figure shows the reaction zone movement in the solid phase; from it the unconverted soda can be read at any length and any time in the reactor.
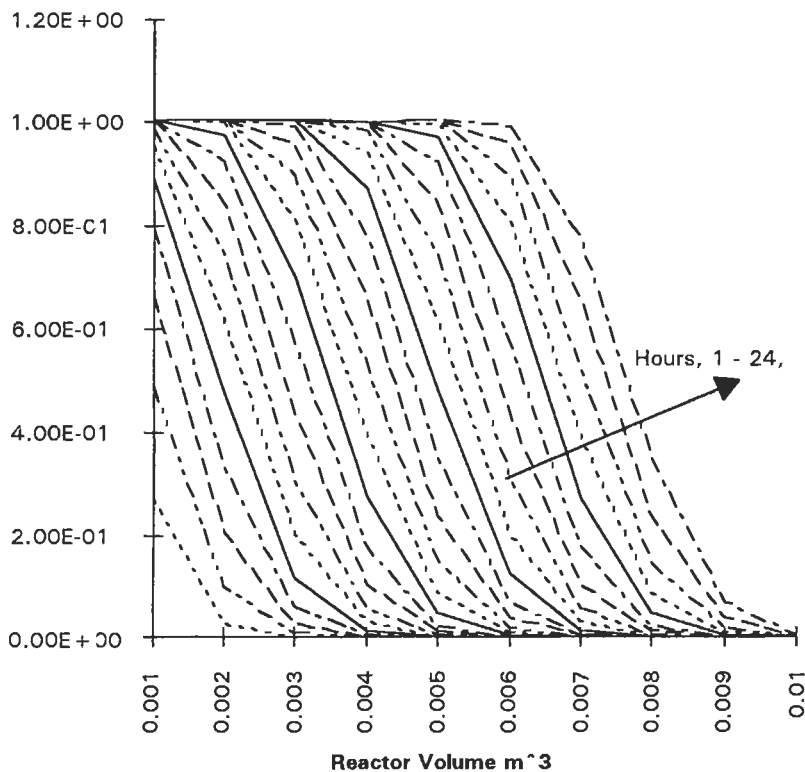
Figure 8.1.7: Consumption of Na$_2$CO$_3$ by Volume and Time

8.2 Handling of Heat in Reactors

Exothermic catalytic reactions are executed in heat exchanger–type multi–tube reactors. Catalyst is in the inside of the tubes, although the opposite can be used, especially if the coolant liquid must be kept at high temperature, and the vapor pressure is high. Some exothermic reactions are also executed in adiabatic reactors of tray–type construction, where the heat removal is effected in the heat exchanger between the stages or trays of the reactor. These are mostly used for reactions where high temperature leads to an equilibrium. Utilization of reaction heat is an important cost–reducing operation for exothermic reactions. To get the maximum value of byproduct heat, the reaction must be executed at the highest temperature permitted by reaction conditions, safety and pollution control.

Endothermic catalytic processes must be supplied with the reaction heat lost, due to generally high temperature required for these reactions. Heat is generally supplied by hot combustion gases or by radiant heat if the catalyst is in tubes. Even if the catalyst is in adiabatic beds, heat can be supplied to the reacting fluid through empty reheater tubes installed between the reactor stages. Another way to supply the heat requirement for endothermic reactions is to combine them with exothermic reactions; internal combustion is a common example. Periodic heating and reaction is just one more way to supply the heat in non–steady–state operation. This method was used in the old Houdry dehydrogenators. In the large catalytic crackers the catalyst is in a moving bed. During cracking, the byproduct coke deposits on the catalyst and decreases its activity. Then the catalyst moves through the regenerator where coke is removed by burning and the catalyst gets hot.

Some of the most common methods of heat transfer with catalytic reaction will be briefly reviewed.

Tubular Reactors

Heat exchanger–like, multi–tube reactors are used for both exothermic and endothermic reactions. Some have as much as 10,000 tubes in a shell installed between tube sheets on both ends. The tubes are filled with catalyst. The larger reactors are sensitive to transient thermal stresses that can develop during startup, thermal runaways and emergency shut downs.

Cooling for exothermic reactions can be effected by circulating liquid coolant in the shell or by boiling coolant. The least expensive coolant is water; for higher temperatures tetralin can be used, or a eutectic mixture of biphenyl and biphenyl–oxide ([5]Dowtherm ®, Therminol®, Diphyl®) chlorinated aromatics, or glycols. Liquid metals (mercury, eutectic mixture of metallic sodium and potassium) and molten salts are available, although some of these have not been used for some time. Others were removed from usage more recently due to toxicity and environmental regulations. The first multi–tube reactor the author saw during World War II was a mercury–cooled reactor for the oxidation of naphthalene to make phthalic anhydride. (In the U.S. there was a mercury–boiling power generating plant on the West Coast.) The general features of a multi–tube reactor are shown on Figure 8.2.1.
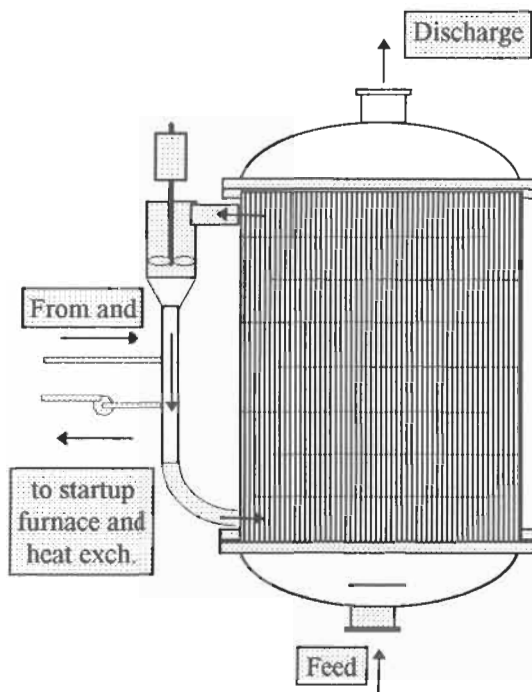
Drawing by the author.

Figure 8.2.1: Tubular reactor.

---

[5] Registered tradenames of Dow Chemical Company, Monsanto, and BASF.

A circulating liquid–cooled tubular reactor is shown on the above Figure 8.2.1. The axial pump, on the left upper corner, circulates the liquid. Flow is upward in the shell. This helps to remove any vapor or inert gas pockets that could have accumulated at some corners above the baffle cuts. Tubes are not tightly fit in the holes of the baffles, so 10–30% of the heat exchange fluid flows through those openings and avoids the path through the baffle cuts. Some designs avoid putting tubes in the baffle cut area because heat transfer will be different, and most likely not as good as in the cross flow area above the baffles. Some reactors have more elaborate fluid distribution systems than shown on the figure, and others just rely on high enough velocities to make up for unevenness of the entrance flow.

Coolant flow is set by the designed temperature increase of the fluid and needed mass velocity or Reynolds number to maintain a high heat transfer coefficient on the shell side. Smaller flows combined with more baffles results in higher temperature increase on the shell side. Reacting fluid flows upwards in the tubes. This is usually the best plan to even out temperature bumps in the tube side and to minimize temperature feedback to avoid thermal runaway of exothermic reactions.

Tube sizes are 1 to 1.5” Ø for exothermic reactions and up to 3 or 4” Ø for endothermic reactions. Reactors with 3” Ø made for an endothermic dehydrogenation in the synthetic rubber program during World War II were later used for exothermic hydrogenation at Union Carbide Corp. In the endothermic reaction, if a cool spot developed at the centerline in the reactor tubes, it cut catalyst utilization but no other loss was incurred. When it was used for exothermic reactions, a nickel catalyst of good quality and long life was deactivated much faster than expected. After more than 20 years of less than perfect performance a detailed thermal analysis and simulation revealed that only a short length of each tube was working and there was a overheating at the center. At the hot spot, catalyst deactivated gradually by organic deposits and solid structure changes, and the working zone moved down to where catalyst was not used (or misused) yet. In weeks, the working zone reached the bottom of the tube and production started dropping abruptly. Then catalyst in the reactor was regenerated by oxidation. During this time the large and reversible loss was converted to a small but permanent loss and production started again. After a few such periods the catalyst had to be changed.

Crystallographic investigation revealed nickel–spinnel formation of the catalyst with the alumina carrier. This needed one hundred or more degrees Centigrade higher temperature than any thermocouple ever indicated.

Reactors with boiling fluid cooling are very similar in construction to liquid–cooled reactors. The main difference is the lack of baffles. Well–designed boiling fluid reactors are similar to reboilers in distillation tower bottoms, in that 10 to 15 times more liquid circulates than is evaporated by the reaction heat. This ensures a reasonably uniform shell side temperature. If the reactor shell discharges vapor only, at the bottom of a 30 foot (10 meter) long reactor tube, the static pressure can be 100 kPa or 1 atmosphere higher. A correspondingly higher boiling point at the bottom may prevent the start of boiling and cause a much lower heat transfer coefficient there. For vapor pressure temperature relationships of water, tetralin, and Dowtherm A ®, see Figure 2.2.5 in Chapter 2.

Charging a reactor with catalyst, making certain that an equal quantity packs quickly into each of several thousand tubes, takes special skills and equipment. The low d_t/d_p ratio of approximately four makes the equal charging especially difficult. By random events, bridging in the tubes can occur at any length between the falling catalyst particles. This leaves an empty length below the bridging and this tube will behave quite differently from the rest of the tubes. If a pre–measured volume of catalyst is charged to every tube, then those tubes that have bridging will have some leftover when the tube is filled to the top.

In reactor construction, the tubesheet is the most expensive part and the possibility of tubes getting loose from the tubesheet is the most dangerous problem. Therefore, large reactors have some limitations on the rate at which they can be heated (for example, 25°C/hour), to avoid developing temperature differences in the body which lead to transient thermal stresses. These stresses can cause tubes to bend and break loose from the tube sheets.

In spite of all these problems and difficulties, tubular reactors are the most important equipment for organic intermediate production in the petrochemicals industry.

Adiabatic reactors

These are less expensive and less troublesome than tubular reactors. All the catalyst volume needed for a given conversion is usually divided in several beds or stages. In large catalyst volumes, the stages may be in separate vessels, or in small volumes in the same vessel but divided into several trays.
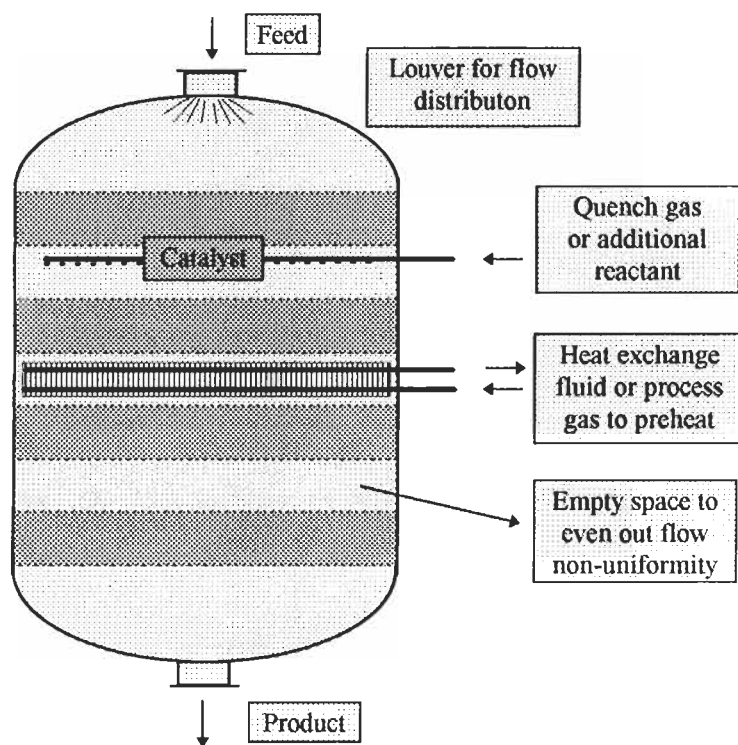
Drawing by the author.

Figure 8.2.2: Conceptual scheme for a tray–type adiabatic reactor.

There are many reasons for division into trays. The best known reason is to limit the temperature change by having a heat exchanger between trays. The other is to give an opportunity to inject a reactant, the concentration of which was limited by safety or selectivity reasons. The final reason is to compensate for uneven flow distribution, the result of uneven catalyst packing across a bed, which happens during catalyst charging. The channels of low resistance to flow have a tendency to extend themselves.

To prevent this the bed must be interrupted, that is cut into multiple layers. In the space between layers there is equalizing of pressure and flow. This way a reasonably equal residence time distribution can be achieved even if every tray has its own non–uniformity.

Exothermic reactions leading to thermodynamic equilibrium are performed in adiabatic reactors. These are SO_2 oxidation to SO_3 in sulfuric acid production, some forms of ammonia synthesis, and methanol production from syngas. Among the endothermic reactions executed in adiabatic reactors is that of naphtha reforming to high octane gasoline. This reaction includes isomerization of paraffins, and forming some olefins and aromatics. Unless aromatics are separated for use as petrochemical starting materials, these are hydrogenated. This is done in a separate unit and is made to stay within the benzene concentration limits permitted for motor vehicle fuels. Ethylbenzene dehydrogenation to styrene is another example.

On Figure 8.2.2 the louver below the entrance nozzle is very important if mass flow is high. In a flow test on a model that was linearly scaled down to one–half size (to one–eighth on a volume basis) a two inch flat vertical cross–section was laid on a black "smoke" table. Moist air was fed at half of the mass velocity expected for the full size reactor. A pulse of phosphorous pentachloride was injected just above the entrance as a flow marker. The inlet gas—expanding not much more than the 14° jet angle—shot through the first tray loaded with catalyst and flowed backwards through the catalyst close to the walls. After this shocking observation, a flow distributing louver was installed, right at the entrance point, and this eliminated the problem.

After the first catalyst tray the injection of additional reactant or unheated feed gas is shown. This latter is for cooling. After the third tray an empty space is used just to even out flow non–uniformities.

The author tried to build various adiabatic reactors for exothermic reactions. Some of the considered models given below are from Berty (1969). One was a tray type reactor in which the finned cooling tubes occupied about as much space as the catalyst tray did. The catalyst holding trays had manholes on the side of the reactor for charging and removing

the catalyst. A model of this was used in the previously mentioned inlet flow distribution experiment.
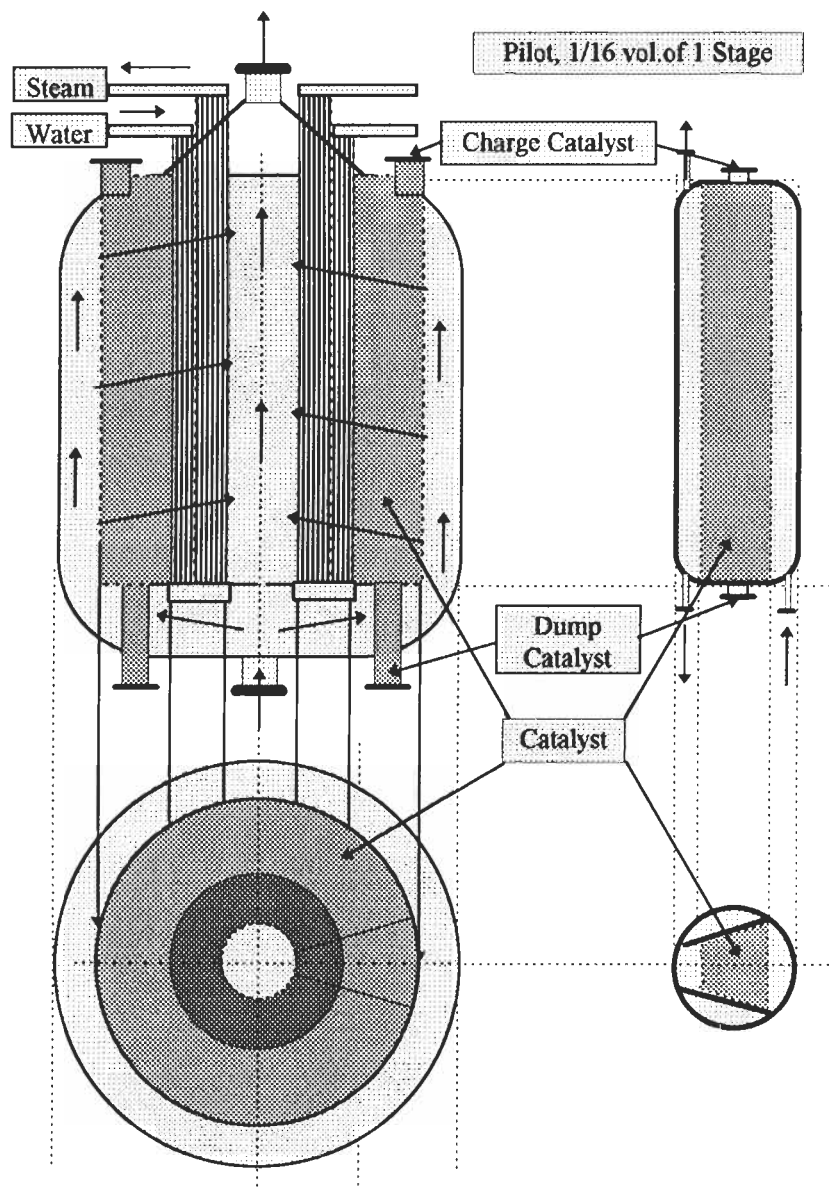
Drawing by the author.

Figure 8.2.3: Radial inward–flow reactor.

For a very large plant a six–stage adiabatic reactor was designed. Every stage was to occupy one large cylindrical vessel and flow was to go in a horizontal direction through a cylindrically shaped catalyst basket. The gas leaving the catalyst was fed directly to heat exchanger tubes and left the reactor through a central discharge tube. Details of the proposed construction are given in Figure 8.2.3.

For testing the basic design of the radial inward–flow adiabatic reactor, an old ethylene oxide production unit was used. This had been shut down but was in operable condition. The recycle compressor was the basic limiting factor for design of the test unit. This was enough to feed about one–sixteenth of a single stage of the new reactor. Therefore, a wedge–shaped sector of the large unit was constructed and placed in a cylindrical pressure vessel. This sector held 18 tons of catalyst (shown in the upper right quarter of Figure 8.2.3.)

The unit was operated on and off for several months, undergoing various improvements, before it was finally shut down. The major problem was that cooling tubes were not installed. This was considered only as a control device to set the inlet temperature to the next stage. Another important role was understood later, and that was the prevention of ignition of homogeneous reactions at the discharge of the catalyst bed. Also, it was necessary to run at high mass velocity to avoid ignition. The resulting pumping cost to overcome the high pressure drop would have used up all the gains, so the project was abandoned.

Fluidized bed reactors

Fluidized bed catalytic reactors seem to have so many advantageous features that they were considered for many processes. One of the advantages is their excellent heat transfer characteristics, due to the large catalyst surface to volume ratio, so very little temperature difference is needed for heat transfer. This would make temperature control problem–free. The second is the uniformity of reaction conditions in the bed.

Even the good heat transfer conditions turned out to be false, however, if the correlation derived for single cylinders by McAdams (1954) were extrapolated to Re_P < 100. Nelson and Galloway (1975) pointed out that at low Reynolds numbers the real heat transfer coefficient could be four

orders of magnitude less than the value calculated by the McAdams method.

In the late 1950s a large oil company had a problem with a very large fluidized bed reactor. Although they hoped for integral reactor performance, the worst they assumed might happen would be a CSTR operation. It was even worse, though, because non–uniformities caused a large part of the gas to bypass at one side while the rest worked as a poorly–stirred reactor. Temperature differences as high as 25°C were measured laterally inside the bed.
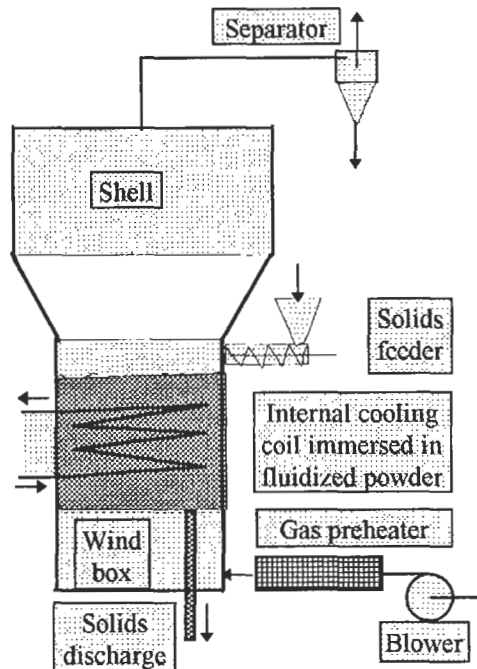
Drawing by the author.

Figure 8.2.4: Fluidized bed reactor

Fluidized bed reactors do not have to perform poorly, but special conditions must be maintained for good performance. A basic process for silicone manufacturing, which is not practiced much anymore, is the reaction of silicon metal with methyl chloride to form dimethyl dichlorosilane:

$$2\,CH_3Cl_{(g)} + Si_{(s)} \xrightarrow{\;Cu\;} (CH_3)_2\,SiCl_{2(g)}$$
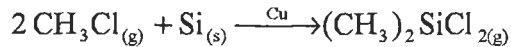
This reaction is carried out in tall fluidized beds of high L/d_t ratio. Pressures up to 200 kPa are used at temperatures around 300°C. The copper catalyst is deposited onto the surface of the silicon metal particles. The product is a vapor–phase material and the particulate silicon is gradually consumed. As the particle diameter decreases the minimum fluidization velocity decreases also. While the linear velocity decreases, the mass velocity of the fluid increases with conversion. Therefore, the leftover small particles with the copper catalyst and some debris leave the reactor at the top exit.

The previous example was a rather unique application and not a typical case for fluidization. Although some fluidized bed reactions are executed at elevated pressure, like the naphtha reforming, most are used at atmospheric or at low pressures. The preceeding conceptual sketch, Figure 8.2.4, gives the most important features of a fluid–bed, catalytic reactor.

Characteristic of fluidized bed reactors is the large "wind box" to equalize pressure. This is a primary requirement to get even flow through the bed. The expanding shell at the upper part is there to retain as much solid as possible in the reactor.

Catalytic reactions performed in fluid beds are not too numerous. Among these are the oxidation of o–xylene to phthalic anhydride, the Deacon process for oxidizing HCl to Cl_2, producing acrylonitrile from propylene and ammonia in an oxidation, and the ethylene dichloride process. In the petroleum industry, catalytic cracking and catalyst regeneration is done in fluid beds as well as some hydroforming reactions.

Several patents exist on carrying out exothermic reactions for manufacture of reactive intermediates where high selectivity is essential. Even this author has a patent to make ethylene oxide in a transport line reactor (Berty 1959). Yet no fluidized bed technology is in use today. Mostly fixed bed, cooled tubular reactors are used for that purpose.

9. Thermal Stability of Reactors

9.1 The concept

The steady–state operation of any reactor requires that the heat removed should equal the heat generated:

$$q_{rem} = q_{gen}$$

where

$$q_{rem} = U \, (S/V) \, (T - T_C),[6]$$

and

$$q_{gen} = (-\Delta H)r, \quad r = k_0 e^{-E/RT} C^n$$

The above statement is obvious. Almost as evident is the statement that since heat generation rate increases with temperature, heat removal rate should increase even faster. This would eliminate continued temperature increase and prevent temperature runaways.
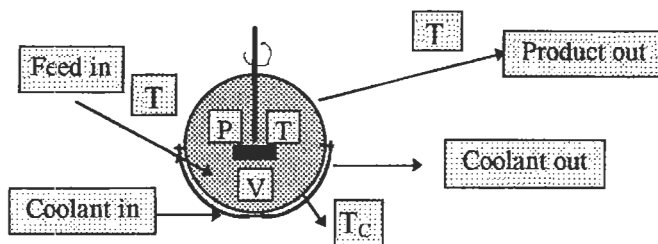
Drawing by the author.

Figure 9.1.1: Thermal stability.

To understand this, consider the following case which is limited to a homogeneous reaction executed in an "isothermal" CSTR as shown in Figure 9.1.1. Isothermal here means feed and discharge are at the reaction temperature, and all heat is removed by heat transfer through the walls.

---

[6] The heat removed includes the heat carried by the sensible heat of the reacting fluid also. If the feed was at a lower temperature than the reactor then $q_{ad} = (F/V) \, \rho \, c \, (T - T_0)$. For the example it was assumed that $T - T_0 = 0$ for simplicity sake as the "isothermal" CSTR.

Assume that the reaction is running steadily with $\Delta T = T - T_C$. This can be very small if **U** (the heat transfer coefficient), or **S** (the surface), or both are large. Assume this, and set $\Delta T = 2$ K. Now some temporary outside cause (a difference in feed purity, catalytic contamination, etc.) makes the reaction and heat generation run faster, resulting in an increase of T by one K and ΔT to 3 K. This increases the heat removal rate by 50 %. The reaction and heat generation rates increase for one degree, e.g., by 15 %. Once the temporary cause is gone the reaction temperature will return to its original value at constant T_C without any outside control action.

Now assume that **U** and **S** are not large and that $\Delta T = 20$ K is needed to keep the heat balance. In this case when something causes the temperature to rise even for a very short time by one K, the reaction rate will increase, just as before, by 15%. The heat transfer rate will increase by a ratio of (21-20)/20, that is by 5 %. The 5 % increase cannot restore the heat balance and the reaction temperature will keep rising. A temperature runaway will occur.

9.2 Intuitive derivation

From the previous thought experiment it is natural to suppose that if reaction temperature increases, the heat transfer rate should increase more than the heat generation rate. This is expressed mathematically as:

$$\frac{dq_{rem}}{dT} > \frac{dq_{gen}}{dT}, \quad \text{and} \quad \frac{dq_{rem}}{dT} = US/V, \quad \frac{dq_{gen}}{dT} = q_{gen}\frac{E}{RT^2}\frac{C}{C_0}, \quad \text{for 1st order.}$$

$$\text{Since} \quad q_{rem} = US/V(T - T_0), \quad \text{and} \quad \frac{dq_{rem}}{dT} = US/V, \quad \text{therefore}$$

$$\frac{dq_{rem}}{dT} = \frac{q_{rem}}{T - T_0}, \quad \text{replacing this into the inequality for slope condition}$$

$$\frac{q_{rem}}{T - T_0} > q_{gen}\frac{E}{RT^2}\frac{C}{C_0}, \quad \text{because } q_{rem} = q_{gen}, \quad T - T_0 < \frac{RT^2}{E}\frac{C_0}{C}$$

The above inequality, called a "slope" condition, is the requirement for thermal insensitivity, expressed here for first order reactions. This form was derived by Perlmutter in (1972.) In most cases it is adequate to define the condition for a stable reactor, but not always. The area of sensitive domain was defined by Van Heerden (1953.)

The first observation of sensitivity–stability was reported by Liljenroth (1918) in connection with the autothermal operation of ammonia oxidation reactors. Papers of Damköhler (1937) and Wagner (1945) went unnoticed. At Union Carbide Corp. Perkins (1938) used zero order kinetics to define a safe range for ethylene oxidation in an unpublished report. His result,

$$T - T_0 < RT^2/E$$

is a conservative estimate for higher than zero order reaction rates. Since for a first guess or orientation at heterogeneous catalytic reactions:

$$E/RT \cong 20, \quad T - T_0 < 0.05\, T$$

The works of Wilson (1946) and Frank–Kamentskii (1939, 1961) finally had the first impact on the industry. The paper of van Heerden (1953, 1958) started the academic investigations. Conceptually significant experimental work was started by Wicke and Vortmeyer in (1959). Schmitz (1975) reviewed the field. His references included almost 300 papers, according to his estimate about 40% of all publications in the field. Of those, only 45 papers reported on experimental work, and only 8 of those on industrially significant processes.

Early investigators did not distinguish between sensitivity and stability. This only started after the Aris and Amundson (1958) paper was published. The main difference is that stability problems include a feedback for heat against the feed flow. In the case of sensitivity there is a solution at every temperature, even if the solution changes rapidly. With stability problems there may be some temperature ranges where either no steady–state can be achieved or the steady–state location will depend on from what extreme it was approached. In a CSTR the backmixing causes the thermal feedback; in an integral reactor the heat conduction against the feed flow is the reason.

9.3 Analytical solution

Aris and Amundson (1958) solved the coupled, time–dependent material and energy balances, linearizing the equations about the operating point by a Taylor series expansion. This made the solution possible by the method of characteristic equations. The solution yielded two equations, one the slope condition and the other recognized by Gilles and Hofmann (1961) as the condition that sets the limits to avoid rate oscillation. This is called the

"dynamic" condition and important only for higher than first order rates. To avoid oscillations the increase of heat removal rate with the increase of temperature must be larger than the difference between heat generation rate increase due to temperature alone and reaction rate decrease due to the concentration drop alone. The rest of the theoretical derivation given by Aris and Amundson (1958) will be omitted here.

Carra and Forni (1974) derived the criteria that Carberry (1976) referred to in his book. These are equivalent to the original derivation of Aris and Amundson (1958). The notation is easier to understand and closer to the notation in this book. Eliminating some typographical errors, the criteria are:

$$\left(1+\frac{1}{Da_I}\right)\left(\frac{1}{Da_I}+U-\gamma\beta\right)+\gamma\beta > 0, \quad \text{slope condition,}$$

$$1+\frac{2}{Da_I}+U-\gamma\beta > 0, \qquad \text{dynamic condition.}$$

These can be rearranged to:

$$1+U_0Da - \frac{\gamma\beta Da}{1+Da} > 0, \quad \text{for slope, and}$$

$$1+U_0Da - \gamma\beta Da + (1+nDa) > 0, \quad \text{for dynamic criteria}$$

9.4 Stability criteria explained

The *material balance function* for a CSTR, m(C,T) is the transient material balance equation:

$$(C_0-C)+\frac{V}{F}r(C,T) = \frac{V\,dC}{Fdt} \equiv m(C,T) \text{where}:$$

$$r(C,T) = k_0 e^{-E/RT} C^n \text{ and} V/F = \theta,$$

$$\frac{\partial m(C,T)}{\partial C} = -1-\theta nkC^{n-1} \text{that is already dimensionl ess,}$$

now using the familiar terms of $Da_1 = \dfrac{rV}{CF} = \theta\,k\,C^{n-1}$

$$\frac{\partial m(C,T)}{\partial C} = -(1+nDa_1), \text{if n} = 1\frac{\partial m(C,T)}{\partial C} = -(1+Da_1)$$

The partial derivative of heat generation rate with respect to temperature is also needed. This we can get from the usual rate law multiplied by the heat of reaction:

$$q_{gen} = (-\Delta H)k_0 e^{-E/RT} C^n, \quad \frac{\partial q_{gen}}{\partial T}\Big|_C = (-\Delta H)\left(\frac{E}{RT^2}\right)k_0 e^{-E/RT} C^n$$

converting this to dimensionless form, by multiplying both sides by $\dfrac{\theta}{\rho c}$,

and using $\gamma = E/RT$, $\theta = V/F$, $\beta = \dfrac{(-\Delta H)C}{\rho c T}$, and $Da_1 = \theta k_0 e^{-E/RT} C^{n-1}$

then the result is $\dfrac{\partial \bar{q}_{gen}}{\partial T} = \gamma \beta Da_1$, where $\bar{q}_{gen}$ is

the heat generation rate in temperature dimension.

The full heat—removed equation and its derivative are still needed. These are:

$q_{rem} = q_{tr} + q_{ad}$, heat is removed by transfer and by sensible heat,

$q_{rem} = \dfrac{\rho c}{\theta}(T - T_c) + U(S/V)(T_0 - T)$ and multiplying this by $\dfrac{\theta}{\rho c}$

$\bar{q}_{rem} = T - T_c + \dfrac{U(S/V)\theta}{\rho c}(T_0 - T)$ is in temperature dimension,

differentiating this with regard to temperature and multiplying by k_0/k_0

$$\frac{d\bar{q}_{rem}}{dT} = 1 + \frac{U(S/V)\theta}{\rho c}, \quad \frac{d\bar{q}_{rem}}{dT} = 1 + U_0 Da, \text{ and } U_0 = \frac{U(S/V)}{\rho c k_0}, \quad Da_1 = k_0 \theta$$

is the dimensionless temperature derivative of the heat removal function.

The Carra–Forni expression can be rearranged once more to the form:

$1 + U_0 Da - \dfrac{\gamma \beta Da}{1 + Da} > 0$, or $1 + U_0 Da > \dfrac{\gamma \beta Da}{1 + Da}$ for slope, and

$1 + U_0 Da - \gamma \beta Da + (1 + Da) > 0$, or $1 + U_0 Da > \gamma \beta Da + (1 + Da)$

for dynamic criteria

The dimensionless groups can be replaced by the corresponding differential quotient expressions for the derivatives as:

$$\frac{d\overline{q}_{rem}}{dT} > \frac{d\overline{q}_{gen}}{dT} \quad or \quad \frac{d\overline{q}_{rem}}{dT} > \frac{\frac{\partial \overline{q}_{gen}}{\partial T}\Big|_C}{\frac{\partial m}{\partial C}\Big|_T}, \quad \text{is the slope}$$

conditions, and using the same terms :

$$\frac{d\overline{q}_{rem}}{dT} > \frac{\partial \overline{q}_{gen}}{\partial T}\Big|_C + \frac{\partial m}{\partial C}\Big|_T, \quad \text{is the dynamic condition.}$$

These are definitive even if the detailed kinetics is not known. While the results of the derivation of the dimensionless functions is limited to the specified conditions, the derivatives are of general value and give experimental guidance.

9.5 Experimental requirements

These requirements can be derived from the above conditions. On the left hand side, the temperature derivative of the heat removal rate can be calculated if the flow over the catalyst is known. This is possible in recycle reactors. On the right hand side, the inequalities represent the two stability criteria, which contain three derivatives:

$$\frac{d\overline{q}_{gen}}{dT}\Big|_C, \frac{\partial \overline{q}_{gen}}{\partial T}\Big|_C, \frac{\partial m}{\partial C}\Big|_T,$$

Of these three, two must be measured experimentally to calculate the stability criteria. In recycle reactors that operate as CSTRs, rates are measured directly. Baloo and Berty (1989) simulated experiments in a CSTR for the measurement of reaction rate derivatives with the UCKRON test problem. To develop the derivatives of the rates, one must measure at somewhat higher and lower values of the argument. From these the calculated finite differences are an approximation of the derivative, e.g.:

$$\frac{d\overline{q}_{gen}}{dT} \cong \frac{\overline{q}_{gen2} - \overline{q}_{gen1}}{T_2 - T_1}, \quad \text{where } T_2 = T + 0.5\Delta T \text{ and } T_1 = T - 0.5\Delta T$$

and T is at the operation point of interest.

One other approach is to measure the rate as a function of a specified argument alone, and then differentiate the function with respect to the argument used. The differentiation can be done graphically, or by fitting an empirical function to the data (like a Fourier series) and differentiating this analytically.

The partial derivative of the material balance function with regard to concentration can be measured because:

$$\frac{\partial m}{\partial C}\Big|_T = -\left(1 + \theta \frac{\partial r}{\partial C}\Big|_T\right), \quad \text{where} \quad r = f(C), \text{ at constant } C_0 \text{ and } T.$$

This is accomplished by measuring the rate at constant temperature and at various concentrations by varying the feed rate. Calculating θ, multiplying by the measured slope at the calculated θ, and then adding one gives the derivative of the mass balance rate with regard to concentration.

The partial derivative of the heat generation rate with regard to the temperature can be measured considering that:

$$\frac{\partial \bar{q}_{gen}}{\partial T}\Big|_C = \frac{(-\Delta H)\theta}{\rho c} \frac{\partial r}{\partial T}\Big|_C$$

by measuring the rate at various temperatures as:

$$r = f(T)$$

at constant C_0 and C.

This is accomplished by constant feed concentrations through adjustment of the feed rate to keep C constant at various temperatures. After plotting the rate versus temperature, the curve can be differentiated, giving the derivative of $\partial r / \partial T$. The change of the thermodynamic values of $(-\Delta H)/\rho c$ are minor and can be neglected and used as a constant multiplier of the measured slope. The $\theta = V/F$ must be calculated for each measurement and also multiplied by the measured slope at the constant value of the concentration C. The technique is similar to the measurement of the activation energy discussed in Chapter 5.2.

The ordinary derivative of the heat generation rate with regard to temperature:

$$\frac{d\overline{q}_{gen}}{dT} = \frac{(-\Delta H)\theta}{\rho c} \frac{dr}{dT}, \text{ where } r = f_1(T,C) \text{ and } C = f_2(T).$$

This measurement is done at fixed θ and C_0, therefore C will change as the rate changes. The measured rate must be multiplied by the practically constant $(-\Delta H)\theta/\rho c$ and this will give

$$\overline{q}_{gen}$$

the heat generation rate in temperature dimension, as the function of T. Differentiating this curve gives values of

$$d\overline{q}_{gen} / dT$$

at given values of T. This type of measurement was done in Berty et al (1982) and results are summarized here.

9.6 Execution of experiments

The experiments were executed in a system shown in Figure 4.2.1. An on–line chromatograph analyzed the feed and discharge alternately. From the repeated analyses, averages and standard deviations were calculated. After a line–out period, a run was done in one to two hours. Before and after the run the condenser was drained and collected products were measured and analyzed. From the combined gaseous and liquid products, reactor discharge concentration and material balance was calculated for carbon, hydrogen and oxygen in various species. Results were presented on the computer output, one of which is reproduced in the table in Figure 9.6.1 (Berty 1982).

On the last column of Figure 9.6.1, notice that the rate of reaction was 20.6 mol/(kg catalyst*hr.) This is the production rate of most methanol plants. Yet accounting for all species has given H, C, and O balances acceptable results. The temperature of reacting gas was kept within 2°C. Since no methane formation was ever noticed, methane was used as an internal standard. Balances were adjusted on a methane in equals methane out mol basis.

Other operating conditions are detailed on the table in Figure 9.6.2 (Berty 1982). Among the listed experimental conditions it is worth noting that the

recirculation to feed ratio was 620±20 with the corresponding low gradients. Residence time was nine seconds at the temperature and pressure of the reaction. Experimental results on methanol synthesis are listed on the table in Figure 9.6.3 (Berty 1982).

		H_2	CO	CH_4	CO_2	H_2O	CH_3OH
Feed	PCT						
	AVG	70.478	14.548	5.883	9.091	0.	0.
	STD	0.088	0.127	0.040	0.076	0.	0.
Moles/	RUN	11.585	2.391	0.967	1.494	0.	0.
Vent	PCT						
	AVG(G)	70.843	11.786	7.008	10.018	0.058	0.345
	STD(G)	0.	0.056	0.037	0.050	0.	0.026
	AVG(L)					0.113	0.887
	STD(L)					0.	0.
Moles/	RUN(G)	9.955	9.656	0.985	1.408	0.008	0.049
Moles/	RUN(GM)*	9.776	1.626	0.967	1.382	0.008	0.048
Moles/	RUN(L)					0.103	0.811
Reactor	CON	66.481	11.060	6.577	9.402	0.744	5.737
Rate mol/kg.hr.							
	AVG	-39.275	-17.714	0.428	-2.086	2.682	20.695
	AVGM	-43.597	-18.433	0.	-2.697	2.679	20.674
	STD	0.511	0.694	0.034	0.130	0.	0.088
Bal	PCT	C	H	O	PrcAtm	Auto	Vent
	AVG	98.881	98.294	98.861		52.020	1.000
	AVGM	100.391	99.868	100.366			
			Con-		Flo M/Hr	Feed	Vent
Temp	C	Bed	densor		AVG	10.493	8.970
	IN	232.000			STD	0.017	0.017
	OUT	234.000	27.000		AVGM	10.493	8.808

Concentrations are in mol%. * indicates results corrected on no change in CH_4 moles basis.
Date: 4/9/80   Run time in minutes=94.00
Time: 13.33 to 15.07   Liquid Collected=27.80 GMS
No. of cycles: 2

Reproduced with permission, © 1982 AIChE.

Figure 9.6.1: Computer printout of experimental results.

Catalyst				
Type	Cu–based	United Catalyst		
Size	$d_p=$	3/16 in. ϕ, 4.76 (10^{-3})m		
		3/16 in. long, 4.76 (10^{-3})m		
Bed volume	V=	20 cm^3, 20 (10^{-6})m^3		
Weight	W=	26.5 g, 26.5 (10^{-3})kg		
No. of pellets		166		
Bed ϕ		1.875 in., 47.6 (10^{-3}) m		
Depth	L=	0.659 in., 16.7 (10^{-6}) m		
Operating Conditions				
Feed rate	F' =	65.7 $(10^{-6})\pm0.35$ (10^{-6}) m^3/s		
		10.55$\pm$0.056 mol/h		
Feed components,	H$_2$	CO	CO$_2$	CH$_4$
mol%				
desired concentration	70.0	15.0	10.0	5.0
actual concentration	69.6$\pm$0.60	15.3$\pm$0.44	9.5$\pm$0.35	5.6$\pm$0.43
Space Velocity (STP)	GHSV=	11,830$\pm$60 hr^{-1}, or 3.29$\pm$0.018 s^{-1}		
Residence time (Tr, Pr)	$\theta=$	9.03 s		
Recycle ratio		620$\pm$20		
Mass velocity	G=	9.2$\pm$0.29, kg/m^2-s		
Reynolds no.	$d_pG/\mu=$	3,050$\pm$150, G/a$\psi\mu$=795$\pm$40		
Blower speed		1500$\pm$50 rpm, 30$\pm$2 s^{-1}		
Operation, pressure	P=	52.0 atm abs.=5.27 MPa		
Temperature	T$_s=$	464 to 533K, variable		
Heat transfer coefficient	U$_o=$	2630$\pm$50 W/m^2–K.		

Reproduced with permission, © 1982 AIChE.

Figure 9.6.2: Average experimental conditions.

On the following table, the sixth column gives the heat generation rate in watts. The seventh column is labeled as heat generation rate in Kelvin units. This was done so that by differentiating this function with regard to temperature a dimensionless expression is received. A well–meaning person corrected this at the last minute in the original publication to "Theoretical Adiabatic Temperature Rise, " which is wrong, and has been corrected in the table reproduced here.

Run No.	Gas T., K	Reaction rate, mol/kg-h		% Conv.*	Heat gen.	Heat gen.	Material Balance		
		H_2O	CH_3OH	to CH_3OH	rate (W)	rate (K)	C	H	O
14-1	464.0	0.35	2.0	1.963	1.81	20.28	102.49	101.88	103.35
14-2	464.0	0.59	3.21	3.241	1.79	19.88	99.74	102.64	100.25
15-1	477.0	1.68	7.10	6.022	4.76	52.69	100.73	100.74	100.89
15-2	477.0	1.80	6.82	6.810	4.82	53.42	101.59	102.20	101.79
14-7.8	477.0	2.03	8.26	8.177	5.18	57.38	99.70	97.24	99.73
21-3	486.0	2.10	11.57	11.562	7.64	85.41	99.49	104.28	99.99
21-4	486.0	1.73	11.46	11.463	7.59	85.02	100.02	104.47	100.33
13-1	491.0	2.14	15.50	15.760	11.30	131.88	102.48	101.32	102.62
15-3	491.0	2.27	13.21	13.174	9.41	106.52	101.62	101.71	101.58
21-1	491.0	1.60	13.64	13.728	9.19	104.65	97.42	97.22	95.37
21-2	491.0	1.63	14.0	13.910	9.36	106.45	96.42	94.13	93.60
12-1	505.0	2.69	20.67	22.082	14.3	159.76	100.39	99.87	100.36
12-2	505.0	2.53	21.05	21.998	15.1	168.38	102.32	99.80	102.86
12-5	519.0	2.50	20.84	21.258	14.5	162.49	100.30	97.43	100.34
12-6	519.0	2.43	20.23	20.667	14.9	168.10	102.85	101.01	103.03
12-3	533.0	2.61	18.90	20.032	12.9	142.22	99.57	100.49	99.47
12-4	533.0	2.62	18.98	19.595	13.9	151.83	102.08	99.97	101.86

* from CO and CO_2

Reproduced with permission, © 1982 AIChE.

Figure 9.6.3: Experimental results on methanol synthesis.

The results of the experiment are summarized in the table on Figure 9.6.4 (Berty 1982).

No assumptions involved		
Temperature	T	477 K
Methanol rate	r_{CH3OH}	10.0 mol/L–h
Water rate	r_{H2O}	2.4 mol/L–h
Heat generation rate	q_{gen}	5.0 W
	$\overline{q}_{gen}$	60.2 K
Maximum ΔT	ΔT_{max}	18.5 K
Slope condition	$d\overline{q}_{gen} / dt$	3.25
These assume first order rate with $(C_{H2}–C_{H2,eq.})$ and consider MeOH reaction only		
Concentration	$(C_{H2}–C_{H2,eq.})$	0.204 mol/L
Ad. Temp. rise pot.	β	1.01
Reaction time	θ	0.00262 h
Damköhler no.	D_a	0.128
Conversion	$X=D_a/(1+D_a)$	0.113
$(\delta q_{gen}/\delta T)\vert_c$	$\varepsilon\beta D_a$	3.68
Arrhenius no.	ε	28.5
Energy of activation	E	112.6 kJ/mol
$(\delta m/\delta C)_\tau$	$-(1+D_a)$	-1.128
Dynamic cond.	$\varepsilon\beta D_a-(1+D_a)$	2.55
Heat transfer coefficient	UD_a	760
$d\overline{q}_{rem} / dT$	$1+UD_a$	761

Reproduced with permission, © 1982 AIChE.

Figure 9.6.4: Summary of experimental results.

On this table, the Arrhenius number E/RT was designated by ε, but this symbol is already used in this book for the empty fraction in a packed bed. The correct symbol for $E/RT = \gamma$ is used here. On the last line in this table the derivative of the heat removal rate is given:

$$dq_{rem}/dT = 761$$

and this is much larger than

$$\gamma\beta Da_I/(1+Da_I) = 3.68/1.13 = 3.26$$

for the slope condition, and

$$\gamma\beta Da_I - (1+Da_I) = 3.68-1.13 = 2.55, \text{ for the dynamic condition.}$$

The conclusion is that the measured data were all collected at stable conditions. The corresponding slopes illustrating the heat removal rates were indistinguishable from perfectly vertical lines. The tangent line shown at low conversion on Figure 9.6.5 is just an example to show graphically that for ignition on the catalyst particles a low heat transfer function would have been needed to require the $\Delta T=18.5$ K. Finally the Van Heerden diagram is shown in Figure 9.6.5 (Berty 1982) constructed from the measured results.
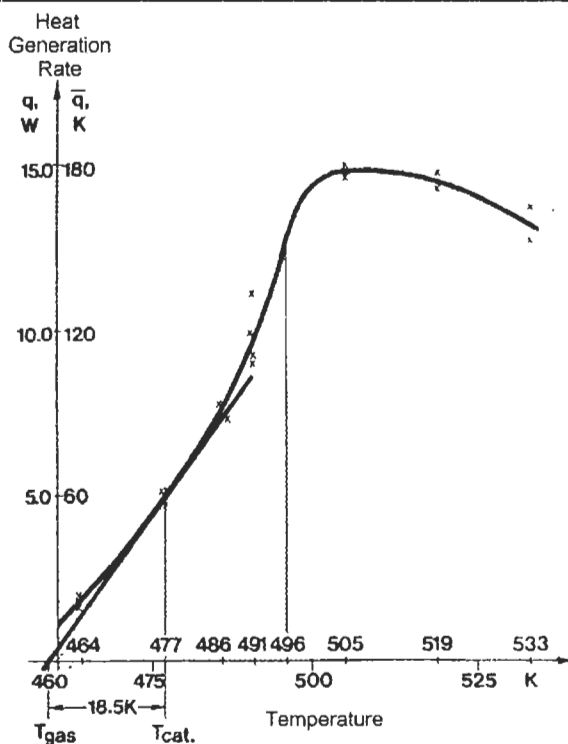
Figure 9.6.5: Experimentally measured Van Heerden diagram for low pressure methanol synthesis.

The original van Heerden diagram, as presented in his paper of 1953, was constructed for an adiabatic reactor case. In that case, at fixed feed temperature, there was a different slope (representing heat removal rate) for each feed rate. There was also a different heat generation versus temperature

curve for each feed rate. The middle intersection was misinterpreted as an unstable condition and locus of ignition in later publications for some time. Bilous and Amundson (1955) declared that as far as the reactor was concerned the unstable state did not exist, but it took a long time before that statement was generally accepted.

The three intersections were the results of the mathematical approach when a low heat removal condition existed: assuming the steady–state first and then solving the algebraic equations. This resulted in 3 solutions. If the transient differential equations for material and temperature were integrated in the time domain until the time derivative vanished, only the upper and lower solution were received. Which one was the actual operating point depended on which end was considered to be the starting point of the experiment. At a low temperature start, the lower point became stabilized. Once ignition occurred and temperature moved to the higher range, lowering the temperature resulted in stabilizing in the upper state.

With a high heat removal rate, corresponding to an almost vertical line, as was the case in the experiments in the CSTR, the full heat generation curve could be measured. An intersection could be achieved between the heat generation curve and the very steep heat removal line at the point where the non–existent middle point was, but this was just one of the many stable solutions possible and not an "unstable point."

Figure 9.6.6 shows an example with a low heat removal rate, in which the ignition point is at the place where the heat removal line touches the heat generation curve from below (point I.) Correspondingly the "flameout" condition is at the high conversion end, where the straight line for heat removal is tangent to the heat generation curve from above (point E.) Between these two loci an uncontrollable region may exist and the curve looks like a hysteresis case. None of these points diminishes the seminal significance of van Heerden's work, which started a new chapter in reactor design.

Aris (1969) pointed out that the mathematical definition of the CSTR stability problem and the catalyst particle problem cooled by the feed flow were essentially identical.

A graphical explanation for the constant flow and variable feed temperature controlled adiabatic CSTR is given in Figure 9.6.6.
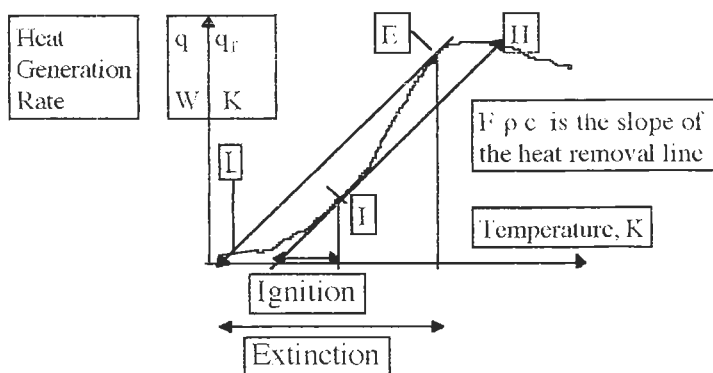
Drawing by the author.

Figure 9.6.6: Thermal stability of an adiabatic CSTR with constant flow and variable feed temperature

In Figure 9.6.6 the two constant slope lines give the ignition and flameout or extinction conditions. If the heat removal is as low as these lines represent, then no stable operation can be maintained in the reactor, or at catalyst temperatures indicated between the two tangent points and the corresponding intersection of the sloping lines and the abscissa. Starting with a cold reactor at constant flow and gradually increasing the inlet allows very low conversions to be maintained. After the ignition temperature is reached at point I, the system moves toward the higher intersection at point H. Thereafter, if the temperature is lowered, high conversions are maintained until the point E is reached where extinction, or flameout occurs and conversion and heat generation drops to a very low level.

9.7 Applications for Design

For adiabatic reactors one example was presented by Berty et al (1968) on a six–stage adiabatic reactor system that had intercoolers between the stages. Every adiabatic stage is always sensitive or unstable but the full six–stage

system can be made insensitive. The problem was stated for this system as follows:

> "If the inlet temperature to a stage changes to a new higher level and enough time elapses to approach a new steady–state, the resultant increase of the inlet temperature to the next stage should be no greater than the temperature rise in the inlet of the preceding stage."

This, in mathematical terms means:

$$dT_{1,N+1} < dT_{1,N}$$

If this can be accomplished without any control action, the system is not sensitive. The system notation can be identified in the following Figure 9.7.1. The expression used in the literature of "jumping" to a new steady–state refers to homogeneous gas–phase reactions in an empty reactor. Heterogeneous catalytic reactors have a large mass of thermal capacity in the catalyst that dampens out short duration disturbances. Therefore the reference for enough time is included in the above statement. Using a quasi–homogeneous, one–phase model cannot account for this. But it can be shown on two–phase models where heat capacity of fluid and solid are separately taken in account as these change in time. This was done in Berty et al (1972).

Temperature of coolant:

Drawing by the author.
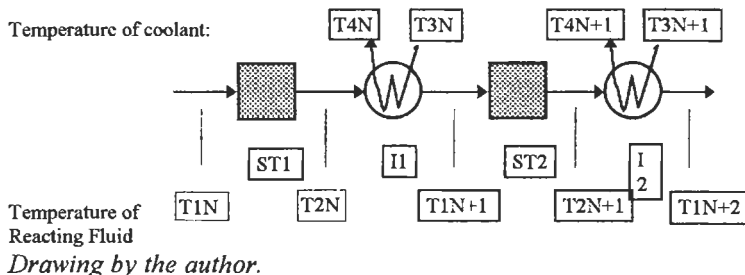
Figure 9.7.1: Staged adiabatic reactor with intercoolers.

Using high heat capacity systems, some experimenters tried to stabilize around the (non–existent) unstable middle intersection, and believed that they had accomplished this. In reality they were seeing a "jump" to a higher

steady–state that had actually lingered in between for several hours before settling into the new, higher steady–state.

$$T_{3N} \geq \frac{T_{2N} - T_{1N+1} e^{\frac{E}{R}\left(\frac{T_{2N}-T_{1N}}{T_{2N} T_{1N}}\right)}}{1 - e^{\frac{E}{R}\left(\frac{T_{2N}-T_{1N}}{T_{2N} T_{1N}}\right)}}$$

The above expression defines the minimum coolant temperature that can be used, with the corresponding **U** and **S** to remove the heat. A lower **U** and **S**, which would require lower temperature, would make the system sensitive. This seems to be counterintuitive in general, yet not for those who remember the introductory explanation at the first page of this chapter.

For cooled tubular reactors, Wilson (1946) derived a stability (Insensitivity) criterion that matched the one developed by Perkins in (1938), i.e.,

$$\Delta T < RT^2/E$$
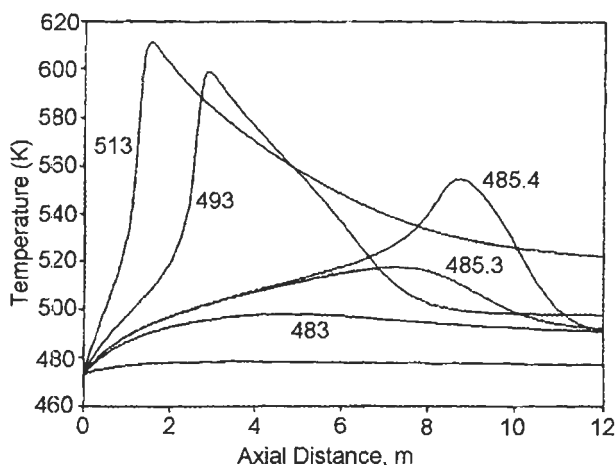
Figure 9.7.2: Plug–flow reactor simulation. Inside temperature vs. Tube length at various tube wall temperatures, in K

This result was very conservative, i.e., too restrictive for production units; much higher temperature differences were observed in the industry (Nelson 1974). The better results measured in CSTRs were still about two thirds of

those observed in large scale. An extensive simulation study done by graduate students at the University of Akron (Bashir et al 1992) showed that the above maximum pertains to the length where the second derivative of the temperature vs. length function becomes zero.
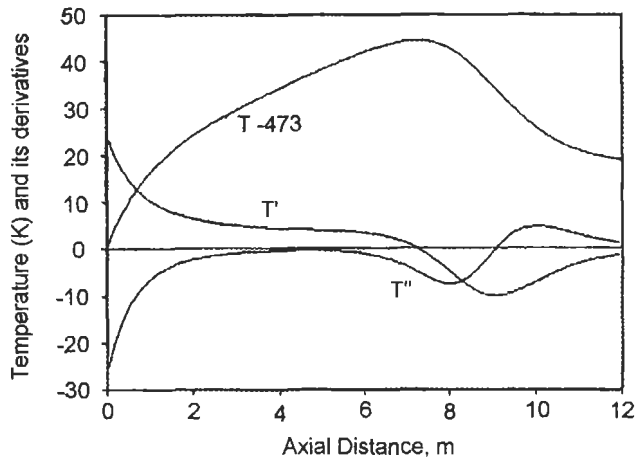
Reproduced with permission from Bashir et al, I&EC Res., 31, p. 2168, © 1992 American Chemical Society.

Figure 9.7.3: Plug–flow reactor simulation at T_wall= 485.3K
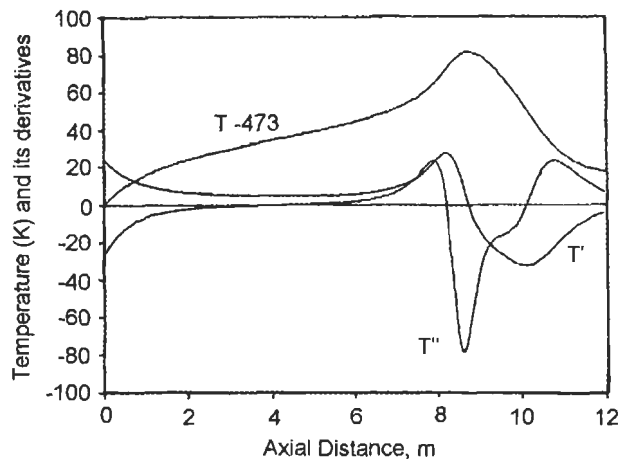
Reproduced with permission from Bashir et al, I&EC Res., 31, p. 2168, © 1992 American Chemical Society.

Figure 9.7.4: Plug–flow reactor simulation at T_wall=485.4K.

If ΔT between gas and wall is incrementally larger than this, a runaway starts. It remains insensitive if it is incrementally lower. This is shown on Figure 9.7.2 and with the temperature derivatives on 9.7.3 and 9.7.4 (figures Bashir et al 1992).

To find and monitor the point of inflection is difficult in the industry while the "hot spot" (the highest temperature) is somewhat easier to find and monitor. Consequently, an expression was derived for this value. This comes from the fact that at the maximum ΔT, all the heat is transferred through the wall, therefore the heat generated must equal the heat transferred:

$$U(S/V)(T - T_w) = (-\Delta H)k_0 e^{E/RT}C^n \quad \text{and} \quad \text{expressing } \Delta T \text{ with the time}$$

constant ratio of U_0 and β, the maximum temperature difference is:

$$T - T_w \leq \frac{T\beta}{U_0}, \quad \text{where} \quad U_0 = \frac{U(S/V)}{\rho c k_t} = \frac{St}{Da_I}$$

This result was checked by simulation of both CSTR measurements and calculations of tubular reactor incipient runaways. It should be noted that the predicted ΔT at inflection from CSTR experiments agrees well with measures in tubular simulation. At hotspot the ΔT to the ΔT at inflection is between 1.4 and 1.8. Using a multiplier of 1.4 as recommended by Nelson (1974) is safe.

The need to keep a concave temperature profile for a tubular reactor can be derived from the former multi–stage adiabatic reactor example. For this, the total catalyst volume is divided into more and more stages, keeping the flow cross–section and mass flow rate unchanged. It is not too difficult to realize that at multiple small stages and with similar small intercoolers this should become something like a cooled tubular reactor. Mathematically the requirement for a multi–stage reactor can be manipulated to a different form:

$$dT_{1,N+1} < dT_{1,N}, \text{is} \quad \text{also} \frac{dT_{1,N+1}}{dT_{1,N}} < 1$$

dividing numerator and denominator by an incremental volume or length of the reactor.

$$\frac{\left(\dfrac{dT_1}{dx}\right)_{N+1}}{\left(\dfrac{dT_1}{dx}\right)_{N}} < 1, \text{ or } \left(\frac{dT_1}{dx}\right)_{N+1} < \left(\frac{dT_1}{dx}\right)_{N}, \text{ or } \left(\frac{dT_1}{dx}\right)_{N+1} - \left(\frac{dT_1}{dx}\right)_{N} < 0$$

Dividing the last expression by the incremental length:

$$\frac{\left(\dfrac{dT_1}{dx}\right)_{N+1} - \left(\dfrac{dT_1}{dx}\right)_{N}}{\Delta x} \cong \frac{\Delta\left(\dfrac{dT_1}{dx}\right)}{\Delta x} < 0 \quad \text{and going to the limit}$$

$$\lim \frac{\Delta\left(\dfrac{dT_1}{dx}\right)}{\Delta x} = \frac{d^2 T_1}{dx^2} < 0$$

$$\text{as } \Delta x \Rightarrow 0$$

This result means that the reactor is insensitive if the temperature profile is concave toward the reactor length axis, and the inflection point is avoided. If the ΔT exceeds that permitted by the previous criterion—the limit set by RT^2/E—an inflection of the temperature vs., tube length will occur and thermal runaway will set in. Just before runway sets in the temperature at the "hot spot" can be 1.4 times higher than RT^2/E.

9.8 Multi–Tube Reactors

It cannot be expected that a reactor containing several thousand tubes would behave as a simple multiple of the single tube. To study this by computer simulation, the Advanced Chemical Reaction Engineering students at The University of Akron were told to assume that a non–uniformity exists among the tubes caused by minor differences in catalyst packing densities. This causes flow differences, since the pressure drop for all tubes must be the same. Simulated experiments were conducted for three levels of variation in the packing density distribution at various wall temperatures Govil (1989). It was observed as that as the reactor approached runaway conditions, the number of tubes suffering runaway increased gradually.

One hundred tubes were taken as the representative sample population and all were integrated for three different density distributions and each at 3 different levels of runaway tubes (few, medium, and many tubes in runaway.) Altogether 900 integrations were performed and the results analyzed. Figure 9.8.1 shows the distribution of observed maximum ΔTs with the hundred tubes with 5% random packing variation and at beginning of runaways at 486 K wall temperatures.
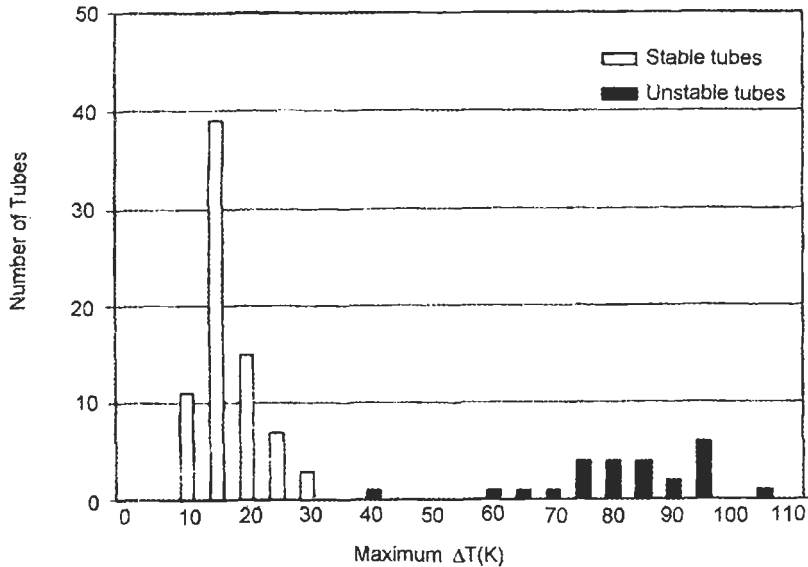
Reproduced from Govil, Hung. J. of Ind. Chem., © 1989.

Figure 9.8.1: Effect of packing density variations

As can be seen most of the tubes were still in a non–sensitive state while about ten were in runaway conditions. This will give an operational feel for how uniform the catalyst charge should be and how closely the system may approach incipient runaway, for a single tube in a multi–tube production unit.

Non–uniformity may be caused by other reasons, like non–uniformity in catalyst activity, etc. Finally, uniformity is not always desirable. In a reactor containing several thousand tubes, for example, uniform runaway in all the tubes at the same time would result in a heat load impossible to control. Disaster would follow.

9.9 Thermal stability in transient state

In the last part of Chapter 7.4 (Transient Studies) the experimental work on ethylene oxidation was shown. There the interest was to investigate what occurs and how fast, after a thermal runaway started. The previous chapter discussed the criteria of how to design reactors for steady–state operation so that runaways can be avoided. One more subject that needs discussion is what transient changes can cause thermal runaways.

The fundamental reason for runaway at transient changes is the large difference in the thermal capacity of the catalyst charge and the flowing fluid, especially if it is a gas–phase reaction. In these cases, if the reaction is running close to the runaway limit but still somewhat below it, sudden changes can start a thermal runaway.

Industrial experience showed that even a change in the gas phase that would slow down the reaction could result in a runaway, if the change was done suddenly. For example, if an oxidation reactor is operated for maximum production and is therefore close to thermal runaway condition, a sudden cut of inlet temperature—a step change down—will cause a runaway. The lower temperature of the gas cools down a short length of the catalyst bed at the entrance and converts less oxygen. The step change in the bed temperature moves slowly because of the large heat capacity of the solids while the increased unconverted reactant concentration moves fast with the gas. The higher reactant concentration reaches the hotter zone of the catalyst that was in steady–state with a lower concentration and accelerates the reaction above the previous level. A temperature runaway thus occurs.

Several other changes that are supposed to slow down the reaction can cause runaway. In the case of ethylene oxidation, chlorinated hydrocarbons are used as inhibitors. These slow down both the total and the epoxidation, although the latter somewhat less. When the reaction is running too high and the inhibitor feed is suddenly increased in an attempt to control it, a runaway may occur. The reason is similar to that for the feed temperature cut situation. Here the inhibitor that is in the ppm region reacts with the front of the catalytic bed and slowly moves down stream. The unconverted reactants reach the hotter zone before the increased inhibitor concentration does.

These phenomena were studied and reproduced experimentally. The necessary dynamic experiments must be done in specially designed pilot-plant sized equipment, and hence these are expensive, as was shown in Chapter 7.4. This type of experiment can be justified only for processes that are practiced in large units and have large economical significance. On the other hand, the computer simulation of this phenomenon is getting easier with the increased calculating speed and capacity. The two–phase model is getting faster to account separately for the thermal changes in the gas and solid phase and in the time and length dimension. Therefore, the success of a mathematical experiment will depend largely on how good the physical and thermodynamic properties and estimated transfer coefficients are for a system.

The basic phenomenon was observed in modeling studies by Bjoreskov and Slinko (1965) that sudden increase in inlet temperature caused a transient drop of the peak temperature. The "wrong–way response" name was given by Mechta et al (1981) after they experienced the opposite: a sudden of inlet temperature resulted in an increase of the peak temperature (which may eventually cause a runaway.) The work used a pseudo–homogeneous reaction model and explained the phenomenon by the different speeds of transient response in gas and solid. The example in the last part of Chapter 7.4 explained the speed difference by the large difference in heat capacity of gas and solid phases. For this a two–phase model is needed and spatial and time changes must be followed.

The final lesson is that no sudden change should be made on catalytic units, especially on the commercial scale reactors. Even if a unit is too close to a dangerous condition, changes should be made gradually in small increments, waiting between incremental changes to reach steady–state before the next incremental change is initiated.

The reader is encouraged to use a two–phase, one spatial dimension, and time–dependent mathematical model to study this phenomenon. The UCKRON test problem can be used for general introduction before the particular model for the system of interest is investigated. The success of the simulation will depend strongly on the quality of physical parameters and estimated transfer coefficients for the system.

Postscript

Experiments were shown in integral reactors from 3 grams to 18 tons of catalyst charged. Most recycle reactors are limited to about 100 grams of maximum charge, yet in a good recycle reactor, experiments can be run at the mass velocity and chemical rate of production units. This reproduces the working conditions in a small, incremental volume of the large reactor and at the conditions that the catalyst experiences there. Mathematical models, developed from recycle reactor studies can be used to design production units. Designs can be optimized for highest economy. The pilot–plant's role can be limited to checking predictions from the mathematical model, and pilots are not needed to execute wide–ranging studies (Berty 1983a). This significantly reduces time and cost of a pilot plant operation. For some standard unit processes, like hydrogenation, the need for pilot plants may be eliminated completely. The use of recycle reactors in catalytic studies opened a more deterministic way to study kinetics and to use the results in engineering new plants.

Literature

Agnew, J.B., "Chemical Kinetics–The Missing Link in Reactor Design," Paper B8a, at CHEMECA 85.

Alcorn, W.R., and T.J. Sullivan, **1992**, *J. Chemical Catalyst News*, August, Englehard Corporation.

Almeida–Costa, C.A., R.S. Quinta Ferriera, and A.E. Rodrigues, **1994**, *Chem. Eng. Sci.*, 49, 24B, pp. 5571–5583.

Anderson, N.K., and C.A. Rowe, **1943**, *J. Ind. Eng. Chem.*, 35, p. 554.

Aris, R., **1966**, *Ind. Eng. Chem.*, 58, pp 32–37.

Aris, R., **1969**, *Chem. Eng. Sci.*, 24, p. 149.

Aris, R., **1975**, *The Mathematical Theory of Diffusion and Reaction in Permeable Catalysts, Vols. I and II*, Oxford University Press, London.

Árva, P. and F. Szeifert, **1989**, in a special issue on "Kinetic Model Development," W.N. Gill, Ed., *Chem. Eng. Comm.*, 76, pp. 195–206.

ASTM Standards on Catalysts, **1980**, PCN 06–432080–12, American Society for Testing and Materials, Philadelphia, PA.

Atwood, G.A., D. Sundaravel and J.M. Berty, **1989**, in a special issue on "Kinetic Model Development," W.N. Gill, Ed., *Chem. Eng. Comm.*, 76, pp.125–140.

Baloo, S. and J.M. Berty, **1989**, in a special issue on "Kinetic Model Development," W.N. Gill, Ed., *Chem. Eng. Comm.*, 76, pp. 73–91.

Bahsir, S., T. Chován, R.J. Masri, A. Mukherjee, A. Pant, S. Sen, P. Vijayaraghavan and J.M. Berty,**1992**, *I&EC Res.*, 31, pp. 2164–2171.

Becker, E.R., and C.J. Periera, ed., *Computer Aided Design of Catalysts*, Marcel Dekker, New York.

Benedek, P. and F. Olti, **1985**, *Computer Aided Chemical Thermodynamics of Gases and Liquids*, John Wiley & Sons, New York.

Bennett, C.O., **1967**, *AIChE Journal*, 13, 5, pp. 890–895.

Bennett, C.O., M.B. Cutlip and C.C. Yang, **1972**, *J. Chem. Eng. Sci.*, 27, pp. 2255–2264.

Berty, I.J., J.M. Berty, P.T. Brinkerhoff, and T. Chovan, **1989**b, *J.I.&EC Res.*, 28, 1589–1596.

Berty, J.M., *Process for Producing Alkylene Oxides, Especially Ethylene Oxide*, **1959**, Östereichisches Patent 201,575.

Berty, J.M., J.H. Bricker and J.O. Hambrik, **1968**, Preprint 10E, at the 63rd National Meeting of AIChE, St. Louis, MO.

Berty, J.M., J.O. Hambrick, T.R. Malone and D.S. Ullock, **1969**, Reprint 42E, at the 64th National Meeting of AIChE, New Orleans, LA.

Berty, J.M., *Process and Equipment for Exothermal Catalytic Reaction in the Vapor Phase*, **1969**, German Patent Disclosure 1,915,560.

Berty, J.M., J.H. Bricker, S.W. Clark, R.D. Dean and T.J. McGovern, **1972**, *Proceedings of the Fifth European/Second International Symposium on chemical Reaction Engineering*, Amsterdam, 2–4 May, Elsevier Publishing.

Berty, J.M., **1974**, *Chem. Eng. Prog.*, 70, 5, pp. 578–584.

Berty, J.M., **1979**, *J. Catal. Rev.–Sci. Eng.*, 20, 1, pp. 75–96.

Berty, J.M., **1979**, *Chem. Eng. Prog.*, September, pp. 48–51.

Berty, J.M., J.P. Lenczyk and V.R. Parekh, **1981**, Paper PD–1, at the 74th National Meeting of AIChE, New Orleans, LA.

Berty, J.M., J.P. Lenczyk and S.M. Shah, **1982**, *J. AIChEJ*, 28, 6, pp. 914–922.

Berty, J.M., **1983a**, *Chem. Eng. Prog.*, July, pp. 63-67.

Berty, J.M., **1983**, "Laboratory Reactors for Catalytic Studies," chapter 3 in *J. Applied Industrial Catalysis I*, B.E. Leach, ed., pp. 41–67, Academic Press, New York.

Berty, J.M., **1983**, "Ethylene Oxide Synthesis," chapter 8 in *J. Applied Industrial Catalysis I*, B.E. Leach, ed., pp. 207–238, Academic Press, New York.

Berty, J.M., S. Lee, V. Parekh, R. Gandhi and K. Sivagnanam, **1983**, *Proceedings of the Third Pacific Chem. Eng. Congress, Kinetics and Catalysis II*, pp. 191–196.

Berty, J.M., S. Lee, K. Sivagnanam and F. Szeifert, **1984**, *Proceedings of ISCRE8, I. Chem. E. Symposium Series No. 87*.

Berty, J.M., **1984**, *Plant/Operation Progress*, 3, 3, July.

Berty, J.M., **1989**, *J. Chem. Eng. Comm.*, 82, pp. 229–232.

Berty, J.M., **1997**, *Ind. Eng. Chem. Res.*, 36, pp. 513–522.

Bhasin, M.M., P.C. Ellgen and C.D. Hendrix, **1980**, UK Patent GB–2,043,481.

Bird, R.B., W.E. Stewart and E.N. Lightfoot, **1960**, *Transport Phenomena*, John Wiley & Sons, New York.

Boersma–Klein, W. and J.A. Moulijn, **1979**, *Chemical Engineering Science*, 34, pp. 959–969.

Bodenstein, M. and S.C. Lind, **1906**, *Z. Phys. Chem.*, 57, p. 168.

Bodenstein, M. and K. Wolgast, **1908**, *Z. Phys. Chem.*, 61, p. 422.

Boreskov, G.K. and M.G. Slinko, **1965**, *Pure Appl. Chem*, 10, p. 612.

Boudart, M., **1956**, *AIChE J.*, 2, p. 62.

Boudart, M., **1968**, *Kinetics of Chemical Processes*, Prentice–Hall, Inc., Engelwood, NJ.

Boudart, M., **1986**, *Ind. Eng. Chem. Fundam.*, 25, pp. 656–658.

Box, G.E.P., W.G. Hunter and J.S. Hunter, **1978**, *Statistics for Experimenters*, John Wiley & Sons, Inc.

Bush, S.F., **1972**, *Advances in Chem. Ser.*, 104, p. 610.

Brunner, E., **1904**, *Zeitschrift für Elektrochemie*, 47, p. 56. (In German.)

Butt, J.B., **1980**, *Reaction Kinetics and Reactor Design*, Prentice–Hall, Edgewood Cliffs, NJ.

Carberry, J.J., **1964**, *J. Ind. Eng. Chem.*, 56, 11, pp. 39–46.

Carberry, J.J., D.G. Tajbl and J.B. Simons, **1966**, *J. Ind. & Eng. Chem. Fundam.*, 5, pp. 171–175.

Carberry, J.J., **1976**, *Chemical and Catalytic Reaction Engineering*, McGraw–Hill, Inc., New York.

Choudhary, V.R. and L.K. Doraiswamy, **1971**, *J. Ind. Eng. Chem. Prod. Res. Dev.*, 10, p. 219.

Christofaratou, E., V. Balakototaiah and D.W. West, **1998**, *AIChE J.*, 49, 2, pp. 394–404.

Clements, Jr., W.G. and K.B. Schnelle, Jr., **1963**, *Ind. Eng. Chem. Proc. Des. And Dev.*, 2, 2, pp. 94–102.

Colburn, A.P., **1933**, *J. Inst. Chem. Eng.*, 29, pp. 174–210.

Cooke, C.G., **1979**, *J. CHEMSA*, 5, 11, pp. 175–176.

Coppens, M–O. and G.F. Froment, **1994**, *Chem. Eng. Sci.*, 49, 24A, pp. 4897–4907.

Crank, J., **1975**, *The Mathematics of Diffusion*, Clarendon Press, Oxford.

Cropley, J.B., **1978**, "Chemical Reaction Engineering," paper 24 in *ACS Symposium Series 65*, pp. 292–302.

Cropley, J.B., L.M. Burgess and R.A. Loke, **1984**, *CHEMTECH*, June, pp. 374–390.

Cropley, J.B., **1987**, *Chem. Eng. Progr.*, February, pp. 44–51.

Damköhler, G., **1936**, *Ztschr. Elektrochem.*, 42, 12, pp. 846–861. (In German.)

Damköhler, G., **1937**, *Der Chemie–Ingenieur III, Part I*, A. Euken and M. Jakob, eds., p. 447. (In German.)

Davis, B.R. and D.S. Scott, **1965**, Paper presented at the 58th Annual Meeting of AIChE, Philadelphia, PA.

Dean, R.D. and N.B. Angelo, **1971**, *J. Chem. Eng. Prog.*, 67, 10, pp. 59–67.

DeLancey, G.B., S. Kovenklioglu, A.B. Ritter and J.C. Schneider, **1983**, *Ind. Eng. Chem. Process Des. And Dev.*, 22, pp. 639–645.

DeLancey, G.B. and S. Kovenklioglu, **1986**, *J. Ind. Eng. Chem. Process Des. Dev.*, 25, 3, pp. 710–717.

Dente, M. and A. Collina, **1964**, *La Chimica E.*, 46, pp. 752-761. (In Italian.)

Difford, A.M.R. and M.S. Spencer, **1975**, *J. Chem. Eng. Prog.*, 71, 1, pp. 31–33.

Dixon, A.G. and D.L. Cresswell, **1979**, *J. AIChE*, 25, 4, pp. 663–676.

Doraiswamy, L.K. and D.G. Tajbl, **1974**, *J. Cat. Rev. Sci. Eng.*, 10, 2, pp. 177–219.

Drucker, G., G. Joos and F. Simon, **1931**, *Zeitschrift für physikalische Chemie*, Supplement.

Ergun, S., **1952**, *J. Chem. Eng. Prog.*, 48, pp. 89–94.

First European Symposium on chemical Engineering, **1957**, Chemical Reaction Engineering, Pergamon Press, Amsterdam, New York.

Frank–Kamenetskii, D.A., **1961**, *Diffusion and Heat Transfer in Chemical Kinetics, 2nd Edition*, Plenum Press.

Froment, G.F. and R. Mezaki, **1970**, *Chem. Eng. Sci.*, 25, pp. 293–301.

Gamson, B.W., G. Thodos and O.A. Hougen, **1943**, *J. Trans. Am. Inst. Chem. Engrs.*, 39,1.

Garanin, V.J., U.M. Korkehi and Kh. M. Minachev, **1967**, *Kinetika I Kataliz.*, 8, 3, pp. 701-703. (Translated from Russian, Kluver Academic/Plenum Publishing.)

Georgakopoulos, K. and R. Broucek, **1988**, *Chem. Eng. Sci.*k, 42, 11, pp. 2783–2784.

Gilles, F.D. and H. Hofmann, **1961**, *Chem. Eng. Sci.*, 15, 328.

Gomezplata, A. and T.M. Regan, **1970**, *Ind. & Eng. Chem.*, 62, 12, pp. 140-147.

Govil, A., E.K. Kazanjian, R. Rastogi, A. Saraf, T.F. Spero, Chien Sze and V.M. Voruganti, **1989**, *Hungarian Journal of Ind. Chem. Veszprém*, 17, pp. 545–561.

Gregory, C.D. and F.G. Young, **1979**, *J. Chem. Eng. Prog.*, 74, 5, pp. 44–48.

Handley, D. and P.J. Heggs, **1968**, *J. Trans. Inst. Chem. Engrs.*, 46, p. 251.

Hanratty, T.J., **1956**, *J. AIChE*, 2, pp. 359–362.

Happel, J., **1978**, *Chem. Eng. Sci.*, 33, p. 1567.

Hougen, O.A., **1951**, *J. Chem. Eng. Progress Monograph Series, AIChE*, 47, 1, pp. 41–73.

Hutchings, J. and J.J. Carberry, **1966**, *J. AIChE*, 12, p. 30.

Jankowski, H., J. Nelles, R. Adler, B. Kubias and C. Salzer, **1978**, Part II, *J. Chem. Techn.*, 30, Heft 9, pp. 441–446. (In German.)

Johnson, P.C., R.C. Lemon and J.M. Berty, *Selective Non–Catalytic, Vapor–Phase Oxiation of Saturated Aliphatic Hydrocarbons to Olefin Oxides*, **1964**, US Patent 3,132,156.

Kehoe, J.P.G. and J.B. Butt, **1972**, *AIChE Journal*, 18, 2, pp. 347–355.

Kelkar, C.P. and J.J. McCarthy, private communication.

Kline, B., J. Tavakoli and J.M. Berty, **1976**, *Proceedings of the Sixth International Symposium on Chemical Oxidation*, April 15–17, pp. 246–253.

Kobayashi, H. and M. Kobayashi, **1974**, *Cat. Rev. – Sci. Eng.*, 10, 2, pp. 139–176.

Kraemer, D.W. and H.I. DeLasa, **1988**, *J. Ind. Eng. Chem. Res.*, 27, 11, pp. 2002–2008.

Krishnan, C., J.R. Elliott, Jr. And J.M. Berty, **1991**, *J. I&EC Res.*, 30, pp. 1413–1418.

Krishnan, C., J.R. Elliott, Jr. And J.M. Berty, **1991**, *Chem. Eng. Comm.*, 105, pp. 155–170.

Kunii, D. and J.M. Smith, **1961**, *J. AIChE.*, 7, p. 29.

Kuni, D., M. Suzuki and N. Ono, **1968**, *Journal of Chemical Engineering of Japan*, 1,1, pp. 21-26.

Larmon, F.P., M.M. Gilbert and R.R. Dean, **1981**, Second World Congress on Chem. Eng. Paper No. 10 03 02.

László, A., **1964**, *International Journal of Heat and Mass Transfer*, 7, p. 423.

Leva, M., **1949**, *J. Chem. Eng.*, pp. 115–117.

Liljenroth, F.G., **1918**, *Chem. Met. Eng.*, 19, p. 287.

Livbjerg, H. and J. Willadsen, **1971**, *Chem. Eng. Sci.*, 26, pp. 1495–1503.

McAdams, W.H., **1954**, *Heat Transmission*, p. 259, McGraw–Hill, New York.

Macdonald, I.F., M.S. El–Sayed, K. Mow and A.L. Dullien, **1979**, *J. Ind. Eng. Chem. Fundam.*, 18, 3, pp. 199–208.

Marcinkowsky, A.E. and J.M. Berty, **1973**, *J. of Catalysis*, 29, pp. 494–499.

Mears, D.E. and M. Boudart, **1966**, *AIChE J.*, 12, 2, pp. 313-321.

Nelles, J., H. Jankowski, R. Adler, B. Kubias and C. Salzer, **1978**, Part III, *J. Chem. Techn.*, 30, Heft 11, pp. 555–559. (In German.)

Nelson, J.R., **1974**, Engineering Department Memorandum, Union Carbide Corp. Nov. 6.

Nernst, W., **1904**, *Zeitschrift für physikalische Chemie*, 47, pp. 52–55. (In German.)

Nielsen, R.P. and H.H. LaRochelle, *Catalyst for Production of Ethylene Oxide*, **1976**, U.S. Patent 3,962,136.

Parekh, V.J., **1980**, "Preliminary Kinetic Study of the Low–Pressure Methanol," MS. Thesis, University of Akron, OH.

Pena, M.A., D.H. Carr, K.L. Young and A. Varma, **1998**, *Chem. Eng. Sci.*, 53, 22, pp. 3821–3834.

Perlmutter, D.D., **1972**, *Stability of Chemical Reactors*, Prentice–Hall, Englewood Cliffs, NJ.

Perkins, G.A., **1938**, *Weekly Progress Report*, 3/15, Carbide and Carbon Chemical Co.

Pinjala, V., Y.C. Yen and D. Luss, **1988**, *AIChE Journal*, 34, pp. 663-1672.

Pirjamali, M., H. Livbjerg and J. Villadsen, **1973**, *Chem. Eng. Sci.*, 28, 328–332.

Price, J., **1968**, *Mechanical and Chemical Engineering Transactions*, 7.

Reynolds, O. **1939**, *Scientific Papers*, 1, pp. 81-85, Cambridge University.

Roduit, B., A. Wokaun and A. Baiker, **1998**, *Ind. Eng. Chem. Res.*, 37, 12, pp. 4571–4590.

Römer, R. and g. Luft, **1974**, *J. Chem. Ing. Tech.*, 45, p. 653.

Sankey, R.H., **1898**, *J. the Engineer*, 86, p. 236.

Satterfield, C.N., **1970**, *Mass Transfer in Heterogeneous Catalysis*, MIT Press, Cambridge, Mass.

Satterfield, C.N. and T.K. Sherwood, **1963**, *The Role of Diffusion in Catalysis*, Addison–Wesley.

Schermuly, O. and G. Luft, **1978**, *J. German Chem. Eng.*, 1, pp. 222–225.

Schmidt, L.D., M. Huff and S.S. Bharadwaj, **1994**, *Chem. Eng. Sci.*, 49, 24A, pp. 3981–3994.

Schwartz, c.E. and J.M. Smith, **1953**, *J. Ind. & Eng. Chem.*, 45, 6, pp. 1209–1218.

Scott, D.S., W. Lee and J. Papa, **1974**, *Chem. Eng. Sci.*, 29, p. 2155.

Silva, J.M., **1987**, *J. Ind. Eng. Chem. Res.*, 26, pp. 179–180.

Smith, J.M., **1968**, *Scaledown to Research*, Preprint 2A at the 63rd AIChE National Meeting, St. Louis, MO.

Smitz, R.A., **1975**, "Multiplicity, Stability, and Sensitivity of States in Chemically Reacting Systems," a review in *Advances in Chem.* Series, 148.

Suter, D., A. Bartoli, R. Schneider, D.W.T. Rippin and E.J. Newonn, **1990**, *Chem. Eng. Sci.*, 45, 8, pp. 2169–2176.

Thiele, E.W., **1939**, *J. Ind. & Eng. Chem.*, 31, pp. 916–920.

Timoshenko, V.I.R., A. Buyanov and M.G. Slink'ko, *Kinetika I Kataliz*, 9, 6, pp. 1358–1363. (English translation.)

Tinkler, J.D. and A.B. Metzner, **1961**, *Ind. Eng. Chem.*, 53, p. 663.

Toor, H.L. and J.M. Marchello, **1958**, *J. AIChE*, 4, p. 97.

Turner, G.A., **1967**, *AIChE J.*, 13, 4, p. 678.

Van de Beld, L., M.P.G. Bijl, A. Reinders, B. Van de Werf and K.R. Westerterp, **1994**, *Chem. Eng. Sci.*, 49, 24A, pp. 4361–4373.

Van Heerden, C., **1953**, *Ind. Eng. Chem.*, 45, p. 1245.

Van Heerden, C., **1958**, *Proceedings of the First European Symposium on Chemical Reaction Engineering*, p. 133.

Vortmeyer, D. and J. Schuster, **1983**, *J. Chem. Eng. Sci.*, 38, 10, 1691–1699.

Wachtel, S.J., L.A. Baillie, r.L. Foster and H.E. Jacobs, **1972**, *J. Oil Gas*, pp. 104–107.

Wagner, C., **1945**, *Chem. Tech.*, 18, p. 28.

Wedel, s. and J. Wiiladsen, **1983**, *Chem. Eng. Sci.*, 38, 8, p. 1346.

Weekman, V.W., **1974**, *J. AIChE*, 20, 5, pp. 833–840.

Weisz, P.B. and C.D. Prater, **1954**, *J. Adv. Catalysis*, 6, pp. 143–163.

Weller, S., **1956**, *AIChE J.*, 2, p. 59.

Whilhelmy, L., **1850**, *Über das Gesetz nach welchem die Einwirkung der Säuren auf dem Rohrzucker stattfindet*, Wilhelm Engelman, Leipzig. (In German.)

Wicke, E. and R. Kallenback, **1941**, *Kolloid Z.*, 97, p. 135.

Wicke, E. and D. Vortmeyer, **1959**, *Z. für Elektrochemi*, 63, p. 145.

Wilhelm, R.H., **1962**, *Pure Appl. Chem.*, 5, p. 403.

Wilke, C.P. and O.A. Hougen, **1945**, *J. Trans. Am. Inst. Chem. Engrs.*, 41, p. 445.

Wilson, K.B., **1946**, *Trans. Inst. Chem. Eng.*, 24, p. 77.

Yang, K.H. and O. Hougen, **1950**, *Chem. Eng. Prog.*, 46, p. 146.

Yagi, S. and D. Kunii, **1963**, *Proc. Heat Transfer Conference*, University of Colorado 1959 and London 1962, p. 750.

Yagi, S. and N. Wakao, **1959**, *J. AIChE*, 5, p. 79.

Zeldovich, I.B., **1939**, *Zhur. Fiz. Khim*, 13, p. 163.

Appendix Summary

A1. The UCKRON–1 Test Problem

Here a four–step mechanism is described on the framework of methanol synthesis without any claim to represent the real methanol mechanism. The aim here was to create a mechanism, and the kinetics derived from it, that has an exact mathematical solution. This was needed to perform kinetic studies with the "true," or "exact" solution and compare the results with various kinetic model predictions developed by statistical or other mehods. The final aim was to find out how good or approximate our modeling skill was.

A2. Explicit Form of the Rate Equation for the UCKRON–1 Test Problem

A brief overview of the form for rate equations reveals that temperature and concentration effects are strongly interwoven. This is so even if all four basic steps in the rules of Boudart (1968) are obeyed for the elementary steps. The expectations of simple unchanging temperature effects and strict even–numbered gas concentration dependencies of rate are not justified.

B. FORTRAN Program for the Exact Solution

This program helps calculate the rate of methanol formation in mol/m^{3}s at any specified temperature, and at different hydrogen, carbon monoxide and methanol concentrations. This simulates the working of a perfectly mixed CSTR specified at discharge condition, which is the same as these conditions are inside the reactor at steady–state operation. Corresponding feed compositions and volumetric rates can be calculated from simple material balances.

C1. Calculation of Operating Conditions and Transport Criteria for NOx Abatement in Air in the Rotoberty®

An example for low pressure operation over a small catalyst is given on page 229-231. This extreme case is the most difficult task for the centrifugal

blower. It is assumed that 2 cm³ of spherical catalyst with 200 micrometer diameter is charged to the catalyst basket. Over this charge the RPM is measured that makes u=58.7 cm/s linear velocity in air at ambient conditions. From the physical properties of air and other information the rest is calculated.

The Excel spreadsheet is constructed so that on page one, the referenced properties are listed in Column C, and the same with conversion factors to SI units in Column D. Conversion formulas and values calculated in SI Units are in Column E. Column F is a duplicate of Column E, and this can be used for additional calculation by changing to other conditions or to an entirely new case. It is recommended toleave Column E alone for a comparison case and to copy Column F to another page to execute calculations.

On page 2, Column C contains the mathematical expressions to caluclate the property named in Column A, and as signed in Column B. Column C contains the the mathematical calculation scheme for the property and Column D lists in Excel notation the source and the calculation method. Column E is the same as Column D, but preceded by an equal sign, which gives the instruction for executing the calculation in Excel. Column F is a duplicate of Column E. If any parameters are changed on page 1 in Column F, this will give the corresponding calculated values for your new case.

On page 3, the dimensionless criteria are listed and the corresponding driving forces are given. These can be compared to recommended maximum values and a decision can be made on acceptance or rejection of results. You can also experiment by changing operationg conditions to minimize the criteria. For example, try using larger particles or higher RPM or lower temperature, etx.

Page 3 gives a summary of the most important result in a figure illustrating in a semi–quantitative way the conditions in the specified CSTR. As can be seen on line 74, Da_I is somewhat larger than the critical value but the concentration difference on line 75 is small, so this result can be accepted with some reservations. The Carberry number is also larger than the criteria, therefore these experimental results are marginal for Nox abatement

experiments. All other criteria are satisfied. On page 6 for the methanol experiments only the Da_{IV} is larger, therefore this is also less than perfect.

C2. Calculation of Operating conditions and Transport Criteria for the UCKRON Test Problem as a Methanol Synthesis Experiment in the Rotoberty®

On pages 232-234 is an example in the other extreme, where a high–pressure, fast reaction is studied on an industrial size catalyst. The layout and calculation schemes are the same as in the NOx example, so these are not repeated here.

D. UCKRON in Excel for Mathematical Simulations

On page 235-241 is the explicit solution used in Excel format to make studies, or mathematical "experiments," of any desired and possible nature. The same organization is used here as in previous Excel applications. Column A is the name of the variable, the same as in the FORTRAN program. Column B is the corresponding notation and Column C is the calculation scheme. This holds until line 24. From line 27 the intermediate calculation steps are in coded form. This agrees with the notation used toward the end of the FORTRAN listing. An exception is at the A, B, and C constants for the final quadratic equation. The expression for B was too long that we had to cut it in two. Therefore, after the expression for A, another for D is included that is then included in B.

Pages 1 and 2 list all the calculation details and execute a calculation for the "center point" condition of the former statistical study. This is done at 70 atmospheres hydrogen, 25 atmospheres carbon monoxide, and 5 atmospheres of methanol (all partial pressures), and at 485 K temperature. This is a test case because we know that the rate is 4 mol/m³s at these conditions, and this is satisfied here.

On pages 3 and 4, the calculations for Chapter 5.3: Range Finding Experiments are calculated for the example. The results listed on page 4 in line 38 are listed again in Table 5.3.1 and shown on Figures 5.3.2 and 5.3.3.

On pages 5 and 6, rates are calculated for five different temperatures and otherwise for fixed conditions for discharge. The five rates are given again on line 38. On line 63, the effective energies of activation are listed, calculated from the rate of the previous lower temperature and that one listed in the column. As can be seen this changes significantly with temperature. This should not be any surprise since four kinetic constants and four equilibrium constants are involved in the calculation and each has its own exponential temperature function. This is just an example that kinetic models, when they formally use the Arrhenius type function, are a good approximation for a narrow range of conditions. Still, extrapolations beyond limits are risky.

E. Regression of Results from Preliminary Studies

In this Appendix the results of the previously simulated experiments are anlayzed after 10% random error is added. To each of the four exact calculated results two different random errors are added, generating eight simulated experimental measurements. For a start of a new kinetic study, a simple power–law expression model is recommended and is used here. On the first and second pages, independent variables are converted to the 1000/K, and the natural logarithm of partial pressure scales. On the second page random numbers are gnerated and the four exact results are changed to the eight error–loaded "experimental" results. On the third page, multivariate regression is executed by Mathcad Plus 6 (MathSoft, Inc.), and results are shown and interpreted.

On page 4, rates are calculated for the four specified conditions. Variance is calculated in the "experimental' results and correlation coefficients are used to show that fraction of the variance in the "experimental" results accounted for by the model. This is over 99%. Finally the experimental error is calculated from the "repeated" experiments on page 5.

F. Reactor Empty Volume and Chemisorption Measurements

In Chapter 7.4, empty reactor volume determination of a perfect CSTR is described by following the discharge concentration from the sudden step–change injection of a non–adsorbing inert gas (solid line in the picture.) Next the same experiment is discussed if made with a chemisorbing gas and shown on the previous picture with a dotted line. In this second case, the reactor

volume looks larger because the discharge concentration is increasing more slowly. The virtual larger volume is the result of material missing because it is chemisorbed on the catalyst surface. This measurement is possible only for large charges of very large surface area catalyst, with the lowest concentration of adsorbing component in the gas phase.

G. Calculation of Kinetic Constants

This calculation was made from the "ignition curve" measurements done by Kline et al, (1966) and analyzed by Berty (1997.) description of the experiments appears in Chapter 5.1. In these experiments every point on the ignition curve represents the final conversion achieved at the specified temperature in an approximately plug–flow isothermal integral reactor. Therefore the integrated form of the first–order kinetic equation is the starting point. On the first page using the vectorize command of MathCad, the series calculation can be executed as fast as a single calculation. This command is illustrated by the long arrow above the calculation instruction. On the second page the linear regression feature of MathCad is used to calculate the effective energy of activation at the specified conditions.

H. Rate of Reaction

The simple form of time derivative of concentration was used in classical experiments in physical chemistry to express the rate of reaction. This must be changed to satisfy the condition in industrial reactors in which many other physical changes, such as flow and diffusion occur and for which conditions are frequently in a transient state. These forms are reviewed here.

Appendix A: The UCKRON–1 Test Problem[7]

A.1 Model for Mechanism of Methanol Synthesis Assumed for the Test Problem

$$2H_2 + CO = CH_3OH \qquad K = M'/H'^2C'$$

$$2(H_2 + X_1 = X_2) \qquad K_1 = k_1/k_{-1} = X_2'/(X_1'H') \qquad (1)$$

$$CO + X_2 = X_3 \qquad K_2 = k_2/k_{-2} = X_3'/(X_2 \cdot C') \qquad (2)$$

$$X_3 + X_2 = X_4 + X_1 \qquad K_3 = k_3/k_{-3} = X_4'X_1'/(X_3'X_2') \qquad (3)$$

$$X_4 = CH_3OH + X_1 \qquad K_4 = k_4/k_{-4} = M'X_1'/X_4' \qquad (4)$$

$$X_1 + X_2 + X_3 + X_4 = 1 \qquad K = K_1^2K_2K_3K_4$$
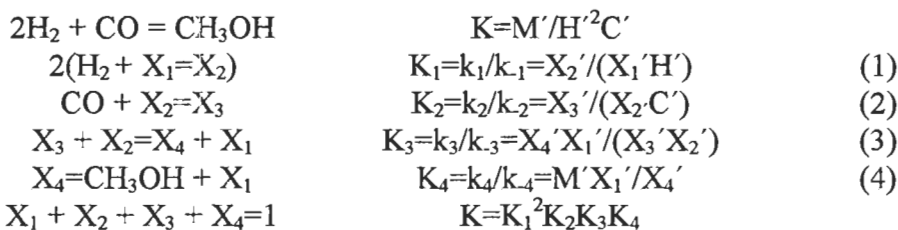
Xs are surface fractions (or active centers), free and covered by chemisorbed species of hydrogen, carbon monoxide, and methanol. H, C, and M are activities of hydrogen, carbon monoxide, and methanol. Primes indicate equilibrium values.

Using the conservation and balance equations for the active centers, but without the assumption of a rate-limiting step, the mathematically rigorous rate expression is the UCKRON–1 Test Problem given below.

Remarks: The aim here was not the description of the mechanism of the real methanol synthesis, where CO_2 may have a significant role. Here we created the simplest mechanistic scheme requiring only that it should represent the known laws of thermodynamics, kinetics in general, and mathematics in exact form without approximations. This was done for the purpose of testing our own skills in kinetic modeling and reactor design on an exact mathematical description of a reaction rate that does not even invoke the rate–limiting step assumption.

A.2 Explicit Form of the Rate Equation for Methanol Synthesis by the UCKRON–1 Test Problem

$$r = \frac{-b \pm (b^2 - 4ac)^{1/2}}{2a} \qquad \text{in mol/(m}^3\text{·s) units.}$$

$$a = K_1 K_2 K_3 \left\{ \left[\frac{\frac{1}{k_4} - \left(\frac{2K_1(1+K_2C)}{k_1} + \frac{K_2}{k_2} \right)}{1 + K_1 H + K_1 K_2 HC + \frac{M}{K_4}} \right] H + \frac{2}{k_1} \right\} \left\{ K_1 \left[\frac{\frac{1}{k_4} - \left(\frac{2K_1(1+K_2C)}{k_1} + \frac{K_2}{k_2} \right)}{1 + K_1 H + K_1 K_2 HC + \frac{M}{K_4}} \right] H + \frac{2}{k_1} C + \frac{1}{k_2} \right\}$$

$$+ \left\{ \left[\frac{\frac{1}{k_4} - \left(\frac{2K_1(1+K_2C)}{k_1} + \frac{K_2}{k_2} \right)}{1 + K_1 H + K_1 K_2 HC + \frac{M}{K_4}} \right] \left[\frac{\left(\frac{2K_1(1+K_2C)}{k_1} + \frac{K_2}{k_2} \right) \frac{M}{K_4} + \frac{1 + K_1 H + K_1 K_2 HC}{k_4}}{1 + K_1 H + K_1 K_2 HC + \frac{M}{K_4}} \right] \right\}$$

$$-b = \frac{1}{1 + K_1 H + K_1 K_2 HC + \frac{M}{K_4}} \left[K_1 K_3 H \left[2K_1 K_2 \left\{ \left[\frac{\frac{1}{k_4} - \left(\frac{2K_1(1+K_2C)}{k_1} + \frac{K_2}{k_2} \right)}{1 + K_1 H + K_1 K_2 HC + \frac{M}{K_4}} \right] H + \frac{2}{k_1} \right\} C + \frac{1}{k_2} \right] + \frac{K_3}{k_3} + 2\frac{\left(\frac{2K_1(1+K_2C)}{k_1} + \frac{K_2}{k_2} \right) \frac{M}{K_4} + \frac{1 + K_1 H + K_1 K_2 HC}{k_4}}{1 + K_1 H + K_1 K_2 HC + \frac{M}{K_4}} - \frac{1}{k_4} \right]$$

$$c = \frac{KH^2 C - M}{K_4 \left(1 + K_1 H + K_1 K_2 HC + \frac{M}{K_4} \right)^2}$$

Appendix B: FORTRAN Program for the Exact Solution

```
   PROGRAM UCKRON
C
*****************************************************************
C   THIS PROGRAM CALCULATES THE RATE OF METHANOL SYNTHESIS
C   REACTION USING THE EXPLICIT FORM OF THE RATE EQUATION
C   PROPOSED BY BERTY J.M., LEE S., SZEIFERT F. AND CROPLEY J.B.
C   IN THEIR PAPER PRESENTED AT THE INTERNATIONAL WORKSHOP
C   ON KINETIC MODEL DEVELOPMENT, AICHE, DENVER, 1983
C   PROGRAMMER - ASHOK SAND
C
*****************************************************************
C
   IMPLICIT REAL (A-Z)
   WRITE (*,10)
10 FORMAT (1X,'INPUT THE EXIT PARTIAL PRESSURES OF HYDROGEN, ',
   &'CARBON MONOXIDE',/3X,'AND METHANOL IN ATMOSPHERES,IN ',
   &'THAT ORDER')
   READ (*,*) H,C,M
   WRITE (*,20)
20 FORMAT (1X,'INPUT THE REACTION TEMPERATURE IN KELVIN')
   READ (*,*) TEMP
C
*****************************************************************
IN THE FOLLOWING SECTION RATE CONSTANTS ARE EVALUATED
C
*****************************************************************
C
   TREF = 485.
   R = 1.987
   RT = (1. / TEMP - 1. / TREF) / R
C
*****************************************************************
C   CONSTANTS OF THE 4 ELEMENTARY REACTIONS RESPECTIVELY
C
*****************************************************************
   SK1 = 0.5 * EXP(-25000.0 * RT)
   SK2 = 20000. * EXP(-15000.0 * RT)
```

227

```
      SK3 = 500000. * EXP(-12000.0 * RT)
      SK4 = 34.047 * EXP(-30000.0 * RT)
C
*******************************************************************
C   K1, K2, K3 AND K4 ARE THE EQUILIBRIUM CONSTANTS OF THE 4
C   ELEMENTARY REACTIONS
C
*******************************************************************
      K1 = SK1 / (3. * EXP(-43000.0 * RT))
      K2 = SK2 / (499984. * EXP(-26400.0 * RT))
      K3 = SK3 / (499936. * EXP(-8000.0 * RT))
      K4 = SK4 / (3.619 * EXP(-10000.0 * RT))
C
*******************************************************************
C   EK IS THE EQUILIBRIUM CONSTANT OF THE OVERALL REACTION
C
*******************************************************************
      EK = (K1**2) * K2 * K3 * K4
C
*******************************************************************
C   THE REACTION IS NOW CALCULATED USING THE EXPLICIT FORM OF
C   THE RATE EXPRESSION GIVEN IN THE PAPER
C
*******************************************************************
      F = (1. / SK4) - ((2. * K1 * (1. + K2 * C)) / SK1 + (K2 / SK2))
      G = 1. + K1 * H + K1 * K2 * H * C + M / K4
      N = F / G * H + 2. / SK1
      I = K1 * N * C + 1. / SK2
      J = (1. / SK4 - F) * M / K4 + (1. + K1*H + K1*K2*H*C) / SK4
      L = J / G
      A = K1*K2*K3*N*I + L*F/G
      B  =  1.  /  G*(K1*K3*H*(2.*K1*K2*N*C  +  K2/SK2)  +  2.*L-
1./SK4)+K3/SK3
      CC = (EK*H**2*C - M)/(K4*G**2)
      RATE = (B - SQRT(B**2. - 4.*A*CC))/(2.*A)
      WRITE (*,120) TEMP
120   FORMAT(1X,'AT TEMPERATURE = ',F8.2,' K')
      WRITE (*,130) RATE
130   FORMAT(1X,'REACTION RATE =',F9.5,' MOLES/M**3/SEC')
      STOP
      END

      _
```

	A	B	C	D	E	F
1	APPENDIX C		Page 1, REACTION:	NO + NO2 + 2 NH3 = 2 N2 + 3 H2O		
2						
3	INPUT VARIABLE	SYMBOL	PROPERTY from reference	SI UNITS	SI DIMENSION	SI DIMENSION
4			Original units			
5	CATALYST & BED PROPERTIES					
6	Particle diam.	dp	200 micron	*10^-6 = m	2.00E-04	2.00E-04
7	Shape factor	Phi	1		1.00E+00	1.00E+00
8	Cat.porosity	Theta	0.3		3.00E-01	3.00E-01
9	Tortuosity Fact	Tau	3		3.00E+00	3.00E+00
10	Charge volum	V	2 cm3	*10^-6 = m3	2.00E-06	2.00E-06
11	Basket diameter	dt	1.95 inches	*0.0254 = m	4.95E-02	4.95E-02
12	Bed porosity	Epsylon	0.35		3.50E-01	3.50E-01
13						
14	FLUID PROPERTIES at T and P of REACTION					
15	Av.mol weight	MW	29 g/mol	*10^-3 = kg/mol	2.90E-02	2.90E-02
16	Heat. cap.	cp	0.256 cal/g*K	*4,184.0 = J/(kg*K)	1.07E+03	1.07E+03
17	Viscosity	mu	0.0331centipoise	*0.001 = kg/m.s	3.31E-05	3.31E-05
18	Thermal condy	kt	121*(10^-6) (cal/cm*sec*K)	*4.184 =W /m.K	5.06E-02	5.06E-02
19	Diffusivity	D	0.180 cm2/sec	*10^-4 = m2/s	1.80E-05	1.80E-05
20	Feed mol fract.	yo	100 PPM	mol/mol	1.00E-04	1.00E-04
21	Conversion	X	90%	mol/mol	9.00E-01	9.00E-01
22	Heat of reaction	deltaHr		kJ/mol	3.01E+02	3.01E+02
23	Stoichiom.coeff	alpha			-1.00E+00	-1.00E+00
24	Expansion coeff	delta			5.00E-01	5.00E-01
25	Effective diffusiv	De	De = (theta/tau)D	m2/sec	1.80E-06	1.80E-06
26						
27	EXPERIMENTAL CONDITIONS					
28	Shaft speed	kRPM	7	min-1	7.00E+00	7.00E+00
29	Linear velocity	u	58.7 cm/sec	*10^-2 = m/s	5.87E-01	5.87E-01
30	Temperature	T	232 C	273 = K	5.05E+02	5.05E+02
31	Pressure	P	1.1 atm	*101325 kg/m*s2 = Pa	1.11E+05	1.11E+05
32	Space velocity	GHSV	25000/h	h-1 (STP)	2.50E+04	2.50E+04
33	Gas constant	R		m3*Pa/(mol*K)	8.31E+00	8.31E+00
34						

	A	B	C	D	E	F
35	A P P E N D I X C		Page 2, REACTION:	NO + NO2 + 2 NH3 = 2 N2 + 3 H2O		
36						
37	CALCULATED VARIABLES					
38	NAME	SYMBOL	FORMULA	CALCULATION SCHEME		
39						
40	Feed rate	Fo	V*GHSV/3600, m^3/s	E10*E32/3600	1.39E-05	1.39E-05
41	Feed rate at Tr,Pr	F'	Fo(T/273)(101325/P)	E40(E30/273)(101325/E31)	2.34E-05	2.34E-05
42	Feed concentratio	Co =	yo*P/R*T, mol/m^3	E20*E31/(E30*E33)	2.65E-03	2.65E-03
43	Discharge conc	C =	(1-X)*y*P/R*T, mol/m^3	(1-E21)*E41	2.65E-04	2.65E-04
44	Basket cross sect	A =	dt^2*Pi/4, m^2	E11^2*Pi/4	1.92E-03	1.92E-03
45	Bed depth	L =	V/A, m	E10/E43	1.04E-03	1.04E-03
46	dimensionless	L/dp =		E44/E6	5.20E+00	5.20E+00
47	Cat.surf/Bed v	S/V =	(6/dp)*91-eps), m^-1	(6/E6)*(1-E12)	1.95E+04	1.95E+04
48	Standard density	rhoo =	MW/0.0224 kg/m^3	E15/0.0224	1.29E+00	1.29E+00
49	Density at Tr, Pr	rho =	rhoo*(273/T)*(P/101250),kg.m^3	E47*(273/E29)*(E30/101250)	7.70E-01	7.70E-01
50	Recyle flow	nF'	u*A, m^3/s, at Tr,Pr	E29*E44	1.13E-03	1.13E-03
51	Space time	V/F =	(3600/GHSV)*alpha. mol/m^3.s	(3600/E31)	1.44E-01	1.44E-01
52	Mass velocity	G =	u*rho, (kg/m^2*s)	*E28*E48	4.52E-01	4.52E-01
53	Reaction rate	r =	(C - Co)*(V/F)*alpha, mol/m^3*s	E23*(E43-E42)/E51	1.66E-02	1.66E-02
54	Recycle ratio	n =	u*A/F'	E29*E44/E41	4.83E+01	4.83E+01
55						
56	DIMESIONLESS VARIABLES					
57	Reynolds No.	Rep =	dp*G/mu	E6*E52/E17	2.73E+00	2.73E+00
58	Prandit No.	Pr =	mu*c/kt	E17*E16/E18	7.00E-01	7.00E-01
59	Schmidt No.	Sc =	mu/(rho*D)	E17/(E48*E19)	2.39E+00	2.39E+00
60	Colburn factor	jH=jD=	1.15*Rep^(-0.5)	1.15*E56^(-0.5)	6.96E-01	6.96E-01
61	Adiab.Temp.	beta =	(-deltHr*C)/(rho*c*T)	(E42*E22)/(E48*E16*E29)	1.92E-07	1.92E-07
62						
63	TRANSFER COEFFICIENTS					
64	Heat transfer	h =	jH*G*c/(Pr^0.67), kW.m^2*K	E60*E52*E16/(1000*E58^0.67)	4.28E-01	4.28E+02
65	Mass transfer	kg =	JD*u/(Sc^0.67), m/s	E59*E28/(E58^0.67)	2.28E-01	2.28E-01
66						
67						

	A	B	C	D	E	F
68	A P P E N D I X C		Page 3, REACTION:	NO + NO2 + 2 NH3 = 2 N2 + 3 H2O		
69						
70	CRITERIA	Dimensionless numbers		Critical values		
71		Driving forces				
72	In flow direction	L = L				
73						
74	DaI =	r L/(C u) =(Ci -C)/C	E53*E45/(E43*E29)	5.00E-02	1.11E-01	1.11E-01
75	Ci - C =	DaI*C	D74*E43, mol/m3		2.94E-05	2.94E-05
76						
77	DaII =	r L deltaHr/(u rho c T)	E52*E44*E22/(E29*E48*E16*E30)	5.00E-03	2.12E-08	2.12E-08
78	T - Ti =	DaII*T	D77*E30, K		1.07E-05	1.07E-05
79						
80						
81	Normal to flow	L =dp/6(1-eps)				
82						
83	Ca =	r dp/(C kg 6(1-eps))	E53*E6/(E43*E65* 6(1-E12))	5.00E-02	1.41E-02	1.41E-02
84	C - Cs =	Ca*C	D83*E43, mol/m3		3.73E-06	3.73E-06
85						
86	DaV	r dp (-deltaHr)/(h T 6(1-eps)	E53*E6*E22/(E64*E30*6(1-E12))	5.00E-03	1.19E-06	1.19E-09
87	Ti - T =	DaV*T	D86*E30, K		5.99E-04	5.99E-07
88						
89						
90	Inside pellet	L =dp/6(1-eps)				
91						
92	PHI =	r dp^2/(De C 6(1-eps)	E52*E6^2/(E25*	5.00E-02	3.56E-02	3.56E-02
93	dC/dl =	PHI*C/dp	D92*E43/E6		4.73E-02	4.73E-02
94						
95	DaIV =	(-deltaHr)r dp^2/(kt T 6(1-ep	E53*E22*E6^2/(E18*E30*6(1-eps))	5.00E-03	2.00E-09	2.00E-09
96	dT/dl =	DaIV*T/dp	D95*E30/dp		5.06E-03	5.06E-03
97						

	A	B	C	D	E	F
1	**A P P E N D I X C**		Page 4, REACTION:	CO + 2 H2 = CH3OH		
2						
3	INPUT VARIABLE	SYMBOL	PROPERTY from reference	SI UNITS	SI DIMENSION	SI DIMENSION
4			Original units			
5	CATALYST & BED PROPERTIES					
6	Particle diam.	dp	0.5 cm	*10^-2 = m	5.00E-03	5.00E-03
7	Shape factor	Phi	sphere		1.00E+00	1.00E+00
8	Cat.porosity	Theta	0.4		3.00E-01	3.00E-01
9	Tortuosity Fact	Tau	2		3.00E+00	3.00E+00
10	Charge volum	V	20 cm3	*10^-6 = m3	2.00E-05	2.00E-05
11	Basket diamete	dt	1.97 inches	*0.0254 = m	5.00E-02	5.00E-02
12	Bedporosity	Epsylon	0.4		4.00E-01	4.00E-01
13						
14	FLUID PROPERTIES at T and P of REACTION					
15	Av.mol weight	MW	11 g/mol	*1 = kg/mol	1.10E-02	1.10E-02
16	Heat. cap.	cp	33.8 J/mol K	/11 = kJ/kg*K	3.07E+00	3.07E+00
17	Viscosity	mu	0.17 centipoise	*1.02(10^-4) Pa s	1.73E-05	1.73E-05
18	Thermal conduct.	kt	0.0438 BTU/(h)(sqft)(F.ft)	*1.73(10^-3) kW/m s	7.58E-05	7.58E-05
19	Diffusivity	D	0.41 cm^2/s	*10^-4 = m2/s	4.10E-05	4.10E-05
20	Feed mol fract.	yo	0.145	mol/mol	1.45E-01	1.45E-01
21	Conversion	X	24%	mol/mol	2.41E-01	2.41E-01
22	Heat of reaclon	deltaHr	98000 J/mol	/1000 kJ/mol	9.80E+01	9.80E+01
23	Stoichiom.coeff	alpha			-1.00E+00	-1.00E+00
24	Expansion coeff	delta			2.00E+00	2.00E+00
25	Effextive diffu	De	De = (theta/tau)D	m2/sec	4.10E-06	4.10E-06
26						
27	EXPERIMENTAL CONDITIONS					
28	Shaft speed	kRPM	7	min-1	2.50E+03	2.50E+03
29	Linear velocity	u	1.1 m/s		1.10E+00	1.10E+00
30	Temperature	T	232 C +	273 = K	5.05E+02	5.05E+02
31	Pressure	P	52 atm	*101325 kg/m*s2 = Pa	5.27E+06	5.27E+06
32	Space velocity	GHSV	12000/h	h-1 (STP)	1.20E+04	1.20E+04
33	Gas constant	R		m3*Pa/(mol*K)	8.31E+00	8.31E+00
34						

	A	B	C	D	E	F
35	APPENDIX C		Page 5, REACTION:	CO + 2 H2 = CH3OH		
36						
37	CALCULATED VARIABLES					
38	NAME	SYMBOL	FORMULA	CALCULATION SCHEME		
39						
40	Feed rate	Fo	V*GHSV/3600, m^3/s	E10*E31/3600	6.67E-05	6.67E-05
41	Feed rate at Tr,Pr	F	Fo(T/273)(101325/P)	E40(E30/273)(101325/E31)	2.37E-06	2.37E-06
42	Feed concentratic	Co =	yo*P/R*T, mol/m^3	E20*E31/(E30*E33)	1.82E+02	1.82E+02
43	Discharge conc	C =	(1-X)*y*P/R*T, mol/m^3	(1-E21)*E41	1.38E+02	1.38E+02
44	Basket cross s.	A =	dt^2*Pi/4, m^2	E11^2*Pi/4	1.96E-03	1.96E-03
45	Bed depth	L =	V/A, m	E10/E44	1.02E-02	1.02E-02
46	dimensionless	L/dp =		E44/E6	2.04E+00	2.04E+00
47	Cat.surf/Bed v	S/V =	(6/dp)*91-eps), m^-1	(6/E6)*(1-E12)	7.20E+02	7.20E+02
48	Standard density	rhoo =	MW/0.0224 kg/m^3	E15/0.0224	4.91E-01	4.91E-01
49	Density at Tr, Pr	rho =	rhoo*(273/T)*(P/101250),kg.m^3	E46*(273/E30)*(E31/101250)	1.38E+01	1.38E+01
50						
51	Space time	V/Fo =	(3600/GHSV)*alpha. mol/m^3.s	(3600/E32)	3.00E-01	3.00E-01
52	Mass velocity	G =	u*rho, (kg/m^2*s)	*E28*E49	1.52E+01	1.52E+01
53	Reaction rate	r =	(C - Co)*F/V*alpha, mol/m^3*s	E23*(E43-E42)E41/E10	5.21E+00	5.21E+00
54	Recycle ratio	n =	u*A/F	E29*E44/E41	9.10E+02	9.10E+02
55						
56	DIMESIONLESS VARIABLES					
57	Reynolds No.	Rep =	dp*G/mu	E6*E51/E17	4.38E+03	4.38E+03
58	Prandlt No.	Pr =	mu*c/kt	E17*E16/E18	7.03E-01	7.03E-01
59	Schmidt No.	Sc =	mu/(rho*D)	E17/(E49*E25)	3.06E-01	3.06E-01
60	Colburn factor	jH=jD=	1.15*Rep^(-0.5)	1.15*E57^(-0.5)	1.74E-02	1.74E-02
61	Adiab.Temp.	beta =	(-deltHr*C)/(rho*c*T)	(E43*E22)/(E49*E16*E29)	6.31E-01	6.31E-01
62						
63	TRANSFER COEFFICIENTS					
64	Heat transfer	h =	jH*G*c/(Pr^0.67), kW.m^2*K	E60*E52*E16/(E58^0.67)	1.03E+00	1.03E+00
65	Mass transfer	kg =	jD*u/(Sc^0.67), m/s	E60*E29/(E59^0.67)	4.22E-02	4.22E-02
66						
67						

	A	B	C	D	E	F
68	APPENDIX C		Page 6, REACTION:	CO + 2 H2 = CH3OH		
69						
70	CRITERIA					
71						
72	Indirection of flow L = V/A					
73						
74	Dal =	r L/(C u) =(Ci -C)/C	E53*E45/(E43*E29)	3.50E-04		
75	Ci - C =	Dal*C	D74*E43, mol/m3	4.83E-02		
76						
77	DalII =	r L deltaHr/(u rho c T)	E52*E44*E22/(E30*E48*E16*E29)	2.21E-04		
78	T - Ti =	DalII*E30	D77*E30, K	1.11E-01		
79						
80						
81	Normal toflow	L =dp/6(1-eps)				
82						
83	Ca =	r dp/(C kg 6(1-eps))	E53*E6/(E43*E65* 6(1-E12))	1.24E-03		
84	C - Cs =	Ca*C	D83*E43, mol/m3	1.71E-01		
85						
86	DaV	r dp (-deltaHr)/(h T 6(1-eps)	E53*E6*E22/(E64*E30*6(1-E12))	1.37E-03		
87	Ts - T =	DaV*T	D86*E30	6.90E-01		
88						
89						
90	Inside pellet	L =dp/6(1-eps)				
91						
92	PHI =	r dp^2/(De C 6(1-eps)	E52*E6^2/(E25*	6.39E-03		
93	dC/dl =	PHI*C/dp	D92*E43/E6, (mol/m3)/m	1.76E+02		
94						
95	DalV =	(-deltaHr)r dp^2/(kt T 6(1-ep	E53*E22*E6^2/(E18*E30*6(1-eps))	9.26E-02		
96	dT/dl =	DalV*T/dp	D95*E30/E6, K/m	9.36E+03		
97						

Appendix D: UCKRON Test Data from Excel

	A	B	C	D
1	APPENDIX D		UCKRON in EXCEL page 1	
2				
3	This program calculates the rate of methanol synthesis using explicit form of the			
4	rate equations proposed by J.M. Berty, S. Lee,F. Szeifert, and J. B. Cropley			
5	on page12-13, in their paper In Chem. Eng. Comm. 1989, Vol.76, PP 9-33.			
6	Exit condition in atm and K			
7	Hydrogen	H		7.00E+01
8	Carbon Monoxide	C		2.50E+01
9	Methanol	M		5.00E+00
10	Reactor temp.K	T		4.85E+02
11		1000/T		2.06E+00
12	Evaluation of "k"			
13	Ref. temp. K	Tref		4.85E+02
14	Gas constant	R		1.98E+00
15		RT		0.00E+00
16	Forward	k1	0.5*EXP(-25000*D15)	5.00E-01
17	kinetic	k2	20000*exp(-15000*D15)	2.00E+04
18	constants	k3	500000*exp(-12000*D15)	5.00E+05
19	at T	k4	34.047*exp(30000*D15)	3.40E+01
20	Equilibrium	K1	C14/(3*exp(-43000*D15)	1.67E-01
21	constants of the	K2	C15/(20000*EXP(-15000*D15))	4.00E-02
22	4 elementary	K3	C16/(499936*EXP(-8000*D15))	1.00E+00
23	reactions at T	K4	C17/(3.619*EXP(-10000*D15))	9.41E+00
24	Overall equ.const	EK	(C20^2)*C21*C22*C23	1.05E-02
25				
26	Rate calc. from explicit form			
27	F =		(1/D19)-(2*D20*(1+D21*D8))/D16+(D21/D17)	-1.30E+00
28	G =		1+D20*D7+D20*D21*D7*D8 +D9/D23	2.49E+01
29	N =		D27/D28*D7+2/D16	3.29E-01
30	I =		D20*D29*D8+1/D17	1.37E+00
31	J =		(1/D19-D27)*D9/D23+(1+D20*D7+D20*D21*D7*D8)/D19	1.42E+00

	A	B	C	D
32	APPENDIX D		UCKRON in EXCEL page 2	
33	L =	D31/D28		5.72E-02
34	A =	D20*D21*D22*D29*D30+D35*D27/D28		6.37E-06
35	D =	(2*D20*D21*D29*D8+D21/D17)		1.10E-01
36	B =	1/D28*(D20*D22*D7*D35+2*D33-1/D19)+D22/D18		5.49E-02
37	CC =	(D24*D7^2*D8-D9)/(D23*D28^2)		2.19E-01
38	Rate =	(D36-SQRT(D36^2-4*D34*D37))/(2*D34)		4.00E+00
39	LN(RATE)			1.39E+00
40	LOG10(RATE)			6.02E-01
41				
42	Material Balance Calculation,		(Fo/V)yjo = -arj + (F/V)yj,	
43	No Methanol in Feed		aM = 1, aH = -2, aC = -1,	
44	Total Pressure	P = H+C+M	D7 + D8 + D9	1.00E+02
45	yH	H/P	D7/D44	7.00E-01
46	yC	C/P	D8/D44	2.50E-01
47	yM	M/P	D9/D44	5.00E-02
48				
49	(Fo/V)yMo=0			
50	(F/V)yM	arM	D38	4.00E+00
51	F/V	arM/yM	D38/D47	7.99E+01
52	(F/V)yH	(F/V)yH	D51*D45	5.60E+01
53	(F/v)yC	(F/V)yC	D51*D46	2.00E+01
54	(F/V), check	yH+yC+yM	D50+D52+D53	7.99E+01
55				
56	(Fo/V)yHo	(F/V)yH-2arM	D52+2*D50	6.40E+01
57	(Fo/V)yCo	(F/V)yC-arM	D52+D50	2.40E+01
58	(Fo/V)	(Fo/V)(yCo+yHo	D56+D57	8.79E+01
59	Fo/V=2rM+F/V	2rM+F/v	2*D50 + D51	8.79E+01
60				
61				
62				
63				

	E	F	G	H	I	J	K
1	APPENDIX D		PRELIMINARY STUDY		page 3		
2							
3							
4							
5							
6							
7	H	80	60	60	80		
8	C	40	30	30	40		
9	M	10	2.5	10	2.5		
10	T	495	495	475	475		
11		2.0202	2.0202	2.10526	2.10526		
12							
13	refT						
14	R						
15	RT	-2.11E-05	-2.11E-05	2.19E-05	2.19E-05		
16	k1	0.84647	0.84647	0.28887	0.28887		
17	k2	27429.2	27429.2	14390.3	14390.3		
18	k3	643750	643750	384240	384240		
19	k4	64.0392	64.0392	17.6262	17.6262		
20	K1	0.11408	0.11408	0.2474	0.2474		
21	K2	0.03146	0.03146	0.05137	0.05137		
22	K3	1.08802	1.08802	0.91608	0.91608		
23	K4	14.3351	14.3351	6.06565	6.06565		
24	EK	0.00639	0.00639	0.01747	0.01747		
25							
26							
27	F =	-0.59319	-0.50838	-4.29594	-5.17588		
28	G =	22.311	14.4807	40.3695	61.8742		
29	N =	0.23577	0.25633	0.53858	0.23137		
30	I =	1.07596	0.87733	3.99739	2.28975		
31	J =	0.7622	0.31478	9.37273	5.64362		

	E	F	G	H	I	J	K
32	**APPENDIX D**		PRELIMINARY STUDY page 4				
33	L =	0.03416	0.02174	0.23217	0.09121		
34	A =	8.2E-05	0.00012	0.00036	-0.00146		
35	D =	0.06771	0.05521	0.4107	0.23525		
36	B =	0.0325	0.03032	0.14844	0.07097		
37	CC =	0.22774	0.22865	0.18987	0.1925		
38	**Rate =**	**7.13695**	**7.77068**	**1.28309**	**2.57578**		
39	LN(RATE)	1.96528	2.05036	0.24927	0.94615		
40	LOG10(RATE)	0.85351	0.89046	0.10826	0.41091		
41							
42							
43							
44	Total Pressure	130	92.5	100	122.5		
45	yH	0.61538	0.64865	0.6	0.65306		
46	yC	0.30769	0.32432	0.3	0.32653		
47	yM	0.07692	0.02703	0.1	0.02041		
48							
49	(Fo/V)yMo=0						
50	(F/V)yM	7.13695	7.77068	1.28309	2.57578		
51	F/V	92.7803	287.515	12.8309	126.213		
52	(F/V)yH	57.0956	186.496	7.69855	82.4251		
53	(F/v)yC	28.5478	93.2481	3.84928	41.2126		
54	(F/V), check	92.7803	287.515	12.8309	126.213		
55							
56	(Fo/V)yHo	71.3695	202.038	10.2647	87.5767		
57	(Fo/V)yCo	35.6847	101.019	5.13237	43.7883		
58	(Fo/V)	107.054	303.056	15.3971	131.365		
59	Fo/V=2rM+F/V	107.054	303.056	15.3971	131.365		
60							
61							
62							
63	Ea						

	L	M	N	O	P	Q
1	APPENDIX D		TEMPERATURE EFFECT page 5			
2						
3						
4						
5						
6						
7	H	64	64	64	64	64
8	C	32	32	32	32	32
9	M	4	4	4	4	4
10	T	470	479.3	489.5	501	513.7
11		2.1276596	2.086376	2.0429009	1.996008	1.9466615
12						
13	refT					
14	R					
15	RT	3.327E-05	1.24E-05	-9.58E-06	-3.33E-05	-5.82E-05
16	k1	0.2176549	0.3667555	0.6353511	1.1492432	2.1442624
17	k2	12142.525	16606.341	23091.719	32953.016	47908.74
18	k3	335423.3	430888.77	560933.03	745524.87	1005721.7
19	k4	12.549803	23.472902	45.38699	92.429198	195.36572
20	K1	0.303329	0.208332	0.1402611	0.0915399	0.0584234
21	K2	0.0584496	0.0460732	0.0358616	0.0273688	0.020594
22	K3	0.8755145	0.9517451	1.0392083	1.1425792	1.262481
23	K4	4.8364752	7.3420199	11.395288	18.308123	30.153422
24	EK	0.022772	0.0139732	0.0083547	0.0047974	0.0026759
25						
26						
27	F =	-7.920796	-2.768449	-0.926168	-0.288004	-0.085285
28	G =	57.550058	34.535835	20.629153	12.207977	7.3358552
29	N =	0.3803382	0.3228796	0.274516	0.2304207	0.1886719
30	I =	3.6918452	2.1525773	1.2321685	0.6749964	0.3527525
31	J =	11.136617	2.9795831	0.7796226	0.195003	0.0488628

	L	M	N	O	P	Q
32	APPENDIX D		TEMPERATURE EFFECT page 6			
33	L =	0.1935118	0.0862751	0.0377923	0.0159734	0.0066608
34	A =	-0.004838	-0.000567	7.138E-05	6.838E-05	2.366E-05
35	D =	0.4315692	0.1983495	0.0883736	0.0369469	0.0145288
36	B =	0.1327995	0.0766465	0.042561	0.0219909	0.0104686
37	CC =	0.186084	0.20869	0.2249909	0.2289891	0.2136818
38	Rate =	**1.3361974**	**2.6700511**	**5.3340265**	**10.773883**	**21.451709**
39	LN(RATE)	0.2898278	0.9820976	1.6741064	2.3771249	3.0658043
40	LOG10(RATE)	0.1258706	0.4265196	0.7270552	1.0323722	1.3314619
41						
42						
43						
44	Total Pressure	100	100	100	100	100
45	yH	0.64	0.64	0.64	0.64	0.64
46	yC	0.32	0.32	0.32	0.32	0.32
47	yM	0.04	0.04	0.04	0.04	0.04
48						
49	(Fo/V)yMo=0					
50	(F/V)yM	1.3361974	2.6700511	5.3340265	10.773883	21.451709
51	F/V	33.404935	66.751279	133.35066	269.34707	536.29271
52	(F/V)yH	21.379159	42.720818	85.344424	172.38212	343.22734
53	(F/v)yC	10.689579	21.360409	42.672212	86.191061	171.61367
54	(F/V), check	33.404935	66.751279	133.35066	269.34707	536.29271
55						
56	(Fo/V)yHo	24.051553	48.060921	96.012477	193.92989	386.13075
57	(Fo/V)yCo	12.025777	24.03046	48.006238	96.964944	193.06538
58	(Fo/V)	36.07733	72.091381	144.01872	290.89483	579.19613
59	Fo/V=2rM+F/V	36.07733	72.091381	144.01872	290.89483	579.19613
60						
61						
62						
63	Ea		-33201.9	-31516.41	-29684.15	-27632.86

Appendix E: Regression of Results from Preliminary Studies

10-7-98, JMB

Model: rate = k exp(-E/RT) P(CO/H)^m P(MeOH)^n

Log form; ln rate = ln k - E/*RT + m*ln(C) + n*ln(M)

Coded: y = b + a1*x1 + a2*x2 +a3*x3

Code:

a1 = -E/(1000*R) X1 = 1000/T

a2 = m X2 = C

a3 = n X3 = M

(Mathcad Plus 6, of MathSoft, Inc. was used)

Independent Variables on log scale

$$
vT := \begin{bmatrix} 495 \\ 495 \\ 475 \\ 475 \\ 495 \\ 495 \\ 475 \\ 475 \end{bmatrix}
\qquad vX1 := \overrightarrow{\dfrac{1000}{vT}}
\qquad vX1 = \begin{bmatrix} 2.02 \\ 2.02 \\ 2.105 \\ 2.105 \\ 2.02 \\ 2.02 \\ 2.105 \\ 2.105 \end{bmatrix}
$$

$$
vPC := \begin{bmatrix} 120 \\ 90 \\ 90 \\ 120 \\ 120 \\ 90 \\ 90 \\ 120 \end{bmatrix}
\qquad vX2 := \overrightarrow{\ln(vPC)}
\qquad vX2 = \begin{bmatrix} 4.787 \\ 4.5 \\ 4.5 \\ 4.787 \\ 4.787 \\ 4.5 \\ 4.5 \\ 4.787 \end{bmatrix}
$$

$$vPM := \begin{bmatrix} 10 \\ 2.5 \\ 10 \\ 2.5 \\ 10 \\ 2.5 \\ 10 \\ 2.5 \end{bmatrix} \qquad vX3 := \overrightarrow{\ln(vPM)} \qquad vX3 = \begin{bmatrix} 2.303 \\ 0.916 \\ 2.303 \\ 0.916 \\ 2.303 \\ 0.916 \\ 2.303 \\ 0.916 \end{bmatrix}$$

Random Numbers generated:

$$r := runif(8, -0.1, 0.1) \qquad\qquad \text{Error-free results}$$

$$r = \begin{bmatrix} -0.1 \\ -0.061 \\ 0.017 \\ -0.03 \\ 0.065 \\ -0.065 \\ 0.042 \\ -0.039 \end{bmatrix} \qquad\qquad vr := \begin{bmatrix} 7.14 \\ 7.77 \\ 1.28 \\ 2.58 \\ 7.14 \\ 7.77 \\ 1.28 \\ 2.58 \end{bmatrix}$$

Results with 10% random error added

$$vR := \overrightarrow{[vr \cdot (1 + r)]} \qquad\qquad vR = \begin{bmatrix} 6.428 \\ 7.293 \\ 1.302 \\ 2.503 \\ 7.601 \\ 7.264 \\ 1.334 \\ 2.479 \end{bmatrix}$$

log of "experimental" results

$$\text{vz} := \overrightarrow{\ln(\text{vR})}$$

$$\text{vz} = \begin{bmatrix} 1.861 \\ 1.987 \\ 0.264 \\ 0.917 \\ 2.028 \\ 1.983 \\ 0.288 \\ 0.908 \end{bmatrix}$$

Multivariate Regression for k=1 degree polynomial and 3 variables:

$$k := 1$$

$$\text{Mxyu} := \begin{bmatrix} 2.02 & 4.787 & 2.303 \\ 2.02 & 4.5 & 0.916 \\ 2.105 & 4.5 & 2.303 \\ 2.105 & 4.787 & 0.916 \\ 2.02 & 4.787 & 2.303 \\ 2.02 & 4.5 & 0.916 \\ 2.105 & 4.5 & 2.303 \\ 2.105 & 4.78 & 0.916 \end{bmatrix}$$

$$\text{vm} := \text{regress}(\text{Mxyu}, \text{vz}, k)$$

$$\text{vm} = \begin{bmatrix} 3 \\ 3 \\ 1 \\ -16.101 \\ 1.045 \\ -0.245 \\ 30.031 \end{bmatrix}$$

y = b + a1*X1 + a2*X2 + a3*X3

y = 30.0 - 16.1*(1000/T) + 1.05*ln(pC) - 0.245*ln(pM)

rate = 10^13*e^(-16100/T)*pC^1.045*pM^-0.245

Ea = 16100*1.98 = 31878 cal/mol

Results Calculated from Regression

$$y1 := 30 - 16.1 \cdot 2.02 + 1.05 \cdot 4.79 - 0.245 \cdot 2.3 \qquad\qquad y1 = 1.944$$

$$y2 := 30 - 16.1 \cdot 2.02 + 1.05 \cdot 4.5 - 0.245 \cdot 0.916 \qquad\qquad y2 = 1.979$$

$$y3 := 30 - 16.1 \cdot 2.11 + 1.05 \cdot 4.5 - 0.245 \cdot 2.3 \qquad\qquad y3 = 0.19$$

$$y4 := 30 - 16.1 \cdot 2.11 + 1.05 \cdot 4.79 - 0.245 \cdot 0.916 \qquad\qquad y4 = 0.834$$

$$r1 := \exp(y1) \qquad r2 := \exp(y2) \qquad r3 := \exp(y3) \qquad r4 := \exp(y4)$$

$$r1 = 6.987 \qquad\quad r2 = 7.232 \qquad\quad r3 = 1.21 \qquad\quad r4 = 2.303$$

Statistical Characterization of Results from Preliminary Experiments

Experiments at 4 conditions, each run twice

2 repeats, listed separately

$$A := \begin{bmatrix} 6.43 & 7.60 \\ 7.29 & 7.26 \\ 1.30 & 1.33 \\ 2.50 & 2.48 \end{bmatrix} \qquad C := \begin{bmatrix} 6.43 \\ 7.29 \\ 1.30 \\ 2.50 \end{bmatrix} \qquad D := \begin{bmatrix} 7.60 \\ 7.26 \\ 1.33 \\ 2.48 \end{bmatrix}$$

In experimental results: Calculated results:

$$\mathrm{mean}(A) = 4.524$$

$$B := \begin{bmatrix} 6.99 \\ 7.23 \\ 1.21 \\ 2.30 \end{bmatrix}$$

$$\mathrm{var}(A) = 7.138$$

$$\mathrm{stdev}(A) = 2.672$$

Correlation of results

$$\mathrm{corr}(B, C) = 0.996 \qquad\qquad \mathrm{corr}(B, D) = 0.997$$

$$C - D = \begin{bmatrix} -1.17 \\ 0.03 \\ -0.03 \\ 0.02 \end{bmatrix}$$

Standard Deviation of Experimental
Results from pairs of Measurements

$$V := \frac{\left[(-1.17)^2 + (0.03)^2 + (-0.03)^2 + (0.02)^2 - \dfrac{(-1.17 + 0.03 - 0.03 + 0.02)^2}{8} \right]}{7}$$

variance in results $V = 0.172$

standard deviation in results s $s := V^{0.5}$ $s = 0.415$

From the original variance in the data var(A) =7.138 after the correlation
only the variance of $V = 0.172$ remained. This is less than 3 % not fitted.
This is not surprising since we fitted straight lines through 2 points.

Appendix F: Chemisorption

$\theta := 0, 0.5 .. 6.0$

$C/C0 = 1 - \exp(-F'/V*t)$
$-F/V*t = \theta$

$$\left(1 - e^{-\theta}\right)$$

0
0.393
0.632
0.777
0.865
0.918
0.95
0.97
0.982
0.989
0.993
0.996
0.998

$$\left(1 - e^{-0.8 \cdot \theta}\right)$$

0
0.33
0.551
0.699
0.798
0.865
0.909
0.939
0.959
0.973
0.982
0.988
0.992

$1 - e^{-\theta}$

$1 - e^{-0.8 \cdot \theta}$
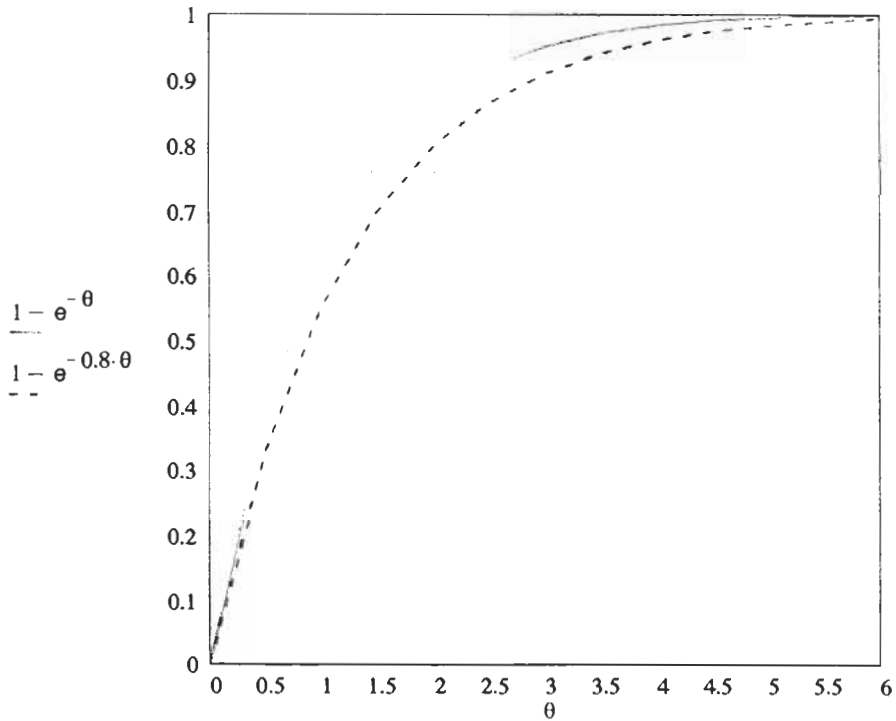
Appendix G: Calculation of Kinetic Constants

Basis: Lafayette Experiments of 7/15/93, Figure 2, Ignition Curve, Reactor 2, MMG catalyst 3, 57.1 PPM TCE, GHSV of 10800

Conversions:

$$K \equiv 1Q$$

$$vX := \begin{bmatrix} 0.001 \\ 0.02 \\ 0.06 \\ 0.35 \\ 0.75 \\ 0.93 \\ 0.999 \end{bmatrix} \qquad vkt := (-\ln(1 - vX)) \qquad vkt = \begin{bmatrix} 1.001 \cdot 10^{-3} \\ 0.02 \\ 0.062 \\ 0.431 \\ 1.386 \\ 2.659 \\ 6.908 \end{bmatrix}$$

Temperature:

$$vT := \begin{bmatrix} 373 \cdot K \\ 423 \cdot K \\ 473 \cdot K \\ 523 \cdot K \\ 573 \cdot K \\ 623 \cdot K \\ 673 \cdot K \end{bmatrix} \qquad vx := \frac{1000 \cdot K}{vT} \qquad vx = \begin{bmatrix} 2.681 \\ 2.364 \\ 2.114 \\ 1.912 \\ 1.745 \\ 1.605 \\ 1.486 \end{bmatrix}$$

$$vy := \ln(vkt) \qquad vy = \begin{bmatrix} -6.907 \\ -3.902 \\ -2.783 \\ -0.842 \\ 0.327 \\ 0.978 \\ 1.933 \end{bmatrix} \qquad k_{623} := 2.659 \cdot \frac{3}{\sec}$$

$$k_{623} = 7.977 \cdot \sec^{-1}$$

Linear Regression of ln(kt) = y with 1000*K/vT = x

$i := 0..6$ vx := vx   vy := vy

$\text{mean}(vx) = 1.987$ $\text{mean}(vy) = -1.6$

$\text{stdev}(vx) = 0.397$ $\text{stdev}(vy) = 2.885$

$\text{var}(vx) = 0.157$ $\text{var}(vy) = 8.325$

$a := \text{slope}(vx, vy)$ $a = -7.247$

$b := \text{intercept}(vx, vy)$ $b = 12.799$

$c := \text{corr}(vx, vy)$ $c = -0.996$

$x_i := i$ $y_i := a \cdot x_i + b$
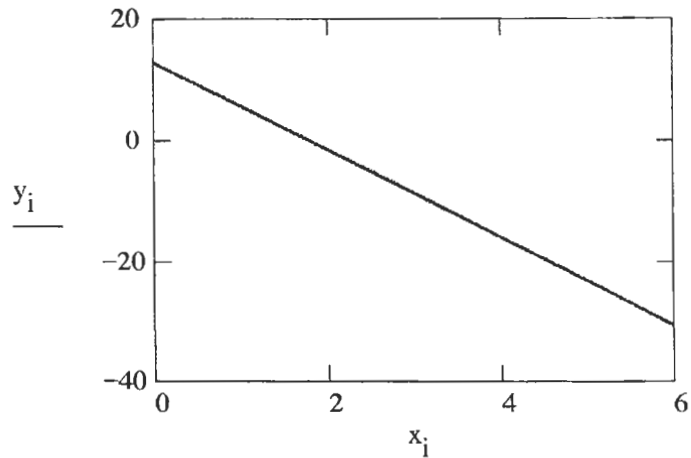
yi = b + a*xi   ln(kt) = ln(kot) - (E/R*K)*1000*K/T $T := K$

$kot := \exp(b)$ $kot = 3.618 \cdot 10^5$ $time := \dfrac{1}{3 \cdot \sec^{-1}}$

$k_o := \dfrac{kot}{time}$ $k_o = 1.086 \cdot 10^6 \cdot \sec^{-1}$ $mol := 0.022412 \cdot m^3$

$R := 8.314 \cdot \dfrac{joule}{mol \cdot K}$ $E := -1000 \cdot a \cdot R \cdot K$ $E = 6.025 \cdot 10^4 \cdot \dfrac{joule}{mol}$

Appendix H: Reaction Rate

Chemical engineering inherited the definition for the reaction rate from chemical kinetics. The definition is for closed systems, like batch reactors, in which most of the classical kinetic studies were done. Inside a batch reactor little else besides chemical reaction can change the concentration of reactant A. In a closed system, for the reaction of:

$$\alpha_A A + \alpha_B B = \alpha_p P + \alpha_s S$$

for example:

$$CO + 2\ H_2 = CH_3OH \text{ or } -CO - 2\ H_2 + CH_3OH = 0$$
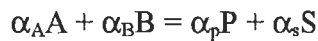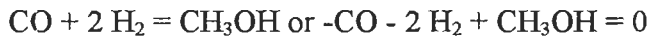
the rate law or its functional form is:

$$r_A = k_o e^{-E/RT} C_A{}^n C_B{}^m$$

for example, methanol synthesis, the UCKRON test problem:

$$r = f(T,\ C,\ H,\ M)$$

where the dimension of the rate is:

$$r_A [=] \frac{mol}{m^3 s}$$

the measure or definition of rate of reaction is:

$$r_A \equiv -\frac{dC_A}{dT}$$

or:

$$r \equiv \frac{dC_A}{\alpha_A dt} = \frac{dC_G}{\alpha_B dt} = \frac{dC_B}{\alpha_p dt} = \frac{dC_F}{\alpha_s dT}$$

for example:

$$r = -\frac{dC_C}{d\theta} = -\frac{dC_H}{2 d\theta} = \frac{dC_M}{d\theta}$$

251

In a closed system the rate of reaction is properly defined by a total time derivative of the concentration, if concentration is based on the closed total volume of the system or on a volume liquid of constant density.

Many large processes of the chemical industry are conducted in continuous flow reactors and these are open systems. In these, where material can get in and out, the concentration of the reactant can be changed by the movement of materials in addition to the change by chemical reaction. While the above definition of rate is valid for closed systems only, the functional form of the rate expression and the dimensions for rate have general validity[8]. A good understanding of the significance of reaction rate can be obtained from the balance equation for reactant A, in a single–phase, homogeneous reaction, in a reactor of constant volume, at non-steady state, and of a general type as was given by Damköhler[9] but presented here for one spatial dimension only:

$$\frac{\partial C_A}{\partial t} = \alpha r + u \frac{\partial C_A}{\partial l} - D \frac{\partial^2 C_A}{\partial l^2}$$

It will be easier to see the importance of the various terms if this equation is rearranged as Hulbert[10] recommended it. For this the reaction term will be put on the right hand side and terms representing physical changes to the left hand side.

From the four changes listed in the first line of the table (next page) only the pertinent terms are given for each type of reactor. In the first line for the batch reactor type, since both the flow and diffusion (dispersion) differential terms drop out, the time derivative remains alone and therefore becomes a total derivative. This is the measure for the rate here. In the next to last line, for the CSTR type, the flow term is in integrated form, since no change is expected there. Multiplying both u and l with the flow cross section will change the flow term to the more familiar $F'(C_{Ao}-C_A)/V$. If both the flow and concentration change, then this is the correct measure for rate:

$$\frac{F'_o C_o - F' C}{V} = -\alpha r$$

---

[8] For catalytic reactions in an open system, V reactor volume contains the catalyst and concentrations are referred per unit of flowing volume, m^3/s.

[9] Damköhler, G in **1937**, *Eucken-Jackob: Der Chemie Ingenieur*, III, Part 1, p. 367.

[10] Hulbert, H.H. as mentioned in Carberry 1976.

Expressions for Rates

Time	Flow	Diffusion	Reaction	Reactor Type
$+\dfrac{\partial C_A}{\partial t}$	$+u\dfrac{\partial C_A}{\partial l}$	$-D\dfrac{\partial^2 C_A}{\partial l^2}$	$=-\alpha r$	General
$+\dfrac{dC_A}{dt}$			$=-\alpha r$	Batch
$+\dfrac{\partial C_A}{\partial t}$	$+u\dfrac{\partial C_A}{\partial l}$		$=-\alpha r$	Flow, not SS, Integral
	$+u\dfrac{dC_A}{dl}$		$=-\alpha r$	Flow, SS, Integral
	$+u\dfrac{dC_A}{dl}$	$-D\dfrac{d^2 C_A}{dl^2}$	$=-\alpha r$	Flow and Dispersion
	$+u\dfrac{C_{Ao}-C_A}{l}$		$=-\alpha r$	Flow, CSTR in SS
$+\dfrac{dC_A}{dt}$	$+u\dfrac{C_{Ao}-C_A}{l}$		$=-\alpha r$	Flow, CSTR, non-SS

Index

STUDIES IN SURFACE SCIENCE AND CATALYSIS

Advisory Editors:
B. Delmon, Université Catholique de Louvain, Louvain-la-Neuve, Belgium
J.T. Yates, University of Pittsburgh, Pittsburgh, PA, U.S.A.

264

266

268